Investigation into the Regulation and Interactions of Myocyte Stress 1 protein

Thesis submitted for the degree of
Doctor of Philosophy
at the University of Leicester

Eva Simone Jordan BSc MSc (Leicester)
Department of Biochemistry
University of Leicester

November 2014

Eva Jordan

Investigation into the Regulation and Interactions of Myocyte Stress 1 (MS1) Protein.

Abstract

Myocyte stress 1 (MS1) also known as Striated Muscle Activator of Rho Signalling (STARS) and Actin-binding Rho activating protein is a stress responsive, muscle specific protein expressed in cardiac, skeletal and smooth muscle. MS1 was first observed to increase in mRNA levels during early states of pressure overload induced left ventricular hypertrophy, making MS1 sensitive to extracellular stress. MS1 is highly involved in actin dynamics, where polymerization of actin leads to the regulation of the myocardin related transcription factor-A and the serum response factor (MRTF-SRF). The SRF pathway plays a critical role in the regulation of the skeletal muscle. While in the heart, MS1 is thought to be implicated in hypertrophic signalling and cardiac remodelling. Previous studies in the lab have shown that MS1 increased in mRNA levels during simulated ischaemia/reperfusion injury but levels were attenuated with the addition of JNK inhibitor SP600125 during simulated ischaemia/reperfusion injury. Although we know MS1 is involved in actin dynamics due to its ability to bind actin at the C-terminal as a result of actin binding domains (located between 234-375 a.a) and also bind actin binding proteins ABLIM-2 and 3, there is limited information on how MS1 becomes upregulated and its specific function.

In this study we wanted to investigate the effect of various stimuli on MS1 promoter activation with the use of luciferase reporter assays. The MS1 promoter was responsive to sorbitol induced osmotic stress, oxidative stress by serum deprivation and hypertrophic agonist phenylephrine. All of these are well known activators of the stress activated protein kinases (SAPKs); JNK and p38. There may be a link between MAPK activation and MS1 regulation.

Investigation of other interacting partners of MS1 was proposed to give some insight into the function of MS1. Binding assays using purified MS1 fragments were used to look at potential interactions in the heart. Interestingly, novel myofibrillar proteins were pulled out of heart extract and identified by mass spectrometry as Myosin-6, troponin I, troponin T, α-tropomyosin, myosin LC2 and actin.

We observed potential phosphorylation sites, located within the N-terminus of MS1. *In vitro* kinase assays using activated JNK, p38 and ERK, allowed for phosphorylation of MS1. Three novel phosphorylation sites Thr24, Thr62 and Ser77 were identified by mass spectrometry. Immunofluorescence studies were used to determine whether phosphorylation alters MS1 subcelluar distribution or interaction with actin. Co-localisation was observed between MS1 and HA-JNK at the cell membrane where there was evidence of membrane ruffling and actin stress fibres present at the periphery. All of these findings in this study are novel and imply that MS1 may be involved in the MAPK pathway and also play critical roles in contractile function, muscle development and cell motility, where phosphorylation may be responsible for its ability to interact with myofibrillar proteins.

Acknowledgements

Firstly, I would like to thank my supervisors Dr. Martin Dickens and Dr. Sally Prigent for their great amount of patience, help, guidance and encouragement throughout this journey for the past few years, especially during the writing of my thesis, thank you for everything.

I would also like to thank my committee members Dr. Mohammed El-Mezgueldi and Dr. Mark Pfuhl for their informative talks and generous gifts.

I would like to thank Dr. Raj Patel, Dr. Mark Leyland, and Prof. Andrew Fry's lab for the generous provision of reagents.

I must also thank my lab partners Dalhee, Juwhan and Naif for making time in the lab enjoyable. A very special mention goes out to Samrein Ahmed for not only becoming my close friend but being supportive and believing in me, you made my days in the lab so much easier. I would also like to thank everyone from lab 2/42 for their help and reagents throughout the years. A special thanks goes to my close friends which I made in Leicester, Shanow, Kim, Fabricio, Tammy and Sian. Friends who became my chosen family, I thank you for everything.

I am especially grateful to my close friend, my sister from another mister and the best flatmate ever, Lara Lewis who has supported me so much during my PhD and believed in me when I didn't believe in myself. Thank you for helping me to keep my sanity. I could not have asked for anyone as kind, understanding and helpful as you. You are truly an angel in human form. Special thanks for allowing me to convert our lounge into my office during my write up!

Special thanks to my friends in Barbados for all of the skype calls and chats when I felt frustrated and homesick. I would also like to thank Scott Bentham, for being there for me, encouraging me and being supportive during my write up...I love you. Also to one of my oldest friends; Andraa Bynoe , her family and Lesley Reece for the prayers and motivational chats. I love you.

Finally, I reserve my greatest expression of gratitude to my parents. My father, who has always believed in me, loved me unconditionally and was always there for me, I know you still watch over me in spirit. To my mother, you are my pillar of strength and without you, this would never have been possible. You have continuously encouraged me throughout my life and constantly brought a sense of calm when I was upset, frustrated and felt down. You are the epitome of strength and I love you so much. All I have ever wanted was to make both of you proud. I dedicate this thesis to you and Daddy!

List of Contents

Table of Contents

Table of Figures

Table of Tables

Abbreviations

ABLIM	Actin binding Lim protein 1
ABP	Actin binding protein
ABRA	Actin binding rho activator
ADP	Adenosine diphosphate
AMP	Adenosine monophosphate
ANF	Atrial natriuretic factor
ANP	Atrial natriuretic peptide
AP-1	Activator Protein 1
ATF2	Activating transcription factor 2
ATP	Adenosine triphosphate
ASK	Apoptosis signal-regulating kinase
Bax	Bcl-2 associated protein X
BCA	Bicinchoninic acid
Bcl-2	B-cell lymphoma/ leukemia-2
BH	Bcl-2 homology domains
BIM	Bcl-2 interacting mediator of cell death
BSA	Bovine serum albumin
cDNA	Complementary DNA
CMV	Cytomegalovirus
c-myc	Cellular myelocytomatosis oncogene
CO-IP	Co-immunoprecipitation
CsCl	Caesium chloride
C-terminus	Carboxy-terminus
DAG	Diacylglycerol
DAPI	4'-6'- diamidino-2-phenylindoe
dH_2O	Distilled water
DIABLO	Direct IAP-binding protein with low
DINA	Distal intergenic activator
DMEM	Dulbecco's Modified eagle medium
DMSO	Dimethyl Sulfoxide
DNA	Deoxyribose nucleic acid
dNTP	Deoxynucleotide triphosphate

dsDNA	Double stranded DNA
DTT	Dithiothreitol
ECL	Enhanced Chemiluminescence
E. Coli	Escherichia coli
ECRs	Evolutionarily conserved regions
EDTA	Diaminoethane-tetra acetic acid
ERK	Extracellular signal regulated kinase
EST	Expression Tagged Sequence
ET-1	Endothelin-1
Et al	Et alia (and others)
ETS	E26 transformation specific
FADD	Fas-associated protein with death domain
FBS	Foetal Bovine serum
FCS	Foetal calf serum
FITC	Fluorescein isothiocyanate
GATA4	GATA-binding protein 4
GFP	Green fluorescent protein
GPCR	G-protein coupled receptor
GPS	Group-based prediction system
GRN	Gene regulatory network
GST	Glutathione S-transferase
HEK	Human embryonic kidney
HPLC	High performance liquid chromatography
HRP	Horseradish Peroxidase
IF	Immunofluorescence
IP	Immunoprecipitation
IPTG	Isopropyl-beta-D-thiogalactopyranoside
JNK	c-Jun N-terminal kinase
kDa	Kilodalton
KIM	Kinase interaction motif
LB	Luria Bertani
LC/MS	Liquid chromatography/mass spectrometry
LIM	Lin11 Isl-7 Mec-3

LVH	Left Ventricular Hypertrophy
MADS	MCMI, AGAMOUS DEFICIENS
MAPK	Mitogen activated protein kinase
MBP	Myelin basic protein
MEF2	Myocyte Enhancer Factor 2
MHC	Myosin heavy chain
MI	Myocardial infarction
MKK	MAPK/ERK Kinase
mM	millimolar
MLK	Mixed lineage kinase
MOMP	Mitochondrial Outer Membrane Permeabilization
mRNA	Messenger Ribonucleic acid
MRTF	Myocardin-related transcription factors
MS1	Myocyte stress 1 protein
MSD1	Myocyte stress domain 1
mTOR	Mammalian target of rapamycin
MyoD	Myogenic differentiation antigen
NaCl	Sodium chloride
NaF	Sodium fluoride
NHS	N-hydroxysuccinimide
N-terminus	Amino-terminal
PBS	Phosphate buffered saline
PE	Phenylephrine
Pen/strep	Penicillin / streptomycin
PKC	Protein kinase C
PLC	Phospholipase C
PMA	Phorbol 12 myristate 12 acetate
PMSF	Phenyl methylsulfonyl fluoride
PUMA	p53-Upregulated modulator of apoptosis
Rho	Ras homolog
ROS	Reactive oxygen species
SAPK	Stress activated protein kinase
SDS-PAGE	Sodium dodecyl sulphate polyacrylamide gel electrophoresis

SINA	Stress intergenic activator
SiRNA	Small interfering RNA
SMC	Smooth muscle cell
SRE	Serum response element
SRF	Serum response factor
STARS	Striated muscle activator of Rho Signalling
SV40	Simian virus 40
TBS	Tris buffered saline
TCF	Ternary complex factor
TF	Transcription factor
TK	Thymidine kinase
TLB	Triton lysis buffer
TNF	Tumor necrosis factor
TRADD	TNF receptor-associated Death domain
U	Unit
µg	Microgram
µl	Microlitre
µM	Micromolar
UV	Ultraviolet
v/v	Volume per volume ratio
WT	Wild-type
W/V	weight per volume ratio
xg	Times gravity
ZAP-70	Zeta chain associated protein -70

Chapter 1. Introduction

1.1. Cardiac Function and Statistics

The cardiovascular system is made up of the heart, blood and blood vessels (capillaries, veins and arteries) found throughout the body which allows for circulation of the blood. This system is a closed circuit that is expandable allowing for movement and stresses to occur without damage. The main function of this system is to maintain homeostasis within the body, which requires the transport of oxygen, nutrients, hormones and cellular waste products. The key player in this system is the heart that acts as a pump and allowing for blood to pump in and out of this organ.

The heart, during embryonic development, is one of the first organs to be formed. This organ grows through proliferation and physiological hypertrophy of cardiac cells (Srivastava and Olson., 2000). This is a muscle that acts as a pump to facilitate circulation, beating approximately 3 billion times without failure during the course of a normal, healthy lifetime (Lifton., 2007). The heart consists of three layers, the epicardium, myocardium and the endocardium. The heart is a four chambered double pump where the four chambers are; the right atrium, right ventricle, left atrium and left ventricle and two types of valves, known as the atrioventricular and semilunar valves (**Figure 1.1).** The left and right side of the heart is separated by a muscular wall of tissue known as the septum (**Figure 1.1)**. The right side of the heart is smaller and receives deoxygenated blood which has circulated throughout the body. The right atrium receives venous blood, where contraction of the heart passes the blood through the tricuspid valve to the right ventricle (Lifton., 2007). The blood is then pumped to the pulmonary artery, where capillaries within the lungs enable oxygenation of the blood which is then received by the left side of the heart enabling its adequate distribution throughout the body (Lifton., 2007). Specialised cells known as cardiomyocytes make up the heart, and are responsible for contraction of the hearts chambers (Lifton., 2007). This system is susceptible to breakdown and assault as a result of different factors. These factors arise due to abnormalities with development and environmental factors or genetic disorders that lead to the development of cardiovascular diseases.

Cardiovascular disease (CVD) is described as complications that occur to either cardiac function or the related vasculature such as blood vessels, capillaries, arteries and veins. CVD which includes heart disease and stroke is the leading cause of death worldwide.

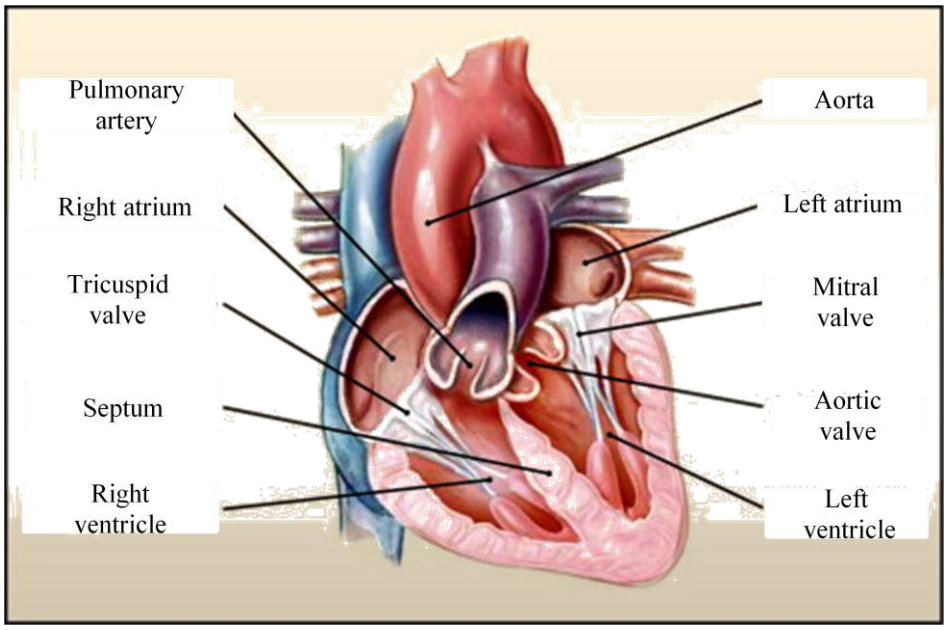

Figure 1.1: The Anatomy of the Heart.
Coronal section of the human heart shows the four chambers which are the right atrium, right ventricle, left atrium and left ventricle along with the valves and vessels responsible for receiving and distributing blood throughout the body. (Picture taken from 'Lasker Award to Heart Valve Pioneers' Lifton., 2007)

Based on the world health organisation statistics from a 2011 study, it was estimated that 17.3 million people died of CVD in 2008, which accounted for 30% of deaths in the world (World Health Organization, 2011). Low and middle-income countries are most affected by this disease which is not gender specific as both men and women are equally affected (World Health Organization, 2011).

1.2. Cardiovascular Diseases

1.2.1. Coronary Heart Disease

Coronary heart disease (CHD) which is also known as coronary artery disease (CAD) and ischaemic heart disease, causes the highest number of deaths amongst all of the CVDs with more than 7.2 million deaths observed in 2008 (World Health Organization, 2011). CHD is described as narrowing of the blood vessels responsible for supplying the heart (myocardium) with blood and oxygen. Build-up of cholesterol rich deposits or plaques known as atherosclerotic plaques or fatty streaks that form within the walls of the artery are often the main reasons for narrowing of these vessels (**Figure 1.2**). Once the artery wall has thickened, and the space for blood flow is reduced blood flow to the myocardium becomes restricted leading to the reduced intake of oxygen and nutrients required. Plaque development begins during injury or infection of the endothelium within the layer of lipid on the arterial wall where macrophages and T-cells are present (Ross, 1999; Napoli *et al.*, 1997; Stary *et al.*, 1994). For over 25 years, it was thought that elevated levels of low density lipoprotein (LDLs) which are the major cholesterol-carrying lipoprotein in the plasma, were the main cause of CHD (Nabel., 2003).

Although these plaques are initially stable with low lipid levels, over time, they become unstable and finally rupture (**Figure 1.2**) (Ashley and Niebauer, 2004). As a result of excessive thickening that causes the arterial wall to remodel in order to retain the diameter of the lumen vessel plaques can become fatal. This can lead to the release of metalloproteinases by macrophages, that degrade the fibrous cap of the plaque and make it susceptible to rupture (**Figure 1.2**) (Liu *et al.*,2004; Galis *et al.*, 1994; Schonbeck *et al.*, 1997). A staggering 70% of all fatal myocardial infarctions and coronary deaths occur as a result of plaque rupture (Naghavi *et al.*, 2001; Falk *et al.*, 1995).

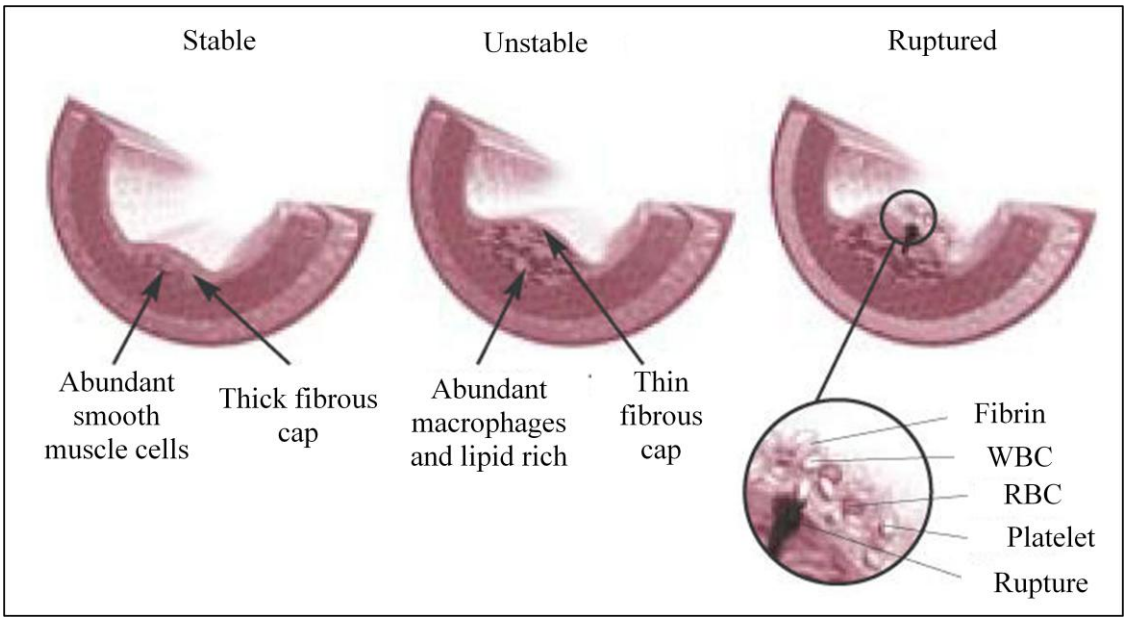

Figure 1.2: Formation and Composition of Atherosclerotic Plaques
Atherosclerotic plaques are initially triggered as a result of injury or infection of the endothelium. The lipid levels and macrophages accumulate gradually within the walls of the artery that are encapsulated by a fibrous cap (a thickened layer within the artery wall as a result of smooth muscle cells that deposit collagen and elastin fibers). As the atherosclerotic plaque thicken, this leads to restricted blood flow as it is within the lumenal space and the cap is susceptible to rupture. (Taken from Ashley and Niebauer., 2004)

Studies have shown that atherosclerotic progression is caused through inflammation. This is as a result of proinflammatory cytokines and growth factors, which are produced in an area within the plaque known to induce monocytes differentiation into macrophages (Virmani *et al.,* 2005; Smith *et al.,* 1995; Van der Wal *et al.,* 1994). Although coronary heart disease is a killer, it can be prevented and is treatable with lifestyle changes and drugs which can regulate LDL cholesterol levels.

1.2.2. Congenital Heart Disease

Congenital heart disease is defined as a cardiovascular malformation of the heart present from birth (Pierpont *et al.,* 2007). Coronary heart disease is the most common cause of congenital disorders found in newborns that can result in perinatal and infant mortality, with approximately 6-13 new-borns out of every 1000 births affected (Tennant *et al.,* 2010; Bird *et al.,* 2006). These cardiovascular malformations are symptomatic and are identified shortly after birth whilst other defects are often detected during infancy (Wren *et al.,* 2008; Gregory *et al*., 1999). During the last 20-25 years there has been an increase in adult patients with congenital heart disease owing to progression in paediatric cardiology and surgery. In the UK, approximately 250,000 adults live with congenital heart disease, which implies that timely diagnosis during hospitalisation and new-born management has reduced mortality rates of CHD (Swan *et al.,* 2006; Gatzoulis., 2006; Tennant *et al.,*2010; Boneva *et al*., 2001).

Heart conditions that develop as a result of congenital heart disease are due to mutations in genes or chromosomes. The most common CHD lesions are atrial septal defects that can cause mitral valve prolapse leading to mitral valve regurgitation (Lifton., 2007). Other common lesions are obstructive lesions of the left or right side of the heart resulting from lost systemic perfusion lost or restricted blood flow (Altman *et al.,* 2014). Problems with the bicuspid and/or tricuspid valves can also be affected. In critical cases, surgery or patient management is required to correct these problems (Altman *et* al., 2014; Brickner *et al*., 2000). In recent years, major advances have been undertaken in the development of effective treatments for valvular disease which causes prolase of the valve (Lifton., 2007).

1.2.3. Deep Vein Thrombosis or Pulmonary Embolism

Deep vein thrombosis is described as the development of blood clots which are termed deep vein thrombi (DVT) that can be found within the leg veins as well as the arms and

cerebal veins which can become dislodged and travel to the heart and lungs (Kucher, N., 2011; Kyrle and Eichinger; 2005; Goldhaber and Morrison., 2002). Pulmonary embolism (PE) occurs as a result of clots that break off from the vein walls, when this occurs they can travel through the heart to the pulmonary arteries. The term used to describe both disorders is called venous thromboembolism (VTE) (Goldhaber and Bounameaux; 2012; Goldhaber *et al*., 2002). Although, studies have shown that DVT and PE can arise spontaneously or be caused by clinical conditions as a result of trauma, surgery or excessive bed rest, these disorders can also occur due to hereditary traits and predisposition which can increase an individual's susceptibility.

PE is the third most common cause of death from cardiovascular disease after heart attack and stroke (Goldhaber and Bounameaux; 2012). So far, studies carried out in Sweden and Norway have confirmed that DVT and PE are not gender specific, however, there is a slightly higher incidence in women than men (Naess *et al.,* 2007; Nordstorm *et al*., 1992). Deep vein thrombosis is rare in children and more prevalent in adults aged 65-89 (Kniffin *et al.,* 1994). Studies confirmed DVT is also prevalent in Caucasian and Blacks based on a British study where 25% Caucasians and 22% Blacks were more susceptible than Asians, who had a significantly lower incidence (Klatsky *et al.,* 2000; Patel *et al.*, 2004).

Symptoms of DVT include days of cramping that intensify over time, followed by leg swelling and discolouration (Goldhaber and Bounameaux; 2012). Patients with PE are asymptomatic leading to a delay in diagnosis that often results in progression of this disease, however imaging tests and ultrasounds are done to correctly diagnose patients. Formation of venous thrombi occurs as a result of low blood flow and low shear stress. Clots are formed of fibrin strands, red bloods cells and platelets that develop in the pockets of calf veins (Goldhaber and Ridker., 2002). DVT and PE are usually treated with blood anticoagulants or in more serious cases, either surgery or a catheter to remove the clot (Goldhaber and Bounameaux; 2012).

1.2.4. Rheumatic heart disease

Rheumatic heart disease develops as a consequence of rheumatic fever which is caused by group A *streptococcus* bacteria and can show symptoms of a sore throat or tonsillitis in children (Cunningham, MW; 2004). During fever, organisms attach to epithelial cells producing enzymes that allow for the invasion of tissues. In acute stages during rheumatic fever, an inflammatory response develops. There seems to be a period

between pharyngitis and rheumatic fever of about 1-5 weeks that allows for the inflammatory response to develop and attack the tissue (Bisno *et al.,* 1995; Stollerman, GH; 1995 and 1991). This leads to activation of streptococcal M-protein types that extend from the cell membrane of the Streptococcal A group bacteria (Cunningham, MW., 2000). The streptococcal M-proteins can mimic the immune system and cardiac antigens, for example the protein myosin and valvular endothelium allow them to invade the tissues without detection (Cunningham, MW; 2004). Cytoskeletal proteins such as tropomyosin, laminin and ECM are recognized by antimyosin antibodies that result in damage to the valves of the heart (Cunningham, MW; 2000). T-lymphocyte production plays a role in the damage to myocardium, endocardium and pericardium resulting in carditis or endocarditis as a result of TNF and release of interleukins (Kaplan 2005; Roberts and Mi; 2008; Guilherme *et al*., 2004).

Rheumatic heart disease is observed in children between ages 5-15 in both underdeveloped and developing countries, where antibiotics are not commonly used for pharyngitis (Kaur *et al.,* 1998). Unfortunately, as a result, complications in the heart such as mitral valve disease and atrial fibrillation can develop. Mitral valve disease is most common in rheumatic heart disease, and is found in around 50% of individuals with rheumatic fever, a disease that is estimated to affect approximate 15 million people worldwide (Cunningham, MW; 2000; World Health Organization., 2004). This is due to the accumulation of calcium deposits or fibrosis in the aortic valve that either prevents the valve closing and causes regurgitation (leaky valve) or results in complete failure known as mitral stenosis (Roberts and Mi; 2008). Atrial fibrillation is another incidence of rheumatic heart disease due to blood clot formation. To date there is still a debate on the pathogenetic mechanism of the development of rheumatic fever and rheumatic heart disease (Kaplan., E.L; 2005), however It has been hypothesised that the virus herpes simplex I could play a role in this disease (Li *et al.,* 2005).

The cardiovascular diseases listed are some examples of a broad range of disorders; however these develop at different stages in life and affect different aspects of the cardiovascular system. These diseases have similar risk factors, for example diabetes, smoking, obesity, limited physical activity and high cholesterol to name a few that can make people more susceptible. Most of these diseases are treatable with dietary management and increased physical activity, however, in severe cases, corrective surgery is required. A greater focus on the physiological aspects of heart diseases with

emphasis on ischaemia/reperfusion injury and cardiomyopathies are discussed in the following sections.

1.3. Pathophysiology of Ischaemia/Reperfusion Injury an Overview

Despite advances in the treatment of acute myocardial infarction (AMI) over the last 30 years, it is still understood to be the most common cause of death in the world (Mewton *et al.,* 2010). Myocardial ischaemia-reperfusion injury can occur as a result of thrombolysis, angina pectoris, embolic vascular occlusion, coronary by-pass surgery, angioplasty or heart transplantation, and can result in cardiomyocyte death by necrosis and apoptosis (Hausenloy and Yellon, 2013; Zhan *et al.*,2007; Dhalla *et al*., 2000 (Sahna *et. al*., 2005). During reperfusion, apoptosis is enhanced, owing to the sudden readmission of oxygenated blood into the tissues after an ischaemic event leading to further tissue damage. Apoptosis is described as programmed cell death and is known to play a role in myocyte death due to ischaemia reperfusion injury, where the inhibition of apoptosis may attenuate injury (Dhalla *et al.,* 2000; Krijnen *et al.,* 2002). There are a series of biochemical and metabolic changes that occur during ischaemia reperfusion injury in the heart, these include; oxidative stress, ATP depletion, inhibition of myocardial contraction, calcium overload, neutrophil mediated endothelial dysfunction, loss of membrane phospholipids and a decrease in microvascular flow (**Figure 1.3)** (Maxwell and Lip.,1997; Hausenloy and Yellon, 2013).

1.3.1. Pathophysiology of Ischaemia

Ischaemia is defined as an insufficient supply of blood to organs as a result of an obstruction that can lead to a reduction of arterial or venous blood flow. This leads to a decrease in oxygen (known as hypoxia) and nutrient supply to the tissues, leading to a series of events which cause tissue damage (Parlakpinar and Sagir, 2013, Vanteeffelen, JW, 2008). Damage as a consequence of ischaemia is dependent on the length of time blood flow is restricted. If occlusion is for less than 40 minutes, metabolic and biochemical changes are reversible and can be treated. However if restriction of blood flow is between 40-50 minutes, this can result in progressive damage and instances where damage is irreversible. Over 50 minutes results in damage so severe that it resembles damage that takes place during reperfusion injury (which is more damaging than ischaemia) (Maxwell and Lip, 1997; Piper *et al.*,1998).

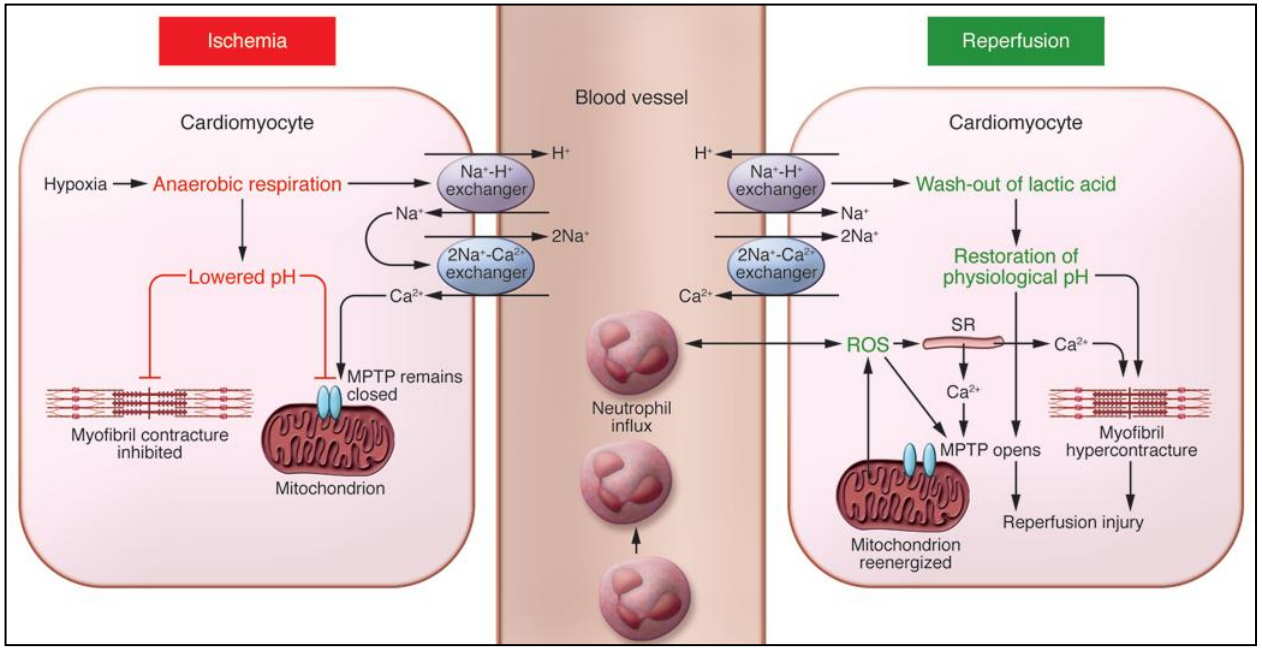

Figure 1.3: An overview of the Pathophysiology of Myocardial Ischaemia-Reperfusion Injury
During myocardial ischaemia restriction of blood flow leads to hypoxia, this triggers a compensatory switch to anaerobic respiration that leads to lactate build up, creating an acidic environment. This induces ATPase mediated pumps Na^+ /H^+ to remove H^+ and leads to the accumulation of intracellular Na^+ that causes a chain reaction activating $2Na^+$ /Ca^{2+} exchanger to malfunction resulting in calcium overload. Na^+ /K^+ ATPase pumps cease to work during ischaemia. At the onset of reperfusion, reactivation of the electron transport chain causes an influx of ROS. This leads to the opening of the mitochondrial permeability transition pore (MPTP) that leads to dysfunction of the sarcoplasmic reticulum. Intracellular accumulation of Ca^{2+} by lipid peroxidation causes cell damage. Rapid restoration of pH balance, allows for the MPTP to open. However all these events during reperfusion leads to further injury within cardiomyocytes. (Picture taken from Hausenloy and Yellon, 2013)

Pathological abnormalities that commence during decreased oxygen tension result in depletion of mitochondrial oxidative phosphorylation, leading to a reduction in ATP production for energy metabolism. Decreased ATP levels trigger a compensatory pathway known as anaerobic glycolysis necessary for ATP production (Maxwell and Lip, 1997). This leads to the accumulation of lactate resulting in decreased pH levels and an increased production of hydrogen ions, causing intracellular acidosis, attenuation of glycolysis and residual energy metabolism (Buja et al., 2010). ATP depletion occurs during ishcaemia when the purine precursors that are necessary for the resynthesis of ATP degrade to hypoxanthine and xanthine (Eltzschig and Collard, 2004; Maxwell and Lip, 2005). During normal physiological conditions, the enzyme responsible for the conversion of hypoxanthine to xanthine is catalysed by xanthine dehydrogenase. However, during ischaemic conditions xanthine dehydrogenase is converted to xanthine oxidase, which requires the use of oxygen instead of nicotinamide adenine dinucleotide (NAD) as the substrate (Eltzchig and Collard, 2004). The inability to catalyse the conversion of hypoxanthine to xanthine, due to lack of oxygen, leads to the accumulation of hypoxanthine allowing for the propagation of toxic reactive oxygen species to form during reperfusion (Kaminski *et al.*, 2002; Maxwell and Lip, 2005). This continued reduction in energy also causes a disturbance in cell electrolyte balance, where there are abnormally elevated levels of potassium and magnesium proton ions (Buja et al., 2005; Maxwell and Lip, 2005; Eltzschig and Collard, 2004). As a result, potassium ions leak rapidly from the intracellular compartment of the cell into the extracellular compartment due to an accumulation of metabolites and inorganic phosphates (Maxwell and Lip; 1997; Buja, L.M,2005).

The Na^+/K^+ ATPase pump responsible for maintenance of the cell membrane potential becomes inhibited during this time (Buja, L.M., 2005). This leads to alterations in ion transport, with a further decline in potassium ions and an increase in sodium ions within the cell. This contributes to the previous elevation of sodium ions based on the Na^+/H^+ ion exchanger that extrudes protons and allows sodium to enter the cell (Avkiran and Marber, 2002; Buja LM., 2005). Increases in sodium ions in addition to already present chlorine ions contribute to cell swelling. The mechanisms essential for maintaining normal calcium concentrations required to carry out functions are driven by ATP.

When these mechanisms cease to work calcium ions accumulate within the cytosol due to the malfunction of the ion transport systems occurring in the sarcolemma and sarcoplasmic reticulum. Calcium overload leads to the activation of phospholipases and

protein kinases (Buja *et al.*, 2005). During phospholipase activation, production of the potent prostaglandin inducer, arachidonic acid which is a free fatty acid (FFA) occurs leading to membrane degradation and the integrity of the membrane becomes compromised (Buja *et al.*, 2005). The reduced pH of the cell as a result of acidosis prevents the opening of the mitochondrial permeability transition pore (MPTP) causing impaired contractility in cardiomyocytes which can cause rigor (Buja *et al.*, 2005; Hausenloy and Yellon, 2013). Although the biochemical changes and mechanisms mentioned contribute to ischaemic injury, it is during reperfusion that damage to cardiomyoctes worsens. This is as a result of an influx in blood restoration that carries reactive oxygen species (ROS) and free radicals causing oxidative stress (Buja et al., 2005; Darwin, 1995; Maxwell and Lip, 1997; Hausenloy and Yellon, 2013)

1.3.2. Pathophysiology of Reperfusion Injury

Reperfusion is termed as the re-establishment of blood flow into ischaemic tissue. Restoration of blood flow to ischaemic tissue was initially thought to prevent permanent damage as a result of ischaemia. Timely reperfusion can salvage cardiomyocytes and decrease cardiac morbidity and mortality. This can, depending on the severity of the injury, even reverse the damage caused by ischaemic injury (Verma *et al*., 2002). However, although reperfusion is beneficial following ischaemia for the prevention of long term damage, it can also have negative effects (Hausenloy and Yellon, 2013; Braunwald and Kloner, 1985).

During reperfusion the sudden influx of blood can contribute to damage already caused by ischaemia, this leads to progressive damage as a result of calcium overload in the cytosol and mitochondria, acute inflammatory response and formation of toxic Reactive Oxygen Species ROS (Braunwald and Kloner, 1985; Napoli *et al.*, 2002; Eltzschig and Collard, 2004). During ischaemia there is an accumulation of hypoxanthine due to the depletion of ATP (as discussed in section 1.3.1). In the presence of oxygen, substrate xanthine oxidise can convert hypoxanthine to xanthine with the restoration of blood flow, with production of by-products such as toxic ROS (Kaminski *et al.*,2002; Berry and Hare, 2004; Li and Jackson, 2002). The production of superoxide radicals (oxygen with an unpaired electron) has been heavily studied in animal models, however some studies have disputed that there is a lack of evidence to show their relevance in humans (Stewart *et al.*, 1986; Maxwell and Lip, 1997, Kloner, 1997). It is thought that the quantities of superoxide radicals may be insufficient to affect humans, although

xanthine oxidase has been found to accumulate in endothelial cells (Maxwell and Lip, 1997). However, oxygen radicals can also be formed by other mechanisms such as mitochondrial respiration and activated neutrophils, which explains why they can still be found in elevated levels within the heart and are considered a major contributor to reperfusion injury based on a series of breakthrough studies supporting this theory (Bolli *et al.,* 1989; Jolly *et al.,* 1984; Zweier and Weisfeldt, 1987; Ambrosio *et al.,* 1989; Ferrari *et al.,* 1989).

During ischaemia, oxygen deprived tissue is primed following metabolic changes, leading to the promotion of damage during reperfusion (Ambrsio and Tritto, 1999). Previously, limitations prevented the capacity to adequately measure the level of oxygen radicals in patients (Kloner, 1993). However, new techniques such as electron paramagnetic resonance spectroscopy have been used to measure oxygen radicals, and have confirmed elevated levels of these radicals cam contribute to damage caused during reperfusion (Ambrosio and Tritto, 1999; Duilio *et al*., 2001).

During early reperfusion there are events that mimic an inflammatory like response mediated by neutrophils (a type of white blood cell). They are considered the "first-responders" of the inflammatory cells whereby they migrate towards the site of inflammation (Palakpinar and Sagir, 2013). Superoxide generation results from neutrophil membrane associated NADPH oxidases that are activated through either proinflammatory cytokines, platelet activating factor (PAF) or particular stimuli (Jordan *et al.,*1999). Neutrophils adhere to both biological surfaces and inflammatory mediators such as interlukin 6 (IL-6), interlukin 8 (IL-8) and tumor necrosis factor alpha (TNF-α) (Jordan *et al.,* 1999; Verma *et al*., 2002; Jacobs *et al.,* 2010). The stimulation of neutophils by pro-inflammatory mediators not only leads to the production of superoxide anions but also hydrogen peroxide and hydroxyl radicals during a respiratory burst (Jordan *et al.,* 1999). The formation of hydrogen peroxide is due to dismutation of superoxide anions (Jordan *et al.,* 1999). The vascular endothelium is susceptible to damage by existing oxygen radicals that result in increased permeability and adherence of neutrophils (Dreisher *et al.,* 1993; Svendsen and Bjerrum, 1992). A reduction in release of endothelium-derived factors that have adverse effects on neutrophils, such as nitric oxide a vasodilator and adenosine can also occur (known cardioprotective properties), this can exaggerate damage and dysfunction (Jordan *et al.,* 1999; Verma *et al.,*2002). Oxygen free radicals further contribute to damage by the production of lipid peroxides and hydroperoxides which can lead to damage of the

sarcolemma and the disruption of membrane-bound enzyme system function (Verma *et al.*,2002; Aceto *et al.*, 1990). Lipid peroxidation is evidence of free radical contribution to reperfusion injury, which was observed in studies of patients following thrombolytic reperfusion after prolonged ischemia of coronary thrombosis (Grech *et al.*,1993 and Davies *et al.*, 1990). Needless to say, there are many studies that support lipid peroxidation as a major contributor of free radical production, (Lau *et al.*, 1991, Weitz *et al.*, 1991; Maxwell and Lipp, 2005).

Changes in calcium homeostasis have also been shown to majorly contribute ti reperfusion injury (Gross *et al.*, 1999). As previously discussed (Section 1.3.1), the calcium concentration increases during prolonged ischaemia and is further exacerbated during reperfusion injury. Increased levels of calcium in the sarcolemma are due to entry through L-type calcium channels and the inhibition of the sarcoplasmic reticulum (Ca^{2+} -ATPase) and sarcolemma (Na^{+}, K^{+}- ATPase) pumps (Verma *et al.*, 2002; Piper *et al.*,1998). As a result of the removal of H^{+} protons, the activation of the Na^{+} / H^{+} exchanger to restore the intracellular pH results in an influx of Na^{+} into the cells through the Na^{+} /Ca^{2+} exchanger, resulting in an increase of Ca^{2+} ions (Schafer *et al.*,2001). Further uptake of calcium ions by the sarcoplasmic reticulum then results in calcium oscillations leading to myocytes going into a state of hypercontracture when exposed to oxygen and re-energization after reperfusion (Inserte *et al.*, 2002; Piper *et al.*, 1998; Schafer *et al.*, 2001; Siegmund *et al.*, 1997; Dirksen *et al.*, 2007). Other consequences of calcium overload during reperfusion, resulting in injury; are the activation of proteases, dysfunction of gap-junctions and membrane rupture (Menown and Adgey, 2001; Dirsken *et al.*, 2007; Ruiz-Meana *et al.*, 1999). Membrane rupture occurs due to a sudden influx of water and cell swelling as a result of intra and extracellular increases in osmolarity during ischaemic events (Piper *et al.*, 1998; Garcia-Dorado *et al.*, 1992). Inevitably, in combination, all of these events contribute to cell death through necrosis or apoptosis.

1.3.3. Prevention of Reperfusion Injury

For years there have been many debates on whether reperfusion injury exists, and if so to what extent is it detrimental to myocytes. This is the major reason for debate on its existence due to major limitations with the methods used to measure severity in clinical experiments (Kloner *et al.*, 1993). Numerous studies using experimental data and clinical trials have, in recent years, validated the occurrence of reperfusion injury in

humans (Ambrosio and Tritto, 1999; Kloner, 1993; Dirksen *et al.,* 2007). The overall aim, is to reperfuse an ischaemic myocardium in the safest way possible without incurring additional damage, therefore reperfusion is carried out in a fast and effective manner in order to avoid further damage. Understanding the mechanisms involved in reperfusion, and ensuring measures are taken to minimise potential damage, are the best solutions to this ongoing problem. Currently, biotechnology and pharmaceutical industries have developed new therapies to deal with reperfusion injury through numerous experimental models which have been proven as effective (Eltzschig and Collard, 2004; Collard and Gelman, 2001; Maxwell and Lip, 1997).

Lipid peroxidation and xanthine oxidase (in animals more than humans) are major contributors to free radical damage (Paradies *et al.,* 1999; Kalogeris *et al*., 2014). Antioxidant therapy has been extensively studied in regard to its protective capacity against oxidative stress in animal studies, through the use of superoxide dismutase, vitamin E (a major lipid-soluble free radical scavenger for free radical damage and lipid peroxidation), allopuritol (competitive inhibitor of xanthine oxidase), iron-chelating compounds, super oxide dismutase, angiotensin converting enzyme inhibitors, mannitol and calcium channel antagonists (to prevent calcium overload) (Maxwell and Lip, 1997; Collard and Gelman, 2001; Marzi *et al.,* 1993). Although the experimental evidence from these studies proves to be beneficial, however the use of this therapy in humans is still under investigation. However, it is still highly regarded as a protective measure against reactive oxygen species (Dhalla *et al.,* 2000).

Ischaemic preconditioning is described as the phenomenon by which tissues are exposed to brief periods of sublethal ischaemia separated by periods of reperfusion, and is used as protection against prolonged Ischaemia/reperfusion injury (Hausenloy and Yellon, 2013; Collard and Gelman, 2001). Experimental evidence using this technique has shown improved ventricular function and a decrease in the accumulation of neutrophils (Jerome *et al.,* 1995; Wang *et al.,* 1999). Unfortunately, there is still limited clinical evidence in humans supporting the efficacy of this method. There is however, a plethora of experimental data using animal models that supports this method (reviewed in Dirksen *et* al., 2007, Collard and Gelman, 2001; Maxwell and Lip, 1997).

Leukocyte mediated ischaemia/reperfusion injury is another therapeutic target in the prevention of reperfusion injury. Inhibition of leukocyte endothelial adhesion and synthesis, and inflammatory mediator release are central to these therapeutic experimental strategies (Panes *et al.,* 1999). Antagonists such as inflammatory

mediators, platelet activation factor and TNF-α are the major targets in antileukocyte therapies (Panes and Granger, 1999) and have been used as mediators to facilitate leukocyte activation. Studies have shown that aspirin can trigger the biosynthesis of a new group of bioactive eicosanoids known as aspirin-triggered lipoxins, of which lipoxins are products generated from arachidonic acid (Chiang *et al.*, 1999). Lipoxins prevent transmigration of neutrophils triggered by leukotrienes, which suggests that lipoxins may act as inhibitors in host inflammatory reactions (Chiang *et al.*, 1999).

The above mentioned therapies are a few of many strategies that support the use of drugs which target the major contributors of reperfusion injury. These therapies are thought to be capable of limiting the size of infarcts prior to or at the onset of reperfusion (Dirsken *et al.*, 2007).

In summary, the extent of injury that myocardial cells sustain is dependent on the length of time that they are subjected to ischaemic conditions. Reperfusion can either reverse the damage caused during ischaemia or increase damage of the cells (Piper *et al.*, 1998). The contributing factors during reperfusion call into question the efficiency of this process, as it might not benefit all patients and could be detrimental due to the manifestations that occur (Maxwell and Lip, 1997). Reperfusion injury exists based on experimental evidence and clinical relevance (Ambrosio and Tritto, 1999; Verma *et al*., 2002; Hansen, 1995; Dirksen *et al*., 2007). Therefore measures taken to prevent injury either before or during early stages of reperfusion could prevent or limit the extent of damage in humans.

1.4. Simulation of Ischaemia and Reperfusion in vitro

There are different methods used in order to simulate ischaemia/reperfusion injury *in vitro* (Bogoyevitch *et al.*, 1996). The most commonly used method for these two processes is the addition of known concentrations of ions and metabolites to cell media in order to mimic the conditions observed during clinical ischaemia/reperfusion. This cell culture method allows for the selection of an appropriate cell line that allows for experimental reproducibility.

In order to simulate reperfusion HEPES (4-(2-hydroxyethyl)-1-piperazineethanesulfonic acid) buffered Krebs (4 mM HEPES pH 7.5, 2 % FCS, 137 mM NaCl, 3.58 mM KCl, 0.49 mM $MgCl_2$, 0.9 mM $CaCl_2$, 5.59 mM glucose) is used to mimic normal physiological conditions which cells tend to thrive in during extended periods of manipulation. As previously mentioned, the characteristics of ischaemic conditions are;

the inhibition of anaerobic glycolysis, depletion of ATP levels, build up of lactate, decrease in pH levels and increase of intracellular calcium and extracellular potassium concentrations. These characteristics are mimicked by the use of inhibitors and chemicals that allow for these effects to be reproduced *in vitro*. The glucose analogue 2-deoxyglucose is used to inhibit hexokinase through blocking the conversion of glucose into glucose-6-phosphate, a committed step in glycolysis. This reaction is attenuated when 2-deoxyglucose is present; therefore inhibition of the glycolytic pathway occurs resulting in decreased ATP production (Mohinder and Belgrave, 1997). Sodium dithionite can also used as an oxygen scavenger to induce hypoxia. Mitochondria require the presence of oxygen for use in the electron transport chain; however, the use of sodium dithionite inhibits this action. Another incidence of ischaemia is the accumulation of lactate that leads to increased pH levels, termed acidosis. Lactate build up during ischaemia can be mimicked *in vitro* by the addition of sodium lactate, this results in a lowered pH replicating the acidic conditions which so commonly occur. Finally, potassium chloride is added to replicate the increased levels of ions observed during ischaemia as a result of the Na^+/K^+-ATPase pump failing to function. This results in the accumulation of extracellular concentrations of potassium, with these elevated concentrations leading to changes in osmolar load within cells causing swelling to occur. Reperfusion was simulated by using unaltered HEPES buffer, which mimicked the normal physiological conditions where cells thrive.

1.5. Cardiac Hypertrophy

Cardiac hypertrophy (CH) can be defined as the enlargement of an organ or tissue as a result of biochemical signalling events and changes in gene expression, leading to protein synthesis and increase in cell size (Marian *et al*., 2008; Kee and Kook, 2011; Frey *et al*., 2004). CH is a disease associated with the thickening of the interventricluar wall; and results in changes in the sarcomeric structure (Frey *et al.*, 2004). CH is seen in heart diseases such as ischemic heart disease, familial hypertrophic cardiomyopathy and valve disease (Frey *et al.,* 2004; Carreno *et al.,* 2006).

Hypertrophy is a myocardial response to biochemical stresses caused by intrinsic and extrinsic stimuli that correct the pumping function of the heart (Frey *et al.,* 2004). Prolonged hypertrophy can lead to heart failure, as cells that have increased in size become overworked in order to compensate for cells which have died. Thickening of the walls of the heart reduces pumping efficiency leading to dysfunction and malignant

arrhythmia (Levy *et al.,* 1990; Ho *et al.,* 1998). For years the mechanisms that are responsible for the progression of hypertrophy to heart failure have been poorly understood (Carreno *et* al., 2006; Frey *et al.,* 2004). However, in recent years studies have been able to identify mechanisms implicated in the pathogenesis of cardiac hypertrophy such as, protein kinase C (PKC), NFAT, M-TOR, IGF-1, MAPK and PI3K-AKT/PKB pathways (Oka *et al.,* 2008; Molkentin *et al*., 1998; Balakumar *et al.,* 2010; Aoyagi and Matsui, 2011; Rohilla *et al*., 2012).

1.5.1. Physiological vs Pathological Hypertrophy

CH can be classed as either physiological or pathological, and can be divided into two sub-classes either concentric or eccentric due to changes in shape that are dependent on the initiating stimulus (Pluim *et al.,* 2000; Grossman *et al.,* 1975). There are two types of hypertrophy which are observed in the heart, hypertrophy which can arise as an adaptation in response to continuous exercise as seen in athletes or alternatively pathological hypertrophy which occurs to compensate for the loss of other myocytes as a result of continuous stress (Levy *et al.,* 1990 and Ho *et al.,* 1998).

Physiological hypertrophy is in response to regular physical activity or continual exercise training that results in increased myocardial muscle mass and pumping ability (Fagard R.H., 1997; Mone *et al.,* 1996). Pathological hypertrophy develops in response to stimuli such as, genetic mutations, hypertension and valvular disease, leading to a compensatory mechanism as previously discussed, increased muscle mass and accumulation of collagen within the myocardium (Sagara *et al.,* 2012). Although physiological and pathological hypertrophy both display an increase in size, there are neither visual differences to the heart nor major differences with the biochemical pathways that lead to their induction (McMullen and Jennings, 2007). During physiological hypertrophy growth factors become activated, whilst pathological hypertrophy is initiated by the activation of paracrine/autocrine factors e.g angiotensin II and endothelin (ET-1) (McMullen and Jennings, 2007; Frey *et al.,* 2004).

The development of hypertrophic growth is initiated in two ways, eccentric and concentric hypertrophy (Barry *et al*., 2008). Eccentric hypertophy is as a result of volume overload leading to dilation and thinning of the heart wall (Watasuki *et al.,* 2004; Dorn *et al.,* 2003). Concentric hypertrophy occurs after pressure overload and leads to reduced left ventricular volume with increased wall thickness (Barry *et al*., 2008; Watasuki *et al.,* 2004). Eccentric hypertrophy leads to cell elongation as a result

of the expansion of the sarcomeres whilst concentric hypertrophy occurs due to enlargement of the sarcomeres in parallel resulting in increased cell thickness (Watasuki *et al.,* 2004; Barry *et al.,* 2008).

1.5.2. The Fetal Gene Program

A characteristic feature observed during pathological hypertrophy is the re-establishment of the fetal gene program. This includes the upregulation of the genes; atrial and brain natriuretic peptides, α-skeletal actin and β- myosin heavy chain (MHC) (Kuwahara *et al.,* 2003; Thurm *et al.,* 2007). These genes are normally expressed during the development of the heart and are repressed in the adult myocardium (Barry *et al*., 2008). Expression of these genes allows for coordinated protein synthesis leading to increased myocyte size (Thurm *et al.,* 2007). The re-expression of these genes has been shown to lead to the downregulation of additional genes normally expressed in adult hearts such as α-MHC and Ca^{2+} - ATPase (McMullen *et al.,* 2003). The foetal gene program is not observed in physiological hypertrophy, which is another feature that differentiates pathological and physiological hypertrophy (McMullen and Sadoshima, 2005; Sadoshima and Izumo, 1997).

1.5.3. Intracellular Signalling Mechanisms involved in Cardiac Hypertrophy

There are various signalling mechanisms that are involved in hypertrophic development including; MAPK, PKC, calcineurin NFAT system, IGF-1, PI3K-AKT/PKB and mTOR. Two major factors which stimulate biochemical stress resulting in pathological hypertrophy are neurohormonal stimulation, and mechanical stress. When biochemical stress occurs, the formation of paracrine and autocrine factors, which includes angiotensin and endothelin, is important for the development of pathological CH (McMullen and Jennings, 2007). This leads to the activation of G-protein coupled receptors (GPCRs), which are responsible for the dissociation of $G_{\alpha q}$ and the activation of downstream signalling molecules such as second messengers; tyrosine kinases, protein kinase C (PKC), and the mitogen activated protein kinases (MAPK) JNK, p38 and ERK (Yamakazi *et al.,*1999; Carreno *et al.,* 2006).

Studies have shown that mechanical stress (for example physical stretching of cultured cells) leads to the activation of phospholipase C (PLC) which produces second messengers, inositol 1,4,5-triphosphate (IP3) and diacylglycerol (DAG) (Dorn *et al.,*2003). Mechanical stress could support the accessibility of membrane-associated

phospholipases to their substrate. In lipid bi-layer systems, PLC activity is increased by the elevation of pressure on the monolayer, leading to expansion of the space found between phospholipids, enabling access of phospholipases to the hydrophobic section of its substrates (Carreno *et al.,* 2006). The activation of PLC leads to the release of IP3 and DAG and the activation of PKC, which is important for the initiation of the early genes such as *c-fos* and *Egr-1* in response to mechanical stress (Dorn *et al.,* 2003; Kumuro *et al.,* 2001). PKC has different isoforms, however the isoforms found within the heart that become activated as a result of DAG or intracellular calcium are PKC α,β,δ and ε (Molkentin, 2004; Carreno *et al.,* 2006). PKC isoforms α and β are both activated in response to intracellular calcium and DAG, whilst isoforms δ and ε are also activated by DAG but not calcium (Molkentin, 2004). PKC activation results in the enhancement of hypertrophic gene expression in the heart (Molkentin, 2004).

The activation of MAPKs c-jun N-terminal kinase (JNK), p38 and extracellular signal regulated protein kinase (ERK) are involved in the stimulation of myocyte growth, environmental stress such as; oxidative stress, UV radiation and DNA damage (Force *et al.,* 1996; Sugden *et al.,* 1998; Carreno *et al.,* 2006). These are serine-threonine kinases known to phosphorylate substrates involved in growth and differentiation, including CH leading to the development of pathological hypertrophy (Carreno *et al.,* 2006). Insulin-like growth factor (IGF-1) induces CH by creating alterations in potassium channels responsible for the generation of action potential repolarisation, (Rohilla *et al.,* 2012). This occurs through the MAPK and PI3K pathways (Rohilla *et al.,* 2012; Kim *et al.,* 2008; McMullen and Izumo, 2006). IGF-1 is involved in the development and progression of physiological hypertrophy of the heart (Rohilla *et al.,* 2012). PI3Kα is another major player in CH based on studies using dominant negative PI3K transgenic mice, which resulted in the inhibition of exercise induced physiological hypertrophy when compared to the wildtype (McMullen *et al.,* 2003). PI3K is also a known heterodimer which consists of the regulatory subunits p85 and p110 found to be expressed in the heart and activated by GPCRs. PI3K (110α) is known to play a crucial role in physiological hypertrophy (McMullen *et al.,* 2003 and 2007) and also involved in the sarcolemmal recruitment of kinases AKT/PKB, these kinases work with PI3K in the progression of physiological hypertrophy (DeBosch *et al.,* 2006). Constitutive overexpression of PI3K-AKT/PKB however, leads to cardiac dysfunction as seen in several animal studies (Heinke and Molkentin, 2006, Balakumar *et al.,* 2010).

The signalling mechanism mammalian target of rapamycin (mTOR) is found downstream of PI3K-Akt and ERK signalling and regarded as a regulator of CH (Shioi *et al.*, 2003). mTOR expression is associated with the beginning of heart failure, where studies have shown that mTOR mRNA and protein levels became elevated in cardiac tissue of patients with heart failure, when compared with healthy patients (Song *et al.*, 2010). Rapamycin inhibition of mTOR attenuates pathological hypertrophy in human and animal models (Shioi *et al.*, 2003; Yang, 2007; McMullen *et al.*, 2004; Song *et al.*, 2010). Recent studies have suggested that mTOR plays a cardioprotective role during left ventricle (LV) pressure overload (Zhang *et al.*, 2010). Experiments which further supported the theory of mTOR being protective against heart injury used cardiac specific transgenic mice that overexpressed wildtype mTOR. Comparison between these and WT mice showed that transgenic mice which overexpressed mTOR were protected against LV pressure overload (Song *et al.*, 2010).

CH remains an ongoing problem not yet resolved in cardiovascular disease. Pathological hypertrophy is a highly complex event that involves different types of stimuli, intracellular signalling cascades, transcription factors, expressed genes and effectors, that when combined, allow for changes in the structure and function of an organ. Determining the pathways and mechanisms involved in hypertrophy can lead to new pharmacological and therapeutic treatments for pathological cardiac hypertrophy and heart failure.

1.6. Mitogen activated protein kinases (MAPKs) in Cardiac Function, Hypertrophy and stress in the heart

The MAPKs are cytosolic signalling proteins that have specialised phosphorylation systems that enable them to become activated in response to a wide range of external stimuli. MAPKs belong to a highly conserved family of Serine-Threonine protein kinases in the human kinome (Lee and Megency, 2005, Johnson and Hunter, 2005; Manning *et al.*, 2002) with extracellular signal-regulated kinase (ERK 1 and 2), c-Jun N-terminal kinase (JNK), p38 and ERK5 known to be the four best characterised MAPK subfamilies (Johnson *et al.*, 2002; Qi and Elion, 2005; Nishimoto and Nishida, 2006). Activation of these kinases requires dual phosphorylation of a specialised motif Threonine-X-Tyrosine (X could be amino acids Gly, Pro or Glu) within a regulatory loop (Marshall, 1994; Canagarajah *et al.*, 1997; Raingeaud *et al.*, 1995). Each of the 4 classic MAPK subfamilies are involved in a well-conserved three-tiered kinase

signalling cascade that is mediated by the upstream MAP kinase kinase kinases (MAPKKKs, MAP3Ks, MEKKs or MKKKs) as seen in **Figure 1.4**. These MAPKKKs activate the MAPK kinases (MAPKKs, MAP2Ks, MEK or MKK) that in turn activate MAPK by phosphorylation which promotes signal amplification and fidelity (**Figure 1.4)** (Chen *et al.,* 2007). The MAPKs play major roles in a broad range of physiological functions such as growth, proliferation differentiation, motility, survival and metabolism (Qi, 2005; Nishimoto and Nishida, 2006; Elion, 2005; Ferrel, 1996). The activity of the kinases are utilised to direct the function by MAPKs (Rose *et al.,* 2010). The MAPKs are further subdivided into two different groups; where prototypic ERK 1/2 is found to be mainly responsive to growth factors (such as fibroblast growth factor FBF) (Ramos, 2008; Rubinfeld and Serger, 2005), whilst JNK and p38 are known as Stress activated protein kinases (SAPKs) due to their response to physical, chemical and physiological stress (UV, osmotic shock, oxidative stress, infection and cytokines) (Kyriakis and Avruch, 2001).

MAPKs are highly specific as they have unique docking sites and binding partners (Caldwell *et al.,* 2006; Zhou *et al.,* 2006; Sharrocks *et al.,* 2000; Remenyi *et al.,* 2005; Raman *et al.,*2007). The docking sites (D sites) and their respective upstream MAPKs allows for the MAPKs to branch into different signalling pathways (Bardwell, 2006; Bardwell *et al.* 2009; Ho *et al.,* 2007; Grewal *et al.,* 2006). Following activation, the MAPKs go on to phosphorylate specific target proteins at serine and Threonine residues within a specific Pro-X-Thr/Ser-Pro motif (Serger and Krebs, 1995). Scaffolding proteins along with negative regulators and positive modulators are involved in bringing together upstream and downstream signalling components (Roux and Blenis, 2004; Nakamura *et al.,* 2003; Dahanasekaran *et al*., 2007). Determination of MAPK activation in stimulated cells is carried out by the use of negative feedback regulation of ser/thr specific, dual specific phosphatases and regulatory inhibitors (Wang *et al.,* 2007; Owens and Keyse, 2007). Although the MAPK signalling cascades are thought to be specific to each other, there is also a great degree of overlap also known as "cross-talk" between them, where different upstream activators and downstream targets can be involved with different subfamilies (Qi and Elion, 2005; Wang *et al.,* 2007). In addition to the kinase phosphorylation cascades there are several non-conanical pathways involved in MAPK activation, adding to the complexity of MAPK signal transduction (Roux and Blenis, 2004). Finally, MAPKs form complex signalling networks in response to an array of

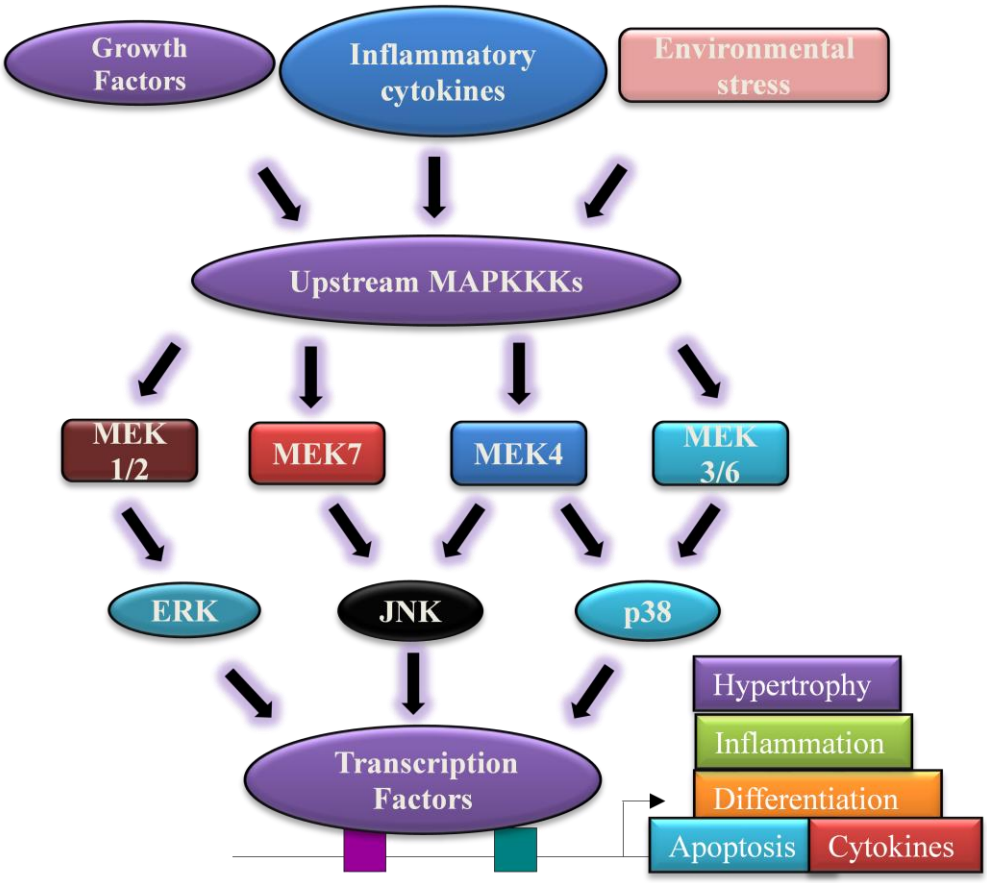

Figure 1.4: A schematic diagram of mitogen activated protein kinase (MAPK) signalling pathways ERK, JNK and p38.
The MAPKs are activated by canonical three-tiered phosphorylation events. The most popular MAPKKs are listed for each MAPK. This is a simplified diagram of the steps between the stimulus and activation of the MAPK and the biological responses as a result of regulation of transcription factors.

external stimuli and achieve specific cellular effects through a multitude of regulatory mechanisms (Rose *et al.,* 2010).

MAPKs are ubiquitously expressed, with great focus having been placed on their function in the heart for over 10 years (Sugden, 2004; Sugden and Clerk, 2006; Muslin, 2008; Petrich and Wang, 2004). Activation of MAPKs is recognised in different stages of heart disease including, hypertrophic cardiomyopathy, dilated cardiomyopathy and ischaemia/ reperfusion injury (Wang *et al.*, 2007).

1.6.1. ERK Pathway and activation

The (ERKs) are one of the most widely studied signalling pathways. In the 1980's ERK was identified because of its ability to phosphorylate the microtubule-associated protein-2 (MAP2) in 3T3-L1 adipocytes in response to insulin stimulation (Avruch, 2007, Rose *et al.,* 2010). As previously mentioned, ERK 1/2 activation occurs via a three tiered signalling cascade following extracellular stimulation by growth factors. The signalling cascade consists of Ras-Raf-MEK-ERK. Rat sarcoma (Ras) belongs to the family of small GTP-binding proteins that act as a molecular switch between tyrosine kinase receptors and downstream signal transduction machinery (Wang *et al.,* 2007). Ras recruits and activates Raf (MAPKKK) at the plasma membrane enabling its translocation from the membrane to the cytoplasm. Once Raf is activated, it phosphorylates and activate MEK 1/2 (MAP2K)1/2, which then activates ERK 1/2 by phosphorylating the Thr or Tyr residue that is located within the Thr-Glu-Tyr motif within the regulatory loop. The activation of ERK 1/2 allows for phosphorylation of downstream targets within the cytoplasm or nucleus (including transcription factors) (Raman *et al*., 2007; Rose *et al.,* 2010).

During cardiac development, the ERK 1/2 pathway plays a major contribution due to its role in growth factor signalling. FGFs are a family of growth factors that are involved in a variety of cellular processes during development which include proliferation, differentiation, cell survival, apoptosis and cell migration (Bottcher and Niehrs, 2004). Three main pathways that are mediated by the FGFs are; Ras-Raf-ERK, phospholipase C/Ca^{2+} and the PI3K/Akt pathway (Daily, 2005).

CH is an adaptative response to external stressors which include mechanical loading and oxidative stresses. As previously mentioned CH can allow the heart to function efficiently after cardiac myocyte death, but prolonged stress on the heart results in changes in gene expression, contractile dysfunction and remodelling of the heart

(Diwan and Dorn, 2007). Earlier studies using cultured myocytes initially showed correlation between Ras and hypertrophy (Fuller *et al.,* 1998; Thorburn *et al.,* 1993). A link was then discovered between Ras expression and the severity of CH given by Ras mRNA measurements from patients who suffered from hypertrophic cardiomyopathy (Kai *et al.,* 1998). There have been many genes discovered in recent times that confirm that the ERK pathway plays an important role in cardiac development and hypertrophy such as GATA4, Elk-1, SMAD 1-4 and cMyc (Reviewed in Wang *et al.,* 2007 and Rose *et al.,* 2010).

Germline mutations in genes such as tyrosine phosphatase (a key regulator for receptor tyrosine kinase mediated MAP kinase activation) SHP2 (Sarkozy *et al.,* 2004; Tartaglia *et al.,* 2001), neurofibromin-1 (NF1) (Xu *et al.,* 1990), K-Ras and sons of sevenless (SOS1 known to be an important cytoplasmic protein of Ras guanine nucleotide exchange factor) were found to cause Noonan syndrome, a condition that affects many parts of the body that results in skeletal malformations and is the major cause of congenital heart disease (Roberts *et al.,* 2006; Schubbert *et al.,* 2007). Mutations in H-Ras, K-Raf and MEK 1/2 are also involved in genetic disorders that result in cardiac defects. These genetic disorders include Costello syndrome, cardio-facio-cutaneous (CFC) and Noonan syndrome with multiple lentigines (LEOPARD) syndrome (Reviewed in Sala *et al.,* 2012). The aforementioned mutations disrupt the biochemical properties of the proteins they encode.

1.6.2. C-jun N-terminal Kinase JNK pathway and activation

The second MAPK subfamily discovered in the 1990's was JNK through its ability to phosphorylate microtubule-associated protein 2 in rat liver, after cycloheximine injection (Reviewed in Rose *et al.,* 2010; Kyriakis *et al.,* 1991). The three genes that make up this MAPK subfamily are JNK1, JNK2 and JNK3 and can generate 10 known isoforms through alternative splicing (Barr and Bogoyevitch, 2001; Davis, 2000). JNK1 and JNK2 are ubiquitously expressed, while JNK3 is found restricted to the heart, testis and brain (Davis, 2000). JNK activation occurs in response to different stimuli and is termed a stress-activated protein kinase (SAPK), where it is highly responsive to inflammatory cytokines and cellular stresses such as ischaemia-reperfusion injury, hyperosmolarity, UV radiation, oxidative stress and DNA damage (Bogoyevitch *et al.,* 1995; Clerk and Sugden, 1997; Laderoute and Webster, 1997; Karin and Gallagher, 2005). This signalling cascade begins with the upstream MAP kinase kinase kinases

(MEKKs) MEKK1, MEKK2 and MEKK3 as well as the mixed lineage kinases MLK1 and MLK2 (Weston and Davis, 2002). These MAP kinase kinase kinases go on to phosphorylate and activate the MAP kinase kinases (MAP2Ks), MKK4 and MKK7 which are involved in the signalling cascade leading to JNK activation (**Figure 1.4**). JNK is activated following the phosphorylation of a conserved Thr-Pro-Tyr motif (Sugden and Clerk, 1998).

Due to the ability of some of these substrates to shuttle between the cytoplasm and nucleus, JNK activation leads to the phosphorylation of many downstream cytoplasmic proteins as well as nuclear targets (Morrison and Davis, 2003; Sugden and Clerk, 1998). JNK plays major roles in many biological processes, such as actin reorganization, mobility, differentiation, apoptosis, proliferation and cytokine production (Bogoyevitch and Kobe, 2006; Davis, 2000). With regards to the heart, JNK activation in a stressed myocardium as a result of mechanical overload or ischaemia-reperfusion injury allows for involvement in heart related hypertrophy and remodelling of the myocardium (Rose *et al.,* 2010).

Investigation of JNK activation and involvement during cardiac hypertrophy was initially thought to be controversial based on conflicting studies with cultured neonatal cardiomyocytes and the use of transgenic mouse models (Wang *et al.*, 1998; Sadoshima *et al.,* 2002; Liang and Molkentin, 2003; Petrich *et al.,* 2004). Studies using cardiomyocytes showed an observed hypertophic phenotype, re-establishment of the foetal gene program and cellular pathology (Wang *et al.*, 1998). Whilst studies with the use of *in vivo* animal models resulted in the failed induction of CH upon JNK activation (Sadoshima *et al.,*2002). Although myocyte hypertrophy was not observed, there was re-activation of the foetal gene program in transgenic mouse models (Wang *et al.* 1998). After 10-15 minutes JNK activity is upregulated during these early stages of pressure overload and reaches maximum upregulation after 30 minutes (Petrich and Molkentin, 2004). Studies have shown that JNK activation is important for pressure overload induced hypertrophy to take place. This is based on *in vivo* studies in rats whereby dominant negative MKK4 was observed to cause disruption in JNK activation leading to inhibition of hypertrophy as a result of pressure overload (Choukroun *et al.,* 1999). Studies have shown that JNK does not become activated during volume overload in the heart (Miyamoto *et al.,* 2004, Sadoshima *et al.,* 2002). The upstream targets of the JNK signalling pathway are also implicated in CH, where inactivation of MEKK1 resulted in the attenuation of G_q induced CH and dysfunction (Minamino *et al.*, 2002). Recently

JunD, a downstream target of JNK was seen to block hypertrophy in cardiomyocytes in response to phenylephrine (a known hypertrophic drug) and pressure overload (Hilfiker-Kleiner *et al.,* 2005 and 2006). This implicates JNK as a negative regulator of hypertrophy. These studies highlight the uncertainty in regard to the function of JNK and other members of this signalling cascade with respect to their influence during CH. A possible reason for this ambiguity could be due to the different isoforms of JNK that become activated and the scaffold proteins that lead to activation of those isoforms (Wang *et al.,* 2007).

1.6.3. p38 pathway and activation in the heart

Another member of the MAPK subfamily of SAPKs is p38, which was discovered around the same time as JNK following isolation as a tyrosine phosphorylated protein in lipopolysaccharide-induced TNF-α expression (Han *et al.,* 1994). There are four different isoforms of p38 identified including p38α, p38β, p38δ and p38γ. Two of these isoforms, p38α and p38β, are ubiquitously expressed in adult tissues, whilst p38γ is found primarily expressed in skeletal and cardiac muscle (Li *et al.,* 1996) and p38δ is found in the lungs, kidneys, pancreas, testis and small intestine (Jiang *et al.,* 1996).

Activation of p38 is similar to the other members of the MAPK family, where p38 is phosphorylated and activated through a signalling cascade that involves three tiers of kinases upstream of p38 that form a canonical activation pathway. p38 is part of the MAPK subfamily of SAPKs and is highly responsive to inflammatory cytokines, UV radiation, osmotic shock, heat and pathogens (Kyriakis and Avruch, 2001; Johnson and Lapadat, 2002; Ono and Han, 2000; Waehre *et al.,* 2011). These stresses initiate the activation of this signalling cascade in combination with the MAPKKKs (MEKK1-4, TAK1 and ASK1), which go on to phosphorylate and activate the downstream MAPKKs (MKK3, MKK6 and MKK4) (Rose *et al.,* 2010). MKK3 and MKK6 do not activate the other MAPKs, which implies, that they are highly selective for p38 activation (Cuenda and Rousseau, 2007, Enslen *et al.,* 1998). The type of MKKs activated is dependent on the type and intensity of stimuli which triggers the signalling cascade (Reviewed in Risco and Cuenda, 2011). The MAPKKs go on to activate p38 through phosphorylation of the conserved Thr-Gly-Tyr motif, within the activation loop enabling conformational changes that lead to the activation of these p38 isoforms (Raingeaud *et al.,* 1996; Enslen *et al.,* 1998; Keesler *et al.,* 1998). Activation of p38 also occurs in two non-canonical MKK independent pathways which include TAB-1

autophosphorylation (Ota *et al.,* 2010; Ge *et al.,* 2002; Tanno *et al.,* 2003) and ZAP-70 which is mediated by T-cell activation that subsequently allows for phosphorylation of p38 at Thr 180, Tyr 182 and Tyr 323 (Salvador *et al.,* 2005). The involvement of p38 in many biological functions such as differentiation, apopotosis, myocyte hypertrophy and cardiac gene regulation has been observed (Thornton and Rincon, 2008; Zarubin and Han, 2005; Baines and Molkentin, 2005; Petrich and Wang, 2004; Liang and Molkentin, 2003; Engel, 2005).

Extensive studies have implicated p38 activation in cardiac development and skeletal muscle development (Keren *et al.,* 2006). A major upstream protein that allows for p38 activation is transforming growth factor-β-activated kinase 1 (TAK1). This is a member of the mitogen activated protein kinase kinase kinase (MAP3K) family that are involved in adaptive immune signalling cascades (Wang *et al.,* 2001). Bone morphogenic proteins (BMP) are essential for cardiac organogenesis during mid-gestation for development of the myocardium (Monzen *et al.,* 1999). BMPs regulate cardiac development through p38 activation via TAK-1 allowing regulation of transcription factors such as GATA-2/4, MEF2C and ATF-2 (Greenblatt *et al.,* 2010; Srivastava *et al.,* 2000 and 2006; Han and Molkentin, 2000; Monzen *et al.,* 1999, Monzen *et al.,* 2001).

The involvement of activated p38 during CH and growth has been extensively studied (Liang and Molkentin, 2003). The use of small molecule inhibitors (such as SB203580 and SB202190) or a dominant negative p38 adenovirus attenuated hypertrophic effects during *in vitro* studies in neonatal rat cardiomyocytes (Liang and Molkentin, 2003; Nemoto *et al*., 1998; Zechner *et al.,* 1997; Wang *et al.,* 1998). A study using an adenovirus in ventricular muscle cells further confirmed that p38 activation was essential for the induction of CH (Wang *et al.,* 1998). Although there are many *in vitro* studies that suggests p38 activation is essential for CH, results from *in vivo* studies showed that activation of p38 did not produce a hypertrophic response (Liao *et al.,* 2001). In addition, agonist-induced hypertrophy did not require p38 MAPK activation carried out in cardiomyocytes (Choukroun *et al.,* 1998). This was as a result of cardiomyocytes treatment with hypertrophic agonist endothelin-1 (ET-1) and inhibitor SB203580, where results showed that the inhibitor had no effect on ET-1 induced hypertrophy suggesting p38 MAPK activation may not be required for CH (Choukroun *et al.,* 1998). In concluding the role of p38 activity on promoting hypertrophy, it can be seen that substantial *in vitro* studies suggest p38 is important for a hypertrophic

response but *in vivo* studies contradict this theory. However, experimental evidence suggests that p38 activity may be important in pathological cardiac remodelling (Reviewed by Rose *et al*., 2010).

The role of p38 in cardiac protection has also been widely studied, where p38 activation was seen to have a cardio protective role during ischaemia-reperfusion injury (Martindale *et al*., 2005; Haq *et al.,* 1998; Mocanu *et al.,* 2000; Zechner *et al.,* 1997; Schulz *et al.,* 2002; reviewed in Zhao, 2013). Other studies have been shown to contradict these previous findings, where p38 activation is detrimental to the state of the myocardium during ischaemia-reperfusion injury and as a result, (Lu *et al.,* 2005; Bell *et al.,* 2008; Saurin *et al.,* 2000) the role of p38 during ischaemia-reperfusion injury remains controversial (Steenbergen C., 2002; Ping and Murphy, 2000; Bassi *et al.,* 2008, reviewed in Vassalli *et al.,* 2011). A possible reason for this contradiction could be variation in experimental conditions, methods, species and inhibitors used to carry out these studies (Rose *et al.,* 2010). During ischemia-reperfusion injury *in vitro*, kinase activity in isolated-perfused rat hearts is subjected to 20 minutes of ischemia and 15 minutes of reperfusion resulting in an approximate 2 fold increase in p38 MAPK activity (Milano *et al.,* 2007). p38 MAPK activation contributes to tissue damage through the induction of the tumour necrosis factor-alpha (TNF-α) in response to the production of hydrogen peroxide generated during reperfusion (Meldrum *et al.,* 1998). However, p38 MAPK activation is seen to have a protective role during ischemic preconditioning, where short periods of ischemia can act as a form of protection to limit cell death and contractile dysfunction (Bolli *et al.,* 2007; Steenbergen *C.*,, 2002).

As previously mentioned, there are different isoforms of p38 that are expressed in the heart. The ability for p38 to be either cardioprotective or detrimental to the myocardium is also dependent on which isoform (p38α or p38β) is activated during this condition (Sicard *et al.,* 2010; Saurin *et al.,* 2000). Recently, a study confirmed that the p38α isoform is required for ischaemic preconditioning but not the p38β isoform (Sicard *et al.,* 2010). Inhibition of p38 activity resulted in protection of the myocardium during ischaemia, with a reduction in scarring and promotion proliferation in cardiomyocytes (Engel *et al.,* 2006). Studies inhibiting the p38α isoform resulted in protection of the myocardium (Saurin *et al.,*2000), whilst p38β was discovered to help facilitate cardio-protection through the phosphorylation of small heat shock proteins (Hsp27) during ischaemic preconditioning (Rouse *et al.,* 1994; Li *et al.,* 2008; Clements *et al.,* 2011). Hsp27 is also involved in the stabilization of actin cytoskeleton. During ischaemia

reperfusion injury p38 was seen to activate a small heat shock protein that can promote cardiac protection (Martindale *et al.*, 2005)

The role of p38 in cardiac protection still remains controversial, and the mechanisms by which different isoforms of p38 are activated within the heart are still a mystery. Therefore the use of p38 as a therapeutic target during ischemic injury still needs to be further assessed.

In summary, the involvement of MAPK signalling in the heart has provided some insight into the members of the MAPK family that play clear roles in cardiac regulation (Wang *et al.,* 2007). The MAPK family has many isoforms, each of which have various substrate affinities and functions. Therefore, pin-pointing the specific isoforms which may contribute to cardioprotection function, remodelling and adverse affects on the myocardium could allow for the development of new therapeutic targets in diseases and conditions of the heart. The advancement in technology, along with a combination of molecular and genetic approaches specific model organisms (mouse to human) may allow for greater insight and potentially reduced contradiction amongst studies. There is still more to be uncovered about MAPKs and their role in development, function and pathogenesis within the heart. The MAPKs not only play major roles within the heart but are also highly involved in skeletal muscle development and regulation where they associate with sarcomeric proteins which are involved in muscle movement, growth and skeletal muscle differentiation.

1.7. Sarcomeric Proteins, the Actin cytoskeleton and actin binding proteins (ABPs)

1.7.1. The Sarcomere and sarcomeric proteins

Striated muscle cells comprising both skeletal and cardiac are made up of sarcomeres (Sanger *et al.,* 2010). Sarcomeres are large, highly ordered and known for their key roles as a contractile apparatus. Made up of a parallel array of thick and thin filaments, these are required to form the molecular motor responsible in powering cardiac contraction (Steinberg; 2013). The thin and thick filaments are actin and myosin respectively with approximate lengths of 7 nm in diameter for actin and 15 nm in diameter for myosin. The thin filaments are made up of three different types of proteins; actin which is comprised of 2 helical strands of actin monomers, tropomyosin molecule (Tm) that associates with actin to form a continuous long strand from end to end and the troponin complex (cTn, cTnI, Tm that binds to cTnT subunit) which associates with tropomyosin (Steinberg ; 2013). Within the sarcomere, there are 6-7 actin molecules per

tropomyosin present. While the thick filaments are comprised of 2 molecules of myosin heavy chain (MHC) complexed with 2 molecules of myosin light chain and 2 molecules of the regulatory light chain (MLC-1 and MLC-2) (Steinberg ; 2013). Actin and myosin are regulators of muscle contraction within the sarcomere and the motor filaments have repetitive patterns throughout of overlapping cytoskeleton (Gautel, 2011).

The sarcomere is approximately 2.5 μm long and made up of many components which include the z-disk (or z-line), A-band, I-band and M-line regions. The z-disk is located at the end of each sarcomere and attached to actin filaments at their plus ends where α-actinin is also present (Figure 1.5). The A-band is the dark band (because it is anisotropic) and the I-band is the light band (because it is isotropic in polarized light) within the sarcomere (Cooper, J.A., 2002; Clark *et al.,* 2002). These bands correspond to the presence or absence of myosin filaments, where the I-band contains only thin filaments (actin) while the A-band contains thick filaments (myosin) (Clark *et al.,* 2002). Myosin and actin overlap is seen in the peripheral regions of the A-band (**Figure 1.5)** (Clark *et al.,* 2002). The actin filaments are attached to the z-disk via their plus ends where α-actinin is also present. Two additional proteins that play keys roles in muscle elasticity, stretch response and sarcomeric organizationd are titin and nebulin (Wang, 1996, Hoshijima, 2006; Clark and Braggs, 1995).

Titin (also known as connectin) is the largest protein in the human body, it is located within the sarcomere with a molecular weight between 3000-3700 kDa (Reviewed by Linke and Kruger, 2011, Meyer and Wright, 2013). In the sarcomere, titin is thought to be a major player in sarcomeric assembly (Ehler and Gautel, 2008), a molecular spring (Tskhovrebova and Trinick, 2010, Maruyama *et al.,* 1985, Soteriou *et al.,* 1993) within muscle cells and more recently a regulatory protein involved in the many signalling pathways within cardiomyocytes that control hypertrophic gene regulation (Linke and Kruger, 2010 and 2011). The N-terminus of titin is embedded in the z-disk, while the c-terminus is found within the M-line of the sarcomere, stretching over half the length of the sarcomere where the elastic region is found within the I-band and myosin binding region found within the A-band as observed in figure 1.5 (Labeit *et al.,* 1992, Labeit and Kolmerer, 1995; Trinick, 1996; Furst *et al.,* 1988 Maruyama *et al.,* 1985).

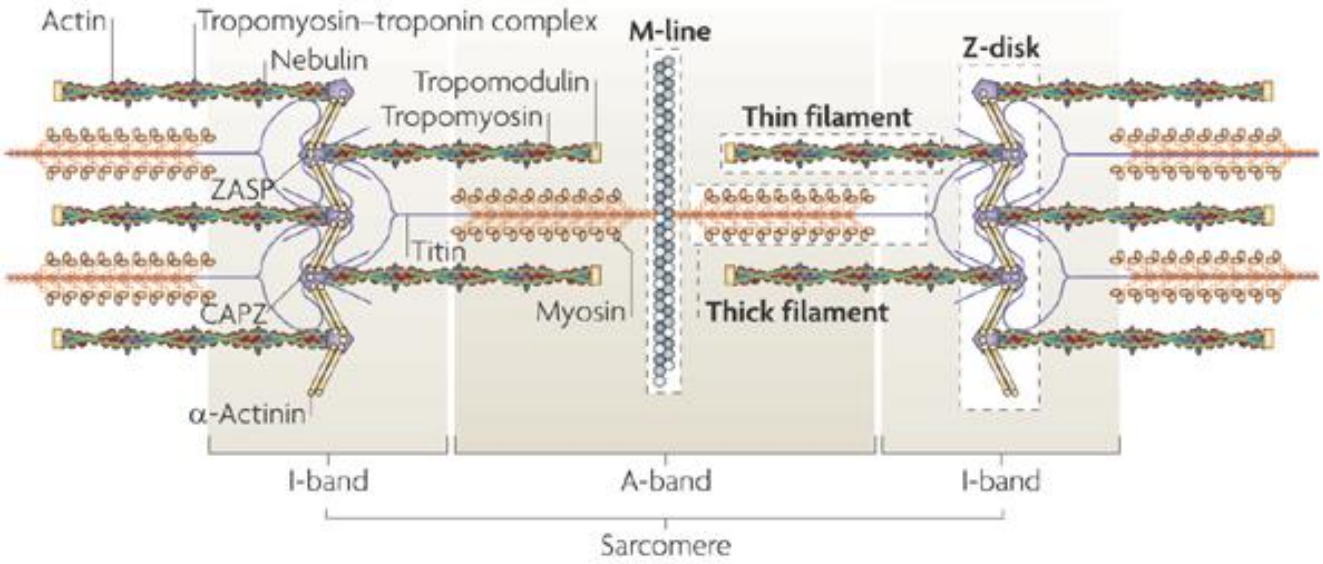

Figure 1.5: Organization of the Sarcomere
The sarcomere is composed of two main filaments; the thin and thick filaments.The thin filaments are crosslinked by actin and anchored by the z-disk. Proteins found within the thin filaments are actin, tropomyosin and the troponin complex. The tropomyosin –troponin complex play an important role in interacting with the thick filament, myosin, which is needed for muscle contract by interacting with actin. Nebulin is also found within the thin filaments and is known to be a regulator protein in thin filament lengthening. Also present are the capping proteins CAPZ and tropomodulin. The thick filaments are located along the M-line and span the A-band region as well. A protein found in the M-line is titin, one of the largest proteins of the sarcomere which spands from the M-line to the z-disk (Figure taken from Sparrow and Schock, 2009).

Titin has phosphorylation sites that are responsible for signalling in the sarcomere. These are found in various areas of titin, which spans across the sarcoemere of the I-band, M-line and z-disk and thought to be a major regulator of myocyte signalling (Reviewed in Kruger and Linke, 2011 and Ahmed and Lindsey, 2009). Since the I-band region of titin is flexible this functions as a spring to determine passive stiffness, a stress sensor and regulation of hypertrophic genes (Reviewed in Kruger and Linke 2010, Ahmed and Lindsey, 2009). Different proteins interact with titin based on the location within the sarcomere. In the I-band region actin, myopalladin and DRAL/FHL-2 interact with titin, while muscle specific RING-finger proteins (MURFs), calmodulin, DRAL/FHL-2 interact with titin in the M-line and lastly within the z-disk are telethonin/T-cap, α-actinin and obscurin are common proteins that interact with titin (Lange *et al.,* 2006). These protein interactions are necessary for communication along the sarcomere in order to allow for genes responsible for muscle expression, development and contractile function.

Nebulin is another giant filamentous protein found in the sarcomere with a molecular weight between 600-900 kDa. Located along the entire length of the thin filament (I-band), nebulin is anchored within the z-disk region by its C-terminus and the N-terminus extends outward towards the centre of the sarcomere (Reviewed in Pappas *et al.,* 2010, Wright *et al.,* 1993). For years, nebulin has been implicated as a key player in the regulation of thin filament lengthening based on studies which used nebulin knockout (KO) mouse models (Witt *et al.,* 2006). The ability of actin and myosin to slide pass each other to facilitate contraction of skeletal muscle is highly important. Actin must be of an appropriate length to facilitate this process, which is regulated by nebulin that acts in a stabilization mechanism (reviewed in Pappas *et al.,* 2010, Georgio *et al.,* 1995, Labeit *et al.,* 2011, Horowists, 2006). F-actin lengthening is regulated by nebulin through interactions with the well-known F-capping protein, tropomodulin (a member of the Tmod gene family) at the N-terminus and the barbed end capping protein CapZ, interacts with nebulin at the z-disk (Gregorio *et al.,* 1995, McElhinny *et al.,* 2001, Pappas *et al.,* 2008). These capping proteins are important for inhibiting actin polymerization and depolymerisation at the filament ends, which are essential for actin assembly and regulation (Gregorio *et al.,* 1995, Mudry *et al.,* 2003). More recently, nebulin KO mouse studies also showed that nebulin is involved in the regulation of muscle contraction (Reviewed in Ottenheijm *et al.,* 2010, Labeit *et al.,* 2010, Ottenheijm *et al.,* 2010, Bang *et al.,* 2009, Chandra *et al.,* 2009).

The filamentous proteins; titin, nebulin and actin all associate with the z-disk, whereas myosin filaments, do not directly associate with the z-disk (Frank and Frey, 2011, reviewed in Clark *et al.,* 2002). The z-disk acts as an anchorage to three of the four main sarcomeric proteins (Reviewed in Clark *et al.,* 2002). The z-disk has actin filaments present which are crosslinked by α-actinin, where they are aligned in an anti-parallel manner and thought to act like the backbone as seen in figure 1.5 (Djinovic-Carugo *et al.,*1999, Frank and Frey, 2011, Gautel S., 2011). Over the last 10 years the role/function of the z-disk has become more defined as it serves as the hub for signalling within the sarcomere, that includes signalling, mechanosensation, mechanotransduction, cell survival and an anchorage for the major cytoskeletal proteins present.

Signalling of the z-disk and M-line, where information is relayed between each other for the control of gene expression, protein synthesis and protein degradation plays a vital role in the function of the sarcomere (Gautel S., 2011, Knoll *et al.,* 2011). A few of the z-disk related proteins that are involved in the many signalling processes within the sarcomere are the LIM domain containing proteins such as muscle LIM protein (MLP), cypher, myotilin, telethonin, zyxin, α-actinin, MURFs and MAPKs (Review in Knoll *et al.,* 2011). Some of the aforementioned proteins are able to shuttle between the z-disk and other subcellular locations within the cell, such as the nucleus and cytoskeleton in order to transmit signals (Reviewed in Frank and Frey, 2011).

There are many transcription factors present within the z-disk. An examples of the z-disk and involvement in nuclear activity is the pathways that involves NFAT, a known target of phosphatase calcineurin involved in the development of maladaptive myocardial hypertrophy (Gautel S., 2008, Knoll *et al.,* 2011). Another shuttling z-disk protein that can shuttle between the z-disk and nucleus is MLP. This protein interacts not only with phosphatase calcineurin, but also telethonin, α-actinin and zyxin (Heineke *et al.,* 2005, Knoll *et al.,* 2010, Knoll *et al.,* 2002, Kong *et al.,* 1997, Louis *et al.,* 1997). MLP is found within the nucleus where it interacts with MyoD, myogenin and MRF4, these are all transcriptional factors responsible for myogenesis (Knoll *et al.,* 2011, Kong *et al.,* 1997).

The z-disk was initially thought to only play a structural role within the sarcomere, supporting the major proteins important for mechanical stability. However, in recent years proteins within the z-disk are not restricted to interacting with each other, but also associate with other proteins located outside the z-disk region within the sarcomere and

subcellular locations within cells. This relationship allows for communication between the sarcomere and nucleus via cytoskeletal components to control gene expression and signalling pathways. There is still more to be determined about the role of z-disk and z-disk related proteins.

1.7.2. The Actin Cytoskeleton and Actin Binding Proteins ABPs

The eukaryotic cytoskeleton is composed of actin microfilaments, microtubules and intermediate filaments (dos Remedios *et al.,* 2005). The actin cytoskeleton functions in contractility, motility, membrane trafficking and cell division (Winder and Ayscough, 2005, Carlier *et al.,* 2005, Chen *et al.,* 2000). Actin assembly and disassembly in response to extracellular signals, plays a fundamental role in some of these processes (Chen *et al.,* 2000).

Actin exists in two distinct forms: a monomeric form called G-actin and a polar, filamentous form known as F-actin, where each unit binds to either ATP or ADP (Chen *et al.,* 2000, Grummt I., 2006, Barbara *et al.,* 2000, Winder and Ayscough, 2005). The minimal concentration of G-actin required to initiate polymerization (actin assembly), is known as the critical concentration (Cc), which is lower for ATP-actin than ADP-actin and allows for cells to maintain their structure and also movement (Carlier and Pantaloni, 1997, Chen *et al.,* 2000). Above the critical concentration of G-actin, polymerization occurs which formation of F-actin, however below the critical concentration of G-actin, results in depolymerisation (Chen *et al.,* 2000). ATP hydrolysis allows for directional actin filament growth which is known as "treadmilling", a known driving force behind the mobility and stability of the cell. The filaments have a pointed end which is slow growing (minus) end with a higher Cc, while the barbed-end of the filament is known as the fast-growing (plus) end with a lower Cc. The term steady-state is used when the net assembly of subunits at the plus end is equal to the minus end. This process is called actin-treadmilling, which allows for equilibrium between the amount of G-actin and F-actin formed (Winder and Ayscough, 2005, Chen *et al.,* 2000, Cooper and Schafer, 2000). In the cytoplasm, changes in cytoskeletal actin dynamics or the assembly transcriptional regulatory complexes have shown implication in the regulation of gene transcription within the nucleus (Sotiropoulos *et al.,* 1999, Grummt I., 2006).

The function of the actin cytoskeleton in skeletal muscle is as a structural scaffold linking the sarcomere and cell membrane. There are many proteins that associate with

the different forms of actin, these proteins are known as actin binding proteins (ABPs). There are different classes of ABPs that aid in controlling actin bundling, nucleation, filament capping, fragmentation and the regulation of monomers within the cytoplasm of the cell (Reviewed in dos Remedios *et al.,* 2003). In recent times the actin has been implicated as a major regulator in transcription (Zheng *et al.,* 2009). There are some ABPs that are capable of shuttling between the cytoplasm and the nucleus. This provides a link between structure and gene regulation within cells (Reviewed in Zheng *et al.,* 2009).

A relatively new ABP is the striated muscle activator of Rho signalling (STARS) or Myocyte stress 1 protein (MS1) (Arai *et al.,* 2002, Mahadeva *et al.,* 2002). This muscle specific protein was identified to be involved in a mechanism with RhoA activation and actin polymerisation (Arai *et al.,* 2002, Kuwahara *et al.,* 2005). The link between actin treadmilling and transcriptional regulation is via MS1 upregulation. After MS1 binds to F-actin, this results in the release of another ABP, myocardin related transcription factor (MRTF-A), that interacts with G-actin (Zheng *et al.,* 2009). As the levels of G-actin decrease within the cytoplasm, this allows for the release of MRTF-A to shuttle from the cytoplasm and translocate to the nucleus where it activates the serum response factor (SRF) (Kuwahara *et al.,* 2005). MS1 is implicated in providing a link between extracellular stress signals and transcriptional regulation.

1.8. Myocyte Stress Protein (MS1)/ Striated Muscle activator of Rho-signalling (STARS)

1.8.1. Discovery of MS1

Myocyte stress -1 (MS1) protein or Striated muscle activator of Rho signalling (STARS), was discovered by two independent labs in 2002 (Mahadeva *et al*., 2002 and Arai *et al.,*2002), the human gene is known as ABRA (Actin Binding Rho Activator). MS1 protein was confirmed to be expressed in muscle as a result of cDNA screening for genes expressed in the heart with the use of mouse embryos (Arai *et al.,* 2002). A novel method known as molecular indexing which was used to quantitatively identify genes expressed, to analyse MS1. This showed strong evidence that during LVH rat models, mRNA levels of MS1 increased significantly in rat hearts as a result of pressure overload induced ischaemia/ reperfusion injury which was caused as a result of aortic banding of the hearts, after one hour (Mahadheva *et al.,* 2002).

Studies carried out by Arai *et al.,* 2002 confirmed that MS1 was involved in the Rho signalling pathway, which leads to the transcriptional activation of the serum response factor, hence the name Striated muscle activator of Rho signalling (STARS). Immunostaining methods, using lysates from adult mouse hearts and COS cells transfected with a MS1 expression vector, confirmed that MS1 was muscle specific, with a confirmed size of 45 kDa based on western blot analysis. Immunofluorescence studies to determine the localisation of MS1 confirmed α-actinin and MS1 protein co-localise with each other. MS1 is found to be localized specifically in the I-band and between the z-lines and to a lesser extent in the M-line region of the sacromere of cardiomyocytes, which confirms that the protein is muscle specific and binds to actin (Arai *et al.,* 2002).

MS1 is thought to be found mainly in the cytosol, but recent studies have confirmed its presence in the nucleus using human skeletal muscle tissue (Wallace *et al.,* 2012), non-muscle COS cells and stressed rat endothelial cells when MS1 was overexpressed in studies carried out by Triodl et al (Arai *et al.,* 2002 and Triodl *et al.,* 2009). Although MS1 has two different names, throughout this thesis it will be referred to as MS1.

1.8.2. Gene and Structure of MS1

The gene which encodes human ABRA is located on chromosome 8 on position 8q23.1 with accession number NP_631905 (Arai *et al.,* 2002). Rat MS1 was used throughout the project, and the rat gene is located on chromosome 7 on position 7q31, while the gene for porcine (pig) MS1 is located on chromosome 4 on position 4q13 (Peng *et al*., 2008). MS1 is an actin binding, muscle specific protein found expressed predominantly in the cardiac muscle, as well as the skeletal muscle and smooth muscle (Mahadeva *et al.,* 2002; Arai *et al.,* 2002; Triodl *et al*., 2009).

Investigation of MS1 with the use of Bioinformatics studies revealed that MS1 has many homologs present in eukaryotes, with the full length of MS1 being 375 amino acid residues. The gene of MS1 although expressed in different species might not necessarily have the same function in each species. The N-terminus of the MS1 protein sequence is not as highly conserved as the C-terminus of MS1 in different species which is observed in **Figure 1.6 (**Uniprot). Initial studies attempted to express full length MS1 in *Escherichia coli* (*E. coli)* were unsuccessful as a result of severe protein

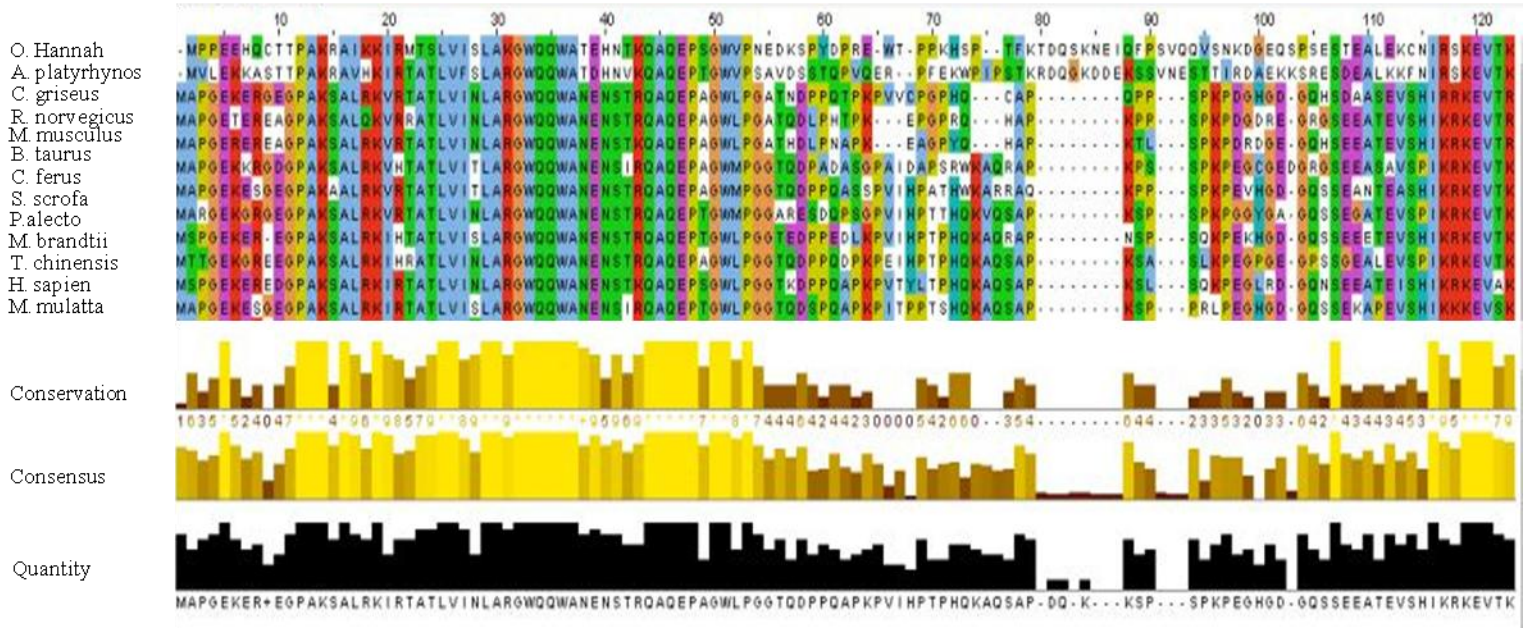

Figure 1.6: An alignment of MS1 amongst 13 different species where the C-terminus is most conserved.
The aligned species are Ophiophagus hannah – king cobra Accession number ERE66548.1, Ana platyrhynchos - Bird accession number EOA96796.1, Cricetulus griseus – chinese hamster (accession number ERE52450.1), Rattus norvegicus – Brown rat (accession number NP787038.1), Mus musculus - mouse (accession number AAM28877.1), Bos taurus – Taurine cattle (NP001179163.1), Camelus ferus – Bactrian camel (accession number EPY77909), Sus scrofa – wild boar (accession number NP001129432.1), Pteropus alecto – Black flying fox bat (accession number ELK08610.1), Myotis brandtii – Brandt's bat (accession number EPQ05312.1), Tupaia chinensis – chinese tree shrew (accession number XP005072681), Homo sapien - Human (AAM27268) and Macaca mulatta – Rhesus monkey (accession number EHH28705)

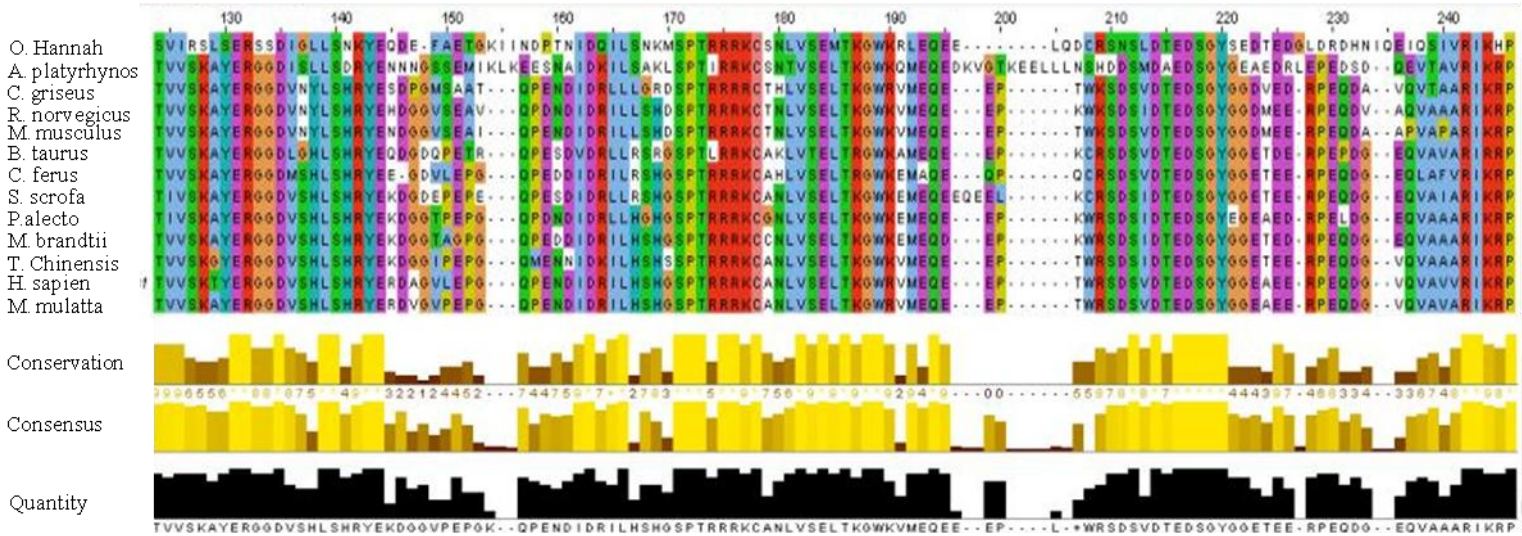

Figure 1.6: Continued.

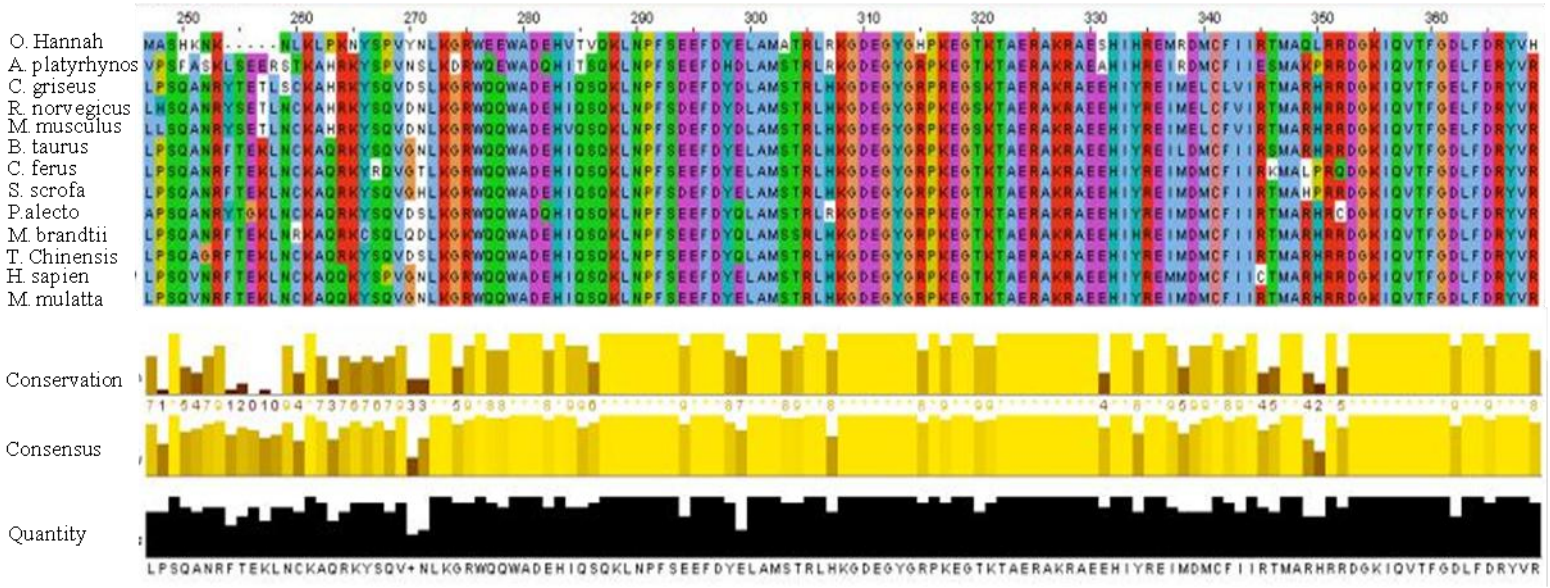

Figure 1.6: Continued.

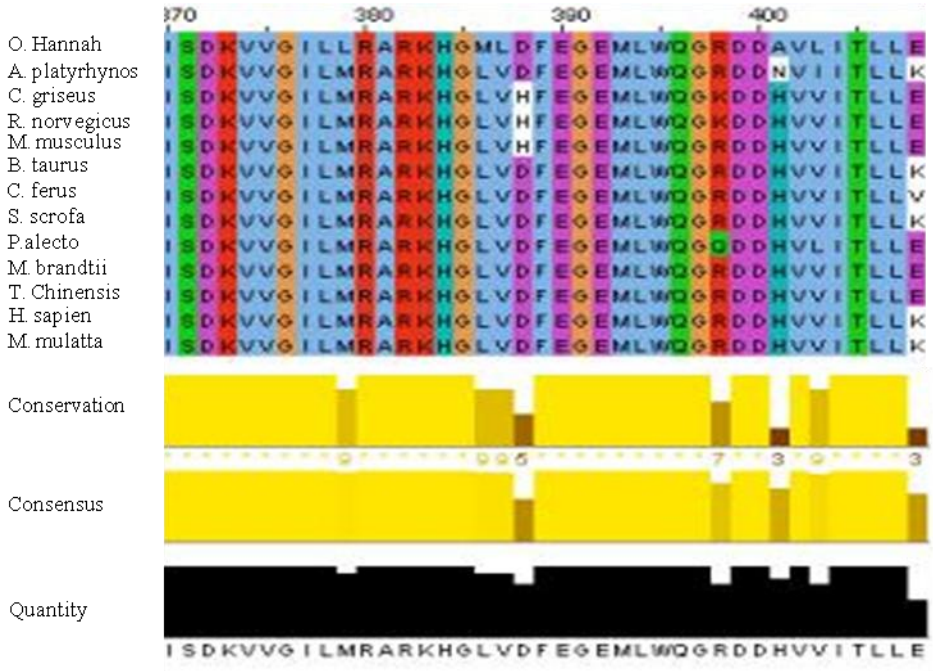

Figure 1.6: Continued.

degradation upon refolding (Fogl *et. al.*, 2011). The degradation of full length MS1 (45 kDa), led to the investigation of putative domains as a result of consistent, well defined bands of smaller sizes between 10 – 20 kDa when protein fragments were expressed (Fogl *et al.*,2011).

Bioinformatics and other computational programs, such as GlobPlot, RONN and Poodle methods were used to investigate the domains of MS1which confirmed that 4 domains are present that overlap each other. These were; MSD1 which covers 2-118 amino acids, MSD2 covers 40 – 196 amino acids and are known as the N-terminal domains, while ABD1 covers 193-296 amino acids and ABD2 which covers 294 – 375 amino acid residues are the C-terminal domains of MS1 (Fogl *et al.*, 2011). The figure below shows the domains of MS1 and where they are located along the full length of MS1 (**Figure 1.7**). There are two actin binding sites located at the C-terminus of the protein in two different domains; ABD1 and ABD2 (Fogl *et al.*,2011). ABD2 and ABD1 are the two well structured domains of the four domains of MS1 and both are located at the C-terminus.

1.8.3. Binding partners of MS1

1.8.3.1. MS1 binds to actin

As previously mentioned, MS1 was discovered to bind to actin as a result of a series of immunofluorescence studies that confirmed co-localisation between MS1 and α-actinin at the M-line and Z-lines to sarcomeric structures, that can be seen in **Figure 1.8A** (Arai *et al.*, 2002). The actin binding region of MS1 was mapped by co-immunoprecipitation experiments. The ability of actin to co-precipitate with wild-type MS1, or C-terminal deletions and point mutations thereof were compared (Arai *et al.*, 2002). The actin binding region was observed to be presemt in two regions of the C-terminus between 234-279 aa and 346-375 aa, as deletions of these areas resulted in loss of interaction with actin. These separate regions were thought to bind actin in a co-dependent manner (Arai *et al.*, 2002). Domain hunting tools were able to identify putatative domains found within full length MS1. Recent literature showed through co-sedimentation assays as well as quantitative fluorescence F-actin binding assays that there are fragments with separate actin binding sites located on two entirely different domains, which were named ABD1 (193-296 aa) and ABD2 (294-375 aa) and both are capable of binding F-actin independently (Fogl *et al.*, 2011). Initially, studies by Arai *et al.*, 2002 used a longer fragment (193-375 aa) and thought that actin binding sites

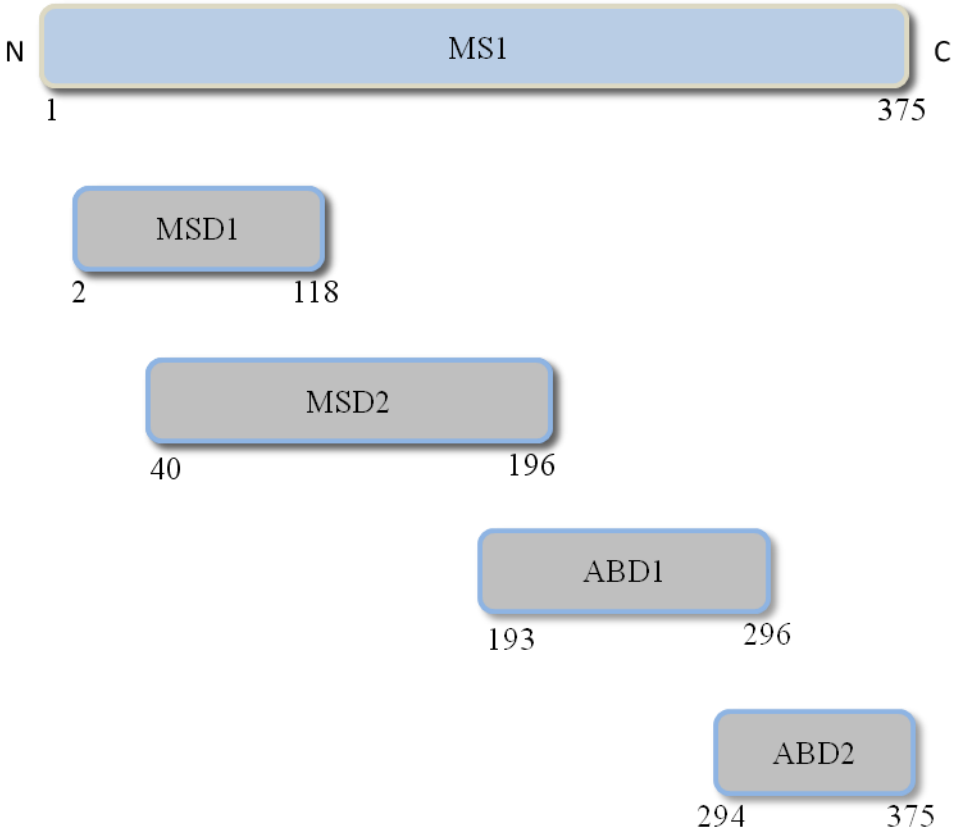

Figure 1.7: Domains of full-length MS1
Positions of the proposed domains found by Domain X. Adapted from Fogl,C; "Structure and Function of the cardiac stress protein MS1" (2011)

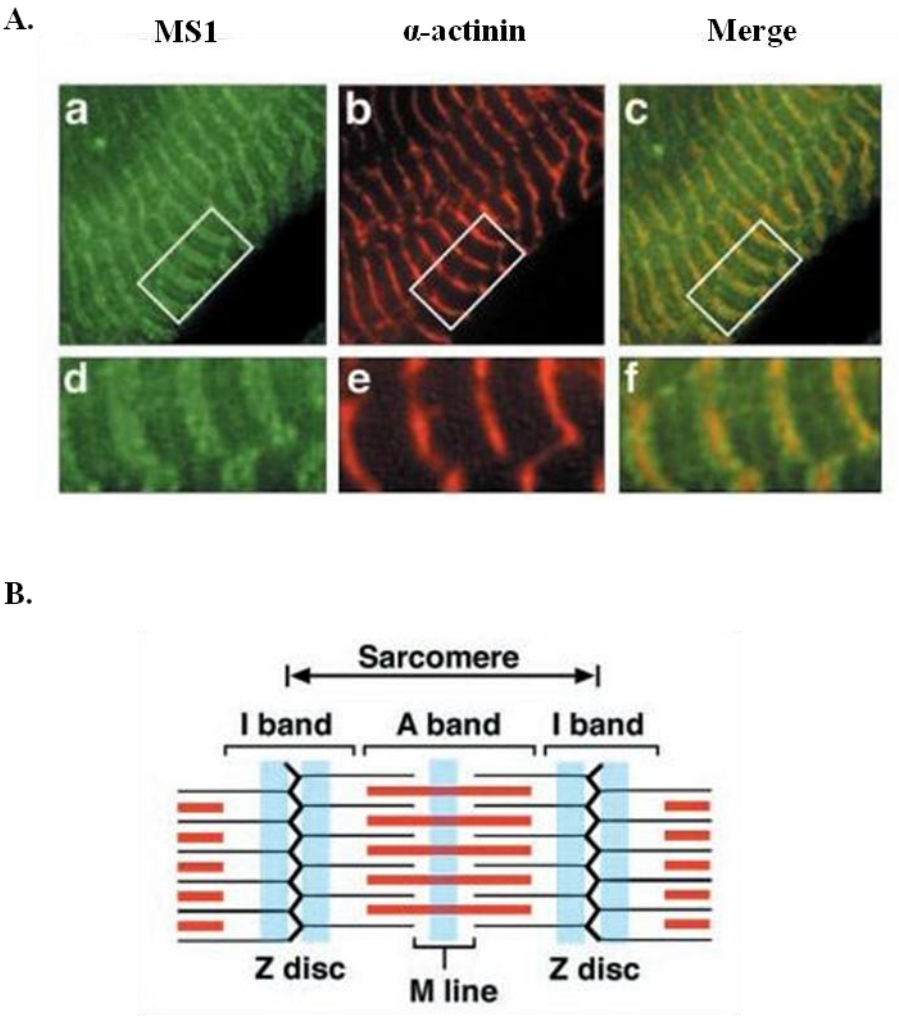

Figure 1.8: Identification of MS1 in the sarcomere
A Immunofluorescence staining of the sarcomere where MS1 is the green fluorescence and α-actinin is stained red shows colocalisation on the I-band and M-line of rat myocytes.
B Schematic diagram illustrating the localization of MS1 and its relation to actin and myosin. Actin is represented by the black horizontal lines and myosin is depicted in red. Blue vertical lines show where MS1 co-localises. (Figure taken from Arai *et. al., 2002.)*

within MS1 were co-dependent for binding to occur. This hypothesis was rejected as the individual fragments established from domain hunting, showed the binding region is located within two separate domains as previously mentioned (Fogl *et al*., 2011). Using MS1 fragments it was shown that ABD1 cosedimented more with F-actin than ABD2; but no cosedimentation with F-actin was observed using fragments derived frim the with N-termimal domains. ABD2 is folded and well structured, while ABD1 is less structurally defined, but ABD1 binds to actin with a higher affinity than ABD2 (Fogl *et al.,* 2011). This could mean that although ABD2 can bind actin, this specific site to be involved in other functions, owing to the role of MS1 in the transcriptional activation of SRF (serum response factor) and the localisation of MS1 within the z-disk of the sarcomere (Kuwahara *et al.,* 2005; Arai *et al.,* 2002).

1.8.3.2. MS1 Binds to Actin Binding LIM (ABLIM) Proteins

MS1 is also known to bind actin binding Lim proteins, ABLIM 2 and 3, observed as a result of yeast two hybrid screening with the use of a skeletal muscle cDNA library and MS1 C-terminus covering 234-375 aa as the bait protein (Barrientos *et al.,* 2007). ABLIM-2 and ABLIM-3 are new isoforms of ABLIM that have a unique characteristic, as they all have four LIM domains. Each LIM domain has a consensus sequence of $CX_2CX_{16-23}HX_2CX_2CX_2CX_{16-21}CX_2$(C/H/D) where X is denoted as any amino acid (**Figure 1.9)** (Schmeichel and Beckerle, 1994). The LIM domains consist of two tandem zinc fingers which are known to be cysteine rich and separated by two residues. The zinc binding residues (1-4) co-ordinate the first Zn-finger and residues 5-8 co-ordinate the second Zn finger ion as seen in **Figure 1.9** (Michelsen *et al.,* 1994). LIM domains have a linker region attached, followed by a 74 aa vilin head domain (Kadrmas and Beckerle 2004). ABLIM- 2 is located primarily in the skeletal muscle and found in the brain, spleen and kidney at lower levels, while ABLIM-3 is found mainly in the heart but also expressed in the liver and lungs (Barrientos *et al.,* 2007).

Investigating the localisation and expression of ABLIM proteins by immunofluorescence, showed that ABLIM-2 has the same co-localisation pattern as MS1, where it is seen to overlap with α-actinin staining in mouse skeletal muscle tissue. The same overlap was also observed with MS1 staining with α-actinin (Barrientos *et al.,* 2007). COS cells transfected with MS1 and either ABLIM-2 or ABLIM-3 were used in co-immunoprecipitation experiments, which showed MS1 co-precipitated with all of the ABLIM proteins (Barrientos *et al.,* 2007). *In vivo* immunofluorescence experiments in

C2C12 cells co-transfected with MS1 and ABLIM2 further supported what was seen *in vitro,* as co-localisation between ABLIM-2 and MS1 was observed (Barrientos *et al.,* 2007). The localisation of ABLIM within the skeletal and cardiac muscle explains the ability of ABLIM to bind proteins found within the z-disk of the sarcomere. The z-disk is known to play a major role in sensing biomechanical stress and leads to signalling which is directed to the nucleus (Frey *et al.,* 2004). The interaction of ABLIM and MS1 was thought to be involved in MS1 dependent transcriptional activation of SRF to assist binding of MS1 to the sarcomere (Barrientos *et al*., 2007).

1.8.4. Transcriptional Regulators of MS1

There is limited information on the molecular mechanism of how MS1 can be able to sense and respond to stress signals within the heart or the skeletal muscle. Analysis of the MS1 promoter identified target sequences that are present for many transcription factors, known to impact on muscle growth, differentiation, arteriogenesis and myogenic proliferation. The list of transcriptional regulators of MS1 are; MEF2, MyoD, ERRα, GATA4 and SRF that will be discussed in detail in this section.

1.8.4.1. MEF2 as a Transcriptional Regulator of MS1

Analysis of the promoter region of MS1 identified essential binding sites for myocyte enhancer factor-2 (MEF2). MEF2 is a member of the MADs box family which are known for their roles as transcription factors that are involved in the regulation of many genes that have a vast amount of biological functions (Shore and Sharrocks; 1995). As a result of stress placed on the heart, cardiac specific expression of MS1 has been hypothesized to be controlled through binding of myocyte enhancer factor 2 (MEF2). MEF2 is known to have DNA binding activity located at the A/T rich element found in promoters of genes involved in skeletal and cardiac muscle development, as well as activation of early stage hypertrophic genes (Wang *et al.,* 2002 and 2003; Black and Crips., 2010). Investigation of the promoter region of MS1 identified two regions, M1 and M2, that resembled the 10bp consensus sequence for MEF2 binding which is CTA(T/A)AAATAG/A (Kuwahara *et al.,*2007).

Regulation of MS1 expression was investigated with transgenic mouse embryo carrying -1581 MS1 LacZ transgene and Luciferase reporter assays with the use of the proximal region of the MS1 promoter with or without deletions of the M1 or M2 regions. These promoters were either normal or mutated and transfected in cardiomyocytes or non-

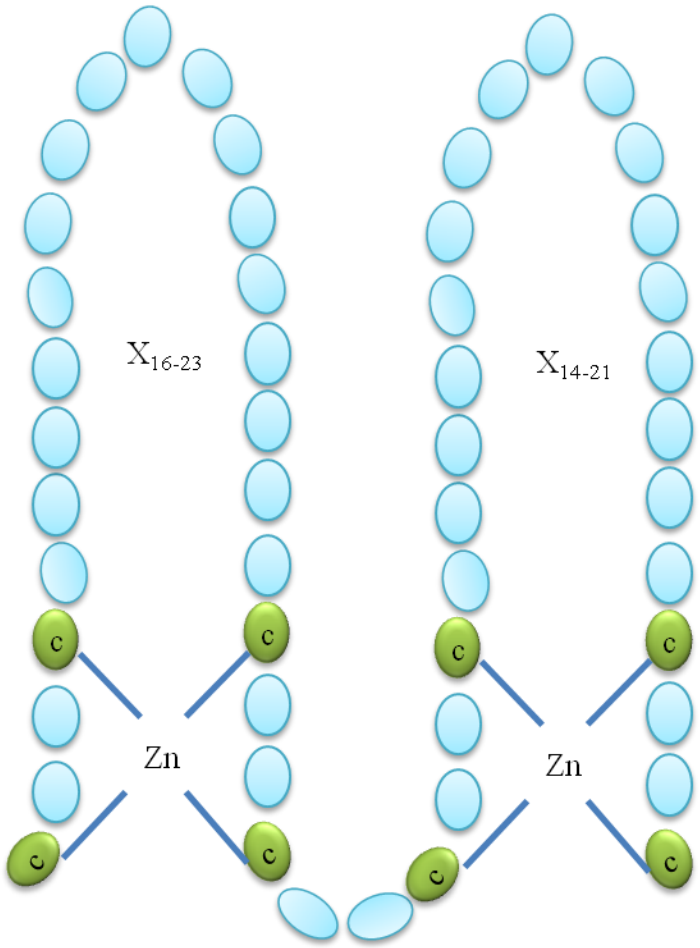

Figure 1.9: Representation of the conserved LIM domain.
The two zinc binding regions are co-ordinated by the presence of cysteine. Where cysteine 1-4 co-ordinates the first Zn, while 5-8 co-ordinates the second Zn finger (cysteines are represented by green colour). X-denotes any amino acid. The separation between cysteines 2-3 and 6-7 by amino acids vary.

cardiac cells (Kuwahara *et al*., 2007). The activity of the promoter region of MS1 was diminished when deletions of either, M1 or M2 region were made, as these particular regions were identified to be involved in MS1 expression (Kuwahara *et al*., 2007). Microarray studies were used to measure the difference of MS1 expression between mouse embryos that were either MEF2C-null embryos or wildtype. Expression profiles confirmed that MEF2C mutants had significantly reduced expression of MS1 compared to the wildtype (Kuwahara *et al.,* 2005). This study demonstrated that activation of wild-type MS1 promoter by MEF2C was 40-fold higher than that of promoter constructs with mutations in the M1and M2 binding regions (Kuwahara *et al.,* 2007).

1.8.4.2. MyoD as a Transcriptional Regulator of MS1 during Myogenic Differentiation

Myogenic differentiation is a highly specialised programme used to generate skeletal muscle. The initial stage of this process, is the formation of mitotically quiescent myoblasts from the mesoderm as seen in **Figure 1.10** (Jiang and Balik., 2013). Activation of myoblasts occurs as a result of exercise, injury or pathological signals that cause myoblasts to proliferate in the muscle (Jiang and Balik., 2013). After proliferation cells exit the cell cycle, differentiate and fuse to the pre-existing myofibrils as seen in **Figure 1.10** (L'honore *et al.,* 2007; Jiang and Balik., 2013). MyoD is among a special group of transcription factors that are able to facilitate myogenic differentiation. MyoD protein is from a family of myogenic regulatory factors (MRFs) which belong to a group that contains a basic helix-loop-helix (bHLH) motif required for heterodimerisation with E-proteins of transcription factors (Tapscott., 2005). These proteins are DNA-binding and act via a highly specific sequence within DNA known as an E-box consensus sequence [CANNTG] found within the promoter regions of most skeletal-muscle specific genes (Berkes and Tapscott., 2005; Tapscott., 2005; Blackwell and Weintraub., 1990).

Studies were carried out to analyse the upstream 5' sequence of the MS1 gene in order to indentify myogenic transcription factor binding motifs (Ounzain *et al.,*2008). Analysis of the proximal promoter identified two E-box sequences (-253/-247 bp and -221/-215 bp) located within evolutionarily conserved regions amongst species. MS1 expression was assessed in C2C12 myoblast cells from the leg muscle of a mouse which differentiate to form myotubes when serum starved. These cells were transfected with

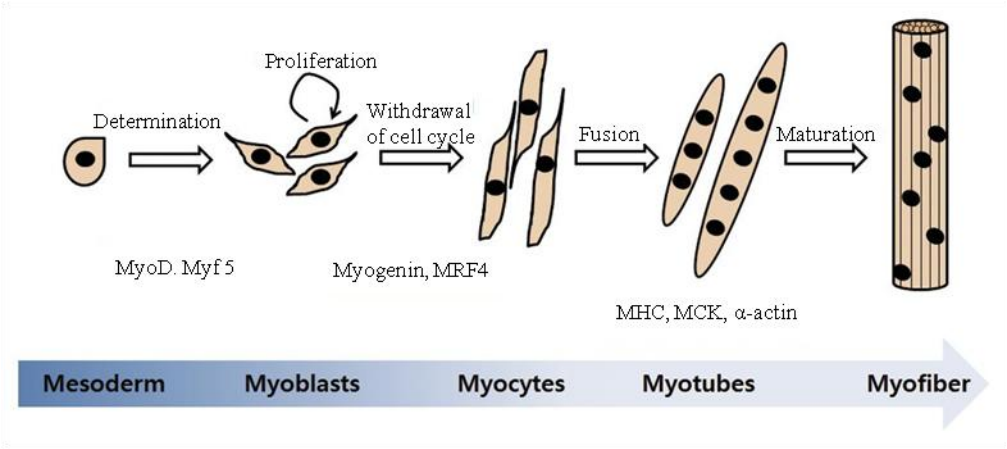

Figure 1.10: Step by step process of Myogenic Differentiation.
The formation of myoblasts initially starts from the mesoderm after the expression of Myo D and Myf5.This allows for the conversion to skeletal muscle myoblasts. After the development into myoblasts, they enter the cell cycle and begin to proliferate. After cells proliferate they exit the cell cycle and differentiation is initiated. The presence of Myogenin and MRF4 facilitates the differentiation process, where they change in appearance and become elongated to become myocytes. Myocytes contribute to the formation of myotubes, where they fuse to other myoctes. The formation of myotubes leads to the expression of muscle specific protein such as alpha-actin, myosin heavy chain (MHC) and muscle creatine kinase (MCK). Matured myotubes become myofibers. (Figure taken from Jang and Balik., 2013 Review)

the promoter region of MS1 that was either wild type or contained mutations to the sites of interest which were the E-Box1,2 and 3 and the TATA binding sites.

Initial experiments were done comparing differentiated C2C12 myoblasts with NIH3T3 fibroblasts, both transfected with the promoter region of MS1. Based on the cell type alone, the promoter activity of MS1 in C2C12 myoblasts increased 4-fold compared with NIH3T3 cells suggesting, that the promoter favours a myogenic environment (Ounzain *et al.,*2008). Experiments carried out in C2C12 cells that were transfected with the MS1 wildtype promoter in combination with MyoD, MEF2D and myogenin, showed that in the presence of MyoD, there was a significant increase seen in the promoter activity of MS1 (Ounzain *et al.,* 2008). This was not seen with the other transcriptional activators, MEF2D and myogenin, where in the absence of MyoD, promoter activity of MS1 decreased. This suggests MyoD is a key regulator in the promoter activity of MS1 (Ounzain *et al.,* 2008). Site directed mutagenesis was done on the promoter region, where the E-box sites possessing the consesensus sequence (CANNTG), essential for MyoD binding were present as well as the TATA box region. These mutations were either single or in combination and compared with the wildtype to determine the effects of the promoters in the presence of overexpressed MyoD on MS1 activity (Ounzain *et al.,* 2008). This experiment played a pivitol role in confirming that mutations to the E1 and E2 regions as well as the TATA box (TATT) reduced the interactions between MS1 and MyoD which caused significant reductions in the promoter activity of MS1 (Ounzain *et al.,* 2008). The promoter region of MS1 is regulated by MyoD binding and is believed to potentially play keys roles in myogenic differentiation and regeneration (Wang *et al*., 2002). Interestingly, MyoD is a transcription factor known to be activated by Akt and PGC-1α (Lin *et al.,* 2002; Guerfali *et al*., 2007). PGC-1α is a transcriptional activator that is known to control genes involved in glucose uptake, mitochondrial biogenesis and fusion as well as being upregulated in muscle during endurance exercise (Lin *et al.,* 2002; Guerfali *et al*., 2007; Cartoni *et al.,* 2005; Michael *et al*., 2001; Russell, A.P; 2010). More importantly PGC-1α works with another transcription factor, ERRα, that also plays a role in the regulation of MS1 (Wallace *et al.,* 2011)

1.8.4.3. Oestrogen-related receptor-α target gene binds to the Promoter region of MS1

Further analysis of the human MS1 promoter region identified that the binding site for oestrogen related receptor-α (ERRα), a member of the nuclear receptor superfamily, is located approximately 150 bp from the transcriptional start site of MS1 (Wallace *et al.,* 2011; Hock and Kralli; 2009). Although this receptor shows similarity to the oestrogen receptor, in terms of DNA and ligand binding, it is not activated by oestrogen nor oestrogen like molecules (Giguere *et al.,* 2008). ERRα plays a key role in mitochondrial biogenesis, aiding in the formation of new mitochondria (Schreiber *et al.,* 2004). Activation of this process occurs as a result of different signals due to cellular stress or in response to environmental stimuli (Hock and Kralli., 2009; Giguere *et al.,* 2008). ERRα works with peroxisome proliferator activated receptor coactivator 1 (PGC-1α), where they are both important regulators of mitochondrial biogenesis and oxidative metabolism (Schreiber *et al.,* 2004). PGC-1α is found in highly specific tissue, the skeletal and cardiac muscle (Kallen *et al.,* 2004).

In order to investigate whether PGC-1α/ERRα can activate the MS1transcriptional programme, C2C12 myotubes were infected with adenovirus either control LacZ or adenovirus expressing human PGC-1α, in the absence or presence of ERRα (which was silenced by SiRNA). There was an observed increase in MS1 mRNA expression by 3-fold compared to the control and a significant decrease in mRNA expression levels when ERRα was silenced (Wallace *et al.,* 2011). The ability for ERRα to bind is dependent on the presence of an oestrogen receptor response element (ERRE) (Schreiber *et al.,* 2004). Within the MS1 promoter is a target sequence, that is identical to the known 9 bp target sequence for ERRα binding 5'-TNAAGGTCA-3' (Wallace *et al.,* 2011).

Determination of how PGC-1α and ERRα interact with the MS1 promoter was investigated by chromatin immunoprecipitation (ChIP) assays. These assays were carried out to identify whether both activators are required to either act directly on the gene of MS1, or whether physical interaction between the activators and MS1 promoter are needed. This study was able to show that Flag-tagged ERRα and PGC-1α were both detected at the ERRE, and knockdown of endogenous ERRα, expression by siERRα resulted in diminished binding of PGC-1α co-activator to the ERRE region of MS1 (Wallace *et al.,* 2011). This showed that ERRα binds directly to the promoter of MS1 and is required for PGC-1α recruitment to the promoter (Wallace *et al.,* 2011).

The transcription factors discussed thus far, MyoD, MEF2c and ERRα/PGC-1α all have a positive effect on the promoter activity of MS1, leading to an increase in its expression (Kuwahara *et al.,* 2007; Ounzain *et al.,* 2008 and Wallace *et al.,* 2011). These transcription factors are all involved in cardiac hypertrophy, myogenic differentiation, strenuous exercise and diabetes (Yoshitake *et al.,* 2013; Mootha *et al.,* 2004). A recent study has shown that the transcription factor GATA4 has an opposite effect which leads to repression of MS1 expression in embryonic, neonatal and adult hearts (Ounzain e*t al.,* 2012). The research has been able to show MS1 can be regulated both positively and negatively by various transcription factors.

1.8.4.4. GATA4 Transcription factor as a repressor of MS1 expression

The GATA-binding protein 4 (GATA4) is from the GATA superfamily that are zinc finger containing transcription factors, and is cardiac specific (Kobayashi *et al.,* 2007 and Zhou *et al.,* 2012). GATA4 recognises a motif seen in the promoters of many cardiac genes that have a consensus sequence 5'-AGATAG-3', which allows for binding of GATA4. It plays a key role in cardiac development, cytoprotection in cardiomyocytes and maladaptation of the heart such as hypertrophy (Oka *et al.,* 2006; Liang *et al.,* 2001 and Molkentin, L, 2000).

Previous investigations analysing the 5 kb of the 5'- flanking sequence upstream of MS1 transcription start site (TSS), identified evolutionarily conserved regions (ECRs) α and β (Ounzain *et al.,* 2008). Investigations by the same group explored further upstream by analysing 20 kb 5'-flanking sequence up stream of the MS1 start site. Two new regions were identified as DINA (distal intergenic activator) located 16 kbp upstream of TSS of MS1 and (SINA) stress intergenic activator located 9 kb (Ounzain *et al.,* 2012). SINA and DINA are cardiac specific cis-regulatory domains for the repression and enhancement of gene expression dependent on different stress signals (Sakabe *et al*., 2012). The two new regions, as well as ECRα were all observed to have GATA recognition sequences and assumed that GATA binding proteins may be involved in the regulation of the MS1 gene (Ounzain *et al*., 2012).

Luciferase reporter assays were performed where 1.6 kbp of promoter region, relative to the MS1 TSS, was amplified and cloned into pGL3-Basic reporter plasmid. Constructs which had deletions of the ECR regions at various positions and SINA and DINA regions were also cloned upstream of the simian virus 40 (SV40) promoter in a luciferase based enhancer/repressor reporter vector pGL3-Promoter (Ounzain *et al*.,

2012). Different cell lines were used, to determine whether the activity of DINA and SINA was tissue sensitive. DINA and SINA domains transfected in H9c2 and neonatal rat ventricular myocytes (NVRMs) had enhanced promoter activity of SV40 by 75 and 110% respectively compared to the control. Where COS7 and NIH3T3 cells did not have any increased activity (Ounzain *et al.,* 2012). Critical analysis of ECRα, SINA and DINA showed the activity of the promoter is dependent on regions that are cardiac cell-specific between -300 to +60 and -300 to -127 and also have GATA elements present (Ounzain *et al.,* 2012). The presence of known distal enhancers such as monomethylation at histone 3 lysine 4 (H3K4mel) and binding by acetyltransferase p300 are associated with regulatory markers are used in CHIP assays to identify active tissue specific enhancers (Heintzman *et al.,* 2007; Pulakanti *et al.,* 2013; Creyghton *et al.,* 2010).

The use of co-transfection gene reporter and ChIP assays, showed GATA4 is able to repress ECRα activity but enhances the activity of DINA. Loss-of-function and gain-of-function approaches exploited, confirmed the role of GATA4 in relation to MS1 expression (Ounzain *et al*., 2012). Embryonic, neonatal and adult cardiomyocytes were used to look at the effects of GATA4 on MS1 regulation. When GATA4 is overexpressed this leads to downregulation of MS1, however when knockdown/knockout of GATA4 was carried out, this resulted in the upregulation of MS1 (Ounzain *et al.,* 2012).

Elucidation of MS1 regulation by GATA4 was investigated with regards to diseases such as diabetes. The use of type 1 and 2 diabetic hearts in this study was to observe the effects of GATA4 on MS1 expression in a pathophysiological environment. Previous studies have demonstrated GATA4 levels are decreased during hyperglycemia as a result of ubiquitination and degradation (Broderick *et al.,* 2012). The mechanism by which this occurs is proposed to be by the E3 ubiquitin ligase CHIP, which mediates ubiquitination and degradation by the ubiquitin proteosome system (UPS) (Broderick *et al.,* 2012; Oka *et al.,* 2006 and Liang *et al.,* 2001). When GATA4 levels are decreased, hyperglycemia is increased which makes the hearts more susceptible to ischaemic injury as a result of an increase in ROS, cardiomyopathy from fibrosis and increases apoptosis (Barouch *et al.,* 2006; Gutkowska *et al.,* 2009). In type 1 diabetic 2-month old FVB mice, where streptozotocin (STZ) treatment, a drug used to destroys pancreatic β cells was used in induced type I diabetes (Islam *et al.*, 2009, Ridolfi *et al.*,1991, Rossini *et al.,* 1977 and Szkudelsk, T., 2001) GATA4 protein levels decreased significantly but

MS1 expression increased by 1.3 fold when compared to the untreated hearts. Similarly, in type 2 diabtetic models, db/db diabetic mice showed a decrease in GATA4 levels with an increase in MS1 expression by 1.3 fold compared to the db/+nondiabetic controls (Ounzain *et al.*,2012).

It can be concluded that GATA4 has a negative effect on MS1, where the dysregulation of MS1 is observed. Furthermore, GATA4 does not only control MS1 regulation but also has major effects on MRTF-SRF signalling in cardiac development and disease. Myocardin related transcription factor- serum response factor (MRTF-SRF) target genes JunB and NPPB were upregulated when GATA4 was depleted in type1 and type 2 diabetic models, which could be expected as MRTF-SRF are direct downstream targets of MS1 in the SRF signalling pathway (Chong *et al.,* 2012, Kuwahara *et al.,* 2005 and Arai *et al.,* 2002). This might however only apply to the activation of the SRF pathway via MS1 and not RhoA which can act independently of MS1 to allow SRF signalling (Sahai *et al.,* 1998,). SRF is a known transcriptional activator of muscle specific genes which are involved in cardiac development, activation of foetal genes during a hypertrophic response in the heart and actin cytoskeleton (Nelson *et al.,* 2005).

1.8.4.5. Regulation of MS1 via a feed-forward loop by the Serum response factor SRF

In vitro studies have shown that SRF is a downstream target of MS1 and the Ras homolog gene family member, RhoA, where MS1 acts in conjunction with RhoA by binding of G-actin (Arai *et al*., 2002 and Kuwahara e*t al.*,2007). The translocation of SRF from the cytoplasm to nucleus through actin dynamics, allows for the regulation of many genes involved in cardiac development, function and structure (Arai *et al.,* 2002; Miano *et al.,* 2004 and Niu *et al.,* 2005). Recent studies with the use of a zebrafish MS1 orthologue (zSTARS) knockdown showed that there were cardiac defects such as abnormalities with the ventricle (decreased size and shortening), enlarged atria and decreased end diastolic dimension in the absence of MS1 expression (Chong *et al.,* 2012). However, with injection of zsrf (serum response factor) mRNA into morpholino embryos, this resulted in the suppression of the cardiac phenotype induced by zSTARS morpholino knockdown (Chong *et al*., 2012). Ectopic overexpression of MS1 in vitro leads to the activation of the proximal promoter, known to contain the conserved SRF binding site at position -305 bp (Chong *et al.,* 2012).

Confirmation that SRF was the cause of this autoregulatory feedback loop was investigated with the use of Luciferase and ChIP assays. H9c2 cells were transfected with the conserved binding region for SRF -1585/+60 and -365/+60, upstream of the MS1 TSS. Luciferase activity confirmed MS1 promoter activity was significantly higher compared to the control (pcDNA without promoter). These effects were reversed in the presence of the inhibitor CCG-1423 when compared to control (without CCG-1423) where the control was 4 times greater, confirming MS1 activity was blocked (Chong *et al.*, 2012). The inhibitor works by preventing MKL1 nuclear localization, which is a co-factor of SRF, that in turn prevents SRF dependent gene expression (Jin *et al.,* 2011, Evelyn *et al.,* 2007 and Miralles *et al.,* 2003). This study along with other research has shown that MS1 does influence SRF transcriptional activity *in vitro and in vivo*. The role of MS1 in the SRF signalling pathway and the other members involved are discussed in greater detail in the following **Section 1.8.5.**

1.8.5. MS1 as a key regulator in SRF transcriptional activity via MRTF-A nuclear translocation

The serum response factor (SRF) is a member of the MADS (MCM1, Agamous, Deficiens, SRF) box domain containing family of transcription factors found in many animal species and fungi (Miano et al., 2003, Miano et al., 2007, Posern and Treisman, 2004). This family of transcription factors are involved in the regulation of skeletal muscle growth and muscle gene expression (Wu *et al.,* 2011, Miano *et al.*, 2007, Shore and Sharrocks, 1995). SRF was discovered and given the name, based on binding activity to the serum response element (SRE) located within the promoter region of a well known proto-oncogene *c-fos,* an immediate early transcription factor involved in cancer (Treisman *et al.*, 1995; Treisman *et al.*1988, Norman e*t al.,* 1988, Wang *et al.,* 2002). Further studies observed SRF binding was dependent on SRE found within the promoter region of many genes controlled by SRF (Shaw *et al.,* 1986). SRF binds to A/T rich DNA sequences that are facilitated through the SRE, where a highly conserved sequence is found within the inner core of SRE known as the CArG box (Shore and Sharrocks, 1995, Pipes *et al.,* 2006). The CArG box is a 10 bp consensus sequence; CC[A/T_6]GG is recognised by SRF and similar to MEF2C from the MEF family, that recognises a 10 bp sequence for binding to DNA as discussed in **Section 1.8.4.1** (Pelligrini e*t al.*, 2005). This explains how regulation of MS1 by both SRF and MEF2 occurs with the CArG-like element found present within the MS1 promoter. MS1 can

facilitate its own transcription that leads to the feed-forward mechanism that requires activation of SRF (Chong *et al*., 2012). A vast number of genes are targets for SRF (over 200) and many of them play roles in cell growth, myogenesis , regeneration and organization of the cytoskeleton (Sun *et al.,* 2006, Miano *et al.,* 2007, Kuwahara *et al.*,2005; Shore and Sharrocks 1995).

MS1/RhoA and MAPK pathways are involved in the transcriptional activation of SRF in skeletal and smooth muscle (Kuwahara *et al.,* 2005, Mahadeva *et al.,* 2002, Murai *et al.,* 2002, Lu *et al.,* 2001, Arai *et al.*, 2002). The link between the RhoA/MS1 signalling pathways and SRF activation is facilitated through changes via actin dynamics that allows for SRF to translocate to the nucleus (Kuwahara e*t al*., 2005). The MAPK signalling pathways facilitate SRF activation through phosphorylation of SRF co-factors, ternary complex factors (TCF), that are part of the Ets domain family e.g Elk1 and SAP-1 (Lee *et al.,* 2010, Iyer *et al.,* 2006, Buchwalter *et al.,* 2004, Janknecht *et al.,* 1993). The involvement of GTPase Ras, allows for the activation of the serine-threonine kinases Raf, MEK and ERK bind to DNA through recognition of an Etf motif [C/A][C/A]GGA[A/T] located near the SRF binding CArG box (Treisman *et al.,* 1994, Shaw *et al.,* 1989, Katsch *et al.,*2012).

The second set of co-factors which allow for SRF activation are the myocardin related transcription factors (MRTFS) that are controlled by MS1/RhoA. RhoA is a ras homolog gene family member, that is a small GTPase, part of the Rho GTPase family that includes Rac1 and Cdc42 (Posern and Treisman, 2006, Hill and Treisman, 1995). Rho A is involved in the stimulation of actin polymerization by activation of Rho kinase (ROCK) and mammalian homolog of diaphanous (mDia) that can stabilize (F-actin) or deplete depolymerised globular actin (G-actin) within the cytoplasm (Mack e*t al.,* 2001, Narumiya e*t al*., 1997 and Sotiropoulos *et al*., 1999). MS1 stimulates SRF activity through Rho A-dependent mechanism, where COS cells were transfected with SM22-luciferase reporter and MS1 or RhoA expression vector which was constitutively active RhoA to determine the effect these had on SM22 promoter activity, a gene known to be regulated by SRF (Arai *et al.,* 2002). The greatest activity of the promoter was seen in the presence of RhoA and MS1 together, however with presence of one or the other, the activity of SM22 promoter decreased by 50% (Arai *et al.,* 2002). Studies further confirmed that activation of SRF by RhoA and MS1 was through actin dynamics with the key involvement of intermediary proteins from the MRTFs family, specifically MRTF-A (Kuwahara *et al.*,2005).

MRTF-A (also called MAL, MKL-1 and BSAC) is a member of the myocardin related transcription factors family, which includes MRTF-B (also called MKL-2 and MAL16) and myocardin (Sakuma *et al.,* 2003, Wang *et al.,* 2002). The MRTFs A and B are found expressed in a wide range of embryonic and adult tissue, while myocardin is found specifically expressed in cardiac and smooth muscle cells (Parmacek M.S., 2007, Pipes *et al.,* 2006, Wang *et al.,* 2001, 2002,2004). Although these have different expression patterns, they have a series of highly conserved domains such as the SAP domain that is a 35 aa motif containing two amphiphatic α-helices that resembles 1 and 2 of the homeodomain (Pipes e*t al.,* 2004, Aravind *et al.,* 2000, Wang *et al.,* 2002). The other conserved domains include, a Q-rich region required for association with SRF and the RPEL domains located at the N-terminal region that mediate cytoplasmic localization and actin binding only in MRTF-A and MRTF-B (Wang *et al.,* 2001, Pipes *et al.,*2006).

There are three RPEL motifs [Arg-Pro-X-X-X-Glu-Leu] essential to the MRTFs that allow for direct interaction with G-actin (Posern and Treisman, 2002). The RPEL domains are thought to bind tightly to G-actin when in the cytoplasm, as observed in NIH3T3 cells in the absence of serum and can also accumulate due to serum stimulation (Kuwahara *et al.,* 2005, Miralles *et al.,* 2003, Guettler *et al.,* 2008). Investigations using the same cell line, co-transfected with MRTFs and MS1 showed that MRTFs translocated to the nucleus without the presence of serum (Kuwahara *et al.,* 2005). Although myocardin is part of the MRTF family, the RPEL motifs do not facilitate binding to G-actin, and the presence or absence of MS1 does not affect translocation to the nucleus (Wang *et al.,* 2003, Kuwahara *et al*., 2005).

MS1 binds to polymerized actin (F-actin) as previously mentioned and depletes the G-actin pool within the cytoplasm (Arai *et al.,* 2002). G-actin is responsible for controlling the translocation of MRTFs into the nucleus, depletion of G-actin within the cytoplasm leads to the activation of MRTF-A that accumulates within the cytoplasm and allows for translocation to the nucleus to activate SRF transcription (Kuwahara *et al.,* 2005). Although MRTFs bind to SRF, the interaction between them is low. To summarize this process of SRF transcriptional activation, due to MS1/RhoA activation a model is represented in **Figure 1.11.**

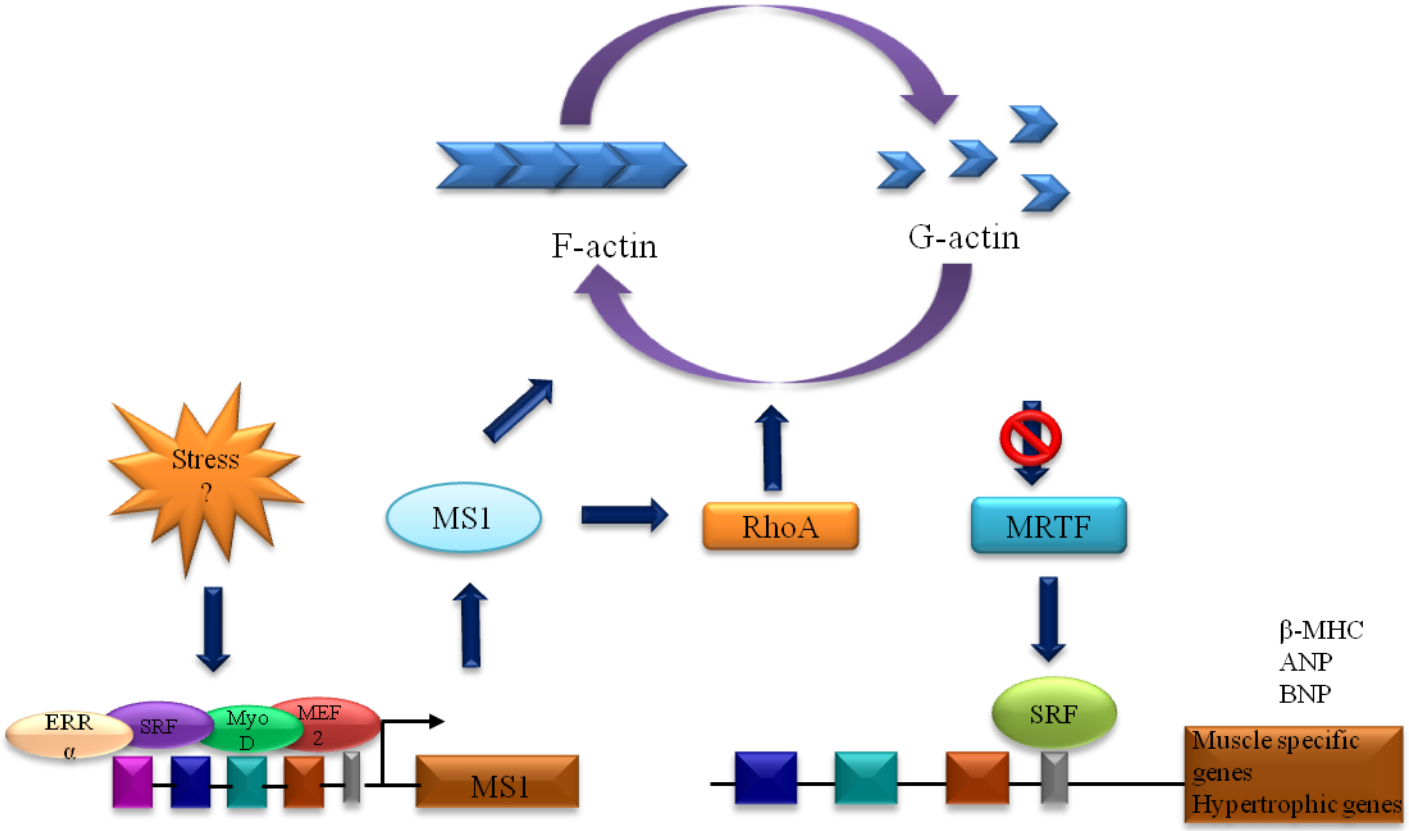

Figure 1.11: A model showing the role of MS1/RhoA on the activation of the SRF.
Different stress signals trigger the activation of transcription factors to regulate MS1 expression. This allows for the polymerization of actin. F-actin polymerization occurs with increased levels of MS1 and/or RhoA. Lower G-actin within the cytoplasm allows for the release of MRTF, a co-activator of SRF to translocate from the cytoplasm to the nucleus to activate SRF. Activation of SRF allows for expression of its target genes that are responsible for cytoskeletal reorganization, hypertrophy, muscle contraction and movement.(Adapted from Kuwahara *et al.*, 2005)

1.8.6. MS1 during Cardiac Hypertrophy

Transcription factors GATA4, MEF2 and SRF are involved in cardiac hypertrophy and are also known regulators of MS1. Cardiac hypertrophy is an adaptation of the heart as a result of the heart coping with increased workload, stress and injury as reviewed in **Section 1.5** (Dorn *et al.,* 2009). MS1 was first observed to increase in expression levels by a study carried out by Mahadeva *et al*. MS1 mRNA levels increased by 3 fold within 1 hr of left ventricular hypertrophy in rats as a result of pressure overload induced by aorticbanding and decreased to basal levels within 24 hrs of post banding (Mahadeva *et al.,* 2002). MS1 is thought to be an early sensor of cardiac hypertrophy based on the early upregulation of MS1 within 1 hr. MS1 is also implicated in sensing mechanical stress which leads to cardiac remodelling in response to LVH (Mahadeva *et al.,* 2002).

Experiments with the use of transgenic mouse models that constitutively expressed active calcineurin (a key mediator in cardiac hypertrophy) under the control of α-myosin heavy chain (α-MHC) promoter resulted in the development of cardiac hypertrophy and cardopmyopathy (Kuwahara *et al.,* 2007). The level of MS1 expression was observed to be 8 times higher in the transgenic mouse hearts when compared to the MS1 expression levels in wild type littermates (Kuwahara *et al.,* 2007). *In vitro* studies showed that when MS1 is overexpressed in H9c2 rat cardiomyocytes compare to the control, there was an increase in cell size (Koekemoer *et al*., 2009). MS1 overexpression significantly induced hypertophic gene marker brain natroiretic peptide (BNP) (Koekemer *et al.,* 2009). Interestingly, MS1 was observed to have a cardioprotective effect against staurosporine-induced apoptosis, where MS1 overexpression resulted in the up-regulation of *Nol3*, a known cardioprotective gene (Koekemoer *et al.,* 2009).

These studies all show the involvement of MS1 during cellular hypertrophy and the potential ability of MS1 to act as an early sensor of cardiac hypertrophy and may also have cardioprotective properties.

1.8.7. Regulation of MS1 during Exercise and Mechanical Stress.

Skeletal muscle is regulated by the increase (hypertrophy) or decrease (atrophy) where these changes elicit an extracellular signal that triggers the intracellular activation of specific genes as a result of changes in size, structure and function (Lamon *et al.,* 2013,

Wallace, A.P., 2010). MS1 expression within the skeletal muscle was seen to be regulated during exercise through actin dynamics. During mechanical stress as a result of contraction, increased loading or immobilization, detection of these extracellular transduction stress signals need to be transmitted within the cells for an appropriate physiological response which is important to the body to determine muscle fate and gene expression (Fluck., 2006 and Russell, A.P 2010). MS1 is upregulated during sensitivity to overload and pathological cardiac hypertrophy as a result of aortic banding of mouse hearts as well as forced overexpression of MS1 in mouse hearts through adenoviral infection that confirmed MS1 as a stress responsive protein (Mahadeva *et al.,* 2002 and Kuwahara *et al.,* 2007). MS1 plays an essential role in the transcriptional activation of SRF (discussed in **Section 1.8.5)** that leads to the expression of proteins essential for muscle growth, contraction and remodelling (Miano *et al.,* 2007).

1.8.7.1. Effects of MS1 during Pro-longed Resistance and Endurance training

Initial studies first observed MS1 increased at mRNA levels in response to hypertrophy induced resistance training in skeletal muscle (Lamon *et al.,* 2009). This study was carried out using males who were subjected to a series of resistance-exercises over an 8-week period. Biopsies were taken post-training which revealed MS1 mRNA increased by 3.4 fold compared to samples taken prior to training (Lamon *et al.,* 2009). MS1 mRNA levels increased as well as the targets downstream of MS1 that include MRTF-A and B, and SRF that all resulted in an over 2.5-fold increase in mRNA levels. Target genes of SRF such as MHC-IIa, α-actin and IGF-1 also increased similarly. Other studies have shown that MS1 expression was affected by plyometric power training in early postmenopausal women (50-57 yrs old) over a 12 month period (Pollanen *et al.,* 2010). The aim of the study was to determine the effects of power training or oestrogen containing HRT on skeletal muscle properties after menopause as previously carried out by Sipila *et al.,* 2001. Although mRNA levels of MS1 increased, the downstream gene targets analyzed from previous studies (Lamon *et al.,* 2009) did not show the same effect (Pollanen *et al.,* 2010). These studies were focused on the expression of genes as a result of exercise over a extended period of time, in all cases MS1 mRNA levels increased increased by 3 fold in skeletal muscle.

Comparative studies were carried out to observe effects of MS1 mRNA levels and members downstream of its signalling pathway MRTF-A and SRF, after 10 weeks of endurance and resistance training (Lamon *et al.,* 2013). After prolonged training regardless of the type of training performed, mRNA levels of MS1 and all downstream targets increased (Lamon *et al.,* 2013). Other comparative studies were done to investigate the regulation of MS1 at the mRNA levels and protein levels, during unilateral eccentric and concentric resistance training over a 12 week period (Vissing *et al.,* 2013). Habitual exercise over a prolonged period, which consisted of either concentric or eccentric resistance exercises, resulted in protein levels of MS1 left unchanged (Vissing *et al.,* 2013).

1.8.7.2. Effects of MS1 during single bout exercise in trained and untrained states

Other studies observed changes in MS1 expression in a short period of time as a result of acute single bout eccentric exercise where MS1 mRNA increased after 3 hrs of exercise, along with its downstream targets by 10-fold (MacNeil e*t al.,* 2010). MS1 mRNA levels also increased by 8 fold and 6 fold at 2.5 hrs and 5 hrs respectively, after a single bout of resistance exercise, however this was not translated to protein level as MS1, MRTF-A and SRF protein levels remained the same (Lamon *et al.,* 2013). Although there was not any increase in MS1 expression during habituated concentric and eccentric exercises over a 12 week period, there was an observed increase in MS1 mRNA levels in both concentric and eccentric single bout exercise. Specifically, a 10-fold increase in MS1 mRNA levels following a single bout eccentric exercise was observed which is consistent with previous studies (Vissing *et al.,* 2013, MacNeil *et al.,* 2010). It should be noted that although there was an increase in MS1 mRNA levels, this was not the same for the other downstream targets MRTF-A and SRF. SRF only showed an increase in mRNA levels post 1 hr concentric exercise but this was not as high as MS1 mRNA levels (Vissing *et al.,* 2013). The same effects were seen for MRTF-A in a different study as a result of training in a habituated state (Lamon *et al.,* 2013).

All studies thus far supported evidence that MS1 was increased at the mRNA levels in skeletal muscle after endurance or single bout exercise whether concentric or eccentric, but this was not seen at the protein level (Lamon *et al.,* 2009, MacNeil *et al.,* 2010, Lamon *et al.,* 2013, Vissing *et al.,* 2013). MS1 is responsive to moderate intensity exercise where test

subjects did single leg cycling until exhaustion (single leg endurance exercise). It was observed that mRNA levels of MS1 increased 3 hrs post exercise but reduced to basal levels 24 hrs after (Lamon *et al.,* 2011). MS1 protein levels also increased 3 hrs post training, but only SRF of the downstream members of the pathway showed an increase but not MRTF-A which could be due to its translocation to the nucleus, as the nuclear extracts were not used for this analysis (Lamon *et al.,* 2011).

1.8.7.3. MS1 decreases as a consequence of Muscle atrophy and Ageing

Atrophy is the term used for the reduction of skeletal muscle as a result of lack of physical activity (disuse), neuromuscular disorders or after musculoskeletal trauma due to diabetes, cancer and AIDS (Doucet *et al.,* 2007, Kim and Choi., 2010). MS1 was seen to decrease in levels during detraining (atrophy) after an 8 week period, of reduced physical activity. Similarly, a decrease in MRTF-A/B and SRF mRNA was observed along with SRF target genes (MHC-IIa, α-actin and IGF-1) which were reduced to the original pre-training levels (Lamon *et al.,* 2009). Unloading as a result of hind limb suspension for 20-days in humans did not show any reduction in MS1 mRNA levels or downstream targets leading to SRF activation (Sakuma *et al.,* 2009). This result differed from a previous study that showed a decrease in MS1 mRNA levels along with the downstream targets (MRTF-A and SRF) in 24-month old mice (Sakuma *et al.,* 2008). The possible reason could be the amount of muscle loss that has to take place to have a negative effect on MS1. This is based on the study using aged mice with muscle loss of over 19%, which was higher than the study with humans which was only 10% (Sakuma *et al* 2008 and 2009). It is logical to believe that since reduction of SRF levels responsible for genes such as α-actin, IGF-1 and MHC-IIa are known to play key roles in muscle regeneration and increase muscle fibres as a result of hypertropy (Schiaffino and Mammucari., 2011, Russell, A.P., 2010). The reduction of IGF-1 involved in the Akt pathway, results in promoting atrophy due to the activation of FoxO/atrogene pathway during ageing, hind-limb suspension and untraining (Leger *et al.,* 2006 and 2008, Crossland *et al.,* 2008, Schiffiano and Mammucari, 2011).

Based on all the evidence in this section, MS1 might be involved in important roles within the skeletal muscle where it is regulated by hypertrophy and atrophy as a result of pro-longed resistance training and disuse. MS1 might also function as an early sensor for

muscular distress in skeletal muscle contractions due to resistance training, and allows for early adaptation during exercise in single bout exercise (Wallace e*t al.,* 2012). This suggests that MS1 might have more of a protective role in the skeletal muscle, where increase in levels of MS1 occurs to protect the sarcomere from any damage due to overloading (Lamon *et al.,* 2013). The importance of knowing the specific role of MS1 and the downstream targets that facilitate SRF activation is important for positive regulation of skeletal muscle mass. This would be vital in the long run for persons with diseases which either result in atrophy or as a result of sarcopenia. Investigating specific pathways as therapeutic targets to enhance skeletal muscle mass would allow for a better quality of life for those suffering from atrophic disabilities that could be combated through repair and muscle growth.

1.8.8. Regulation of MS1 in Diabetes, Angiogenesis and SMC proliferation

1.8.8.1. MS1 Regulation in Type 2 Diabetes

Diabetes is a growing concern worldwide, in 2010 a staggering 285 million people were diagnosed with diabetes and it was estimated that by the year 2030, nearly 439 million individuals could be affected by this disease (Shaw *et al.,* 2009). Insulin resistance is associated with type 2 diabetes (T2D) as this is one of the early detectable metabolic defects observed in humans (Tabak *et al.,* 2009). To date the molecular basis of insulin resistance is still not fully understood, but it is known that one of the causes of insulin resistance is due to reduced glucose uptake into the skeletal muscle (Saltiel and Kahn., 2001). A recent study showed that type 2 diabetes, increased upregulation in the serum response factor and its coactivator MRTF-A (Jin *et al.,* 2011).

The study used muscle biopsies from patients that were either full blown type 2 diabetics, non-diabetic subjects with one or both parents with T2D (FH+) and non-diabetic (FH-) subjects to identify phenotypes that are associated with insulin resistance through skeletal muscle gene expression. As mentioned previously SRF and MRTF-A are downstream targets of MS1 (Kuwahara *et al.,* 2005). In T2D patients MS1 was identified to be the highest differentially expressed gene and showed a 2.5-fold increase as compared to healthy non-diabetic patients (FH-) (Jin *et al*., 2011). Mouse models that were made insulin resistant by high-fat feeding were also showed a 3-fold increase in MS1 when compared to

the controls (Jin *et al.,* 2011). This finding is not a surprise since MS1 facilitates SRF activation by sequestering G-actin in the cytoplasm by converting it to F-actin, and causes the release of SRF coactivator MRTF-A, that allows for SRF gene expression as discussed in more detail in Section **1.8.5** (Arai *et al.,* 2002, Kuwahara *et al.,* 2005 and 2007).

Further exploration into the SRF signalling pathway was to determine the effects of reduced MS1 on insulin uptake and glucose in myotubes. Silencing of MS1 in L6 myotubes resulted in a decrease in MS1 protein expression by 54% and increased Akt-phosphorylation by 1.7-fold as a result of insulin stimulation (Jin *et al.,* 2011). Reduced MS1 expression also affected the basal and insulin-stimulated glucose uptake in myotubes by 3.7-fold and 3.6-fold respectively (Jin *et al.,* 2011). Knockdown of MS1 expression also resulted in the increase of plasma membrane GLUT4 localization in basal and insulin-stimulated states (Jin *et al.,* 2011). GLUT4 is a key component of insulin-stimulated glucose transport in muscle cells and adipose tissue and found mainly in these tissues (Stockli *et al.,* 2011). Diabetic mouse models were used in a more recent study, to look at the effects of GATA4 expression or depletion on MS1 regulation as discussed earlier in Section **1.8.4.4** (Ounzain *et al.,* 2012). Diabetic induced cardiomyopathy occurs as a result of hyperglycemia-induced depletion of GATA4 (Kobyashi *et al.,* 2007). This evidence is still not enough to determine whether MS1 is a key player that contributes to insulin resistance in diabetic muscle but based on human and mouse models, it is worth doing further investigations.

1.8.8.2. MS1 Regulation in Arteriogenesis and Smooth Muscle Cell Proliferation

Arteriogenesis is defined as the increase in diameter of pre-existing collateral vessels which is facilitated by fluid shear stress (FSS). FSS is the physical stimulus responsible for acting on endotheial cells responsible for controlling these processes, that attract circulating cells to the collateral walls where monocytes are known to play a major role during arteriogenesis (Helisch and Schaper.,2003; Triodl and Schaper.,2012). MS1 was identified as a key regulator of arteriogenesis as a result of upregulation in growing collaterals during elevated FSS that resulted in a 7-fold increase (Triodl *et al.,* 2009). Depletion of the stimulatory effect of FSS on collateral growth was done with the use of a nitric oxide (NO) inhibitor L-NAME, resulted in complete repression of MS1 transcription (Triodl *et al.,*

2009). The blockage of NO proves that it can be a possible mediator in FSS activity that also controls MS1 expression. To determine the function of MS1 in arteriogenesis *in vivo*, adenovirus infection of the collaterals of rabbits exposed to femoral artery ligation (FAL) without the use of an AV-shunt was performed (Triodl *et al.,* 2009). Overexpression of MS1 resulted in the improvement of collateral conductance in rabbits after FAL, while deletion of MS1 resulted in impaired arteriogenesis (Triodl *et al.,* 2009). MS1 was further investigated to determine the functional role it has during arteriogenesis.

During arteriogenesis proliferation of smooth muscle cells (SMC) occurs which is essential for vessel maturation (Pipp *et al.,* 2004). Overexpression of MS1 resulted in proliferation and metabolic activity of smooth muscle cells (SMC) in A10 rat cell line (Triodl *et al.,* 2009). During arteriogenesis the activation of the Rho/ROCK pathway is initiated and functions to help the remodelling of small arteries (Van Oostrom *et al.,* 2008). The Rho pathway is also involved in the signalling of SRF transcription which is known to be controlled by MS1 or by a Rho-A dependent pathway (Kuwahara *et al.,* 2005). However, in this case MS1 seems to facilitate the activation of this pathway where increased expression of RhoA was observed in overexpressed MS1 collateral vessels of rats, then decreased in MS1 deficient mice (Triodl *et al.,* 2009). Arteriogenesis usually occurs in areas that are underperfused as a result of an obstruction that causes tissue ischaemia (Triodl and Schaper., 2012; Schaper and Scholz., 2003). MS1 is upregulated during ischaemia/reperfusion injury in mice (Mahadeva *et al.,* 2002) and is also involved in the RhoA pathway (Arai *et al.,* 2002; Kuwahara *et al*., 2005) which is required during arteriogenesis for actin polymerization, necessary for the remodelling of arteries and improve collateral growth (Triodl *et al.,*2009). Based on the results of this study, there is strong evidence that MS1 may act as a sensor during ischaemia that initiate pathways responsible for induction of arteriogenesis. This could imply that MS1 may play a key role in structure and function.

There is no doubt that MS1 has a key function within the cardiac, skeletal and smooth muscles. It has been demonstrated to be a major participant in muscle adaptation and the link between sensing stress and intracellular activation of specific pathways for an accurate physiological response. Although steps have been taken to understand the structure of MS1, more has to be done in this respect. With regard to MS1 upregulated at the protein level,

this needs to be investigated in the future as not many studies have looked at the stability of MS1 or how exactly it is upregulated at the protein level. The goal is to eventually use MS1 as a pharmaceutical target in disease conditions that gear towards prevention of muscle loss and also increase of muscle development based on the different roles it is involved with in different studies.

1.9. Hypothesis and Aims of the Study

1.9.1. Hypothesis of this Study

MS1 is a stress responsive protein, expressed predominantly in skeletal, cardiac and to a lesser extent smooth muscle. Overexpression of MS1 in conjuction with Rho leads to actin polymerization by increasing the binding of G-actin to F-actin, which leads to the transcriptional activation of SRF (Arai *et al.,* 2002 and Kuwahara *et al.,* 2005). This leads to activation of intracellular signalling pathways that are responsible for the transcriptional regulation of genes that play key roles in cardiac and skeletal muscle hypertrophy, stabilization of the sarcomere, reorganization of the actin cytoskeleton due to damage, diabetes, proliferation and differentiation of myocytes. However the specific physiological role of MS1 is yet to be identified.

Previous studies in the lab showed MS1 mRNA expression was attenuated by JNK inhibitor SP600125 during simulated ischaemia/reperfusion injury. This was of interest because it is still unknown what pathway is responsible for the regulation of MS1. Based on these results, the MAPK pathways might be responsible for the regulation of MS1 and should be further investigated.

To date there are only three known proteins that interact with MS1, these are actin and ABLIM-2 and ABLIM-3. Based on the localisation of MS1 to be very specific, it is of interest to explore any other potential binding partners of MS1within the heart, that would allow for further characterization of the MS1 protein and also give a better understanding of the pathways it is involved with based on potential protein interactions.

Finally, there are potential MAPK phosphorylation motifs located at the N-terminus that to date, have not been investigated. The potential interaction between MS1 and MAPK pathways, could play a role in the regulation of MS1 activity. Therefore we wanted to determine whether there is a link between MS1 and the MAPK pathways, which allows for

phosphorylation of MS1 in response to stress stimuli, that results in a change in MS1 conformation or even lead to its activation, in order to facilitate protein interaction.

1.9.2. Aims of Study

The aim of this project was to therefore use biochemical, cell and molecular biology based assays to investigate the regulation and interactions of MS1in the cardiac muscle.

The specific experimental objectives are defined as follows:

1. To determine the effect of endogenous MS1 protein expression in cardiac cells in response to different physiological conditions with the use of an MS1 antibody.

2. Develop a reporter system to investigate the promoter activity of MS1 in response to different physiological conditions and stresses. We used the promoter region of MS1 (-1585/+60) cloned into a firefly luciferase pGL3 reporter vector and transfected in cardiac cells to observe luciferase activty.

3. To investigate potential interactions in the cardiac muscle with establishing a binding assay, where GST and His-tagged domain fragments of MS1 were used as bait in mouse heart extracts. Proteins found to potentially interact were identified by mass spectrometry.

4. Finally, to investigate whether potential MAPK phosphorylation motifs located at the N-terminus of MS1 can be phosphorylated by one of the MAPKs; ERK, p38 or JNK. Phosphorylation of these sites was carried out by radiolabelled *in vitro* phosphorylation assays.

Chapter 2. Materials and Methods

2.1. Materials

2.1.1. General Chemicals and Reagents

All general chemicals and reagents were purchased from Sigma (Dorset, UK) or Fisher Scientific (Loughborough, UK) unless otherwise stated. Centricon columns were purchased from Millipore (Billerica, MA, USA).

2.1.2. Antibodies

Mouse monoclonal anti-Green Fluorescent Protein antibody (anti-GFP) (G6539-2mL, 057k4785), mouse monoclonal anti-α-tubulin (B-5-1-2) and anti-γ-tubulin (T6557, Clone GTLI-88) and mouse monoclonal anti-FLAG M2 antibody (F3165), FLAG antibody (F1804), Anti-Actin (A4700), Anti-His (H1029), were purchased from Sigma. Rabbit polyclonal antisera (2221 and 2222) were raised against MS1 and were produced at Cambridge Research Bioscience. Anti-STARS (Cat No. Ab21986) was purchased from Abcam (Cambridge,UK), anti-HA(Y-11) (sc-805), Anti-STARS (Cat No. Sc-98151), anti-cjun (D-11) (Cat.No sc7481), anti-p38 (N-20) (Cat. No. Sc-728-G), anti-ERK1 (k-23) (Cat. No. Sc-94), Anti-JNK (Cat. No Sc-571), anti-p21 (c-19) (Cat. No. Sc-397) and anti-RhoV (N-12) (sc-160741) were purchased from Santa Cruz (Santa Cruz, California,U.S.A). Phospho-SAPK/JNK (Thr183/Tyr185) (Cat. No.9255), phospho-ERK and anti-phosphop38 (Thr180/Tyr182) (Cat.No.9215) were purchased from Cell Signalling Technology (Dundee,UK). Horse-radish peroxidase (HRP) conjugated anti-rabbit and anti-mouse secondary antibodies used in western blotting were purchased from Amersham Biosciences.

2.1.3. Mammalian Cell Culture and Transfection Reagents

The H9C2 rat myoblast cells (2-1) (Cat No. 88092904) were purchased from the ECACC (Salisbury, UK), HEK-293 (human embryonic kidney cells) were a kind gift from Dr. Joanna Hay (previous PhD student, Department of Biochemistry, University of Leicester, Leicester) and HL-1 cardiac cell line were a kind gift from Dr. Nina Storey (Department of Cell Physiology and Pharmacology, University of Leicester, Leicester). COS-1 (African Green Monkey cells) were a kind gift from Dr. Raj Patel (Department of Biochemistry,

University of Leicester, Leicester). Dulbecco's Modified Eagle's Medium (DMEM), L-glutamine, streptomycin, heat inactivated Foetal Calf Serum (FCS), Horse Serum (HS) and penicillin were purchased from Invitrogen (Paisley, UK). Collagen IV (Sigma C-5533) was purchased from Sigma.

ExGen500 in vitro transfection reagent (R0519) and TurboFect in vitro transfection reagent (R0531) were purchased from Fermentas JetPEI transfection reagent was purchased from Poly-Plus (N.Y, U.S.A).

2.1.4. Molecular Biology and Biochemistry Reagents

Restriction enzymes used were purchased from Roche (Lewes, U.K). Plasmid Preparation kits were purchased from Qiagen (Crawley, U.K). DNA Markers were purchased from Fermentas (York, U.K). Ethidium bromide was purchased from Invitrogen (Paisley, U.K). Gateway cloning enzymes were gifts from Prof. Andrew Fry (Department of Biochemistry, University of Leicester). Quikchange site directed mutagenesis kit was purchased from Stratagene (La Jolla, CA, USA). The BCA assay kit for protein quantification and Compat-Able Protein Assay prep reagent (Cat. No. 1858576) were purchased from Thermoscientific (Rockford IL,USA). Luciferase assay system kits were purchased from Promega (Essex, UK). 1 Kb Plus DNA ladder (10787-018) was purchased from invitrogen.

For western blot analysis Nitrocellulose membranes (Protran) was purchased from Schleicher abd Scheull (Dassel, Germany) and Immobilon P (cat no. IPVH00010) was purchased from Amersham Biosciences (Little Chalfont, U.K). Protein A sepharose beads were purchased from Sigma (Poole, U.K). Precision plus prestained protein markers (10-250 kDa range) were purchased from Biorad (Hemel Hampstead, U.K) while prestained molecular weight markers (Cat No. SDS7B2) were purchased from Sigma (Poole, U.K). Prestained marker (250-4 kDa range) was purchased from invitrogen

2.1.5. Plasmids

pCMV2-FLAG-MS1 generated during previously in the lab, GST-MS1 (1-192 a.a) was made by Lara Lewis. Gateway vectors pcDNA-DEST53 and pDONR201 was purchased from Invitrogen (Paisley, U.K). pEGFP-C1 (GFP) was purchased from Clontech pETM-11-MS1, pLEICS-03-MS1 and p-LEICS-07-MS1 expression plasmids were generous gifts

from Dr. Mark Pfhul (University of Leicester, Biochemistry Department). Renilla Luciferase reporters pRL-SV40 vector, pRL-TK vector, pRL-CMV, Luciferase reporter construct Rat MS1 promoter pGL3-MS1 (-1585/+60) and the pGL3-Basic construct were generous gifts from Dr. Nelson Chong (Glenfield Hospital, Department of Cardiovascular Sciences, Leicester,UK). Below is a list of additional MS1 constructs, showing the residues covered, were received as gifts from Dr. Mark Pfhul (Department of Biochemistry, Leicester, UK).

Table 2.1: MS1/STARS construct names and the residues which they contain.

MS1 Constructs	Residues of MS1/STARS (a.a)
MSD1	2-118
GST- MS1	2-196
MSD2	40-196
ABD1	193-295
C-terminal Tandem (ABD1 + ABD2)	193-375
ABD2	193-295

2.1.6. Primer Sequences for pCMV2-FLAG-MS1

Table 2.2: Forward 5'-3' (F) and the reverse primer 3'-5' (R) that were used to generate FLAG tagged MS1 to study localisation

Primer Name	Primer sequence 5'-3'
N-CMV-30	F AAT GTC GTA ATA ACC CCG CCC CGT TGA CGC
C-CMV-24	R TAT TAG GAC AAG GCT GGT GGG CAC

2.1.7. General Laboratory Buffers

Table 2.3: General Lab Reagents Solutions and their compositions.
A list of a number of general buffers used in the lab:

Luria-Bertani Medium	5 g (w/v) Bacto-Tryptone, 2.5 g (w/v) Bacto-Yeast Extract, 5 g (w/v) NaCl in 500 ml dH_2O with addition of 50 µg Ampicillin or Kanamycin
LB agar Plates	10 g/l (w/v) Bacto-Tryptone, 5 g/l (w/v) Bacto-yeast, 10 g/l (w/v) NaCl, 10 g (w/v) Agar in 1000 ml dH_2O with appropriate antibiotics
Ampicillin	Stock Solution 50 mg/ml in dH_2O. Use 1:1000
Kanamycin	Stock Solution 25 mg/ml in dH_2O. Use 1:1000
***Ge*ntamycin**	Stock Solution 20 mg/ml in dH_2O. Use 1:1000
50 x TAE	40 mM Tris base, 20 mM acetic acid, 1mM EDTA
10 x Tris Buffer Saline (TBS)	500 mM Tris-Base, 1.5 M NaCl
1 x TBST	1 x TBS, 0.1% (v/v) Tween-20
10 x Phosphate Buffer Saline (PBS)	80 g NaCl, 2.0 g KCl, 14.4 g Na_2HPO_4, 2.4 g KH_2PO_4 in 1L dH_2O

Blocking Buffer	5 % (w/v) BSA or skimmed milk in 1 x TBST
Tris – EDTA (TE)	10 mM Tris, 1 mM EDTA , pH 7.4
Extraction buffer	50 mM Na_2HPO_4, pH 7.4, 0.5 M NaCl, 10 % glycerol (v/v), 5 mM Benzamidine, 2 µg/ml PAL, 1 mM PMSF
Start Buffer	50 mM Na_2HPO_4, pH 7.4, 0.5 M NaCl, 10 mM Imidazole
Elution Buffer	50 mM Na_2HPO_4, pH 7.4, 0.5 M NaCl, 0.5 M Imidazole
50 x TAE	40 mM Tris-base, 50 mM EDTA, 5.72 % (v/v) glacial acetic acid, pH 7.4
HiLO Buffer	50 mM Tris, 5 mM EGTA, 150 mM NaCl, 25 mM Benzamidine, 1 % Triton x-100, 1 mM PMSF, 2 µg/ml PAL
3x Sample Buffer	36 % (v/v) glycerol, 12 % (w/v) SDS, 150 mM Tris, 0.01 % bromophenol blue, pH 6.8
Coomassie Stain	45 % (v/v) MeOH, 10 % (v/v) glacial acetic acid, 1.25 g coomassie brilliant blue R-250

Coomassie Destain Solution	25 % (v/v) MEOH, 7 % (v/v) glacial acetic acid
Enhanced Chemiluminescence Buffer A	90 mM p-Coumaric acid in DMSO
Enhanced Chemiluminescence Buffer B	250 mM Luminol-5-amino-2,3-dihydro-1,4-pthalazinedione in DMSO
Transfer Buffer	48 mM Tris, 39 mM Glycine, 20 % (v/v) methanol
Stripping Buffer	62.5 mM Tris-Cl, 2% (w/v) SDS, 0.8% (v/v) β-mercaptoethanol, pH 6.7

2.2. Methods

2.3. Cell Culture

2.3.1. Maintenance of Cell Lines

All cell lines were maintained in a humidified atmosphere 5% CO_2 at a temperature of 37°C, in Dulbecco's Modified Eagle's Medium (DMEM) containing L-glutamine (2 mM), supplemented with 10% (v/v) Foetal Calf Serum (FCS) or 5% (v/v) Horse serum with 100 units/ml of penicillin-streptomycin antibiotics. Cells were plated in 75 cm^2 flasks (Nunc) at 37ºC in 5% CO_2. When cells were approximately 70% - 90% confluent, they were passaged. To passage cells, growth media was removed from adherent cells and then they were washed once with 1x PBS that was supplemented with 0.25% trypsin/1 mM EDTA for 2 min to detach them. Cells were diluted in fresh pre-warmed Dulbecco's Modified Eagle's medium (1:5) and then replated into 75 cm^2 flasks, 6-well plates or 60 mm dishes as needed.

2.3.2. Storage of Mammalian Cell Lines

For long-term storage, cells were frozen in liquid nitrogen. Confluent cells were washed once in 1x PBS and harvested using 1x PBS supplemented with trypsin-EDTA (0.25% trypsin/ 1mM EDTA) for 2 min before being resuspended in 5ml of supplemented medium. Cells were centrifuged at 1100 rpm for 5 min and medium was removed before they were resuspended in FBS supplemented with 10% (v/v) DMSO. The cells were then transferred to cryotubes to be frozen slowly in an insulated box at -20ºC o/n, then at -80ºC for approximately 12 hr then transferred to a liquid nitrogen cell bank.

2.3.3. Transient Transfection of Mammalian Cell Lines

All transfection reagents used were derived from linear polyetheylenimine and acted as cationic polymers in order to act as a "proton-sponge" which was first hypothesized by Behr et al., 1997. The transfection incorporates a high concentration positively charged nitrogen atoms which allows for condensing of DNA to form polyplexes which allows DNA to be taken up via endocytosis into the cell.

2.3.3.1. Transfections of Mammalian cells with ExGen-500 Transfection Reagent

HEK-293 and H9c2 cells were transfected with CsCl purified plasmid DNA using ExGen-500 (cat no. R0519) transfection reagent. This was performed according to the protocol provided by the manufacturer's instructions. Cells which were seeded on appropriate tissue culture dishes (24-well plates, 6-well plates, 60 mm or 10 cm) were grown until they were approximately 50-70% percent confluent. After 24 hr, plasmid DNA and Exgen-500 reagent were mixed at a ratio of 1:3.3. For a 10 cm tissue culture dish 8 µg of plasmid DNA was diluted in 500 µl of 150 mM NaCl before the addition of 30 µl of ExGen-500. The diluted DNA and Exgen-500 were mixed thoroughly and left to incubate for 10 min at room temperature. The mixture was then added dropwise to the medium and after 24 - 48 hr the cells were then used for appropriate treatments.

2.3.3.2. Transfections with JETPEI

HEK-293, H9c2 and COS-1 cells were transfected with CsCl purified plasmid DNA using JETPEI transfection reagent. This was done based on the protocol provided by the manufacturer's instructions. Cells which were seeded on appropriate dishes (6-well plates, 60 mm or 10 cm) were grown until they were approximately 50-60 percent confluent. After 24 hr, transfections were carried out based on the manufacturer's instructions of a mixture of DNA to JetPEI at a 1:2 ratio. The DNA and JetPEI were first, separately diluted in 150 mM NaCl. The mixture of JetPEI and NaCl solution was added to the DNA diluted with NaCl. The solution was vortexed and allowed to incubate for 30 min at room temperature. The mixture was then added dropwise to the medium and after 48 hr the cells were lysed in either SDS-PAGE sample buffer (2X) or Triton Lysis Buffer and analysed on an SDS-PAGE gel.

2.3.3.3. Transfections with Turbofect Transfection Reagent

HEK-293 fibroblasts and H9c2 cells were transfected with CsCl purified plasmid DNA using turbofect transfection reagent. Cells which were seeded on appropriate tissue culture dishes (24-well plates, 6-well plates, 60 mm or 10 cm) were grown until they were approximately 70-90 % percent confluent. Transfections were carried out according to the manufacturer's instructions of DNA to Turbofect reagent (1:2 ratio). For a 10cm tissue

culture dish 10µg of plasmid DNA was diluted in serum free medium (1 ml) before 20 µl of turbofect was added. The diluted DNA and transfection reagent were mixed thoroughly and left to incubate for 17 min at room temperature. The mixture was then added dropwise to the medium and after 24 - 48 hr the cells were then treated appropriately.

2.3.4. Cell Treatments

2.3.4.1. Simulated Ischaemia and Reperfusion

H9c2 cells were plated onto 6 cm dishes and grown in DMEM supplemented with 10% FBS (v/v) and 100 units/ml of streptomycin-penicillin at 37ºC in 5% CO_2 humidified incubator. When the cells were 90% confluent, the medium was removed and the cells were washed once with PBS and transferred to 5ml of Hepes buffered Krebs (4 mM Hepes pH 7.5, 2% FBS (v/v), 137 mM NaCl, 3.58 mM KCl, 0.49 mM $MgCl_2$, 0.9 mM $CaCl_2$, 5.59 mM glucose, 2 mM L-glutamine) and left to equilibrate for 30 min at 37 ºC in the absence of CO_2. The buffer was removed and the cells were subjected to simulated ischaemic stress by transferring to Hepes-Buffered Krebs supplemented with 16 mM KCl, 1 mM sodium dithionite, 20 mM lactate, 10 mM 2-deoxyglucose and acidified to pH 6.5. After 1hr, ischaemic buffer was removed and the cells were then washed twice in 1x PBS. Cells were reperfused by incubating in Krebs buffer at 37°C prior to extraction in SDS-PAGE sample buffer at specified times.

2.3.4.2. Sorbitol Treatment

H9c2 cells which were seeded onto 6 well plates or 6 cm dishes were either transiently transfected with pGL3-MS1 plasmid or pGL3-basic vector or in some experiments transfected with pGL3-MS1 or untransfected. The cells were treated with DMEM with 0.5 M sorbitol for 1 hr. After treatment, the media was removed and replaced with supplemented DMEM with 10 % FBS and allowed to recover over time. Cells were lysed at certain time points.

2.3.4.3. UV Treatment

H9c2 cells which were seeded onto either 6 well plates or 6 cm dishes were transfected with either pGL3-MS1, pGL3-basic or left untransfected and left in supplemented DMEM.

After 24 hr the cells were transferred to 1x PBS and subjected to 2 min UV exposure. The cells were then transferred to supplemented DMEM with 10% FBS and left to recover over a period of 13 hr. After the cells were then lysed and assayed (**Section 2.4.8**).

2.3.4.4. Treatments with Hypertrophic Agonists

H9c2 cells were grown onto either 6-well plates or 60 mm dishes. The cells were transfected with pGL3-MS1 plasmid. Cells were left for 24 hr before serum starving overnight. Cells were either left in fresh serum or Krebs buffer for 30 min to equilibriate. After, either 100 nM of endothelin-1 (ET-1) or 100 µM of phenylephrine (PE-1) was added to the cells and left to incubate for 1 hr at 37ºC. After stimulation, the media was removed and the cells were washed in cold 1x PBS. The 1x PBS was removed and the cells were then extracted in passive lysis buffer. After extraction, cell lysates were pretreated and luciferase activity and protein concentration were measured.

2.3.5. Cell Lysis

Cells which were used for western blots were lysed in SDS-PAGE 2x sample buffer which was diluted from a 6x concentrated stock (6x: 0.35 M Tris pH 6.8, 0.25% bromophenol blue, 10% SDS, 0.6 M DTT, 30% glycerol). Dishes of cells which were used for immunoprecipitations (IPs) were lysed in HiLo buffer (50 mM Tris pH 7.4, 0.825 M NaCl, 1% NP-40, 2 µg/ml Pepstatin, Antipain, Leupeptin (PAL); these are protease inhibitors used to prevent the activity of protease enzymes, 1 mM Na_3VO_4, 1 mM PMSF, 1 mM NaF). Cells were washed with ice cold PBS (1x) and 1 ml of lysis buffer was added to each 10 cm tissue culture dish. The dishes were then left on ice for one minute, before the cells were scraped and lysates were then aspirated using a 1 ml Gilson pipette and transferred to pre-chilled eppendorf tubes. Cells which were grown in 10 cm dishes, which were used in vitro kinase assays were lysed in Triton lysis Buffer (TLB) (20 mM Hepes,pH 7.5, 137 mM NaCl, 25 mM β-glycerol phosphate, 2 mM sodium pyrophosphate (NaPPi), 2 mM EDTA, 10% glycerol, 1% Triton X-100, 2 µg/ml Pepstatin Antipain, Leupeptin (PAL), 2 mM benzamidine, 0.5 mM DTT, 1 mM Na_3VO_4, 1 mM PMSF, 1 mM NaF). After treatments the dishes were washed with 2 ml of cold 1x PBS. The PBS was removed and 1 ml of TLB with protease inhibitors was added to each dish and allowed to incubate on ice for 1 min.

The cells were scraped and lysates were pelleted at 14,000 x g for 10 min at 4°C. The supernatant was removed and placed in a clean eppendorf tube and left on ice until time for use.

2.3.6. Sonication and Centrifugation

Cell lysates which were used for immunoprecipitation were sonicated in methanol/dry ice using Soniprep 150 (10 mm probe, amplitude 12 µm) using 3 cycles of 15 sec sonication bursts at 200-300 W followed by cooling for 10 sec in 1.5ml tubes. The lysates were then centrifuged at 13,000 rpm in a sorvall SS34 rota for 20 min at 4°C. The lysates were then aspirated into a syringe through a 25G needle taking the layer between the upper lipid layer and the precipitated material. This was placed in a fresh clean tube and repeated to ensure the purity of the lysate. These were then placed on ice until they were ready for use.

2.4. Molecular Biology Techniques

2.4.1. Generation of chemically competent E. coli Cells

The principle of preparing competent E. coli (DH5α and BL21-DE3) cells is to enable cells walls to become permeable in order to facilitate DNA to enter easily. This is done by suspending E. coli cells in a calcium solution which creates pores in the cells to make them competent (Chung et al., 1989). E. coli (DH5α) were streaked onto LB-agar and incubated overnight at 37 ºC. A single colony was picked and used to inoculate 5 ml of Luria Bertani (LB) broth which was grown without ampicillin at 37ºC with shaking at 255 rpm overnight. An aliquot of the overnight culture (1 ml) was placed into a flask incubated with, 100 ml of fresh LB and grown to an OD_{600nm} between 0.4-0.45 (approx. $2x10^8$ cells/ml). The culture was then chilled on ice for 10 min and transferred to two pre-cooled 50 ml falcon tubes for centrifugation at 3000 x g for 5 min at 4 ºC. The supernatant was discarded and the pellet was resuspended gently in 25 ml of ice-cold 20 mM $MgCl_2$ using a pipette which was pre-cooled. The cells were centrifuged again and resuspended in 25 ml of ice-cold 0.1 M $CaCl_2$. The suspension was incubated on ice for 2 hr and pelleted again as before. The pellet was resuspended gently in 5 ml 0.1 M $CaCl_2$ with 15% glycerol and left to incubate on ice for 10 min. The cells were aliquoted into eppendorf tubes, snap frozen in liquid nitrogen and stored at -80 ºC.

2.4.2. Transformation of DH5α *E. coli*

Plasmid DNA (1 µl) was added to 50 µl competent E. coli (DH5α) and incubated on ice for 30 min. The bacteria were then heat shocked for 2 min at 42ºC and placed on ice for 2 min. The bacteria were then incubated in 500 µl LB broth with shaking at 245 rpm for 1 hr at 37 ºC. Aliquots of the culture (50 µl and 200 µl) were then plated onto LB-agar with appropriate antibiotics and incubated overnight at 37ºC. Single colonies were picked and inoculated into LB broth prior to miniprep and restriction digestion analysis.

2.4.3. Preparation of Glycerol Stocks

Overnight E. coli cultures were mixed with 0.5 ml sterile LB/50 % glycerol in cryotubes and stored at -80 ºC.

2.4.4. Small-scale Preparation of Plasmid DNA

Small scale plasmid preparation was carried out using the QIAprep Spin Miniprep Kit. A single colony was picked from a plate of transformed E. coli (DH5α) and used to inoculate 5 ml overnight LB- medium at 37 ºC with shaking (225 rpm). The bacterial cells were then pelleted by centrifugation at 13,000 x g for 2 min in an eppendorf tube at room temperature. The supernatant was removed and the pelleted cells resuspended in 250 µl P1 buffer containing RNase A which is used to remove any RNA present. The cells were then lysed in 250 µl P2 buffer and mixed thoroughly but gently by inverting the tube, ensuring the lysis reaction did not continue for over 5 min. Buffer N3 (350 µl) was added and mixed by inverting the tube. The mixture was centrifuged at 13,000 x g for 10 min in a bench-top centrifuge. The supernatant was then placed in a QIAprep spin column and centrifuged for 1min. The flow-through was discarded and the spin column was washed with 0.75 ml buffer PE and centrifuged again for 1 min. The column was placed in a clean microcentrifuge tube and the DNA was eluted by centrifugation for 1 min with 50 µl buffer EB (10 mM Tris-Cl, pH 8-8.5) and centrifuged for 1 min.

2.4.5. Large Scale Preparation of Plasmid DNA (Caesium Chloride Method)

A single bacterial colony was used to inoculate 10 ml LB broth containing the appropriate antibiotics and left to grow overnight. Fresh LB broth (500 ml) with appropriate antibiotics

was inoculated with 0.5 ml of the overnight culture and left to grow overnight at 37 ºC with shaking at 225 rpm. The bacteria were pelleted by centrifugation at 5,000 rpm for 10 min. The supernatant was removed and the cell pellet resuspended in 20 ml P1 solution (50mM Tris-HCl, pH 8.0, 10 mM EDTA, 100 µg/ml RNase A) which removes the presence of RNA. The suspension was then lysed in 20ml P2 solution (200 mM NaOH, 1% SDS) which denatures DNA and destroy the cell membrane, and was left to incubate for 5 min before being neutralised in 20ml of ice-cold P3 solution (3.0 M KAc pH 5.5) which renatures the plasmid DNA was added. The mixture was centrifuged at 5,000 rpm for 10 min. The supernatant was collected and filtered through cheesecloth and the pellet discarded. Plasmid DNA was precipitated with 0.7 volumes of isopropanol and collected by centrifugation at 10,000 x g for 10 min. The pellet was dried and resuspended in 5.5 ml Tris-EDTA (10mM Tris pH 7.9/1 mM EDTA). Caesium chloride (6 g) was added along with ethidium bromide (5 mg/ml) to the resuspended pellet and the mixture centrifuged at 6,000 x g for 5 min to remove insoluble material. The solution was then loaded into Beckman heat sealable tubes and centrifuged overnight in the Beckman ultra centrifuge at 540,000 x g at 20 ºC. Isolation of the supercoiled plasmid DNA (lower band) was carried out with the use of a needle and syringe. The ethidium bromide was removed by solvent extraction using several washes of water-saturated butanol. Plasmid DNA was precipitated with 6 volumes of ethanol and placed at -20 ºC before centrifugation at 10,000 rpm for 30 min, then washed with 70% ethanol. DNA concentration was calculated by the measurement of absorbance at 260 nm.

2.4.6. Restriction Enzyme Digestion

To verify the identity of the plasmid, a 1µl aliquot of plasmid approx. 2µg DNA was digested with appropriate restriction enzymes in appropriate buffers in a final volume of 10 µl for 2 hr at 37 ºC. The digested products were then separated by agarose gel electrophoresis in a 0.8% gel.

2.4.7. Site Directed Mutagenesis

2.4.7.1. Oligonucleotide Design

Oligonucleotides used for site directed mutagenesis were 29 bp in length. Both of the primers consisted of the desired mutation, on opposite strands of the plasmid. The mutation was in the middle region of the primer with 10-15 bases of correct sequence on either side (**Table 2.4**).

Table 2.4: Oligonucleotides for Site-Directed Mutagenesis. Forward (F) and reverse (R) primers that were used to introduce point mutations into the MS1 sequence in order to test for potential phosphorylation sites.

Oligo Name		Primer Sequence (5' – 3')
MS1- Thr62A	F	GACCTACCTCACGCACCTAAAGAACCGGG
	R	CCCGGTTCTTTAGGTGCGTGAGGTAGGTC
MS1- Thr62E	F	GACCTACCTCACGAGCCTAAAGAACCGGG
	R	CCCGGTTCTTTAGGCTCGTGAGGTAGGTC
MS1-Ser77A	F	CCCAAACCTCCGGCACCAAAGCCAGATGG
	R	CCATCTGGCTTTGGTGCCGGAGGTTTGGG
MS1-Ser77D	F	CCCAAACCTCCGGATCCAAAGCCAGATGG
	R	CCATCTGGCTTTGGATCCGGAGGTTTGGG

2.4.7.2. Site Directed Mutagenesis Reaction

Site-directed mutagenesis was carried out according to the manufacturer's protocol, using the Quikchange site-directed mutagenesis kit (Stratagene Cat No. 200519). Primers were designed under the guidelines of the manufacturer's protocol in order to carry out the desired mutation. The sample reaction for PCR was set up containing 1x reaction buffer, 50 ng of dsDNA template (Flag-MS1 or his-tagged MSD1), 125 ng of oligonucleotide primer 1, 125 ng of oligonucleotide primer 2, 1 µl of dNTP (10 mM) and the volume was made up to 50µl with ddH_2O. After mixing, 0.05 U of PfuTurbo DNA polymerase was added to the reaction mix. The PCR reaction was carried out for 1 cycle at 95 °C for 30 seconds, followed by 16 cycles, at 95 °C for 30 sec 55 °C for 1 min and 68 °C for 5 min. After completion of temperature cycling, the reaction was placed on ice for 2 min. The amplified reaction mixtures were then incubated with 1µl Dpn 1 restriction enzyme (10U/µ) and left

to incubate at 37 °C for 1 hr. After incubation the Dpn 1 treated DNA (1 µl) product was transformed into Xli-blue super competent bacteris according to the protocol supplied with the kit. A miniculture was set up from one colony of the transformed bacteris and plasmid DNA extracted using a miniprep kit (QIAGEN). Confirmation of the mutation was verified by sequencing carried out by PNACL. After confirmation of mutants, they were transformed in BL-21-DE3 or DH5α E. coli.

2.4.8. Luciferase Assay

H9c2 cells were transfected with either pGL3-Basic empty vector or pGL3-MS1. After 24 hr cells were treated with appropriate treatments (**Section 2.3.4**) and then lysed as described in the Promega kit protocol for luciferase reporter assays (E1900). Then, pretreated (**as described in Section 2.5.11**) to remove interfering substances for the determination of the protein concentration. The luminescence from the firefly enzymes were measured using a spectrophotometer.

2.5. Biochemical and Cell Biology Techniques

2.5.1. Immunoprecipitation

Immunoprecipitation is a method used in order to isolate a protein antigen out of solution with the use of an antibody specific to the protein of interest. 20 µl of Protein G-sepharose 4B Fast Flow beads (Sigma P3296) was used for each immunoprecipitation (IP). The beads were resuspended in 1 ml of 1x PBS (3 times) and pelleted by brief centrifugation. After the PBS was removed from the beads, 5µg of antibody Anti-HA, Anti-Flag or IgG (Rabbit or mouse) were added to each tube and left to tumble overnight at 4°C. The tubes were removed from the cold room after overnight tumbling and left to incubate at room temperature for 30min before the lysates were added. Lysates were made after appropriate stimulation of the transfected cells, based on the method mentioned previously (**Section 2.3.5**). Aliquots of the clarified lysate (100 µl) were placed in clean eppendorf tubes while the remainder of the lysate was added to tubes containing antibody bound to protein G-sepharose beads. The beads were left to incubate with the lysates with tumbling for 3 hr at 4°C. The beads were then centrifuged briefly and washed three times with 1 ml of appropriate lysis buffer (either HiLo buffer for Co-immunoprecipitations or TLB for in

vitro Kinase assays). The samples for the in vitro kinase assay were placed on ice until required for use. The samples used for western blotting were taken up in 50 µl of 2x SDS-PAGE sample buffer. In some immunoprecipitation experiments 2x sample buffer without DTT was used with heating at 100 ºC for 5 min in order to prevent bonds of the IgG heavy and light chains breaking.

2.5.2. *In vitro* Kinase Assay

After immunoprecipitation of the samples as previously mentioned (**section 2.5.1**), the pelleted beads were then resuspended in kinase buffer without ATP (25 mM Hepes pH 7.4, 25 mM β-glycerophosphate, 25 mM $MgCl_2$, 0.5 mM Na_2VO_4, 0.5 mM DTT). The appropriate protein substrate, 50 µM cold ATP (added to increase ATP concentration so reaction is optimal), 2 µl [γ-P^{32}] ATP were made up as a master mix in 100 µl kinase buffer and 50 µl was added to immunocomplexes from stimulated and unstimulated cells. Tubes were left to incubate for 30 min at 30 °C. After incubation, reactions were terminated by the addition of 25 µl of 3x SDS-PAGE sample buffer and then boiled for 5 min at 100ºC prior to SDS-PAGE (sodium dodecyl sulphate polyacrylamide gel electrophoresis) and autoradiography/phosphoimager analysis. Samples were either run immediately on a SDS-PAGE gel or stored at -20°C to run on gels the next day.

2.5.3. Sodium dodecyl sulphate – Polyacrylamide Gel Electrophoresis (SDS-PAGE)

Cells were removed from the incubator and extracted in 2x sample buffer (6x: 0.35 M Tris pH 6.8, 0.25 % bromophenol blue, 10 % SDS, 0.6M DTT, 30 % glycerol) and boiled for 5-10 min at 100 ºC. The protein in cell lysates were loaded and resolved on appropriate sodium dodecyl sulphate polyacrylamide gels as seen below in **Table 2.5** and **Table 2.6** along with prestained Precision plus protein molecular weight markers (Biorad). The proteins present in the sample were separated by electrophoresis for approximately 2 hr 30 min at 150 V using the Laemmli method, 1970. The percentage of the acrylamide gel used was based on the molecular weight of the protein as seen in the tables below (**Table 2.5 and 2.6**).

Table 2.5: Table shows separating gel composition of the different percentage SDS-PAGE gels.

Percentage Gel	**10%**	**12%**	**15%**	**20%**
H_2O	18 ml	16.2ml	13.5ml	9ml
1.5M Tris ,pH 8.8	9 ml	9ml	9ml	9ml
30% Acrylamide	9 ml	10.8ml	13.5ml	18ml
SDS (10%)	100 µl	100 µl	100 µl	100 µl
APS (10%)	300 µl	300 µl	300 ml	0.30ml
TEMED	14 µl	14 µl	0.014ml	0.014ml

Table 2.6: Table shows the stacking gel composition.

Reagents	**Volumes**
H_2O	6.4 ml
0.5M Tris-HCl pH 6.8	2.5 ml
30% Acrylamide	2 ml
APS (10%)	0.1 ml
TEMED	5 ml

2.5.4. Coomassie Staining of SDS-PAGE Gels

This method allows for proteins to be visualized by the coomassie brilliant blue dye binding to all proteins which are present in gels. Coomassie staining of gels was carried out using coomassie stain solution (0.1% w/v) of Coomassie brilliant blue G250 overnight (**Table 2.3**). The gels were then destained with destain solution (7% (v/v) acetic acid, 25% (v/v) MeOH) for several hrs and a picture taken using GenSnap and dried using a gel dryer (Biorad) at 80 ºC for 2 hr.

2.5.5. Western Blotting

SDS-PAGE gels with the resolved proteins present were removed after electrophoresis and soaked in Western Transfer Buffer and the proteins were transferred to nitrocellulose

membrane (Whatman) or Immobilon P (Millipore) by electroblotting using a semi-dry transfer apparatus (Biorad) running at 22V for 60 min. The membrane was washed briefly for 10 min in Tris buffer saline with tween TBST (0.2% (v/v) Tween-20, 50 mM Tris, 150 mM NaCl, pH 7.4). The membrane was then blocked for 1hr in TBST/ 3% BSA (0.2% (v/v), 50 mM Tris, 150 mM NaCl, pH 7.4, 3% BSA (w/v)) or milk / TBST (5% w/v) semi-skimmed milk 0.1% Tween-20 50 mM Tris, 150 mM NaCl; pH 7.4) depending on the antibody used and the manufacturer's instructions. The primary antibody was then diluted for 1 hr or overnight (**Table 2.7**). The solution of primary antibody was removed and the membranes washed three times for 15 min with 1x TBST. HRP-conjugated secondary antibodies (**Table 2.8**) were diluted with 3% (w/v) BSA/ TBST or 5% (w/v) milk/TBST and added to the membrane to incubate for 1 hr and then washed with 1x TBST over a 15 min period for 1 hr.

The tables below show the antibodies and their dilutions of the antibodies indicated on next page:

Table 2.7: Table shows primary antibodies used for western blotting with their respective catalogue numbers, dilutions and incubation times.

Antibody	Company	Cat. No.	Dilution	Incubation
Actin	Sigma	A4700	1:1000	Overnight,4°C
His	Sigma	H1029	1:1000	Overnight,4°C
Flag	Sigma	F1804	1:2000	Overnight, 4ºC
Flag	Sigma	F3165	1:2000	Overnight, 4°C
HA	Santa Cruz Biotechnology	Sc805	1:2000	Overnight, 4°C
ERK	Santa Cruz Biotechnology	Sc 94	1:1000	Overnight, 4°C
Phospho-ERK	Cell Signalling Technology	9101S	1:1000	Overnight, 4°C
P38	Santa Cruz Biotechnology	Sc728G	1:2000	Overnight, 4°C
Phospho-p38	Cell Signalling	9215S	1:1000	Overnight, 4°C

	Technology			
JNK	Santa Cruz Biotechnology	Sc571	1:2000	Overnight, 4°C
Phospho-SAPK/JNK	Cell Signalling Biotechnology	9255	1:2000	Overnight, 4°C
Rho-V	Santa cruz	Sc160741	1:1000	Overnight, 4°C
α-tubulin	Sigma	T5168	1:2000	Overnight, 4°C
γ-tubulin	Sigma	T6557	1:2000	Overnight, 4°C
GFP	Sigma	G6539	1:2000	Overnight, 4°C
STARS	Abcam	Ab21986	1:1000	Overnight, 4°C
MS1	Cambrid*ge* Research Biochemicals		1:2000	Overnight, 4°C

Table 2.8: Secondary Antibodies

Antibody	Company	Cat No.	Dilution	Incubation
Anti-Mouse IgG HRP	Jackson Immunoresearch laboratories	115-035-146	1:10000	1hr , RT
Anti-Rabbit IgG HRP	Jackson Immunoresearch laboratories	115-035-144	1:20000	1hr,RT
Anti-Goat IgG HRP	Jackson Immunoresearch laboratories	305-036-003	1:5000	1hr, RT

2.5.6. Enhanced Chemiluminescence (ECL

Blots were then developed using Enhanced Chemiluminescence (ECL) reagent which was 20 µl of solution A (Table 2.3) and 50 µl of solution B (Table 2.3) to 0.1 M Tris pH8.5,

which was followed by 3 µl H_2O_2 and incubated for 1 min. The membrane was then wrapped in saran wrap and exposed to x-ray film (Fuji).

2.5.7. Reprobing Immobilon P or Nitrocellulose Membrane

In order to re-probe a membrane with different antibody, the memebrane was stripped using a stripping buffer. Blotted membranes were first washed with 1x TBST to remove chemiluminescent substrate (**Table 2.3**) and incubated in blot strip buffer for 1 hr at 55 ºC with agitation. The buffer was then removed and the membrane was washed 3 times in 1x TBST for 15 min each wash at room temperature. The stripped membrane was then blocked before the addition of antibodies.

2.5.8. MS1 Fusion Protein Production and Purification

2.5.8.1. MS1 Fusion Protein Expression

Expression plasmids which were used were gifts from Dr. Mark Pfuhl's Laboratory. pETM-11 expression plasmids were transformed in BL21-DE3 E. coli or Arctic Express E. coli for fusion protein expression of His-tagged MS1 or GST-MS1. A single colony from transformation experiments was used to inoculate 10 ml of fresh LB-medium which was supplemented with antibiotics. Cells were left to grow overnight at 180-225 rpm at 37 ºC. Saturated culture (1 ml) was used to inoculate 500 ml of fresh LB-medium with appropriate antibiotics. The saturated culture was then added to 2 litres of fresh LB-medium and left to grow for 1 hr with appropriate antibiotics. Expression of fusion proteins by IPTG induction was done at 37 ºC with shaking for 6 hr or at 13 ºC with shaking for 18 hr.

2.5.8.2. Protein Purification of His-tagged MS1/STARS fusion proteins

Columns which contained charged Nickel Sepharose 6 Fast Flow Resin (GE Healthcare) (2 ml), were used to purify each of the his-tagged proteins. Recombinant-protein expressing cells were resuspended in FF6 wash buffer (20 mM Na_2HPO_4, 20 mM NaH_2PO_4, 500 mM NaCl, 10 mM Imidazole, 100 µl BME, 0.02% NaN_3) and cells were then extracted in a French Press and spun down for 90 minutes at 18000 rpm (Beckman JA25.50 rotor in a Beckman Coulter Avanti J-30 I centrifuge or Sorvall SS34 rotor in a Sorvall Evolution RC centrifuge).

The Columns which contained the nickel chelating sepharose 6 Fast Flow resin were prepared by first washing 4 column volumes (4 x 12 ml) of FF6 wash buffer. The supernatant from the centrifugation previously mentioned was diluted with FF6 wash buffer by 50% and poured over the charged nickel sepharose columns and allowed to elute by gravity. A sample of the flow-through (20 µl) was collected to run on an SDS-PAGE gel. The column was then washed 4 times with FF6 wash buffer and those fractions were also collected where a sample of the wash fractions (20 µl) was taken to run on an SDS PAGE gel. After the resin with the bound his-tagged protein was washed, a column volume (12 ml) of FF6 elution buffer (20 mM Na_2HPO_4, 20 mM NaH_2PO_4, 500 mM NaCl, 500 mM Imidazole, 100 µl BME, 0.02% NaN_3) was used to elute the protein of interest. The sample was collected and 20 µl was taken to run on an SDS PAGE gel. Samples which required a further purification step were concentrated up using vivaspin concentrators and left to dialyze overnight.

2.5.8.3. Protein Purification of GST-tagged Proteins

For GST-tagged protein purification, pellets from recombinant-protein expressing bacteria (**Section protein 2.5.8.1**) were resuspended in extraction buffer (20 mM Tris pH7.4, 1 M NaCl, 0.2 mM EGTA, 0.2 mM EDTA with protease inhibitors and βeta-mercaptoethanol), followed by sonication on methanol/dry ice using soniprep (150, 10mm probe, amplitude 12 µm) using 3 cycles of 15 sec sonication bursts at 200-300 W followed by 10 sec cooling. The cell lysate was then clarified by centrifugation at 20,000 x g for 20 min at 4°C. After centrifugation the clarified supernatant was dialysed against the column buffer (1 M NaCl, 2.7 mM KCl, 10 mM Na_2PO_4, 1.8 mM KH_2PO_4 pH 7.3). Protein concentration was determined before the addition of the protein to the glutathione sepharose by the BCA assay (Section 2.5.12). 1 ml of glutathione sepharose (GE Healthcare; 17-0756-01) was washed in the column buffer and the supernatant was added. The supernatant (GST-MS1) was left to tumble with the sepharose for 2 hr at 4°C. After tumbling, the slurry was removed and placed in a 10 ml column to settle. The flowthrough was collected and the beads were washed repeatedly (3 times) in the column buffer with 0.1% Triton X-100. The beads with the bound GST-tagged protein, was eluted with elution buffer (100 mM Hepes pH 8, 50 mM reduced glutathione (Sigma; G-4251), 0.2 M NaCl and 0.1% Triton- x100).

The protein was eluted in 500 µl aliquots. After elution a protein assay was performed to determine the concentration and the fractions were run on a gel along with a sample of the beads to ensure the protein had eluted. The fractions were then pooled together and allowed to dialyze against the buffer required for coupling for NHS-activated sepharose (0.2 M $NaHCO_3$, 0.5 M NaCl, pH 8.5).

2.5.8.4. Buffer Exchange

Proteins were placed in dialysis membrane (spectrapore) of an appropriate molecular weight cut off according to their molecular weight. The protein of interest was then dialyzed against the desired buffer with at least 2 changes done overnight in a 4L or 5L beaker.

2.5.8.5. Purification by Gel Filtration

Further purification, if required, was done by gel filtration chromatography. Gel filtration, is a known chromatographic technique which separates proteins based on size exclusion. The column is packed with a resin which allows for proteins smaller than its pore size to be trapped, while larger proteins will elute faster through the column. Proteins which required a further purification step were dialyzed against Gel filtration buffer (20 mM NaH_2PO_4, 20 mM Na_2HPO_4, 250 mM, NaCl, 2 mM DTT, 0.02% NaN_3) prior to purification by size exclusion chromatography. This was done with a Superdex 75 HiLoad 16/60 prepacked column (GE Healthcare) with a volume capacity of 120 ml. Äkta Purifier 9 and Unicorn software (GE Healthcare) was used to carry out this process. The concentrated protein (5 ml) was left to run on the column at a flow rate of 1 ml/min for 120 ml. Flow through was collected in 5 ml aliquots. Samples were taken from each aliquot and separated by SDS PAGE to determine which aliquots should be pooled together.

2.5.9. Protein Concentration of proteins using concentrators

Protein concentrators (Vivaspin 500) of appropriate molecular weight cut-offs were used to concentrate MS1 proteins after purification and dialysis. Water was first added to the concentrators and left to spin at 2000 rcf at 4 °C for 20 min in an Eppendorf 5804R centrifuge. After, the protein was poured in the concentrator and centrifuged at 2000 rcf, 4

°C for 20 min. The protein concentration was then checked before use and centrifugation was repeated as required.

2.5.10. Coupling of Fusion Protein to NHS-activated Sepharose.

1 ml of N-hydroxysuccinimide (NHS)-activated sepharose beads (GE Healthcare) were washed twice with dH_2O then washed 10-15 times with cold 1 mM HCl (pH 8.5). The washed sepharose was incubated with the dialyzed protein of interest of known concentration and left to tumble overnight at 4°C. After coupling, the beads were pelleted at 2000 rpm for 1 min at 4ºC and the supernatant was removed. The beads coupled with protein was left to incubate with cold blocking buffer (0.5 M ethanolamine, 0.5 M NaCl pH 8.5) which was used to block any non-reacted groups present on the sepharose for 2 hrs at 4ºC. The coupled protein bound sepharose was then pelleted by centrifugation. The medium was then washed alternating between two different buffers, a high pH (alkaline) buffer (0.1 M Tris-HCl, pH 8.5) and a low pH (acidic) buffer (0.1 M acetate buffer, 0.5 M NaCl pH 4.5). The washing was done 3 times with alkaline buffer, followed by three washes with acidic buffer, which was 5 times to remove any unwanted proteins. After subsequent washes the coupled medium was then placed in 1x PBS with 20 mM NaN_3 which is an inorganic preservative used to avoid any microbial contamination at 4 °C until ready for use. Samples of the supernatant were collected during the coupling process and run on a SDS-PAGE gel to determine that the protein was successfully coupled to the NHS-activated sepharose.

2.5.11. Pretreatment of Protein Samples for Protein Assays

Compat-Able pretreatment kit (Thermo scientific) was used to treat samples which might contain any interfering substances which would not be compatible with the BCA assay kit. The protocol was followed based on the manufacturer's instructions. 50 µl of each protein sample was placed in a clean microcentrifuge tube. 500 µl of CompatAble protein assay reagent 1 was added to each tube, mixed and allowed to incubate at room temperature for 5min. 500 µl of Compat-Able protein assay reagent 2 was then added to each of the tubes and centrifuged using the benchtop centrifuge at 10,000 x g for 10 min at 4 °C. After centrifugation the supernatant was discarded and the pellet was either stored in the fridge

until ready for use or resuspended in 50 µl of 1X PBS. Samples were then ready to be assayed.

2.5.12. BCA Protein Assay

The concentration of protein samples was carried out using the Thermo scientific Pierce BCA Protein Assay kit (Cat no. 23225) according to the manufacturer's instructions. They were assayed for protein concentration spectrophotometrically at an absorbance of 565 nm. A standard curve of bovine serum albumin (BSA) containing a range between 2-30 µg of protein was used to create a standard curve to calculate the protein concentration.

2.5.13. Preparation of Mouse Heart Extracts for Isolation of MS1 interacting proteins

1-2 mouse hearts were removed from the -80°C and washed with ice cold PBS (1x). The hearts were then homogenized in 1-1.5 ml TLB (20 mM Tris, pH 7.5, 137 mM NaCl, 25 mM βeta-glycerophosphate, 2 mM sodium pyrophosphate (NaPPi), 2 mM EDTA, 10% glycerol, 1% Triton X-100, 2 µg/ml Pepstatin Antipain, Leupeptin (PAL), 2 mM benzamidine, 0.5 mM DTT, 1 mM Na_3VO_4, 1 mM PMSF, 1 mM NaF) or Guba-straub buffer (50 mM KH_2PO_4, 100 mM K_2HPO_4, 300 mM KCl, 1 mM EDTA, pH 6.7). After homogenization, the extract was left on ice for 15 min before centrifugation at 14,000 rpm for 20 min at 4°C in the Eppendorf centrifuge model 5417R. After the pelleting of debris and tissue the supernatant was transferred to a clean pre-chilled 1.5 ml eppendorf tube. The protein concentration was determined using the BCA assay

2.5.14. Binding Assay

Protein coupled to NHS-activated sepharose or NHS-activated sepharose without coupled protein were removed from the fridge and washed in appropriate buffer (based on what the extracts were made in or purified proteins). ~10 mg of mouse heart extract was added to coupled sepharose beads and left to tumble for 2hrs at 4°C. After the incubation with the extract the sepharose beads were pelleted at 2000 rpm for 15 sec. The supernatant was removed and an aliquot (200 µg) was taken to run on a gel. The pelleted sepharose was then placed in a 5ml column and the sepharose was washed with 3-4 column volumes of 1x TLB (**Recipe previously mentioned in section 2.3.5**). After the final wash, elution buffer

(50 mM sodium acetate, 0.5 M NaCl pH4.5 or 0.1 M glycine-HCl; pH 2.5) was added to the column which was twice the volume of the sepharose. Tris-Base (1 M) pH 8 (one tenth the volume of the eluted protein) was added to prechilled eppendorf tubes to neutralize the proteins which were eluted. After eluting the attached protein 2X SDS-PAGE sample buffer was added to each sample and boiled for 5 min at 100°C. The samples were later run on a SDS-PAGE gel and coomassie stained before being taken to PNACL for mass spectrometry analysis.

2.5.15. Extraction of Actin from Sheep Cardiac Muscle Acetone Powder

100 ml of G-actin buffer (2 mM Tris-HCl pH8, 0.2 mM ATP, 0.1 mM $CaCl_2$, 0.5 mM DTT, 1mM NaN_3) was added to 5 g of minced sheep cardiac muscle acetone powder and left to stir slowly for 30 min. The mixture was then centrifuged at 18000 rpm for 20 min at 4 °C using the Sorvall RC5C centrifuge. The supernatant was then filtered through glass fibers and the pellet was resuspended in G-actin buffer to repeat the process. The supernatants were pooled together and a volume of 10x KME buffer (100 mM tris HCl pH8, 500 mM KCl, 25 mM $MgCl_2$, 10 mM EGTA, 10 mM NaN_3) which represented a tenth of the supernatant volume was added to allow for polymerization of G-actin, which was left to incubate in a water bath at 30 °C for 2 hrs. The solution was brought to a concentration of 0.8 M KCl and left to stir slowly for 20 min at room temperature. The mixture was then centrifuged at 43,000 rpm for 90 min at 4°C using the T865 ultra centrifuge. After centrifugation, the supernatant was discarded and the F-actin pellets were washed with dH_2O and then left to soak over weekend in ATPase buffer. The pellets were then resuspended and the protein concentration was checked. The remaining pellets were soaked in G-actin (10 ml) and left to dialyze for 48 hr against G-actin to remove any contaminants and depolymerise the actin. The concentration was determined spectrophotmetrically at 290 nm. Fractions which produced a peak at 290 nm were pooled together and polymerised using 0.1 volumes of 10 x KME buffer and then incubated at 80 ºC for 45 min. The mixture was then centrifuged at 42, 000 rpm using a T1250 rotor for 2 hr at 4ºC. Pellets were resuspended in 5 ml ATPase buffer and stored at 4 ºC.

2.5.16. Actin Co-sedimentation Assay

Co-sedimentation experiments were carried out to determine the binding of actin to the different purified MS1/STARS protein fragments in the presence of myofibrillar proteins (Kind gifts from Dr. Mohammad El-Mezgueldi, University of Leicester). 10 µM of actin was diluted in actin binding buffer (10 mM tris pH 7.5, 0.2 mM DTT, 1 mM EGTA, 0.1 mM $CaCl_2$, 2 mM $MgCl_2$, 50 mM KCl) which was added to protein(s) of interest which were made up to a volume of 100 µl in actin binding buffer with protease inhibitors. A negative control was the actin without any other proteins added, while the positive control was the actin mixed with a known expressed fragment of MS1 which is known to bind actin.

The samples were then incubated at room temperature in Beckman polycarbonate centrifuge tubes (7 x 20 mm) for 20 min and then centrifuged for 30 min at 85,000 rpm using a TL-100 Beckman rotor in a Beckman Optima Max E ultracentrifuge. After centrifugation, the supernatants were transferred to eppendorf tubes and (6X SDS PAGE sample buffer was added to each sample (25 µl). The pellets were then resuspended in 125 µl of 1.5x SDS-PAGE sample buffer. Both the pellets and supernatants were boiled at 100 °C for 5 min and loaded on an SDS-PAGE gel (12 %) which was coomassie stained.

2.5.17. Preparation of Coverslips

Glass coverslips with a thickness of approximately 22 µm were first rinsed with distilled water in a glass beaker. The coverslips were then incubated with 1 M HCl for 30 min, followed by thorough rinsing with dH_2O. The acid-treated coverslips were then sterilized by the addition of absolute ethanol for 30 min to overnight. Coverslips were then dried on a piece of clean blue roll and placed in a clean glass beaker, then baked at 240ºC for 4 hrs. After the coverslips were sterilized and cooled, then placed in a sterile 10 cm plate.

2.5.18. Immunofluorescence Microscopy

H9c2 cells were seeded onto acid treated coverslips and grown to 70-80% confluency before transfections were done using the plasmids of interest. 24 hr after transfections the cells were subjected to appropriate treatments. The media was removed and cells were washed once with PBS (1x). The cells were then fixed with 3.7% paraformaldehyde at

room temperature for 20 min. After fixation, cells were washed 3 times with PBS (1x) before adding permeabilization solution (0.1% Triton X-100, 1x PBS) for 10 min. The permeabilization buffer was removed and the cells were then blocked in 3% BSA (w/v) in PBST (1x PBS, 0.1% Triton X-100 (v/v), Tween-20) for 30 min at room temperature. For staining of actin filaments, Phalloidin-Texas Red (1:50 dil) was added directly on coverslips and left to incubate for 30 min. After the incubation, the coverslips were inverted on Nesco film on which 200 µl of anti-Flag (1:200) had been placed, diluted in PBST containing 3% BSA and incubation was performed for 1 hr. The coverslips were removed and washed 3 times with PBS before the addition of secondary antibody (anti-mouse which has been conjugated to a fluorophore. The coverslips were covered in foil and left to incubate for 1 hr. After incubation, coverslips were washed 3 times with 1X PBS and Hoechst 33258 was diluted in PBS, added and left to incubate for 5 min at room temperature in order to stain the nuclei of cells. The coverslips were washed again with PBS three times and mounted onto slides using mounting medium (1% (w/v) DABCO (1,4 diazabizyclo[2.2.2] octane), 90% (v/v) glycerol, in 10% (v/v) 10x PBS) and sealed around the edges with nail varnish.

Images were captured using the Nikon TE300 inverted fluorescence microscope at the cell imaging facility (in the Department of Biochemistry, University of Leicester).

Chapter 3. Investigation of MS1 regulation by Western blot analysis and promoter studies

3.1. Introduction

Mycocyte stress 1 protein (MS1) is known to be a stress responsive, muscle specific protein where the mRNA levels increased in response to cardiac hypertrophy as a result of aortic banding which leads to pressure overload (Arai *et. al*.,2002 and Mahadeva *et al.*,2002) .

Previous work in the lab showed that MS1 mRNA increases as a result of simulated ischaemia/reperfusion injury (Hay, unpublished). During ischaemia/reperfusion injury it is known that the MAP kinases JNK, p38 and ERK all become activated at different points during this process (Vassalli *et al.,* 2012). Experiments using inhibitors of MAP kinase pathways identified JNK as a potential kinase involved in MS1 mRNA expression during simulated ischaemia/reperfusion (Hay, 2006). Although these studies demonstrated that MS1 expression increases at the mRNA level, it was not known whether this increased mRNA was being translated into protein.

Since MS1 mRNA expression is known to increase during left ventricular hypertrophy it was of interest to determine which pathways may be involved in the increase of MS1. This would also allow for the possibility of determining what potential role it could play during hypertrophy.

3.2. Aims of this Chapter

We aimed to investigate MS1 expression at the protein level during simulated ischaemia/reperfusion injury by western blotting. This was achieved by using an antibody raised against full length MS1 protein which had been produced in the lab previously. A Second aim was to determine whether the promoter region of MS1 is responsive to cell stress as a result of stress inducers which cause the activation of the JNK pathway such as sorbitol and hypertrophic agonists. This was done using a pGL3-Basic reporter construct containing a 1645bp fragment of the rat MS1 promoter cloned upstream of the firefly luciferase gene (Ouzain *et al*., 2006). The pGL3-Basic promoterless vector was used as a control in these experiments.

3.3. Results

3.3.1. Characterization of MS1 Antisera

In order to determine whether or not MS1 is expressed at the protein level following simulated ischaemia/reperfusion, a reliable antibody was required that would detect endogenous and exogenous levels of protein. At the start of the project, there were no commercial antibodies available for MS1. Therefore full length rat MS1 expressed in *E. Coli* using a pET11-MS1 construct was purified and sent to Cambridge Research Biochemicals Ltd for the production of antisera in rabbits. Two polyclonal antisera were produced MS1 2222 and MS1 2221, and purified by affinity chromatography. Production and purification of these antibodies have been described in a previous study (Jordan. E, 2008). The antibodies were compared by western blot analysis using lysates which were made from HEK293 cells transfected with pCMV-MS1 plasmid DNA. Based on a comparison between the two it, the MS12222 antisera was selected because it produced blots with less non-specific binding (data not shown). The antiserum was repurified using two different methods. In the first of these the antiserum was purified by binding to a His-tagged fusion protein MS1, ABD2 (294-375) which was bound to nitrocellulose membrane (Jordan, E., 2008). The antisera was then eluted from the membrane with sodium citrate buffer pH 2.8 and neutralized with 0.5M Tris Base and TBST and 3% BSA. In the second method, a purified MS1 fragment corresponding to amino acids 294-375 ABD2 was covalently coupled to NHS-activated sepharose beads and was used as an affinity column to purify the antiserum. Bound antibody was eluted using 20 mM sodium citrate pH 2.8 and subsequently neutralized with 0.5M Tris (Jordan, E., 2008). The antiserum used for western blotting in this section was purified using the first method.

3.3.1.1. Detection of Exogenous MS1 in HEK293 cells

The availability of an antibody that detects the MS1 protein at the correct molecular weight when overexpressed in cells, and also the endogenous protein, is important for the characterization of the protein. A reliable antibody which is specific and does not detect non-specific bands is also important for western blot analysis. Therefore we did a comparison using a newly available commercial antibody with the antisera which we had produced and purified. HEK293 (human embryonic kidney) cells were used for

transfections as they do not express MS1, and only overexpressed MS1 would be detected. They also have a good transfection efficiency. These cells were transfected with a pCMV-Flag-tagged MS1 construct (**Chapter 2.3.3.3**) and varying amounts of the cell lysate were analysed by western blotting using anti-Flag antibody (**Chapter 2.5.5**), the commercially available anti-MS1 antibody from abcam and purified MS1 2222 (**Figure 3.1**). Different volumes of cell lysate were used to determine what volume would generate the best signal with the antibody. The western blot shows a band of ~45kDa which is the predicted molecular weight of MS1, detected by the antiserum MS1 2222, in the extract from transfected cells but not in the untransfected. The antiserum detects two bands which are quite close in size at ~45kDa. The lower band was probably due to a proteolytic cleavage of MS1 protein. The commercial antibody Abcam was used did not detect the overexpressed Flag-MS1 and had many non-specific bands present on the blot (**Figure 3.1**). In subsequent experiments the antiserum made by Cambridge Research Biologicals and repurified by myself was used. The probe for α-tubulin was used as a loading control..

3.3.1.2. Expression of Endogenous MS1 in H9c2 cells during Simulated Ischaemia/Reperfusion Injury.

The initial aim of this experiment was to determine whether the increase in MS1 mRNA observed following simulated ischaemia/reperfusion correlates to what is seen at the protein level. In order to carry out this experiment we used H9c2 cells, which are rat cardiomyoblasts. This cell line was used previously in the mRNA studies and is widely used for in vitro studies focusing on cardiac diseases, as they have been derived from embryonic rat ventricular tissue (Hescheler *et al.,* 1991) and mimic cardiomyocytes due to the morphology of the membrane, and the GPCR proteins which are expressed (Hall and Lefkowitz, 2002).

In a series of three independent experiments we wanted to determine whether the antisera would be able to detect endogenous MS1 during simulated ischaemia/reperfusion injury in H9c2 cells. The experiments were carried out under the same conditions where the cells were initially subjected to 1 hr simulated ischaemia and then transferred into “reperfusion” buffer for different lengths of time as explained in **Chapter 2**. The cells were then solubilised in sample buffer and extracts loaded onto a gel, together with a positive control

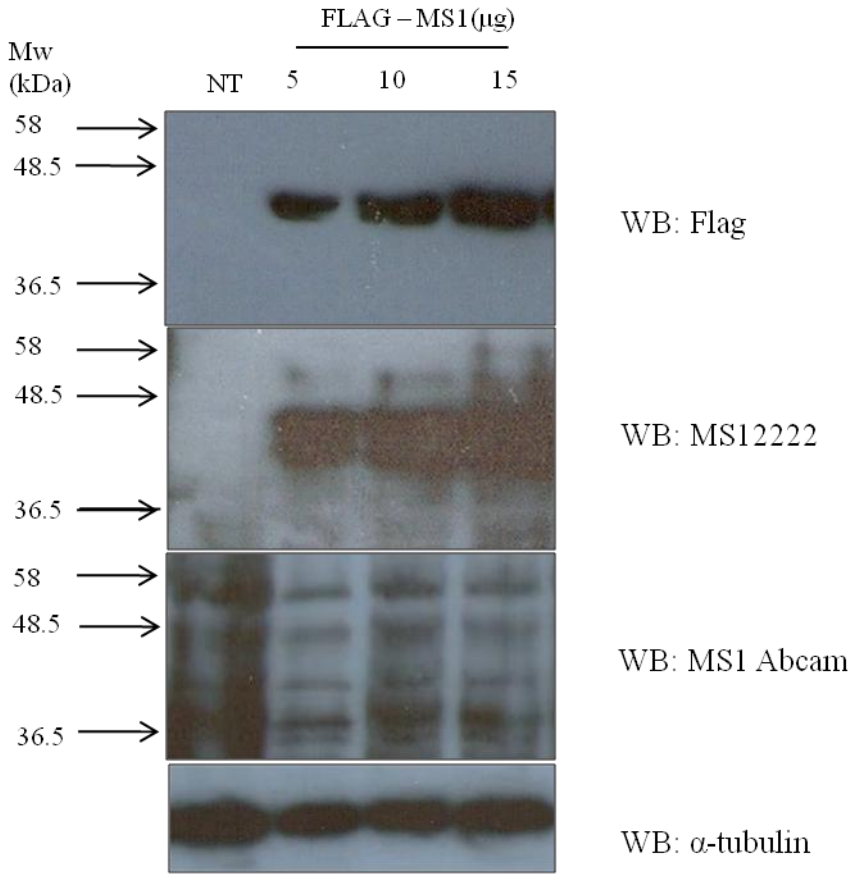

Figure 3.1: Western Blot Analysis of MS1 overexpressed in HEK293 cells
HEK 293 cells were seeded in a 6 well plate and grown until ~80% confluency.HEK293 cells were then transfected with ~2µg of pCMV2-FLAG-MS1 plasmid DNA using turbofect transfection rea*ge*nt. The transfected cells were then extracted in 2X sample buffer and analysed by western blotting using anti-Flag, and anti-MS1 2222 and MS1 (abcam) antibodies. Blots were also probed with an anti-α-tubulin antibody. Non-transfected cells (NT) were analysed for comparison.

which was pCMV-Flag-MS1 expressed in HEK-293 cells. Western blot analysis using the purified MS1 2222 antiserum detected a band which was ~47kDa which co-migrated with the positive control pCMV-Flag-MS1 expressed in HEK-293 cells. The results in figure 3.2A, show the band increased with intensity after 2hr and 4hr reperfusion but then decreased after subsequent time points. Figure 3.2B shows that equal amounts of protein were present in each sample. By comparing the results from the simulated ischaemia/ reperfusion experiment with the 0hr control, there was a 1.5 fold increase in MS1 protein after 1 hr of reperfusion but there is no change seen after 1hr of ischaemia (Figure 3.2C). There is a 1.8 fold increase seen after 2 hr reperfusion with a further increase to 2 fold after 4hr. After 6 hrs of reperfusion there was a decrease in MS1 protein expression which continued up to 24 hrs. The 25hr control had the highest level of expression which increased by 2.6 fold higher than the control at the beginning of the experiment (Figure 3.2C). This was not expected as the 25hr control was not subjected to stress, and only remained in Krebs buffer which is supposed to simulate normal physiological conditions.

3.3.2. Effects of Cell Stress on MS1 promoter activity.

The aim of these studies was to determine whether or not the promoter region of MS1 responds to cell stress and hypertrophic agonists. Since MS1 has previously been shown to be induced during hypertrophy and studies in this lab have shown the MS1 mRNA is induced by simulated ischaemia/reperfusion in a JNK dependent manner, we aimed to investigate the effect of cell stress and hypertrophic agonists on the MS1 promoter. Previous studies in the lab have also established a role for JNK in the induction of MS1 mRNA expression during simulated ischaemia/reperfusion. Therefore we also wanted to look at the effect of JNK activation in response to other stresses such as UV and osmotic shock. The effects of UV and sorbitol on MS1 promoter activity were investigated. Sorbitol causes osmotic stress in cells which is one of the main types of stress which contributes to tissue damage during ischaemia (Ferdinandy *et al.,* 2007). UV irradiation is also a known inducer of SAPK/JNK activation (Helbig *et al*., 2011; Fritz and Kaina., 2006).

In order to determine the effects of cell stress on the promoter activity of MS1 we performed luciferase reporter assays, which are a quantitative method to determine gene expression in mammalian systems. The rat MS1 promoter sequence -1585/+60 (Figure 3.3)

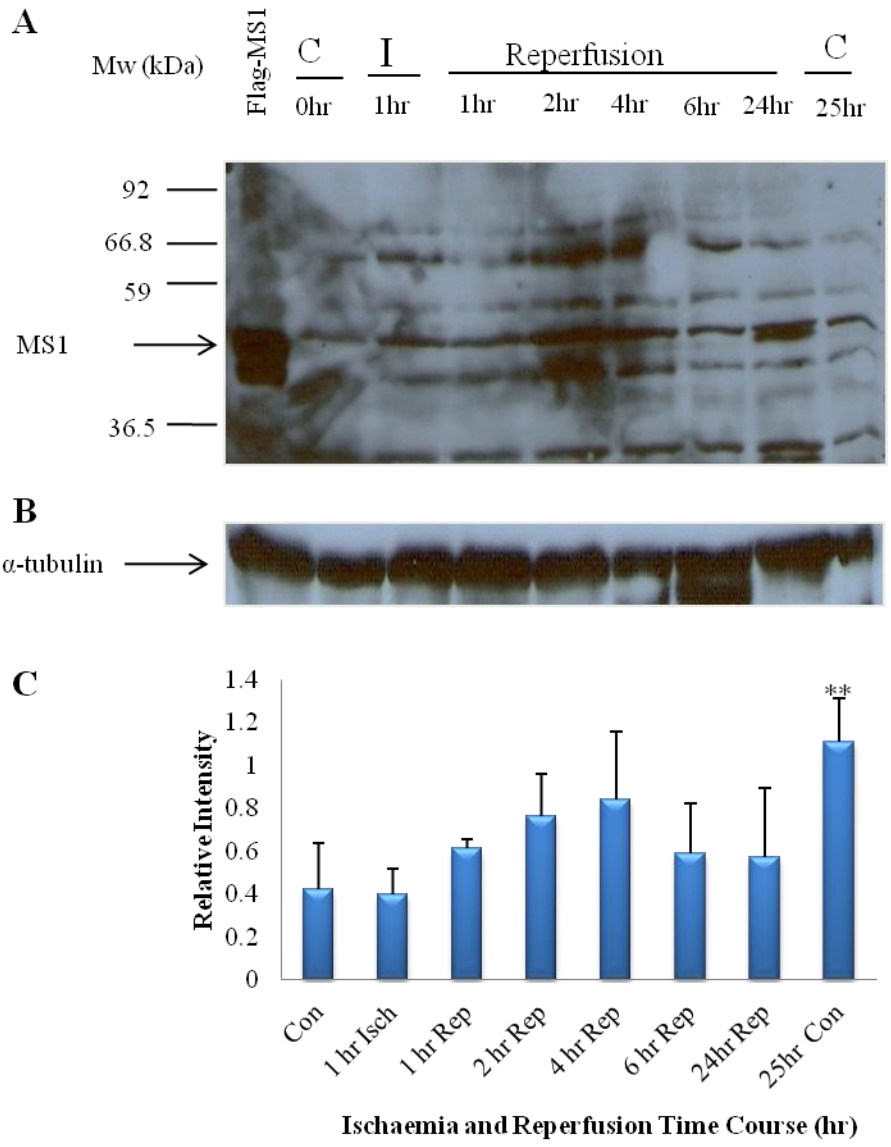

Figure 3.2: Western blot analysis of Endo*ge*nous MS1 protein Expression during simulated Ischaemia/Reperfusion Injury.

A. H9c2 cells were subjected to ischaemia for 1 hr using modified Kreb's buffer (I) then transferred to krebs buffer for different time periods as indicated above (Reperfusion). The cells were extracted in sample buffer and loaded on a 12% SDS-PA*GE ge*l with a positive control which was cell lysate from HEK293 expressing flag-MS1 and MW markers. For comparison cells were left in krebs buffer and extracted at 0 and 25 hr (C) The membrane was then western blotted using MS1 2222 antisera 1:2000. **B**. Blots were reprobed with an antibody against α-tubulin which was used as a loading control. **C**. Data from three independent experiments (n=3) was quantified using ima*geJ* and the mean value ± SEM is shown.Statistical significance was assessed by paired t-tests and significant change compared to the control is indicated by an asterisk ** ($p<0.01$).

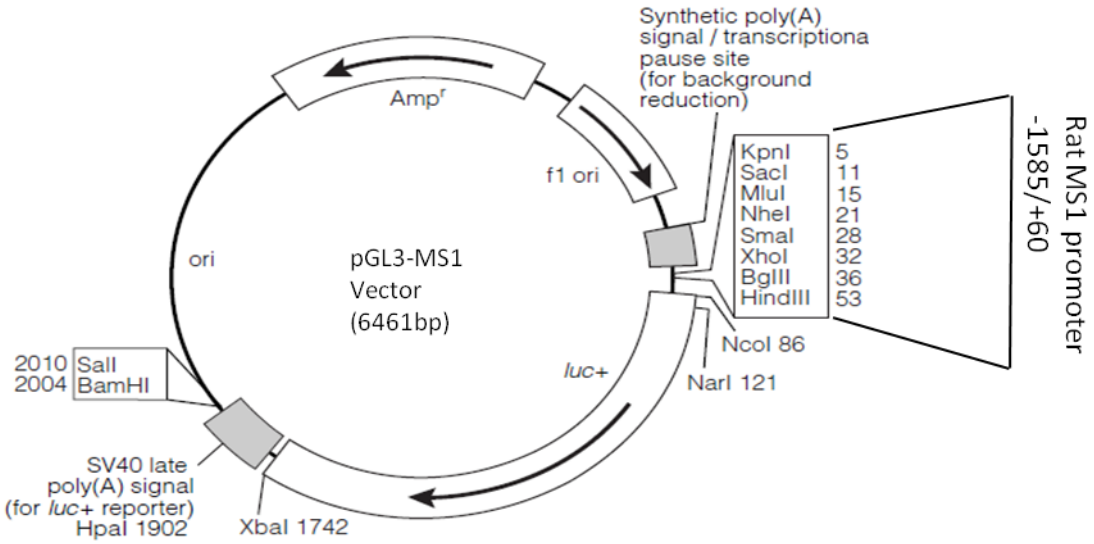

Figure 3.3: Vector map of pGL3-MS1 used for Luciferase reporter Assays.
The promoter region was cloned into the vector, where it is located upstream of the luciferase gene which is denoted as luc+. Amp^r is the Ampicillin resistence gene and the arrows indicate the direction of transcription.

was cloned into the expression vector (pGL3-Basic) upstream of the luciferase gene, which was transfected into H9c2 cells. The cells were then assayed and the reporter gene was identified based on the emission of light as a result of the combination of luciferase enzyme with the luciferin substate (Allard and Kopish., 2008). In the first set of experiments, H9c2 cells were transfected either with the luciferase reporter containing the rat MS1 promoter pGL3-MS1 (Figure 3.3) or the vector alone, pGL3-Basic (promoterless). Cells were subjected to either 1hr of 0.5M sorbitol treatment (in the presence of serum free medium) or 2 mins UV treatment. After the treatments, the cells were left to recover in media which had 10% serum present for 13hrs. Cells were then extracted in passive lysis buffer and then this was added to the firefly luciferase substrate. Readings were recorded using the luminometer which measures the light emitted as a result of the luciferase activity. The amount of luciferase produced reflects the activity of the of the MS1 promoter.

Results showed that there is a ~10 fold increase in luciferase activity in cells transfected with pGL3-MS1 upon sorbitol treatment, when compared with the controls which were either untreated cells left in serum or serum starved for 1 hr then incubated in medium with serum for 13 hr (Figure 3.4). The cells which were exposed to UV treatment showed a two fold increase in luciferase activity compared with the untreated pGL3-MS1 (Figure 3.4). The promoterless pGL3-Basic plasmid (Figure 3.4) plasmid also responds similarly to the stress inducers, but levels were lower. The preliminary data indicates that the MS1 promoter is stress responsive, and furthermore responsive to stress which causes the activation of JNK and p38.

Based on the results seen in Figure 3.4, the MS1 promoter activity was responsive to sorbitol treatment. The aim was to determine whether this response increased over time. A time course was carried out using pGL3-MS1 reporter only during the experiment, as there was no effect on the pGL3-basic reporter in previous experiments. The pGL3-MS1 reporter was important to compare the effects of the reporter with and without sorbitol treatment over a time period of 14 hours (Figure 3.5). The H9c2 cells were transfected with pGL3-MS1 only, and treated for 1 hr with 0.5 M sorbitol while other cells were left untreated. After sorbitol treatments the cells were left to recover over different time periods in normal DMEM with 10% serum. A 2 fold increase in MS1 promoter activity was observed after 1

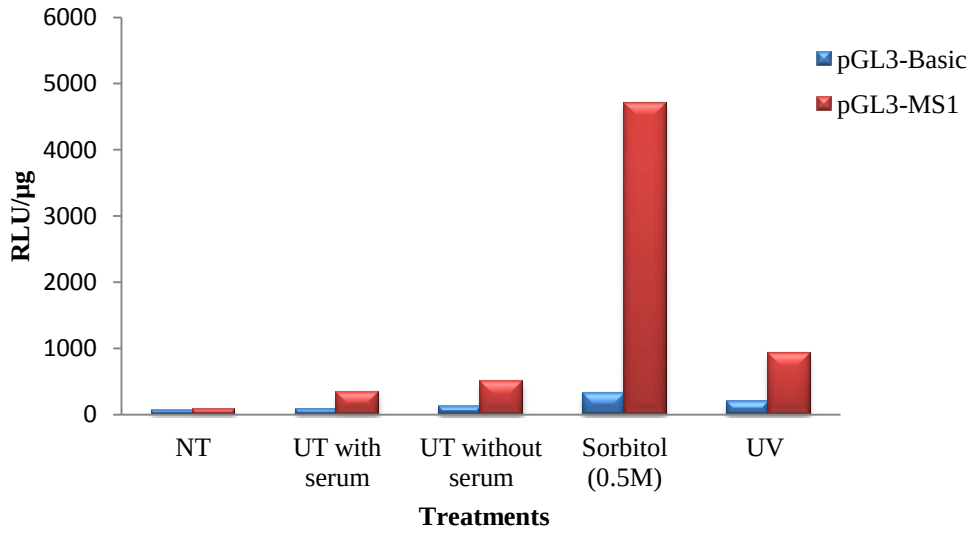

Figure 3.4: Luciferase assay to investigate the sensitivity of the MS1 promoter to stress.
H9c2 cells were transiently transfected with either pGL3-Basic or pGL3-MS1 plasmid in 6 well plates. After 24 hrs of transfection, the medium was removed from the plates and the cells were washed with PBS (1X). After washing, the PBS was removed and the cells were then subjected to either sorbitol (0.5M) treatment for 1hr or UV treatment for 2 min on ice in the presence of PBS. After the treatments the cells were then placed back in DMEM with 10% FBS and allowed to recover over a space of 13 hrs. The cells were then washed and extracted in passive lysis buffer (1X) and the protein concentration and luciferase activity were measured. Protein concentration of the samples was used to normalize luciferase readings in order to plot bar charts. This experiment was carried out by Dominic Patel under my supervision. Diagram above also shows non-transfected cells – NT, Untreated cells in the presence of serum – UT with serum, Untreated cells without serum – UT without serum values.

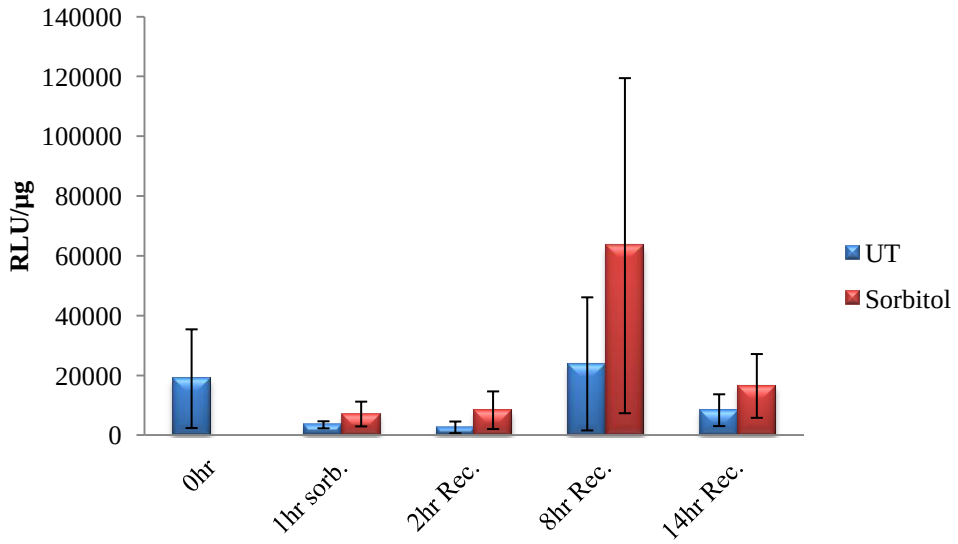

Figure 3.5: Effects of Osmotic Stress on the MS1 promoter
Subconfluent H9c2 were transiently transfected with pGL3-MS1 (0.75µg) plasmid in 60mm dishes. After 24hr the cells were subjected to 0.5 M sorbitol treatment for 1 hr and then left to recover in DMEM with 10% serum at different time points. After extraction in passive lysis buffer, luciferase activity and protein concentration were measured for normalization. Above are the results which represents the mean from three independent experiments and the ±SEM.

Having shown that sorbitol, an inducer of JNK and p38 can increase MS1 promoter activity and JNK and p38 were activated, we wanted to explore the effects of other stresses. We next looked at the effect of serum withdrawal. These studies were carried out by an undergraduate student Dominic Patel under my supervision. H9c2 cells were transfected with the promoter gene luciferase construct pGL3-MS1. The transfected cells were left in serum free medium over the course of 2 days, during which cells were extracted at varying time points and assayed for luciferase activity (Figure 3.7). There was no major increase seen in MS1 promoter activity during the first 24 hrs, however after 48 hrs the activity of the promoter showed a significantly large increase of almost 6 fold in comparison to the 2 hr time point and a ~2.5 fold increase in relation to the control in which H9c2 cells were incubated in the presence of serum supplemented DMEM for 48 hr. This indicates that reduced serum levels have an effect on the promoter region of MS1.

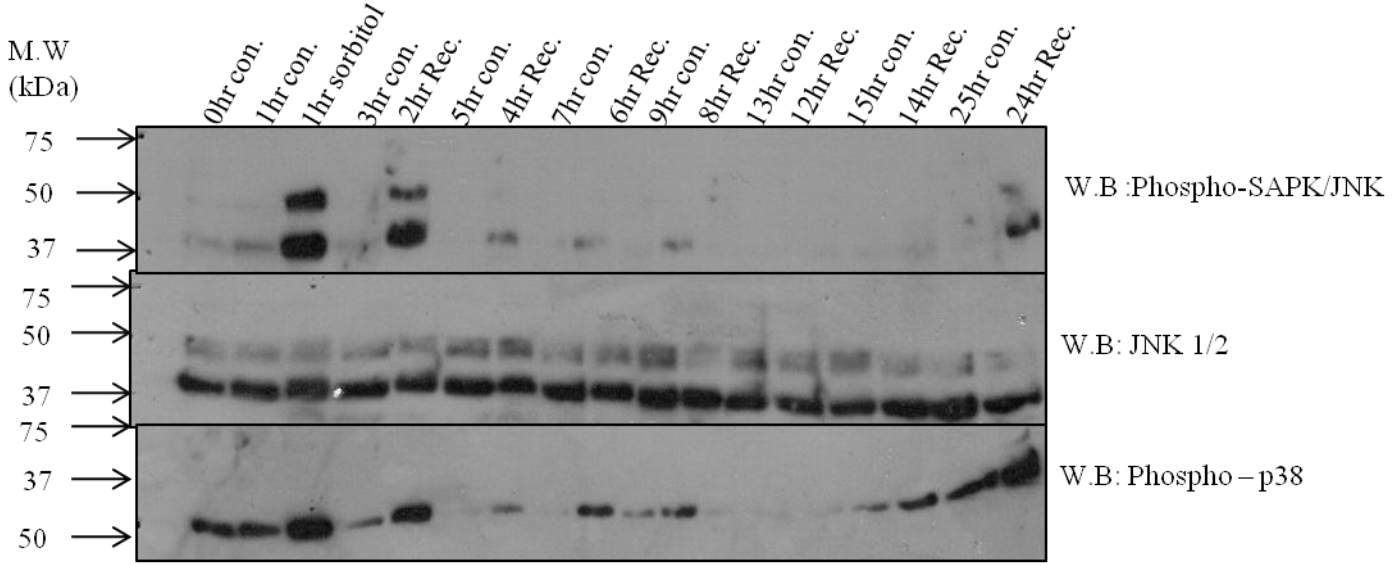

Figure 3.6: Western blot to determine activation of phospho-JNK and phospho-p38 by Osmotic stress.
Subconfluent H9c2 were transiently transfected with pGL3-MS1 (0.75µg) plasmid in 60mm dishes. After 24hr the cells were subjected to 0.5 M sorbitol treatment for 1 hr and then left to recover in DMEM with 10% serum at different time points. After extraction in passive lysis buffer, lysates were loaded onto an SDS-PAGE gel and subjected to western blotting using anti-phospho JNK, anti-phospho-p38 and anti-JNK antibodies. Above shows the antibodies used for each blot and the lysates loaded from each time point.

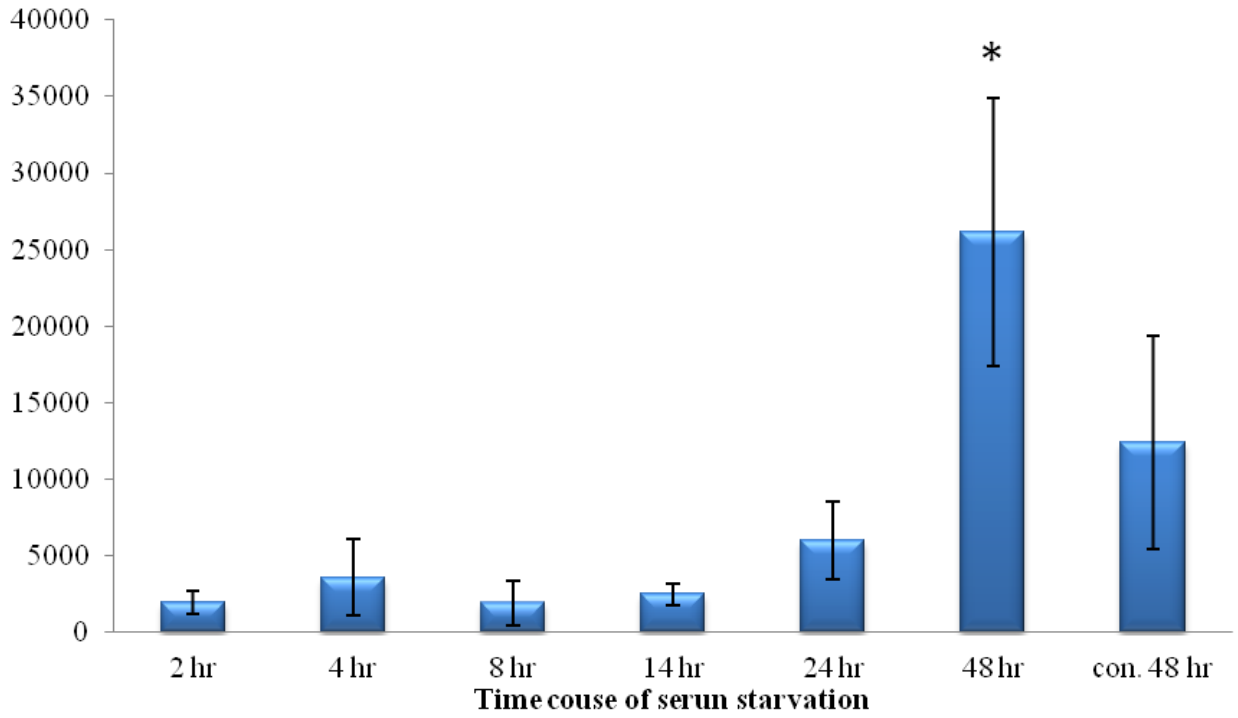

Figure 3.7: The Effects of serum deprivation on MS1 promoter activity
H9c2 cells were grown in 60mm dishes in the presence of DMEM, then transfected with pGL3-MS1 DNA. After 24 hrs of transfection, the cells were then placed in serum lacking medium and were extracted at varying time points. The samples were then assayed for luciferase activity and protein concentration in order to normalize results. Results are expressed as the mean of three independent experiments ± SEM (n=3) . Statistical significance was assessed by paired t-test and significant change at 48 hr compared to 2hr is indicated by an asterisk ($p<0.05$

3.3.3. The Effect of Hypertrophic Agonists on the MS1 Promoter Activity

Studies have shown that MS1 is responsive to hypertrophic stimuli such as calcineurin activation, or aortic banding which caused induced pressure overload in the heart (Mahadeva et al., 2002 ; Arai et al., 2002). H9c2 cells were used for the promoter studies for hypertrophic response, as they are rat cardiomyoblasts which display hypertrophic-associated traits seen within the body, such as re-expression of the proteins α-actinin, ANF and BNP proteins. They also have characteristic membrane morphology (Hescheler *et al.*, 1991 and Watkins *et al*., 2011). We used two well known hypertrophic agonists, phenylephrine (PE) and Endothelin-1 (ET-1) to investigate whether the activation of their associated receptors could cause the promoter activity of MS1 to go up after treatment (Sugden and Clerk., 1998).

H9c2 cells were seeded onto 60 mm dishes and left to reach to ~75% confluency. The cells were then transiently transfected with the pGL3-MS1 reporter plasmid and left for 24 hr before treatment with 100 nM of ET-1 or 100 μM of PE for 1 hr, and then cells were extracted in passive lysis buffer, and the substrate was added before luciferase readings were taken. After one hour of exposure to PE, there is a 2.5 fold increase in MS1 promoter activity compared to the control, of untreated cells (Figure 3.8). However there was very

little change in the activity of the promoter with the addition of ET-1 when compared to the control that was untreated (Figure 3.8).

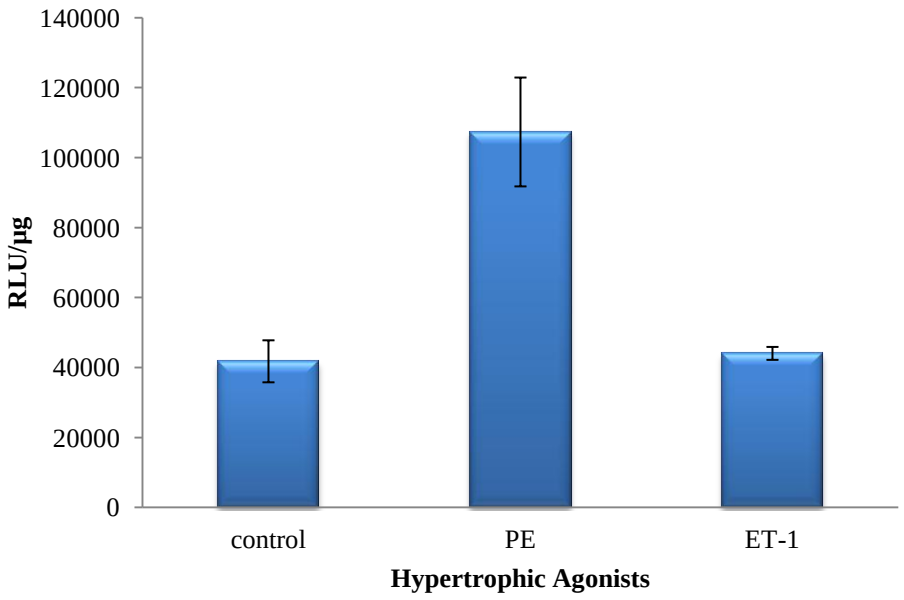

Figure 3.8: Effects of Hypertrophic Agonists on MS1 promoter Activity after 1hr
H9c2 cells were transfected with pGL3-MS1 plasmid. Cells were then left for 24 hours before being serum starved overnight. Cells were then placed in Krebs buffer for 30 min to equilibriate before adding 100 nM ET-1 or 100 µM PE-1. The cells were then extracted in passive lysis buffer before luciferase activity and protein concentration were measured. The results are expressed as the mean of three independent experiments ± SEM (n=3)

3.4. Discussion

3.4.1. Expression of Endogenous MS1 at the Protein Level during Simulated Ischaemia/Reperfusion Injury

At the outset of these experiments MS1 mRNA levels had been observed to increase in a simulated model of ischaemia/reperfusion. If this increase in expression is of physiological relevance we would expect to see an increase in levels of MS1 protein. These studies had not been possible as no suitable antibody was available. A rabbit polyclonal antiserum was produced and purified. This was able to recognise MS1 when overexpressed in cells. A band of corresponding size was also observed in H9c2 cells, which was thought to be endogenous MS1, when cells were subjected to simulated ischaemia/reperfusion. An increase of MS1 expression was observed after 2 hr and 4 hr of reperfusion (Figure 3.2), which supported the observations made previously when experiments measured mRNA levels.

Simulated ischaemia/reperfusion injury in H9c2 cells proved difficult to undertake when optimizing the experiment, the overnight control showed high levels of expression detected by the antisera (Figure 3.2). The antisera was not sensitive enough to detect low levels of MS1, and the specificity also caused problems in terms of the many non-specific bands which were seen throughout experiments. To date, there are not any good commercially available antibodies which could detect endogenous and overexpressed MS1. The antiserum used was a polyclonal rabbit antiserum and considerations should be made to develop a monoclonal antibody that could potentially have a higher specificity to detect MS1.

Extensive studies undertaken to investigate simulated ischaemia/reperfusion injury in the myocardium, suggest that during reperfusion JNK becomes activated during this phase (Armstrong *et al.*, 2004; Wang, 2007; Yin *et al.*, 1997). This occurs as a result of the biochemical changes, such as the production of the reactive oxygen species (ROS). Oxidative stress is a known activator of JNK (Giordano, 2005; Wang, 2007; Clerk *et al.*, 1998). Therefore the fact that MS1 is detected during simulated reperfusion and not during ischaemia does suggest that perhaps they might be involved in the same pathway. Other experiments carried out, were to observe the effect of hypertrophic agonists, and known JNK activators on the increase in MS1 expression at the protein level. There were not any obvious changes seen in terms of an increase in levels of MS1 (Data not shown). It would be of interest to inhibit JNK using pharmacological inhibitors, or knock down its expression using RNAi to determine whether this

abolishes the increase in MS1 protein seen during reperfusion. Problems with the antibody such as the presence of non-specific bands and the inability to detect endogenous MS1 caused issues and it was decided not to proceed using the antisera in the remaining experiments.

3.4.2. The Effect of Sorbitol and UV on the Promoter Activity of MS1

There is strong evidence which suggests that MS1 mRNA expression could be induced by JNK based on previous studies in the lab. Preliminary experiments described in this chapter support these observations. MS1 has been observed to increase in protein levels during early stages of reperfusion injury (Figure 3.2). The fact that using well known activators of JNK/SAPK such as sorbitol and UV, resulted in MS1 promoter activation as seen in Figures 3.4 and 3.5 supports that there is an association between MS1 expression and JNK activation. The fact that there is evidence which suggests that the promoter of MS1 has MEF2 and MyoD binding sites which are activated by p38 and JNK, strongly suggests that the SAP kinases could play a role in controlling MS1 activation.

3.4.3. Serum Deprivation leads to increase in MS1 promoter activity

Experiments carried out where H9c2 cells were transfected with the reporter plasmid pGL3-MS1, showed a 6 fold increase observed after 48 hr of serum deprivation (Fig. 3.7). The effect of serum deprivation results in the activation of JNK, and also p38 as a result of cellular stress and leads to cardiac myocyte apoptosis (Wang *et al.*,1998).

Apoptosis which occurs in the heart is an ordered form of cell death, where cardiac remodelling can occur during cardiac failure or even during ischaemia/reperfusion injury (Haunsteller *et al.,* 1998). Previous studies have shown that serum withdrawal has a proapoptotic action (Malhorta *et al.,* 1999). Therefore this can lead to the assumption that perhaps MS1 could potentially be playing a role in cardiac remodelling, which confirms what was previously thought by previous studies carried out by Kuwahara's group which focused on the promoter region of MS1 (Kuwahara *et al.,* 2007). MEF2 is controlled by transcription factors which are activated via JNK/SAPK, these are in turn activated upstream as a result of upstream kinases (Black and Cripps., 2010, Passier *et al*., 2000 and Wu *et al*., 2000). The promoter region of MS1 has MEF2 binding sites which have been implicated to regulate the gene expression of MS1 since experiments showed loss of expression of MS1 in MEF2C null mice (Kuwahara *et al.,*

2007). It would be interesting to determine whether serum withdrawal could have a pro-apoptotic effect on the H9c2 cells and whether or not MS1 could be involved. This could be achieved by over expressing MS1, or doing knock down studies of MS1, in order to determine whether MS1 could have an effect on apoptosis induced by serum-withdrawal.

3.4.4. Responsiveness of MS1 promoter to Hypertrophic Agonists

Hypertrophic agonists such as PE and ET-1 are well known JNK/SAPK activators in the myocardium (Sugden and Clarke., 1998). The pathway which these agonists act through is the diacyglycerol- induced PKC pathway (Bogoyevitch *et al*., 1994). These agonists are both known to stimulate the hydrolysis of phosphatidylinositol 4,5-bisphosphate which leads to the formation of diacylglycerol (Hilal-Dandan *et al*.,1992). The use of 100 µM PE did show a major effect after just 1hr as compared with ET-1 which did not show much of a change in relation to the control (Fig. 3.8). There needs to be further investigation into the possibility that the PKC pathway could regulate the levels of MS1 as a result of acting on the promoter. A simple experiment would be to treat H9c2 cells with PMA and look at the MS1 mRNA and protein levels.

There was extensive optimization done on these experiments looking at the promoter region of MS1. Dual luciferase reporter assays were initially performed using Renilla luciferase under the control of varying promoters such as CMV, SV40 and TK (thymidine kinase) as an internal control. This led to problems affecting the reporter as it seemed very sensitive when co-transfected with the internal controls resulting in high reporter activity in the absence of treatment. H9c2 cells used for this experiment did not transfect well. This has led to many issues in terms of inconsistent results. A different cell line should be considered when doing these reporter experiments.

Overall we were able to determine that MS1 was detected at the protein level during simulated ischaemia/reperfusion injury. Studies revealed that the promoter is responsive to cell stress and hypertrophic agonists which result in the activation of JNK and p38. These findings are supportive of the hypothesis that MS1 could be regulated by either JNK or p38.

A more direct approach to activate JNK to confirm its role in MS1 induction should be considered. Attempts were made to introduce constitutively active MKK7 into H9c2 cells in addition to the reporter. MKK7 is a direct activator of JNK. The introduction of an additional plasmid into H9c2 cells proved problematic again, highlighting the need

for an alternative cell line. If we could establish a simple reporter assay where introduction of active MKK7 into cells could activate the MS1 promoter, this would open up many opportunities to generate mutant reporter constructs to identify the JNK responsive element.

Chapter 4. Investigation of Potential Binding Partners of MS1

4.1. Introduction

Myocyte Stress 1 (MS1) protein is specifically expressed in the cardiac, skeletal and smooth muscle and is known to have a highly conserved C-terminal region (193-375). As previously mentioned, MS1 was observed to interact with polymerized F-actin, through two actin binding domains, ABD1 and ABD2 located at the C-terminal end between 234-279 and 346-375 amino acids (Arai et. al.,2002). MS1 also interacts with actin binding LIM proteins, ABLIM 2 and 3, which was discovered through yeast two-hybrid screening, the actin binding domain of MS1 as bait and a cDNA library from skeletal muscle (Barrientos *et al*., 2007). ABLIM 2 and 3 are thought to enable MS1 to bind to the sarcomere, where it binds to actin (Barrientos *et al.*, 2007). As a result of the relationship between MS1 and actin as well as the actin binding proteins, ABLIM-2 and 3, great focus has been placed on the C-terminal region of MS1 and not the N-terminus. The N-terminus of MS1 has yet to be investigated and given the fact that it has potential phosphorylation sites within this region, this was considered cause to investigate. The domain structure of MS1 was determined by Dr. Claudia Fogl using a program called DomainX (Reich *et al*., 2006, Fogl *et al.*, 2011). Therefore, it was thought to use the different domains which covered varying sections of the full length of MS1 as bait proteins for the binding assays.

4.2. Aims of this Chapter

The aim of this chapter was therefore to establish a binding assay using different MS1 domains as bait proteins to determine whether there were any other proteins expressed in the heart that might bind to MS1. Different domains were expressed and purified for use and mouse heart extracts were used to carry out experiments. This investigation would give greater insight into the function of MS1 and the pathways MS1 associates with, based on the proteins that may potentially interact with MS1 in the heart.

4.3. Results

4.3.1. Expression and Purification of the MS1 proteins

GST fused MS1 N-terminal tandem (has both Myocyte stress 1 Domain 1 (MSD1) and Myocyte stress 1 Domain 2 (MSD2) domains) and His-tagged C-terminal tandem protein (has both ABD1 and ABD2 domains) were used as bait proteins for the binding assays. The GST-tagged N-terminal tandem protein, C-terminal tandem protein and the other expressed His-tagged MS1 proteins are seen in **Figure 4.1**, which shows the sequence coverage for each compared to the full-length of MS1. Other his-tagged constructs were successfully expressed and purified as seen in figure 4.2 and 4.3. Only ABD2 was used in preliminary experiments and the following binding assays used His-tagged C-terminal tandem protein (193-375 a.a.) and GST-tagged MS1 N-terminal tandem protein (1-196 a.a.). The two tandem proteins, together, covered the full-length of MS1, so it was decided to use both of them as bait proteins in the binding assays.

4.3.1.1. Expression and Purification of MS1 C-terminal tandem

The C-terminal tandem protein which is His-tagged at the N-terminus and covers the amino acids (193-375) was expressed in BL21-DE3 (Invitrogen) *E. Coli* by isopropyl-beta-D-thiogalatopyranoside (IPTG) induction. The first step of purification was via metal ion affinity chromatography using a nickel column as seen in Figure 4.4. Samples from each step of expression and purification were run on a gel and the gel was coomassie stained (Figure 4.4). In figure 4.4 lane 1 shows a band which is of the correct size of 34 kDa after IPTG induction. After purification by the nickel column, the column was washed and the protein was eluted from the column. A sample of the purified protein was loaded in lane 3. A distinct band of the correct size was seen on the coomassie stained gel. The second lane in figure 4.4 shows a fraction collected during the wash step which removes any unbound proteins that are not His-tagged proteins from the column. The C-terminal tandem protein should not be seen in this fraction, however a residual amount was present as a result of the nickel column overloaded with the protein.

The eluted fraction containing C-terminal tandem protein was relatively pure, however, a second purification step was carried out using gel filtration chromatography in Figure 4.5. The x-axis of the gel filtration column shows the elution volume that passed through the gel column, while the y-axis is the signal in milli-absorbance units (mAu)

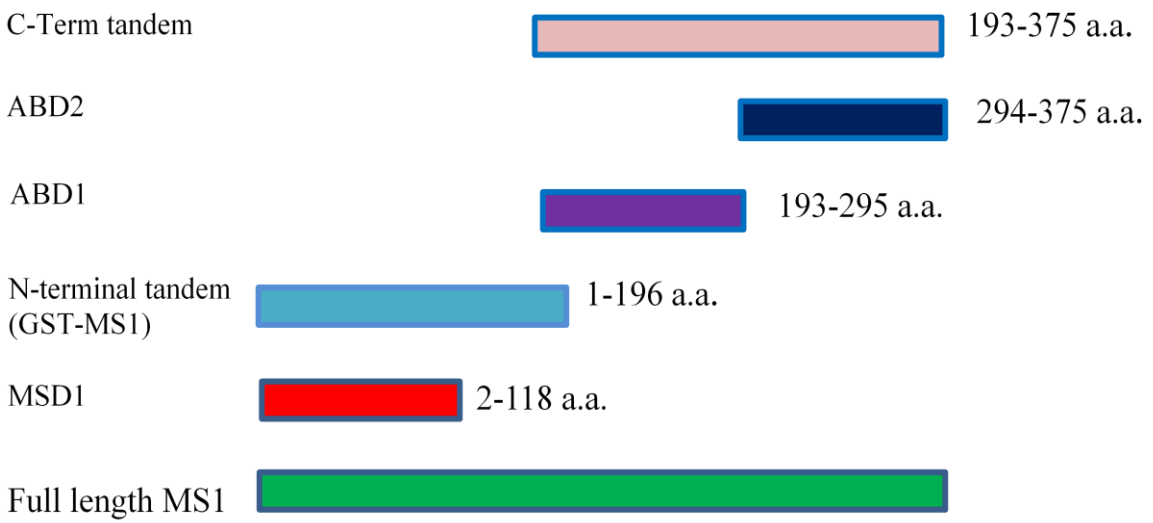

Figure 4.1: Position and residue number for domains encoded by different MS1 constructs
Various protein fragments of MS1 were produced for use in these studies as indicated above. C-terminal tandem, ABD2, ABD1 and MSD1 were His-tag*ge*d constructs *ge*nerated in Dr. Mark Pfuhl's laboratory, while GST-MS1 (N-terminal tandem) was separately made in our lab and was *ge*nerated with a GST tag.

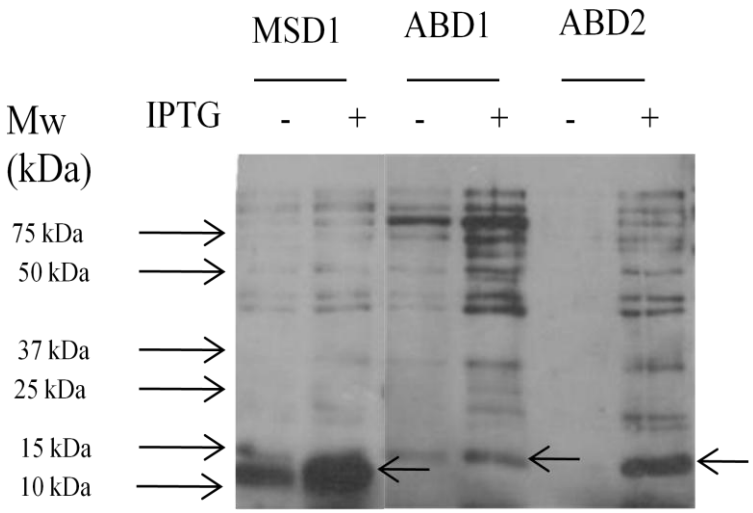

Figure 4.2: Expression of His tag*ge*d MS1 Constructs and detection by western blot Analysis

Western blot showing MS1 lysates, from MS1 constructs which were expressed in BL21DE3 *E.* coli by IPTG induction and lysates were collected, along with uninduced BL21DE3 cells and run on an SDS-PA*GE ge*l to determine whether the expressed protein was detected via western blot analysis using MS12222 antiserum. The arrows show the expression of the proteins at their correct sizes above

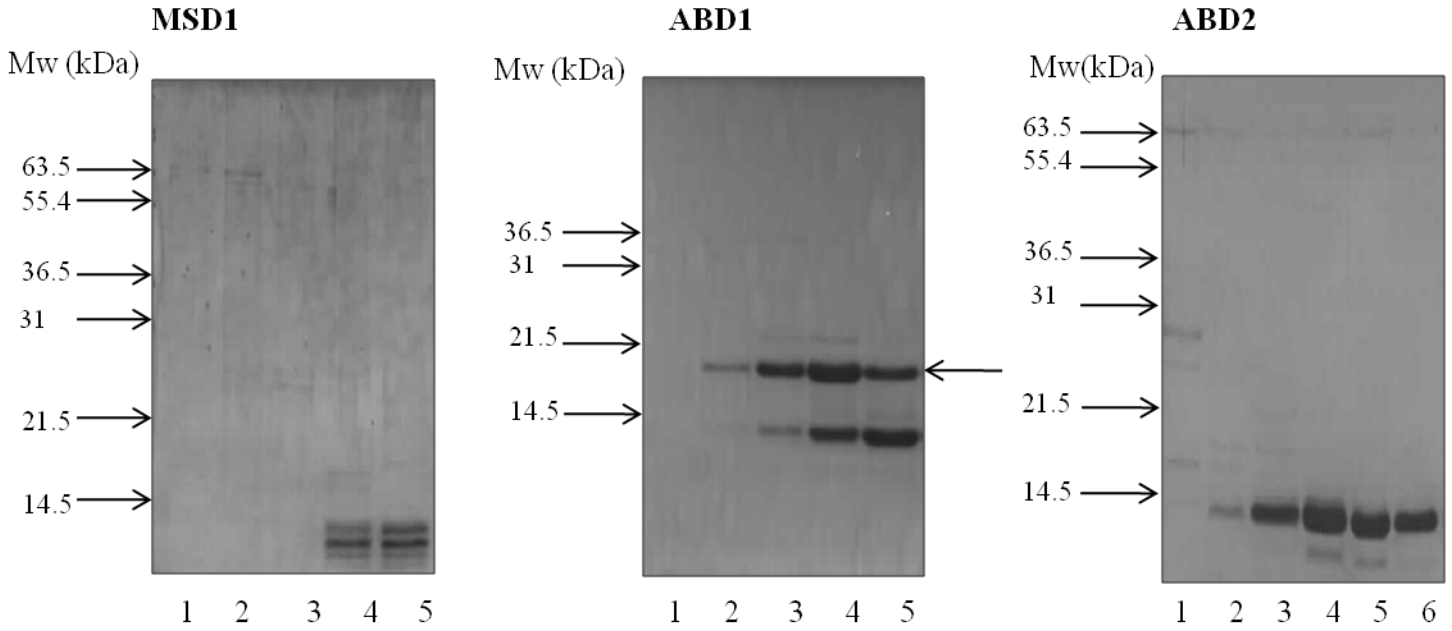

Figure 4.3: Coomassie stained *ge*ls showing the eluted proteins following *Ge*l filtration
Figures above show the protein fragments of MS1 after the bacterial lysates were purified via nickel ion affinity chromatography, followed by *ge*l filtration chromatography. *Ge*l filtration chromatography was executed using the sephadex hi-load 16/60 prepacked column to elute the MS1 His-tag*ge*d proteins. 5 ml aliquots were run on the column at a flow rate of 1 ml/min. After the proteins were eluted, samples of the fractions were run on an SDS-PA*GE ge*l and coomassie stained as seen above. Lanes 1-5 on the *ge*l are the eluted fractions

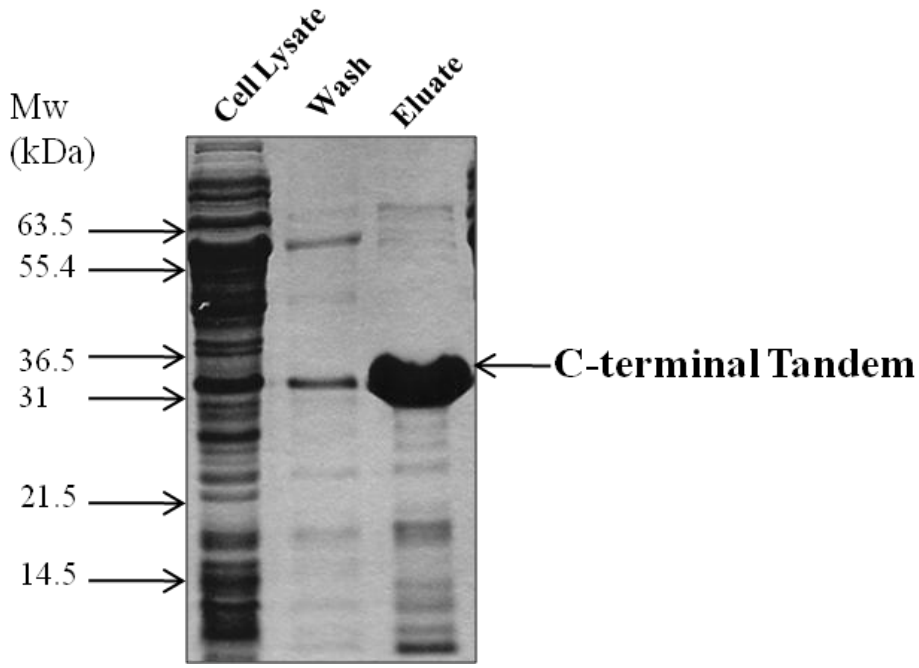

Figure 4.4: Expression and Metal ion affinity Purification of MS1 C-terminal Tandem
After the IPTG induction, MS1 C-terminal tandem was purified by nickel ion affinity chromatography using its His-tag to bind to the column. After binding, the column was washed and the protein eluted with 0.5 M imidazole. During each purification step, a sample was taken. The figure above shows the samples from the induced lysate, final wash and eluted protein on a coomassie stained SDS-PA*GE ge*l.

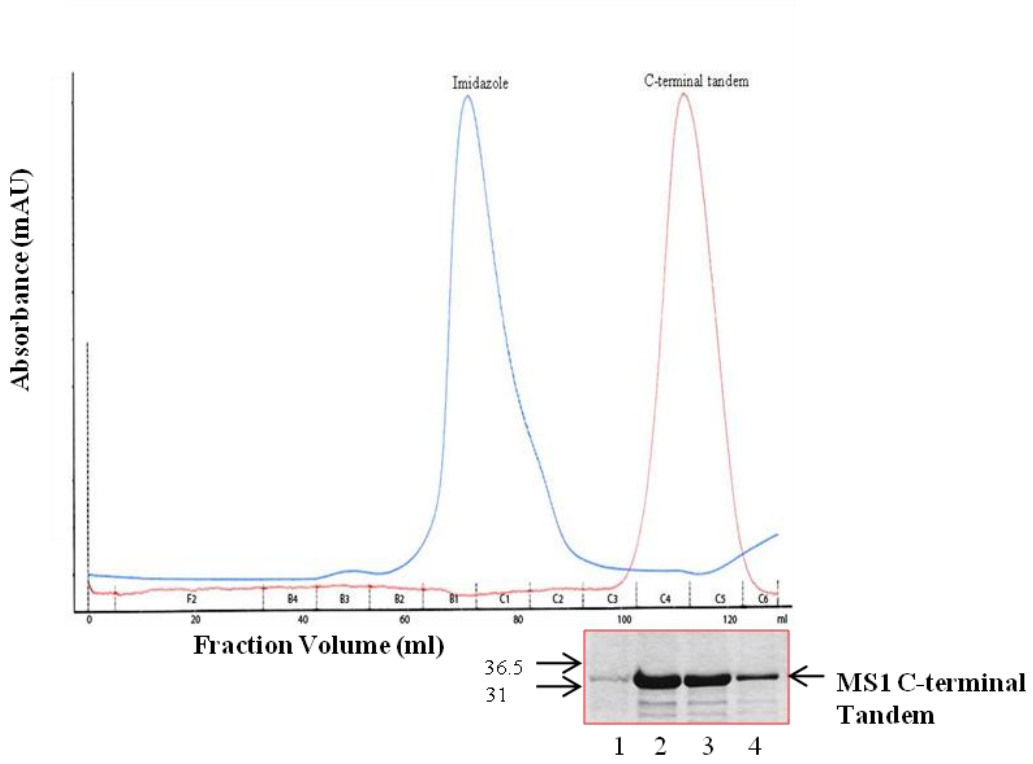

Figure 4.5: *Ge*l Filtration Chromatograph of Elution Profile MS1 C-terminal tandem
*Ge*l filtration chromatography was executed using the sephadex hi-load 16/60 prepacked column to elute the MS1 his-tag*ge*d proteins. 5 ml aliquots were run on the column at a flow rate of 1 ml/min. Elution of C-terminal tandem MS1 is shown by the red peak, while the blue peak shows the elution of imidazole, which was used to elute the protein from the nickel metal ion column. Samples of the eluted fractions from *ge*l filtration were run on a SDS-PA*GE ge*l (12%). Lanes 1-4 contain the eluted fractions of MS1 C-terminal tandem which had a molecular weight of ~31 kDa

measured at 280 nm. The elution of C-terminal tandem protein is displayed in red, while the blue peak is the high concentration of the imidazole which was used to elute the His-tagged protein from the initial nickel affinity column. The eluted fractions from the gel filtration column were run on an SDS-PAGE gel (Figure 4.5). Fractions (2-4) which had the protein C-terminal tandem present were pooled and dialyzed against (PBS).

4.3.1.2. Expression and Purification of N-terminal Tandem protein

The N-terminal tandem (1-196) protein which was fused with GST at the N-terminus and GST, were both purified by glutathione sepharose affinity chromatography. GST was used as a negative control for the binding assays. Proteins were expressed in BL21 (STAR) DE3 cells for GST-MS1 and BL21-DE3 cells for GST as stated in the material and methods section (Chapter 2 Section 2.8.2.1).

The N-terminal tandem protein expressed at the predicted molecular weight of ~53 kDa and the GST protein was expressed at 25 kDa (Figure. 4.6). The columns with the bound protein were washed and the proteins eluted using reduced glutathione. Samples of the eluted fractions from both columns were run on an SDS-PAGE gel. Although the N-terminal tandem protein eluted from the column, there were lower bands of around ~25 kDa (Figure. 4.6B). The fractions containing proteins were individually dialyzed against PBS buffer in order to remove any of the reduced glutathione, and to replace the buffer for one which would be compatible with the resin used to bind the three proteins for the binding assays.

4.3.2. Optimisation of binding assay using C-terminus of MS1 ABD2 as the bait protein

The first binding assay was done using ABD2, which has the second actin binding domain found within the C-terminus of MS1, covers the amino acid residues 294-375. This was to test if the C-terminus of MS1 could interact with actin by the binding assay experiment, as expected from previous work (Arai et al., 2002). Since ABD2 is His-tagged, a nickel chelating sepharose column was used in this experiment. Optimization was necessary to determine adequate protein concentration necessary for a successful binding assay. The first binding assay attempted used ~15 µg of ABD2 bound to nickel chelating sepharose beads, and 25 µg of clarified purified cardiac actin obtained from sheep heart. After the pulldown was completed the samples were run on an SDS-PAGE gel, which was coomassie stained to detect the bands present as shown in Figure 4.7.

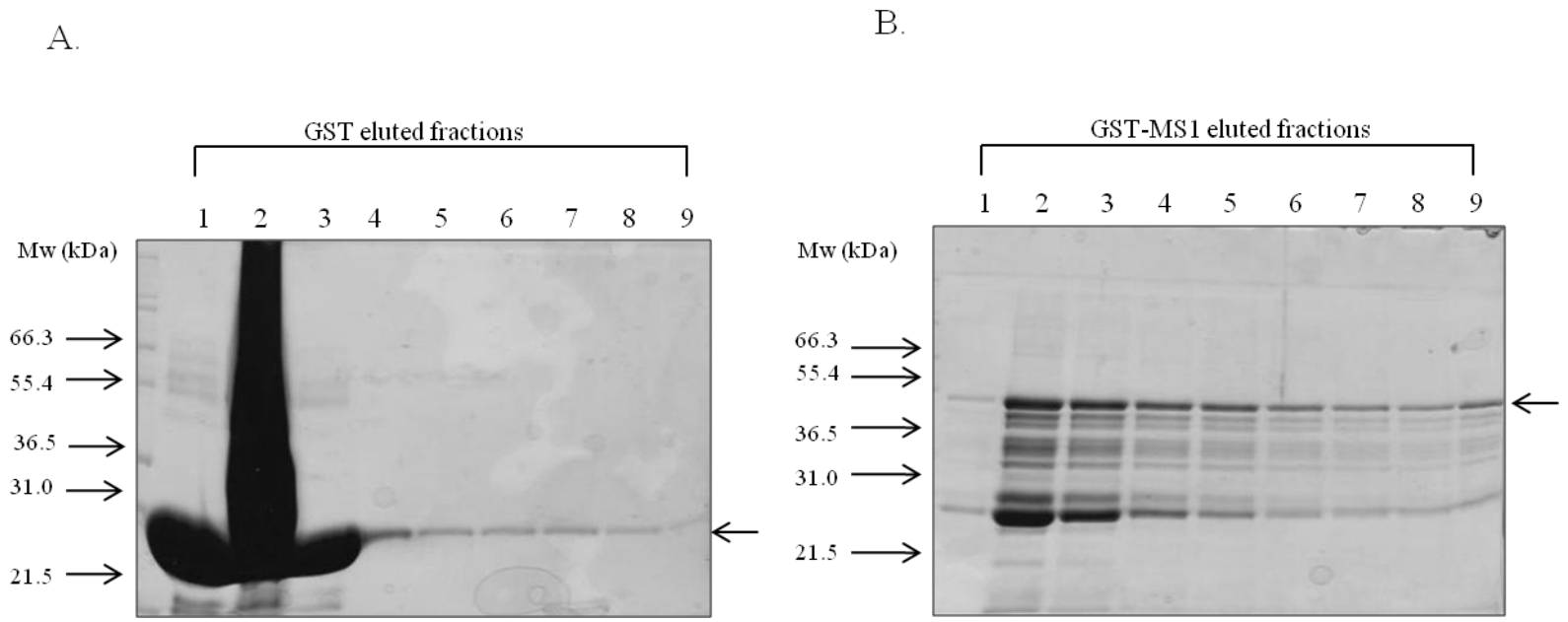

Figure 4.6: Elution of GST and GST-MS1 N-terminal tandem from GST-beads with Reduced Glutathione
GST and GST-MS1 were purified from bacterial lysates using glutathione agarose beads. The beads were washed and the protein eluted with 100 mM reduced glutathione by tumbling for two hours. Beads were then applied to the column and fractions were collected. A sample of each was analysed by SDS-PAGE gel and coomassie stained. Above shows coomassie stained gels of collected fractions that were loaded. The arrows indicate the proteins eluted; figure A is GST and figure B is GST-MS1.

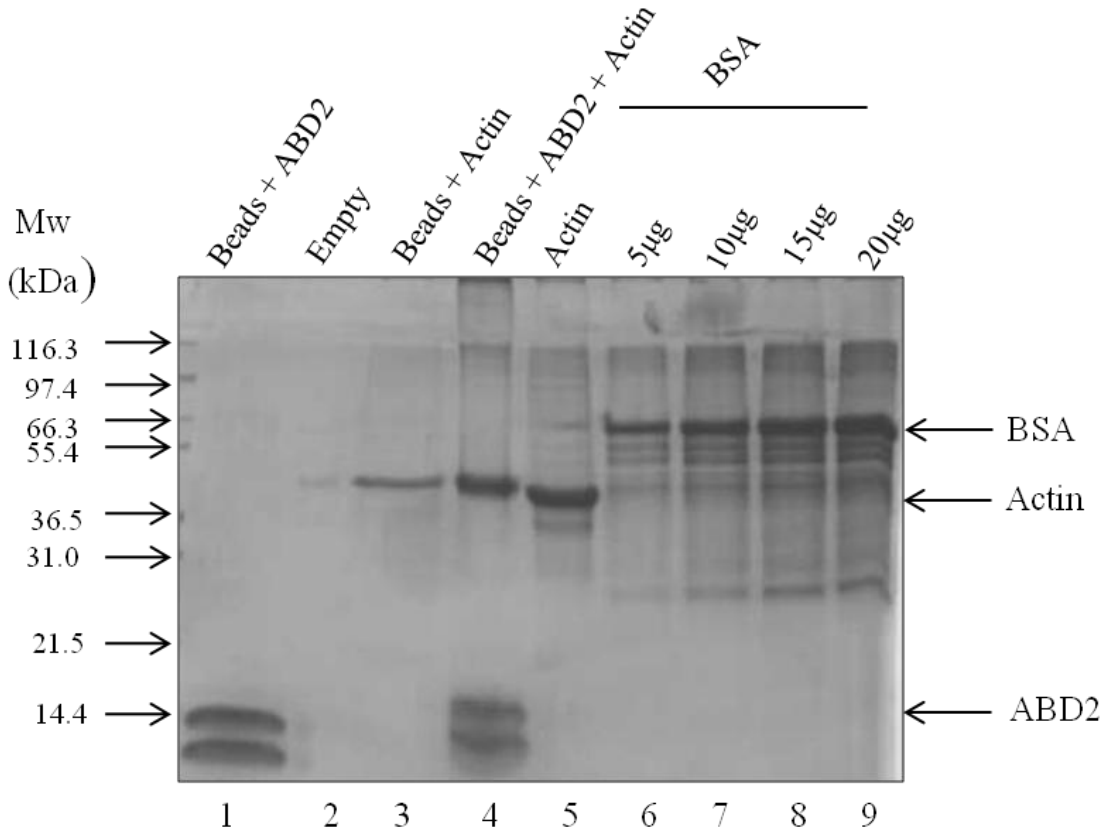

Figure 4.7: Binding assay with ABD2 and actin using charged nickel chelating sepharose beads.

Nickel chelating sepharose beads with bound ABD2 (25 µl) were subjected to tumbling with the actin (25 µg) protein for ~2 hr. After tumbling beads were washed 3x before boiling in SDS-PAGE sample buffer at 100 °C and loaded onto a 12% gel. The gel was then coomassie stained in order to visualize the proteins. The arrows indicate the proteins of interest ABD2 in lane 4 and actin indicated in lanes 5. Molecular weights are indicated.

In lane 1 of Figure 4.7 there were two distinct bands seen, this was ABD2 (294-375) protein bound to the beads only. The upper band of approximately 14.4 kDa corresponded to ABD2. The lower band of a molecular weight of ~12kDa was a proteolytic cleavage product of ABD2, identified by mass spectrometry. The two bands were also seen in lane 4, which had an additional band with an approximate molecular weight of ~46 kDa, believed to be actin, since it co-migrated with the band in lane 5 of figure 4.7. The lower bands were the same size as those seen in lane 1 with ABD2 only. The cleavage taking place, occurred at the C-terminal end of the protein as it was still able to bind to the nickel chelating resin with its N-terminal His-tag. Lane 3 had samples from the actin mixed with nickel chelating sepharose beads that was a negative control, however there was some non-specific binding of actin to the nickel chelating sepharose beads based on the faint actin band which co-migrated with actin in lanes 4 and 5.

Although there was a band in lane 3, this was less than what was seen in lane 4 where ABD2 precipitated more actin. Twenty-five micrograms of actin was loaded in lane 5 in figure 4.7 and analysed on the SDS-PAGE gel to give an idea of how much actin was binding to the beads non-specifically and the bait protein in lanes 3 and 4 respectively. Lanes 6-9 of figure 4.7 were varying known amounts of BSA to quantify what was in each lane. It was estimated that approximately 15 µg was binding to the MS1-ABD2 protein and 8 µg binding non-specifically to the nickel sepharose.

4.3.3. Non-specific binding of Mouse heart extract to beads

After testing the ability of ABD2 to bind purified actin *in vitro*, by a binding assay using mouse heart extract was performed to determine if any proteins including actin would bind to the ABD2 protein immobilised on the nickel chelating sepharose beads. After the binding assay was carried out, samples were run on a SDS PAGE gel, then coomassie stained to visualize the proteins (Figure 4.8). ABD2 was able to bind to cardiac actin, based on the band seen at ~47 kDa in lane 3 of figure 4.8. This band co-migrated with the band observed in lane 6, which contained 25 µg of actin. Numerous bands were observed in lane 4 of figure 4.8, which was a sample from ABD2 with the mouse heart extract (MHE). However, one band was observed to co-migrate with the bands of same size seen in lanes 3 and 5, which was purified cardiac actin. The other bands which were distinct could be seen at molecular weights of 150 kDa, 95 kDa, 79 kDa, 76 kDa, 35.5 kDa and 30.2 kDa respectively. Unfortunately, the negative control

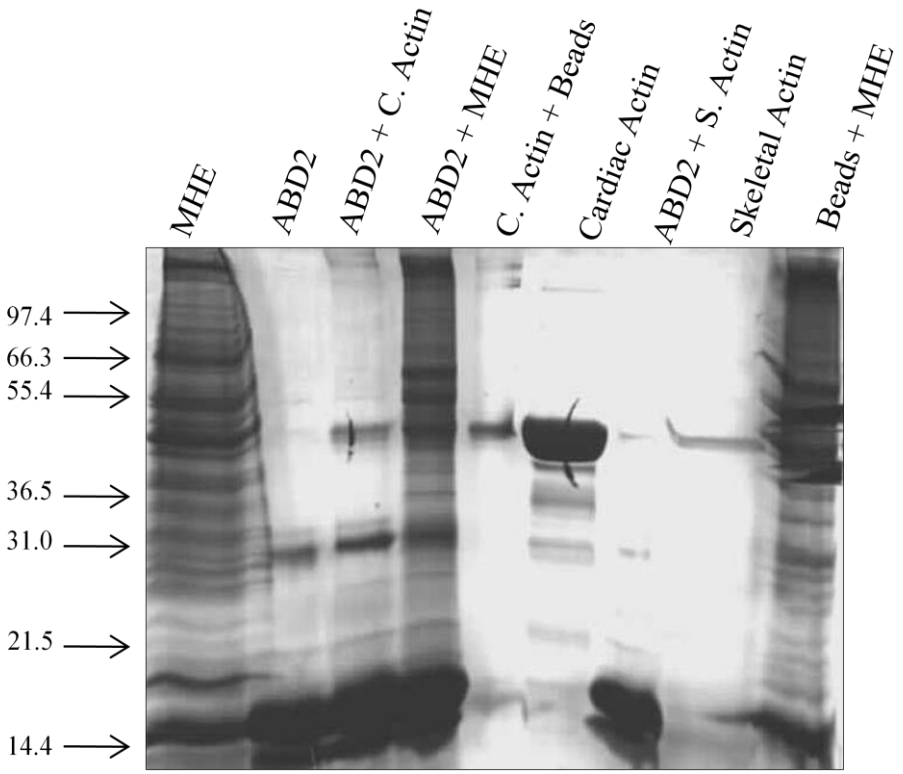

Figure 4.8: Binding assay using mouse heart extract using ABD2 bound to Nickel chelating sepharose beads.

Binding assay where ABD2 was bound to nickel chelating sepharosebeads. 75µg of mouse heart extract was used in this experiment to determine whether any proteins could be successfully pulled from the extract. The positive control was ABD2 and actin, while the negative control was the char*ge*d beads without any bait protein which was left to tumble with the mouse heart exctract MHE. C. actin is cardiac actin, while S. actin is skeletal actin. The *ge*l shows the results after samples from the binding assay were boiled in 3X sample buffer and boiled at 100°C.

which was the beads without any protein bound mixed with mouse heart extract in lane 9, also precipitated many non-specific proteins of the heart to the beads.

The proteins that bound non-specifically to the nickel chelating sepharose column, was possibly due to the presence of histidine-rich proteins. Other resins were tested to assess non-specific binding. Three different types of resins were tested to determine which would be compatible for future binding assays. Quantities of 50µg and 100µg of heart extract was mixed with G50-sephadex, nickel chelating sepharose beads and glutathione sepharose beads. These were washed to remove anything unbound and loaded on a gel to determine whether protein from the extract would bind non-specifically (Figure 4.9). Lanes 1 and 2, showed proteins precipitated by nickel charged chelating sepharose beads, had close to the same amount of protein bound to them as seen in the lane 7 of figure 4.9 with 100 µg of extract alone. The G50 sephadex in lanes 3 and 4 and glutathione sepharose in lanes 5 and 6 of figure 4.9 did not have any presence of extract. Both, GST-MS1, and the negative control, GST only eluted from the column with the extract. This resulted in the tagged proteins masking the unidentified proteins present and restricted a clear visual of other eluted proteins seen in the SDS-PAGE gel (data not shown). Another resin had to be selected in order to combat the issue with the bait proteins eluting from the columns.

The two MS1 proteins used for the binding assays have different tags present, where the N-terminal tandem protein is GST tagged while the C-terminal MS1 protein is tagged with poly-His. A resin was selected that would be compatible with both proteins and minimized variation between binding assays. The resin selected for the binding assays was N-hydroxysuccinimide (NHS-activated sepharose).

4.3.4. Binding Assay using C-terminal Tandem protein with mouse heart extract

The resin, NHS-activated sepharose contains N-hydroxysuccinimide ester functional groups, which react with primary amines in proteins to form stable covalent bonds. This does not require the use of tags to bind to the resin but binds to the purified protein which has the presence of amine groups. Steps were taken to ensure only the bait protein was bound and not any other proteins by blocking the non-reacted sites, after coupling in buffer containing 0.5 M ethanolamine and 0.5M NaCl (pH 8.3). The resin

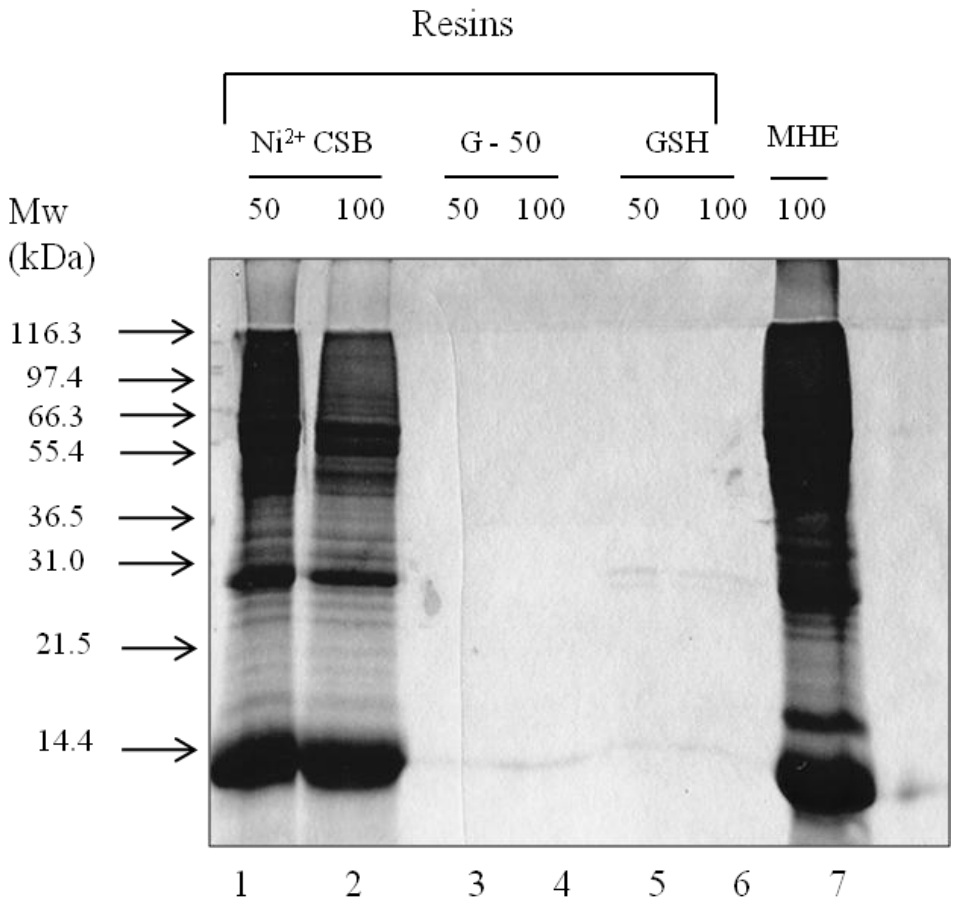

Figure 4.9: Investigating non-specific binding of extract to different resins
Mouse heart extract was incubated with various resins nickel chelating sepharose (Ni^{2+} CSB), sepharose G50 (G-50) and glutathione agarose (GSH) in quantities of 50 and 100 (µg). Lanes 1 and 2 are the eluted samples of the nickel chelating sepharose beads alone. Lanes 3 and 4 were eluted samples from G-50 sephadex resins and lanes 5 and 6 were eluted samples from glutathione sepharose resin. The last lane consisted of mouse heart extract.

with the bound protein was then washed repeatedly with high and low pH buffer. After these washes the proteins bound to the resins were ready for use.

After the binding assay was optimised, experiments using the C-terminal tandem protein (193-375 a.a) were done. This fragment was selected because as previously mentioned it has both actin binding domains present and is essentially half of the full length MS1 protein. The Tandem protein was expressed by IPTG induction and then purified by metal ion affinity chromatography and then by gel filtration as seen in figures 4.4 and 4.5. The protein was eluted from the gel filtration column, and dialyzed into buffers compatible with the NHS-activated sephaorse beads before it was added to the beads to bind. The NHS-activated sepharose beads form a covalently linked bond with the protein of interest and can not be removed from the beads. In order to determine whether or not the protein was successfully bound to the beads a sample of the protein was taken before binding and after binding which would determine whether or not successful binding occurred as seen in Figure 4.10. Lane 1 shows a sample of the proteins before the addition of the beads while lane 2 in Figure 4.10 shows the uncoupled protein following incubation with the NHS-activated sepharose beads. From the results shown, coupling was very efficient with approximately 25 mg of protein was bound to 3ml of beads.

The binding assays were scaled up to increase the chance of proteins in the mouse heart extract binding to the resin. Beads containing approximately 0.5 mg of coupled C-terminal tandem were mixed with 10 mg of the mouse heart extract. The negative control was the beads with reactive sites blocked that were left to tumble with the same amount of mouse heart extract.

Beads were washed and bound proteins were eluted and analysed by SDS-PAGE. Figure 4.11, shows a gel with all the eluted fractions from the binding assay seen in lanes 2-9. Three distinct bands were detected corresponding to putative MS1 binding proteins. The molecular weights were approximately 45 kDa, 40 kDa, 35 kDa and 29 kDa in size were observed in lanes 6 and 7 in figure 4.11. The gels were sent to University of Leicester PNACL, where the bands were excised from gels for Mass spectrometry analysis to identify proteins from the binding assay. The four proteins were identified as actin, troponin T, α-tropomyosin and RhoV respectively. An experiment which followed the same protocol for the binding assay used uncoupled NHS-sepharose with mouse heart extract as a negative control (Figure 4.12). A sample

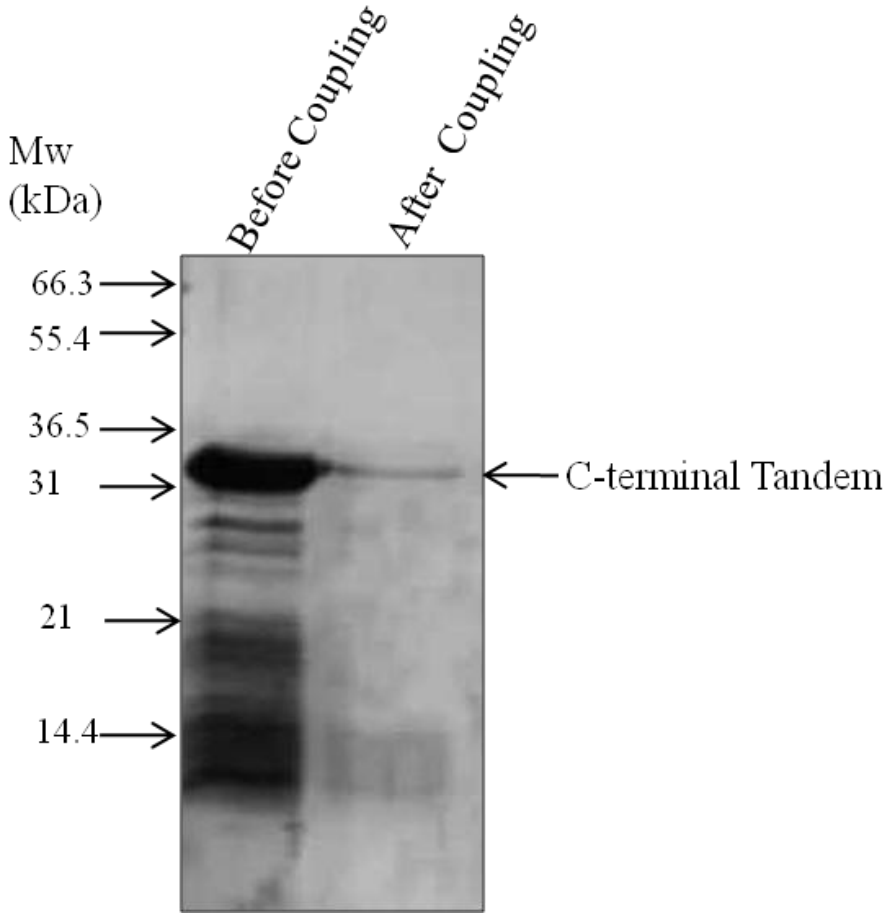

Figure 4.10: Confirmation of coupling of C-terminal tandem protein to NHS-activated Sepharose beads

Coomassie stained *ge*l showing a sample of the supernatant of C-terminal tandem protein before coupling to NHS activated sepharose and after coupling to NHS-activated sepharose beads to determine whether the protein immobilized to the resin.

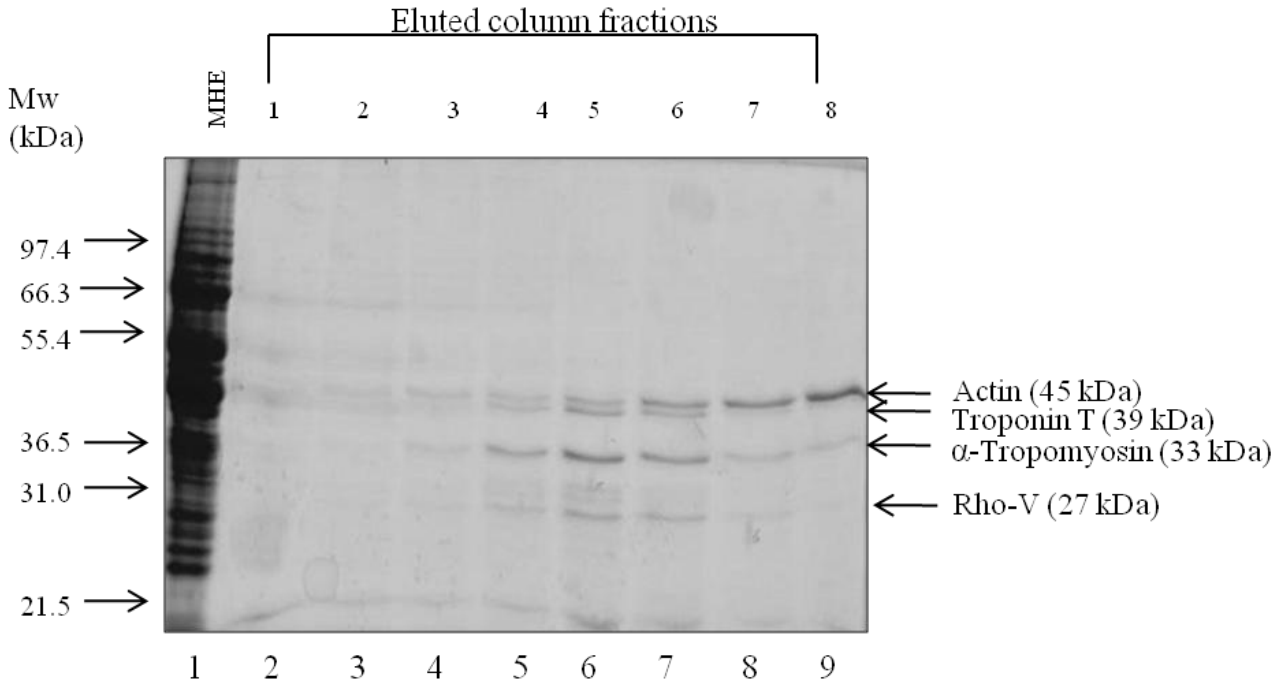

Figure 4.11: Binding Assay using His-tagged C-terminal Tandem to investigate protein interactions with proteins found in mouse heart extract. His-tagged C-terminal Tandem protein was expressed in BL21 star E. coli and purified by metal ion affinity chromatography and then by gel filtration. The purified his-tagged protein was dialyzed and then immobilized to NHS-activated sepharose beads. The Bound protein was then washed 4 times to remove unbound protein and left to tumble with mouse heart extract for 2 hrs. The supernatant was removed and the beads were then washed again in a column and the protein which was bound was eluted from the column with sodium acetate pH 5.5 in column fractions of the same volume (100µl). The fractions which were collected from the column were then neutralized with Tris base . The collected fractions were then concentrated using microcentrifuge concentrators, and sample buffer (3X) was added. Samples were boiled and loaded onto a SDS-PAGE gel (12%)

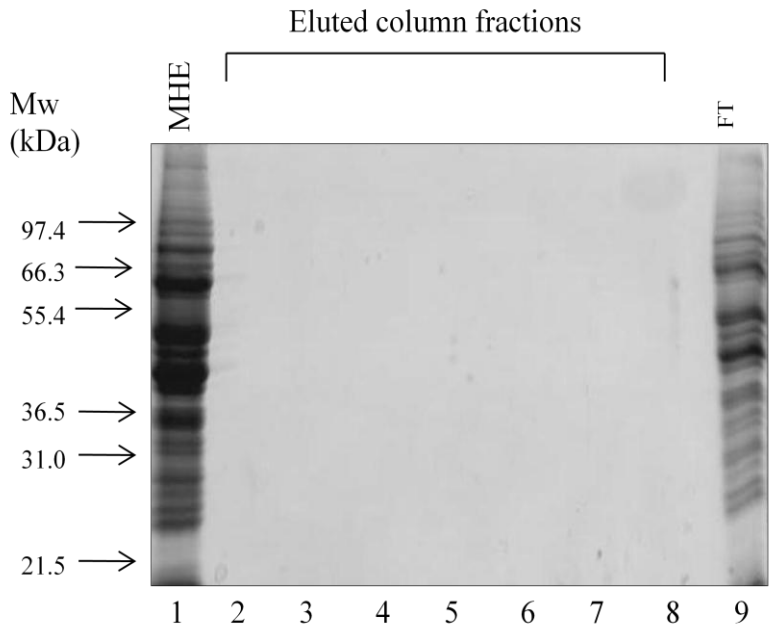

Figure 4.12: MHE proteins do not bind to NHS-sepharose non specifically
NHS activated sepharose beads without any bound protein were incubated with mouse heart extract (MHE), washed and bound protein eluted. Samples were run on a SDS PAGE gel which was stained with coomassie. Lane 1 is the marker, Lane 2 is the mouse heart extract before binding and lanes 3-9 are the eluted fractions from the column and lane 10 is the flowthrough (FT) after the incubation with the beads.

of the extract used in the experiment was run on the gel along with collected fractions after the binding assay was complete. Eluted fractions were run in lanes 2-9 in Figure 4.12 and coomassie stained. The coomassie stained gel did not show any bands which suggests lack of non-specific binding from proteins in the extract. This is an indicator that the proteins are essentially binding as a result of the bait protein and not the NHS-activated sepharose beads which were used to immobilize the protein. One of the bands taken for mass spectrometry analysis was confirmed to be actin in Figure 4.11. The eluted fractions were run on a SDS-PAGE gel for further analysis. Bands observed in the eluted fractions were also found in the lane labelled MHE (mouse heart extract) in lane 2 (Figure 4.11). Actin was purified from the MHE with the use of C-terminal tandem MS1, this validated the approach, and also confirmed previous findings (Arai *et al.,* 2002, Fogl *et al.,* 2011).

Western blot analysis of actin, using an anti-actin monoclonal mouse antibody was carried out as a confirmatory test to identify actin, shown in figure 4.13. Some of the samples from the eluted fractions were run on a separate gel for western blot analysis as seen in Figure 4.13 in lanes 3-7 which were eluted fractions and a sample of the mouse heart extract was also loaded onto the gel to determine whether the large band was the actin protein which could be seen in lane labelled MHE in Figure. 4.13. Western blot analysis confirmed the band at ~46kDa was actin, picked up by the antibody and also present in lanes 3-6 where they co-migrated with the band in the lane labelled MHE in figure 4.13. Unfortunately there were no readily available antibodies which could detect α - Tropomyosin or troponinT identified from mass spectrometry, while RhoV was only observed once and was not identified again in subsequent binding assays.

4.3.5. Binding Assays using N-terminal tandem to determine binding Partners

GST-MS1 Tandem which is made from the first half of MS1 has two domains (MSD1 and MSD2). The binding assay previously mentioned involved a His-tagged protein, immobilized on NHS-activated sepharose beads and when eluted from the column the bait protein would not elute due to the covalent link with the resin. The N-terminal Tandem tagged with GST, encountered problems when binding assays were carried out using the protein coupled to glutathione beads; such as the tag*g*ed protein eluting from the beads. Due to its size it was difficult to see any bands which were present in the binding assay that could have come from the mouse heart extract.

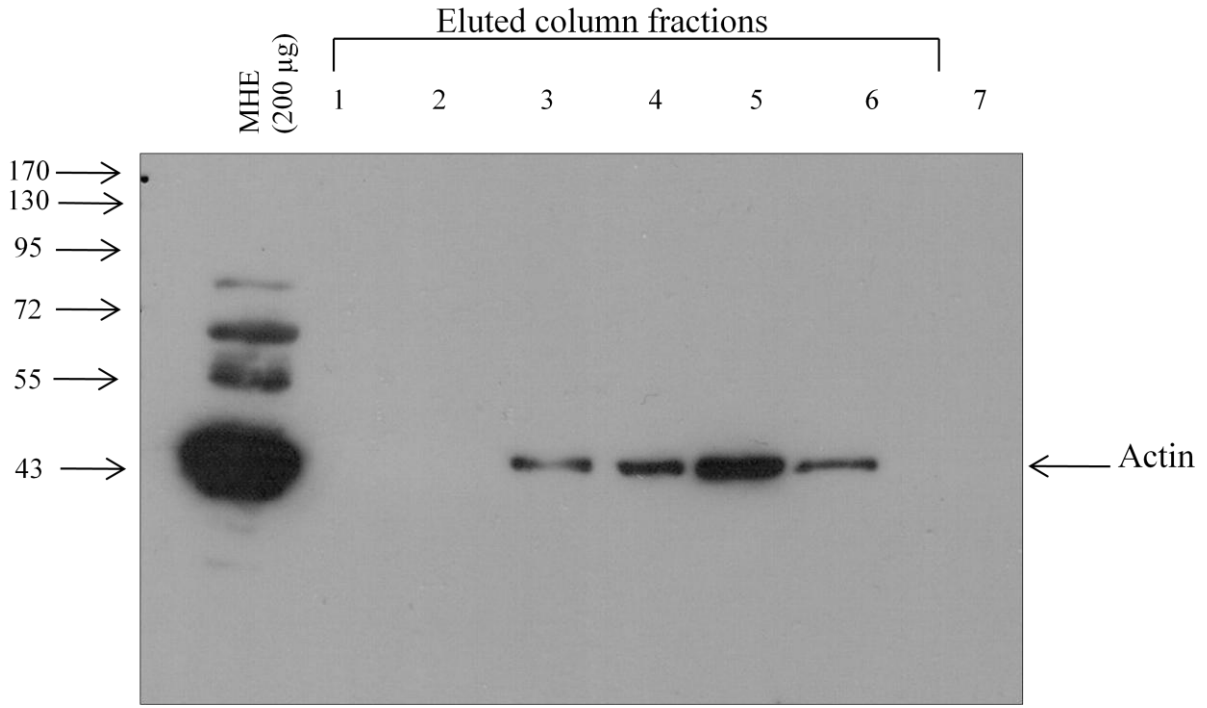

Figure 4.13: Confirmation by western blotting of actin binding to MS1 in binding assay with mouse heart extract using C-terminal Tandem. Western blot analysis confirming actin binding to MS1 C-terminal tandem coupled to NHS activated sepharose beads. 200 µg of mouse heart extract (MHE) was analysed along with samples of eluted fractions from the NHS-activated sepharose column. The samples were separated by SDS PAGE gel (12 %) and western blotted using mouse anti-actin antibody (1:1000 dil).

After expression and purification of GST-MS1, the protein was first eluted from glutathione sepharose beads, dialyzed to remove reduced glutathione and then coupled to NHS-activated sepharose beads. Elution of the GST-MS1 (N-terminal tandem) protein from the glutathione-S-transferase column proved difficult. However there was enough protein to allow binding assays to be performed. As previously mentioned, a negative control was used to ensure binding did not occur non-specifically to the tag and any interactions were specific to the MS1 portion of protein. Two negative controls were used in these binding assays; GST protein immobilized to NHS-activated sepharose beads and NHS-activated sepharose beads only. These were to rule out non-specific binding of proteins. The binding assays were carried out as explained previously and the eluted fractions were resolved by SDS-PAGE. The gel was then coomassie stained in order to visualize the bands (Figure 4.14).

A comparison must be made between the negative controls which were the gels in Figure 4.14 with the gel in Figure 4.15 which are the eluted fractions from the GST-MS1 tandem protein. It could be seen that there are 4 significant bands which are present in Figure 4.15 that are not in the control gels.

The control gel and the gel with the eluted samples were sent for mass spectrometry to identify the bands from the binding assay. The largest band which had a molecular weight of ~224.2 kDa was Myosin-6, the band of molecular weight of 42.3 kDa was actin from skeletal muscle, α-tropomyosin was the band identified at 33 kDa, 24 kDa was troponin-I and myosin regulatory light chain 2 the last band seen at 19 kDa (Figure 4.15).

4.3.6. Binding Assays using Guba-Straub buffer Vs. Triton lysis buffer.

Binding assays using MS1 C-terminal tandem and GST-MS1 N-terminal tandem, yielded different proteins that were pulled out of the heart extract as seen in Figure 4.11 and 4.15 respectively. However, results from both binding assays, showed there were myofibrillar proteins present which included actin. To date, there are no reports in the literature that suggests the N-terminus of MS1 interacts with actin. Myosin was identified as one of the proteins pulled from the mouse heart extract when GST-MS1 N-terminal tandem was used as a bait protein and not MS1 C-terminal tandem. A possible reason for the presence of actin binding to GST-MS1, might be indirect interaction

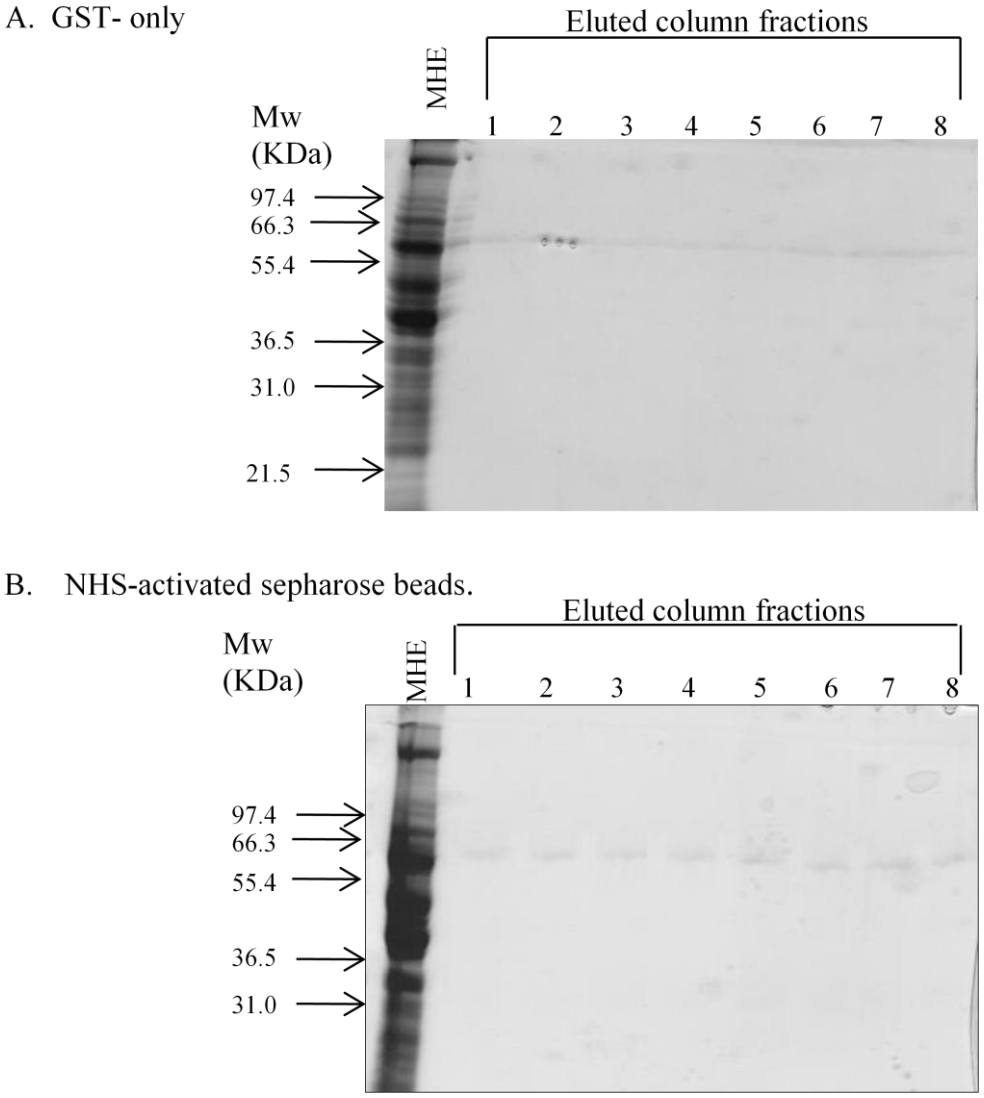

Figure 4.14: Binding assay with control beads; GST-Sepharose or NHS-activated sepharose that had been quenched with no protein

A. GST was expressed in BL21 DE3 ***E. coli*** and purified by binding to glutathione coated agarose beads. The purified protein was then eluted and the isolated protein was immobilized to NHS-activated sepharose beads. After coupling the non-reacted sites were blocked and beads were washed. Beads with immobilized protein were left to tumble with mouse heart extract (MHE). The supernatant was removed and the beads were washed again. The resin was then placed in a column and eluted .The eluted fractions were then neutralized with Tris buffer and sample buffer 3X was added and run on a 15% SDS –PAGE above shows the mouse heart extract used in the binding and eluted fractions. **B.** NHS-activated sepharose beads were washed and the reactive sites were blocked with the same buffer previously mentioned in A. After removing the buffer and washing the beads, they were then left to tumble with mouse heart extract for 2 hrs, the same method was used in order to isolate any bound proteins from the beads if any were present. Samples were the run on a SDS-PAGE gel (15%). Figure shows a sample of the mouse heart extract used and samples

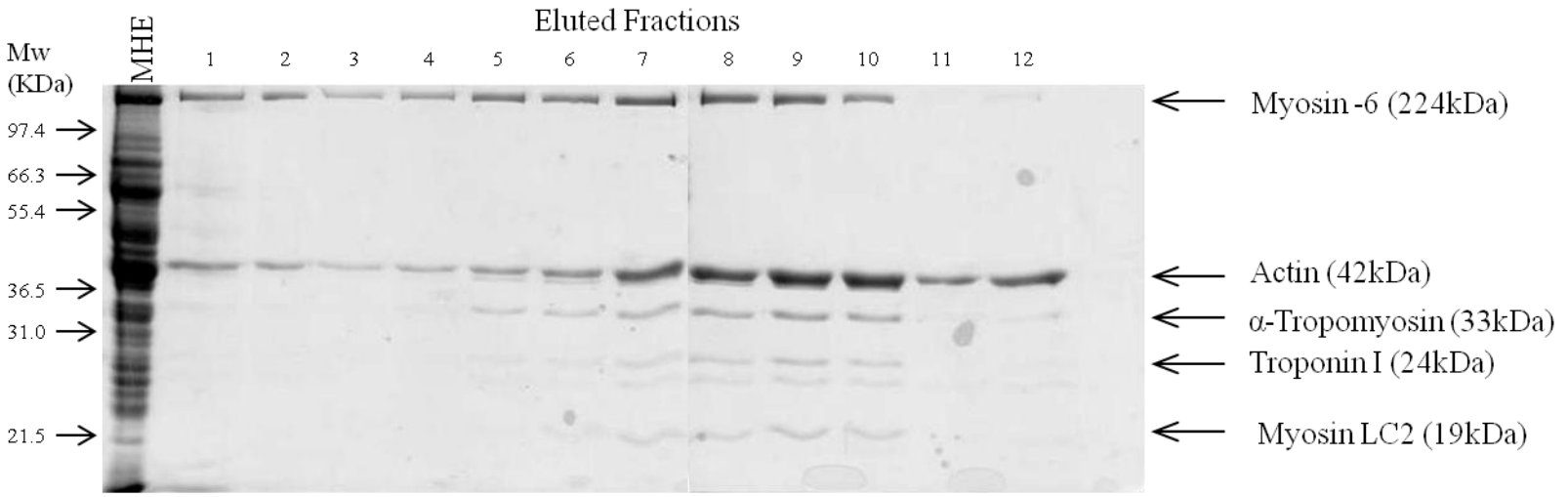

Figure 4.15: Binding Assay using N-terminal region of GST-MS1 N-terminal Tandem to investigate interactions with unknown proteins in mouse heart

The N-terminal region of MS1 (1-196 region of MS1) which is GST-tagged was expressed in BL21 stars ***E. coli*** and purified by binding to glutathione coated agarose beads. The purified protein was then eluted from the beads with 100mM Hepes buffer containing reduced glutathione (50 mM) to isolate the purified protein. The protein was dialysed and then the MS1 (1-196) Tandem protein was immobilized to NHS-activated sepharose beads. The coupled beads were then placed in a buffer (ethanolamine 0.5 M and NaCl 0.5 M) to block any non-reacted groups. The beads were then washed in a high and low pH buffer and then left to tumble with mouse heart extract (7 mg) for 2 hrs. The supernatant was removed and the beads were washed again three times. The resin was then placed in a column and any bound proteins were eluted with pH 5.5 sodium acetate buffer . The eluted fractions were then neutralized with Tris buffer , sample buffer (3X) was added and samples were run on a 12% SDS –PAGE gel.

rather than direct interaction. The proteins identified can be found in complex with each other in myocytes.

To eliminate the possibility of indirect interaction between GST-MS1 N-terminal tandem and actin, Guba-straub buffer was used in the binding assays to dissociate myosin from actin. Guba-straub buffer is used to dissociate myosin from actin with the use of a high salt concentration (Buffer details are in Chapter 2). A comparison should be made between binding assays using the normal buffer (triton lysis buffer) and Guba-straub buffer.

The results from the experiment carried out in Figure 4.16, shows an increase in actin binding in the presence of GST-MS1 N-terminal tandem than with C-terminal tandem protein in Guba-straub buffer. A comparison was made between the two buffers as seen in Figure 4.16. There was more proteins eluted using Guba-Straub buffer than using triton lysis buffer (Figure 4.16). The results from these experiments were inconclusive, however a control should be in place to determine the actomyosin complex dissociated in the presence of Guba-Straub buffer.

4.3.7. Actin Co-sedimentation Assay

In order to determine the role of MS1 in complex formation with the identified proteins, an actin co-sedimentation assay was performed. This allows the determination of direct binding of proteins to F-actin in an *in vitro* assay. Therefore using this method would aid in determining whether or not the MS1 domains were binding directly with actin, or whether they were bound to another protein that interacts with actin which resulted in actin being pulled down.

The experiment carried out used all of the known proteins which were identified by mass spectrometry. These were previously purified and provided by Dr. Mohammed El-Mezgueldi (University of Leicetser). An actin co-sedimentation experiment was carried out as described in chapter 2. It is known that that the C-terminal tandem protein binds directly to actin through the two actin binding domains present, this was used as a positive control and the negative control used was GST. In these co-sedimentation experiments the concentration of MS1 protein used was 50 µM, Actin was 50 µM and the purified proteins were prepared at a molar ratio of 7:1 compared to F-actin concentration. Figure 4.17 shows the various combinations of purified proteins

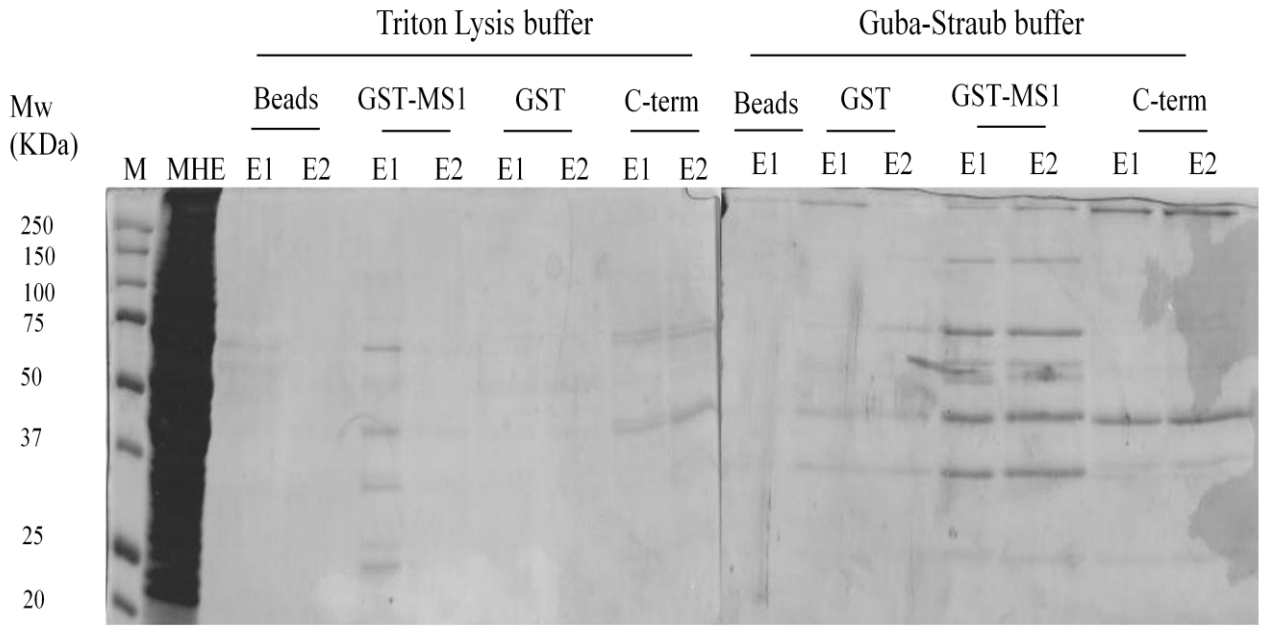

Figure 4.16: Binding assays using Mouse heart extract in Guba Straub buffer or TLB
Binding assays were performed using mouse heart extracts made in either triton lysis buffer or guba-straub buffer. 75 µl of beads with immobilized protein or without anything bound to them were left to tumble with 2 mg of MHE. After binding, any bound proteins were eluted, loaded onto an SDS-PAGE gel and coomasie stained with sample buffer for analysis. Above shows the eluted fractions from the respective proteins used in the binding assays

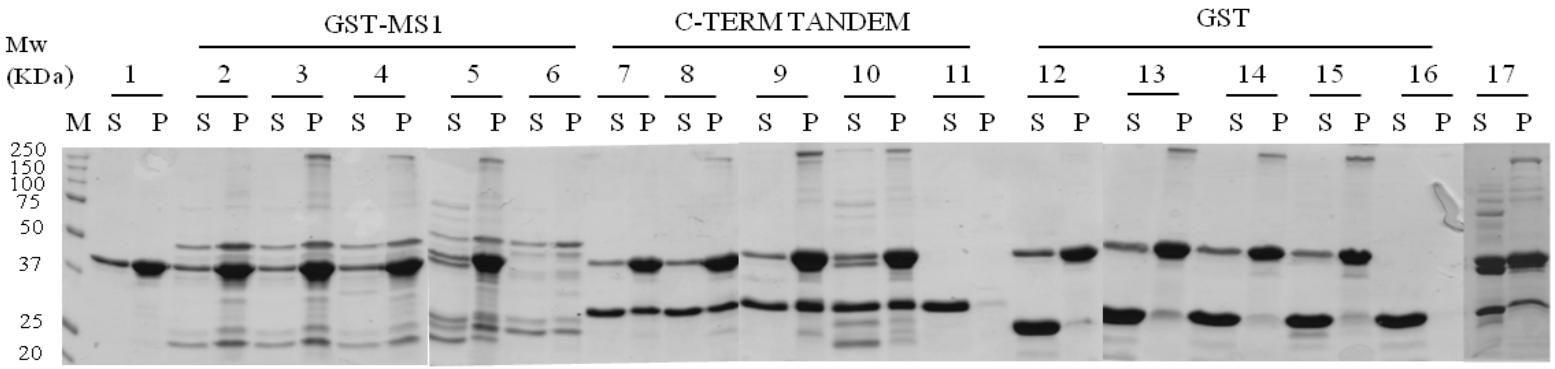

Proteins / Tube No.	1	2	3	4	5	6	7	8	9	10	11	12	13	14	15	16	17
F-actin	+	+	+	+	+	-	+	+	+	+	-	+	+	+	+	-	+
Myosin	-	-	+	+	+	-	-	+	+	+	-	-	+	+	+	-	+
Tropomyosin	-	-	-	+	+	-	-	-	+	+	-	-	-	+	+	-	+
Troponin	-	-	-	-	+	-	-	-	-	+	-	-	-	-	+	-	+
N-term tan	-	+	+	+	+	+	-	-	-	-	-	-	-	-	-	-	-
C-term tan	-	-	-	-	-	-	+	+	+	+	+	-	-	-	-	-	-
GST	-	-	-	-	-	-	-	-	-	-	-	+	+	+	+	+	-

Figure 4.17: *In vitro* Co-sedimentation assay of GST-MS1, MS1 C-terminal tandem with F-actin and myofibrillar purified proteins.
After each fusion protein was incubated with F-actin and the different myofibrillar proteins in F-actin buffer, the mixtures were sedimented by ultrcentrifugation. The supernatant was carefully removed from the pelleted protein and both pellet and supernatant. Sample buffer was added and samples loaded and run on an SDS-PAGE gel, then coomassie stained. The lane labelled M is the molecular weight marker, S represents the supernatant while the P, represents the pellet in the above figure of each set of proteins.The table above shows the proteins added to each lane.

(tropomyosin, myosin, troponin complex) that were incubated with either N-terminal tandem, C-terminal tandem or GST and subjected to ultracentrifugation.

A comparison was made between the sedimentation assays with different proteins and F-actin after centrifugation. Lane M contains the molecular weight marker, S and P is referred to as the supernatant and pellet fractions that were run on a SDS-PAGE gel after the co-sedimentation assay was performed. Purified F-actin alone was predominantly present in the the pellet and to a lesser extent in the supernatant (Figure 4.17 in lane 1). MS1 C-terminal tandem protein on its own remains in the supernatant after centrifugation; this was seen in lane 11S of figure 4.17 where there was a band of correct size of ~35 kDa. C-terminal tandem in the presence on actin and the other proteins which co-precipitate with actin, was present in both the supernatant and pellet as seen in lanes 8,9 and 10 in figure 4.17.

GST-MS1 N-terminal tandem was present in both the supernatant and pellet in lanes 6S and 6P without the presence of actin. This is an indication that GST-MS1 N-terminal tandem precipitated during high speed centrifugation during the co-sedimentation assay. GST-MS1 N-terminal tandem protein in the presence of actin only, was present in lanes 2S and 2P in figure 4.17. There was no major difference where GST-MS1 was present when compared with GST-MS1 N-terminal tandem in the absence of actin in lanes 6S and 6P except for lanes 3S and 3P. Lane 3P is GST-MS1 in the presence of actin and myosin, where myosin seemed to show a more distinct band. A comparison was made between GST-MS1 N-terminal tandem with actin only in lane 2 with GST-MS1 N-terminal tandem in the presence of actin and the other purified proteins myosin, tropomyosin and troponin complexes in lane 5S and 5P, where there was no major difference.

The GST protein was used as a negative control to determine whether there would be any type of protein-protein interaction between the tag and the other proteins. The GST protein did not sediment during the co-sedimentation assay which meant the protein did not precipitate as a result of high speed centrifugation as seen in lane 16 comparing the supernatant with the pellet (S and P) in figure 4.17. The negative control, GST was not seen in the pellet in the presence of actin (lanes 12 P and S) and all co-sedimentation experiments showed GST was not present in the supernatant (S). With the addition of myosin and other myofibrillar proteins, there was no GST protein being pelleted (lanes 12-15).

The results from the co-sedimentation assay, confirms that MS1 C-terminal tandem binds to actin, based on the observations without the presence of actin, C-terminal tandem was present in the supernatant. However, when C-terminal tandem is in the presence of actin, it is found in the supernatant as well as the pellet. MS1 C-terminal tandem has both actin binding domains present; ABD1 and ABD2. This was the positive control in these experiments and confirmed previous findings where the C-terminal region is known to bind actin (Arai *et al.,* 2002, Fogl *et al.,* 2011 unpublished data). The negative control; GST was found present in the supernatant after ultracentrifugation, this did not change with the presence of actin or the other purified proteins, which suggests no interactions with the other myofibrillar proteins. GST-MS1, N-terminal tandem precipitated during the co-sedimentation assay, where the protein was found both in the supernatant and the pellet, when GST-MS1 N-terminal tandem was on its own. However although this was seen, it is still possible that one of the myofibrillar proteins that are bound to actin, binds to the N-terminal region of MS1. Alternative experiments should be explored to test the binding affinity to the proteins, which do not require high speed centrifugation. This experiment was repeated three times and yielded the same results.

4.4. Discussion

The experiments described in this chapter were carried out in order to identify new binding partners for the MS1 N-terminal domain. Extensive research has been done on the C-terminus of MS1, two actin binding domains that allow for binding to actin as well as the actin binding LIM domain proteins; ABLIM-2 and 3 have been identified (Arai *et al.,* 2002; Barrientos *et al.,* 2007). However, the N-terminus of MS1 has been so far poorly investigated. Analysis of the sequence showed there are some phosphorylation sites within the N-terminal region of MS1 which are not present at the C-terminus. We explored the use of two tandem proteins which covered the entire length of MS1 at the N-terminus and C-terminus. N-terminal tandem covered amino acids 1-196, while His-tagged MS1 C-terminal tandem covered amino acids 193-375. An *in vitro* binding assay was optimised and the purified MS1 proteins were used as bait proteins, coupled to NHS-activated sepharose resin. Mouse heart extract was used as a source to determine new interacting proteins with MS1. MS1 is a highly specific cardiac, skeletal and smooth muscle protein. Investigating new interactions might

provide more insight into the cardiac function of MS1 and the pathways the protein is connected with in the heart.

4.4.1. Novel Proteins Identified by Mass Spectrometry

Mass spectrometry analysis of bands from the binding assays identified new putative interactions with MS1. The binding assays with MS1 C-terminal tandem confirmed α-tropomyosin, Troponin T, RhoV and actin. Mass spectrometry results identified bands from binding assays with GST-MS1 (N-terminal tandem) as myosin-6, actin, α-tropomyosin, troponin I and Myosin LC2. All experiments were repeated a minimum of three times and negative controls were used to ensure binding of proteins was independent of the resin used to immobilize the bait proteins.

MS1 binding to actin at the C-terminal end confirmed previous findings (Arai *et al.,* 2002). However, actin binding to the N-terminal region of MS1 is a new finding, since there are no studies which suggested MS1 has actin binding domains present within the N-terminus. The other proteins Troponin T, Troponin I, Myosin-6, Myosin LC2 and alpha-Tropomyosin are myofibrillar proteins that have important roles in cardiac and skeletal muscles. These roles are muscle contraction, muscle structure and mutations in these genes can also lead to defects found in the heart (Goll *et al.,* 2008; Canton *et al.,* 2011; Hoffman *et al.,* 2001; Reviewed in Clark *et al.,* 2002; Kerkela and Force, 2006). Rho V is a member of the Rho GTPase family of small GTP-binding proteins involved in cytoskeleton organization, migration and transcription (Bustelo *et al.,* 2007; Hall, 1998). Rho V was observed to play a role in the reorganization of the actin cytoskeleton via JNK activation but it is still poorly understood (Aronheim *et al.,* 1998). RhoA which is from the same family of RhoV is known to interact with MS1 in the cytoplasm to facilitate SRF signalling (Kuwahara *et al.,* 2005). Unfortunately, RhoV was only identified once in the binding assays and there is no evidence that it is found in the heart (Aronheim *et al.,* 1998).

The myofibrillar proteins identified are localized in the same region of the sarcomere as MS1. MS1 is found localized in the I-band, z-disk and to a lesser extent the M-line (Arai *et al.,* 2002). The proteins actin, tropomyosin and the troponin complex are found within the thin filaments of the sarcomere in the I-band region, while myosin and myosin LC2 is found within the A-band of the sarcomere (Fauci *et al.,* 1998; Seidman and Seidman, 2001, Kruger and Linke, 2011). The interaction between myosin and actin is necessary for movement. In order to give an idea of how all these proteins are in complex, figure 4.18 shows the arrangement of the proteins within the sarcomere.

.

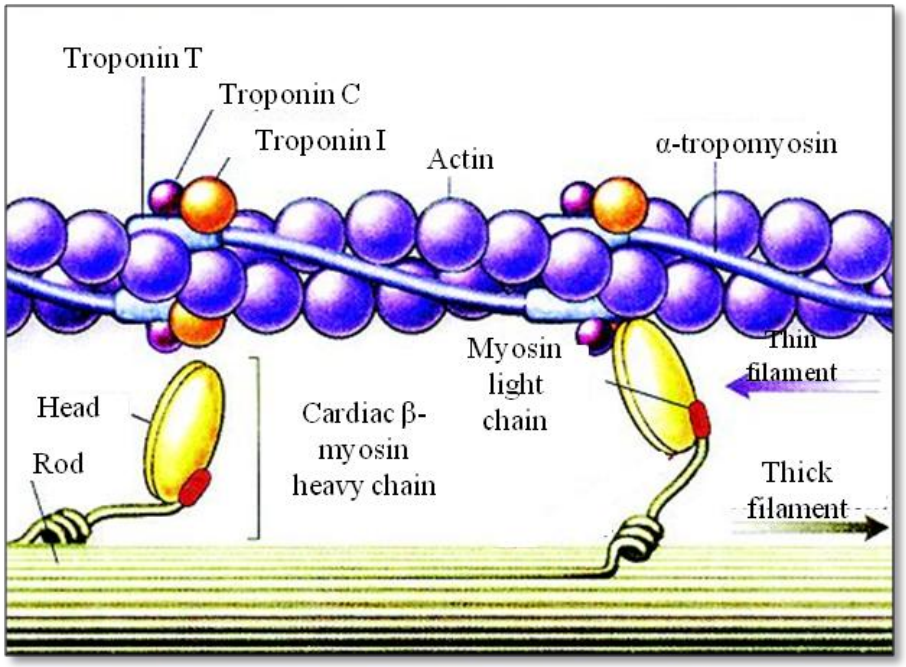

Figure 4.18: Organization of the myofibrillar proteins within the sarcomere
The thin filaments are made up of actin, α-tropomyosin, and the troponin complex (I, C and T). The proteins within the thin filaments are also known as regulatory proteins. In their arrangement in the sarcomere, tropomyosin is found along the length of actin. The proteins in the troponin complex have different functions; Troponin I inhibits myosin binding to actin, troponin C is the calcium binding component and Troponin T binds to tropomyosin which allows the entire troponin complex to bind. The thick filaments consist of myosin and myosin LC2. Myosin binds to actin to facilitate movement. (Figure adapted from Kamisago *et al.*, 2000).

Myosin was identified in the binding assays with GST N-terminal tandem (1-196 a.a) as the bait protein, however myosin was not present in any of the binding assays using MS1 C-terminal tandem. The presence of myosin might have influenced actin being pulled out from the mouse heart extract in the binding assays. This led to further investigation, to determine whether separation of actin and myosin from each other confirms whether these proteins are direct interacting proteins or whether they are binding as a result of the presence of one protein, which has bound to the others as a complex and not individually to MS1.

4.4.2. Comparison between Extracts made in Guba-Straub Buffer and Triton Lysis buffer

Binding assays were carried out using extract prepared with Guba-Straub buffer. Guba-straub buffer is commonly used to allow for the dissociation of actin and myosin. The addition of high concentrations of salts and phosphate to an actin-myosin complex, leads to the dissociation of myosin from actin (First discovered by Straub, 1942; Barany and Barany, 2003). The result observed in Figure 4.16 did not show that there was a difference with binding assays using Guba-Straub buffer. It could be clearly seen that the extract which used the mouse heart extract made with the Guba-Straub buffer, showed the presence of myosin present in the binding assay using MS1 C-terminal tandem protein. This was never observed in previous experiments using extracts prepared in triton lysis buffer. Another theory as a result of myosin binding to C-terminal tandem in the presence of Guba-Straub buffer was; the dissociation of actin from myosin could have caused a conformational change in myosin that allowed for binding to the C-terminus. Therefore a control was necessary to ensure dissociation between the two proteins should be included (comparisons should be made with and without ATP). The presence of ATP dissociates myosin from actin, however when ATP is hydrolysed actin and myosin rebind (Szent-Gyorgyi, 2004). The results for N-terminal tandem (1-196 a.a.) showed that myosin and actin were still pulled out from the binding assay. A possible explanation is that actin and myosin are separated, myosin binds independently and actin may remain in complex with tropomyosin and the troponin complex. In the myofibril the protein are bound to each other in a complex, where there is a troponin-tropomyosin-actin-myosin arrangement (Smith, 2007).

A new approach was taken to look at the binding of these proteins and to confirm interactions between them and the bait proteins. The use of an *in vitro* co-sedimentation

assay would be useful to determine whether actin is binding directly with the bait protein GST-MS1 or whether these proteins need to bind in complex.

4.4.3. *In vitro* Co-sedimentation Assay to determine Actin Binding

The results confirmed C-terminal tandem is binding directly to the actin, which was known before. More importantly this confirmed the experiment itself was working efficiently. The focus in this case was the N-terminus of MS1 as there are no reports of actin binding activity or an actin binding site in the N-terminus. The results from the assay showed that although there was co-sedimentation of MS1 protein with actin, there was a small amount of the N-terminal tandem protein seen in the pellet when centrifuged at the high speed on its own. The experiment was repeated three times and each time there was a small amount of protein in the pellet, however only once was it seen that there seemed to be more protein with the presence of actin. The experiment had certain limitations since the GST-MS1 N-terminal tandem protein precipitated during centrifugation at high speed, which made it hard to analyse the results for this particular protein. This could have been due to the choice of buffer used for the co-sedimentation assay was not compatible with the proteins or the salt concentration resulted in obstruction of the proteins binding (Srivastava and Barber, 2008).

Testing the interactions via co-immuoprecipitation could have been another method for confirming these interactions, however due to time constraints this proved to be problematic. Experiments were carried out using the purified proteins individually in binding assays to confirm their binding to MS1. However this proved to be a problem in terms of getting the purified proteins to bind; possibly because individual protein requires the presence of the other proteins for interactions to occur. The conditions of the heart *in vivo* may have proteins which are phosphorylated and also working together in a complex. Whereas *in vitro*, these conditions are not the same using the purified proteins, which are in a buffer which does not mimic *in vivo* conditions well.

It is possible that the proteins pulled from the binding assay, bind weakly and may not be detected or become detached during the wash steps as the washes were quite stringent to avoid any nonspecific binding of the proteins. It can be assumed that the bands seen from the binding assays are strongly interacting proteins given the stringency of the washes. Another approach using extract from stressed hearts with the bait proteins would be of interest, since MS1 is known to be a stress responsive protein.

Despite the limitations encountered during these experiments, the proteins identified could be genuine interactions, given the location of the proteins in proximity to MS1 and their functions. MS1 is implicated in movement such as eccentric and concentric exercise (MacNeil *et al.,* 2010; Russel A.P, 2010; Vissing *et al.,* 2013). Myofibrillar proteins are responsible for muscle contraction and cardiac contraction (Cooper, 2000; Behrmann *et al.,* 2012; King, 2014). MS1 is thought to act as a mechanosensor where extracellular stress that leads to intracellular signals results in a link to contractile function within the muscle through MS1 (Reviewed in Wallace *et al.,* 2012). The myofibrillar proteins are well involved in diseases of the cardiac and skeletal muscle where mutations in actin, myosin and tropomyosin can lead to serious conditions such as cardiac hypertrophy and heart failure (Seidman and Seidman, 2001; Canton *et al.,* 2011; Robinson *et al.,* 2006; Yamada *et al.,* 2005).

The myofibrillar proteins; actin and myosin may bind to MS1 while they are in complex. The C-terminus of MS1 binds actin which is connected to myosin and the tail of myosin could bind to the N-terminus of MS1, since actin interacts with myosin via the myosin head (Lodish *et al.,* 2000). A protein known to bind to actin and myosin while they are in complex is the myosin binding protein C (MyBP-C), where it acts as a bridge between the thick and thin filaments, binding to myosin at the C-terminal end and actin at the N-terminal region (Luther *et al.,* 2011; Shaffer *et al.,* 2009; Kensler *et al.,* 2011).

These potential interacting proteins are of particular interest and should be further investigated, since they might provide further insight into MS1 in cardiac function.

Chapter 5. Investigation of MS1 as a Potential substrate of MAPKs

5.1. Introduction

MS1 is implicated in many roles within the cardiac and skeletal muscle, where it is involved in early stages of cardiac hypertrophy, myogenic differentiation, proliferation, regulation of skeletal muscle and actin dynamics (Reviewed in Wallace *et al.,* 2012; Lamon *et al.,* 2014). The C-terminus of MS1 has been the main focus of research since there are two actin binding domains present, which facilitate the involvement of MS1 in the SRF signalling pathway (Fogl e*t al.,* 2011). MS1 co-precipitates with ABLIM proteins and is thought to play a role in strengthening its ability to bind to the sarcomere, which substantiates the role MS1 plays in the downstream signalling in the muscle (Barrientos *et al.,*2007). The localization of MS1 in cells is seen predominantly in the cytosol; however, recent studies have shown that MS1 binds to DNA and can be found within the nucleus, but the ability for MS1 to translocate to the nucleus or what function it plays is unclear (Fogl, Unpublished data; Wallace *et al.,* 2011).

Increased MS1 expression leads to the transcriptional activation of SRF in the nucleus via polymerization of actin within the cytosol (Arai *et al.,* 2002). MS1 acts independently or in association with the Rho GTPase, Rho A to facilitate this process (Arai *et al*., 2002 and Kuwahara *et al.,* 2005). The exact mechanism which allows MS1 and Rho A to interact is not known. This raises many questions as potentially how MS1 and Rho A interact during the intracellular signalling pathway and the different processes within the muscle tissue that allows for the expression of muscle specific genes. The MAPK signalling cascade also plays an active role in the transcriptional activation of SRF within the nucleus by phosphorylation of ternary complex factors (TCFs) which are a subclass of Ets-type co-factors (Buchwalter *et al.,*2004). The subfamily of the MAPKs, the stress activated kinases (SAPKs) JNK and p38 have been well studied in their roles in hypertrophy, environmental stress, pathological remodelling within the cardiac and skeletal muscle (Gertis *et al.,* 2007 and Rose *et al.,* 2010). The MAP kinase ERK is known to be heavily involved in some aspects of cardiac development which would explain the role it plays in myogenesis and pathology such as many diseases of the heart. An example is hypertrophic signalling within cardiac muscle by activating the PI3K pathway and Rho signalling pathway upstream (Reviewed in Rose *et al*., 2010).

Post-translational modification by phosphorylation is used in signal transduction and important to determine the molecular mechanism of how proteins are activated. This type of modification allows for the control of many cellular processes such as growth, differentiation, motility, membrane transport and metabolism (Manning *et al.*, 2002). MS1 is found within the sarcomere, where proteins located in the z-disk are phosphorylated by ERK upon its activation, to facilitate the expression of muscle specific genes which are controlled by SRF (Carnac *et al.,* 1998). MS1 is heavily involved in actin dynamics and skeletal muscle regulation (Reviewed by Lamon *et al.*,2014). To date there is no published data associated with the functional activity of the N-terminus of MS1. MS1 is not known to have any kinase activity or known to be a downstream substrate for MAPK proteins or any other kinases.

Analysis of the protein sequence of MS1/STARS shows three potential phosphorylation sites which display a characteristic motif for phosphorylation by the SAPKS, p38 and JNK. The motifs characteristic to phosphorylation by the MAPKs are Pro-X-threonine/Serine motifs which are followed by an extra proline in some cases; located in the -2 position relative to ser/thr in proteins targeted for substrate phosphorylation (Cargnello *et al.*, 2011; Rose *et al.*, 2010). Previous experiments in the lab showed that MS1 mRNA expression was decreased with the use of JNK inhibitor SP600125 during simulated ischaemia/ reperfusion injury. This decrease in mRNA expression was not seen with the use of ERK and p38 inhibitors (Hay., 2009).

5.2. Aims of this Chapter

We wanted to determine whether the motif present at the N-terminal region of MS1 could be a potential substrate of MAPKs JNK, p38 and ERK. This would help to determine what signalling pathways regulate MS1, as it is unclear the upstream targets of MS1.

5.3. Results

5.3.1. Potential phosphorylation sites of MS1/STARS at the N-terminal region of the protein.

Analysis of the protein sequence of MS1 revealed three potential sites which have a motif characteristic of MAPK/SAPK substrate phosphorylation. The potential sites are located at the N-terminal region of MS1 at residues Thr62, Ser77 and Ser150 (Figure 5.1). Based on sequence alignments using sequences from different species, amino acid Ser150 is conserved in the rat, mouse, pig and human (Figure 5.2). In order to carry out this investigation a radioactive *in vitro* kinase assay was performed in order to determine whether or not MS1 could potentially act as a substrate for any of the MAPKs, JNK, p38 or ERK.

To test whether MS1 is a substrate for the MAPKs, we used HEK-293, Human Embryonic Kidney cells to facilitate the overexpression of the kinases to be used in immune-complex kinase assays. Plasmids which encoded the MAPKs HA-ERK, HA-JNK and Flag-p38 were transfected into HEK-293 cells. The cells were subjected to 0.5 M sorbitol treatments to induce activation of p38 and JNK or 1 µM PMA to induce activation of ERK.

MS1 proteins which were bacterially expressed and purified as discussed in Chapter 4 and used as substrates for the activated MAPKs (Figure 5.3). Three of the constructs were used in these phosphorylation assays. MSD1 (Myocyte stress Domain 1) protein, which is the N-terminus of MS1 (residues 2-118 aa) is 17.9 kDa with a His-tag. This domain has two of the three amino acid residues predicted to be phosphorylated (Thr62 and Ser77). The N-terminal tandem construct, which covers the amino acid residues 1-196 (Fig. 5.3) is fused to GST at the N-terminus is a 54 kDa fusion protein. This has the first domains, MSD1 (2-118 aa) and MSD2 (40-196 aa). The sequence of this construct covers all three of the predicted phosphorylation sites, Thr62, Ser77 and Ser150. The C-terminus of MS1 was used as a negative control, which is referred to as C-terminal tandem (193-375 aa). The construct used had a His-tag fused to the N-terminus. The amino acid residues covered in this construct is between 193-375 aa and has two of actin binding domains ABD1 and ABD2. Another negative control used was the

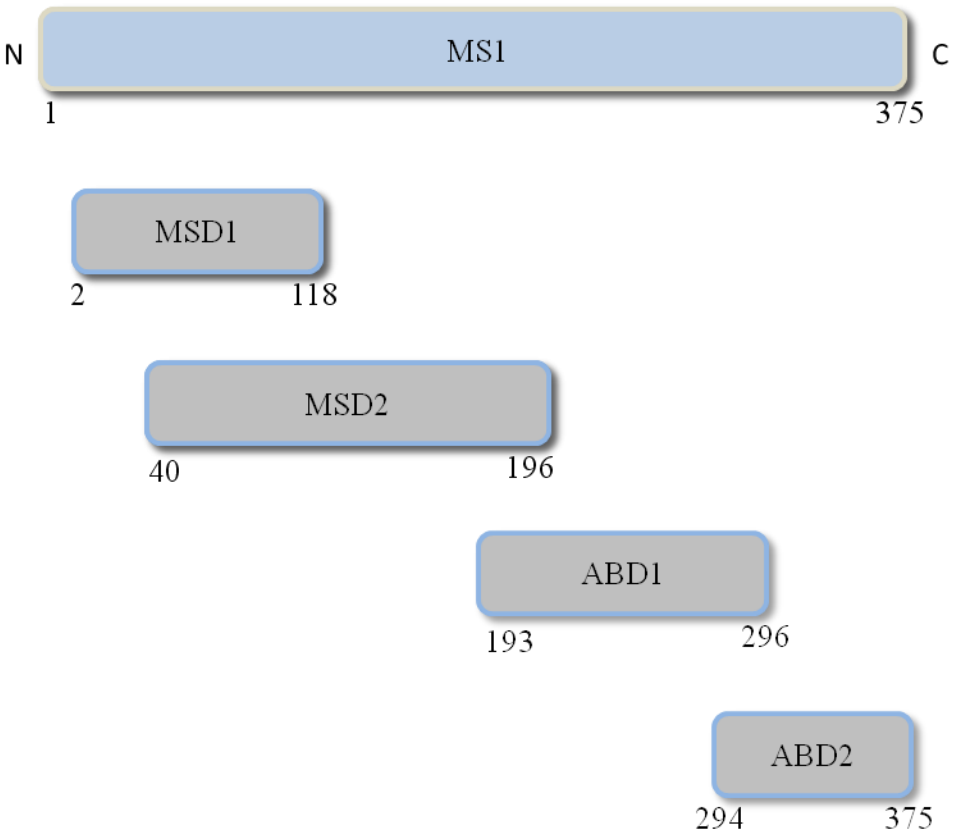

Figure 5.1: Potential phosphorylation sites within the N-terminal region of MS1 within MSD1 and MSD2 domains,
A. Schematic representations showing the sequence of MS1 (1-375 a.a) and the position of predicted phosphorylation sites Thr 62, Ser 77 and Ser 150 at the N-terminus. **B.** The full protein sequence of Rat MS1 showing the highlighted motifs in red which are for MAPK substrate phosphorylation by JNK and p38.

Figure 5.2: An Alignment using Clustalw showing the N-terminus of MS1 where one of the predicted phosphorylation motif is conserved in 4 different species

The alignment which was done using MS1 from pig, rat, mouse and human shows that T62 (underlined in black) is not conserved throughout the species however, S77 is conserved in rat, mouse and pig which is grouped by the black box. In human, there is an upstream SP present which is circled. S150 is seen conserved in all species which is grouped by the red box. Above the species are; Q8K4K7 – Rat, B5SNZ6.1-Pig, Q8BUZ1.1- Mouse and AAM2768.1- Human.

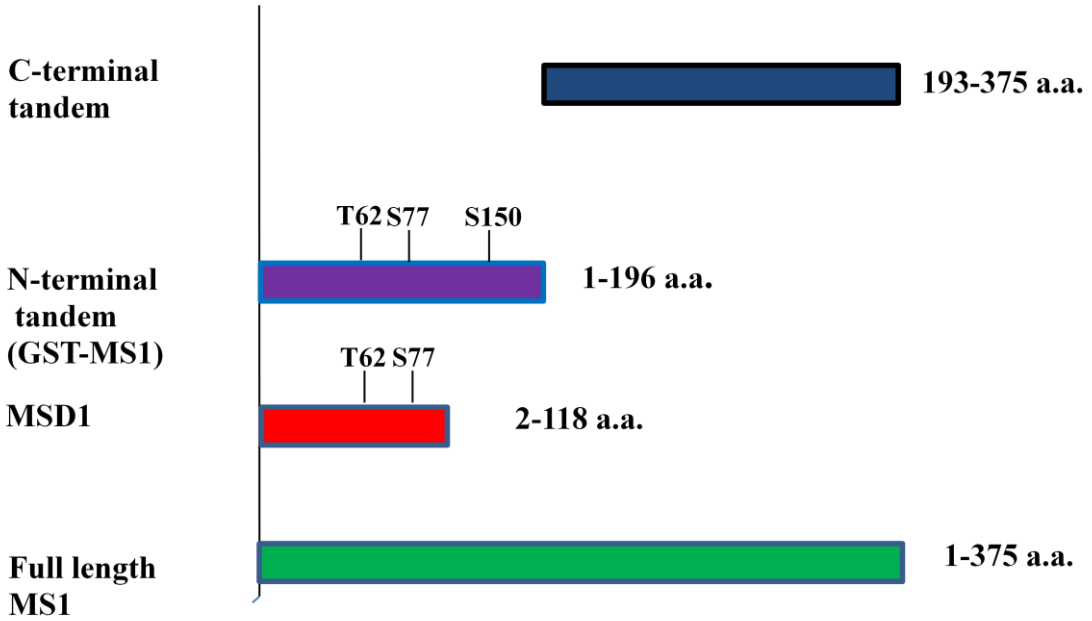

Figure 5.3: Protein fragments which were used in the *in vitro* phosphorylation assays
Above shows the covera*ge* of each protein fragment with the positions of their phosphorylation sites where C-terminal tandem and MSD1 are His-tag*ge*d, while N-terminal tandem is GST-tag*ge*d

recombinant protein GST, which would confirm any phosphorylation observed in the case of GST-MS1, was specific to the MS1 protein and not the GST tag.

5.3.2. Activation of transfected and endogenous MAPKS: JNK, p38 and ERK

HEK293 cells were plated onto 10cm dishes and grown to 85-90% confluency before being transfected with plasmids expressing, either HA-ERK, HA-JNK or Flag-p38. After transfection, cells were placed in culture medium 24 hr post transfection and then serum starved for 16 hr. The cells were then either left untreated or subjected to treatment with 0.5 M sorbitol for 30 min, to induce osmotic shock to activate JNK and p38 or phorbol 12-myristate 13-acetate PMA (1 µM) for 30 min to activate ERK. Sorbitol treatment was chosen because it has been widely used in order to activate predominantly JNK and p38 (Kayali *et al.,* 2000). PMA is a very strong hypertrophic agonist which is known to activate the PKC pathway, which leads to the activation of ERK (Keshari e*t al.,* 2013). Cell lysates were prepared and a sample was analysed by western blotting to confirm that the kinases were successfully transfected and phosphorylated. The remaining lysates were then used for *in vitro* phosphorylation assays.

The cell lysates were run on a 12 % SDS-PAGE gel and western blots were probed with an anti phospho-JNK antibody (1:1000) (Figure 5.4A). Sorbitol treatment resulted in phosphorylation of endogenous and overexpressed JNK which showed bands at approximately 54 and 44 kDa and represents JNK1 and 2 (Figure 5.4A). Western blots were also done with anti-JNK antibody to detect total JNK in order to ensure the same levels were loaded and the apparent activation of the JNK and transfected JNK is not due to unequal loading. It should be noted that the bands which are also seen in figure 5.4A in lanes 2 and 6 are endogenous phospho-JNK and the additional band present in lane 4 is overexpressed phospho-JNK. The activation of phospho-p38 was also successful as indicated by an increase in intensity of the band detected with the anti-phospho-p38 antibody seen in figure 5.4B. To confirm cells were successfully transfected with pCDNA3-Flag-p38, blots were probed with anti-FLAG antibodies as seen in figure 5.4B, which shows a band of ~38 kDa present in the lanes where lysates from cells transfected with FLAG-p38 were present. Transfected cells with constructs encoding FLAG-p38 showed an increase in p38 phosphorylation following sorbitol treatment, although the untransfected cells, showed less phosphorylation in lane 2, activation of phospho-p38 was seen in lanes 4 and 6 (Figure 5.4B).

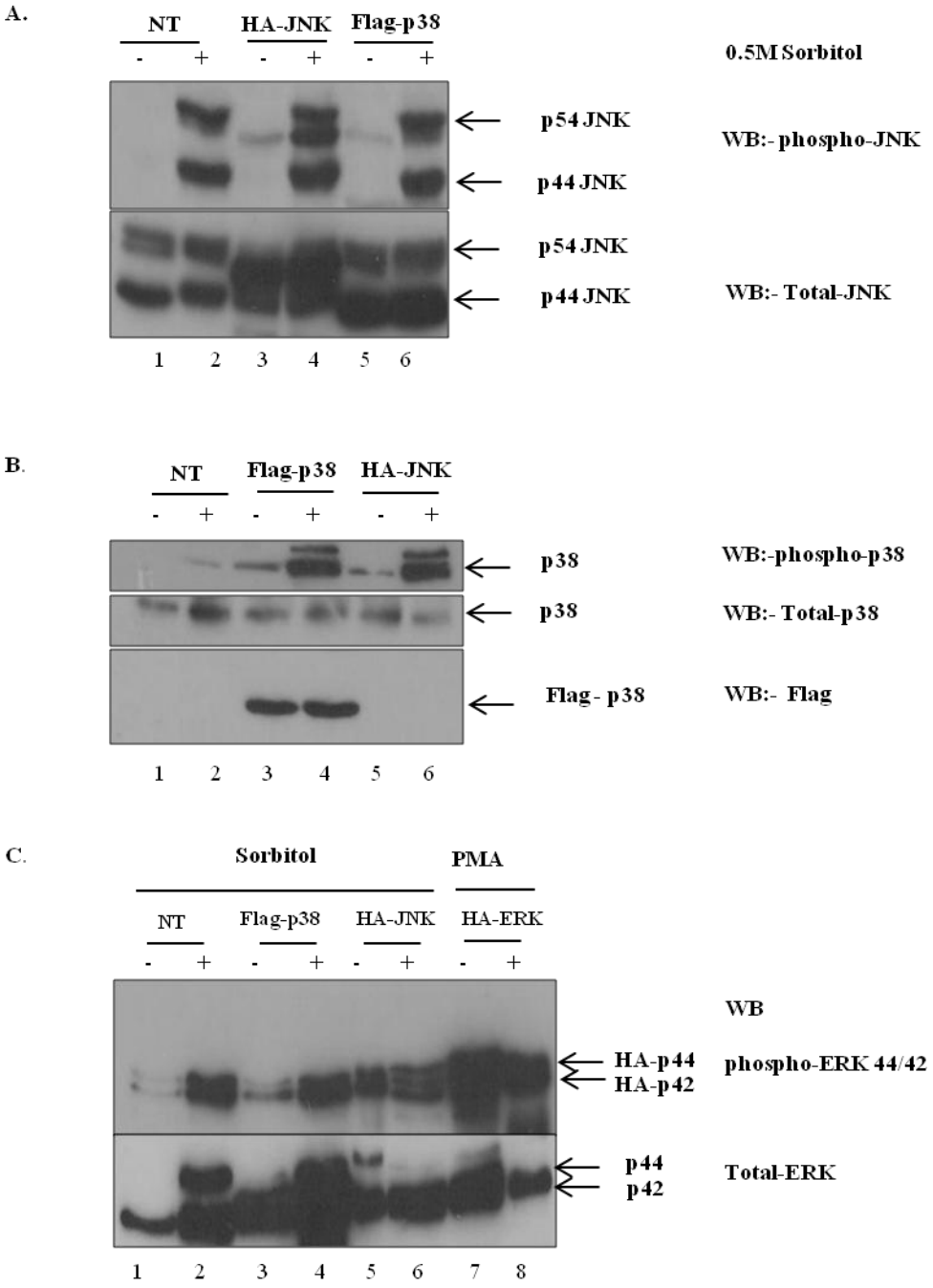

Figure 5.4: Western blot to determine phosphorylation of kinases: JNK, p38 and ERK. HEK293 cells were transiently transfected with 10 µg of HA-JNK, Flag-p38 or HA-ERK DNA constructs before the cells were treated with a stimulus of either sorbitol (0.5 M) or PMA (1 µM) for 30 min. After treatments, cells were lysed and proteins were immunoprecipitated. A sample of lysate was run on an SDS-PA*GE ge*l and subjected to western blotting using phospho-specific antibodies as indicated or antibodies detecting the specific MAPKs. Remaining samples were used for in vitro phosphorylation assays

There was successful overexpression and activation of ERK, which was confirmed by western blot analysis using anti-phospho ERK 44/42 as a result of cells subjected to PMA treatment (Figure 5.4C). Although, the cells in lanes 2,4 and 6 were not treated with PMA but with 0.5 M sorbitol, this resulted in endogenous sorbitol activation of ERK. Sorbitol treatment was shown previously to activate ERK via MAP3K which is responsible for activating JNK and p38 during osmotic stress (Fusello *et al,*. 2006; Petrich *et al.,* 2011 and Kayali *et al,*. 2000). PMA promoted a large increase in intensity of the band detected with anti-phospho ERK antibody (Figure 5.4C).

The lysates which were made from cells transfected with pcDNA3-Flag-p38 were subjected to immunoprecipitation of p38 using anti-Flag antibody and both lysates and immunoprecipitates were run on a SDS-PAGE gel, then western blotted using anti-FLAG antibodies against the tag. The Flag-tag of p38 was detected as seen in figure 5.5 in both the treated and untreated samples while the immunoprecipitates from cells which were either untreated or treated with sorbitol, confirmed that the overexpressed protein was immunoprecipitated with the protein G-sepharose antibody bound beads as seen in figure 5.5 lanes 7 and 8. Lanes 5 and 6 were the negative controls which were the lysates from untransfected cells added to protein G sepharose beads with anti-Flag antibody bound to it. These lanes did not show any presence of the Flag-tagged p38 protein which was predicted to be ~38 kDa. Bands at approximately 50 and 25 kDa seen in the IP samples correspond to heavy chain and light chain IgG bands (Figure 5.5).

Lysates were also analysed by western blotting using anti-HA antibody to confirm the successful transfection of HA tagged proteins JNK and ERK (Figure 5.6). Bands corresponding to HA-JNK and HA-ERK are seen in samples from transfected cells which had HA-tagged JNK (lanes 3-6) and lysates from cells transfected with pcDNA3-HA tagged ERK (lanes 7 and 8) which is slightly smaller in molecular weight (Fig. 5.6). These experiments confirmed that HEK-293 cells, were successfully transfected with the proteins to be used as imuunoprecipitates for *in vitro* kinase assays and confirmation that all MAPKs were phosphorylated; which were identified by antibodies to detect their tags and overexpression at the correct size.

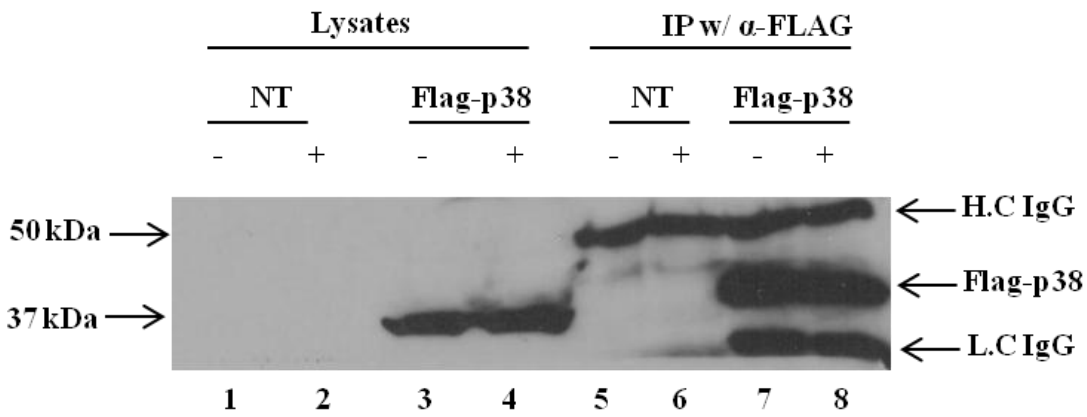

Figure 5.5: Western blot analysis of HEK293 cell lysates and immunoprecipitates from cells transfected wit Flag-p38
HEK 293 cells were transfected with 8 µg of pCMV-Flag-p38 DNA. 24 hr post transfection, cells were stimulated with 0.5 M sorbitol for 30 min or left untreated. After treatments cell lysates were prepared, centrifu*ge*d and supernatants immuoprecipitated with anti Flag-antibody. Immunoprecipitates were loaded onto a 12 % *ge*l. Lanes 1-4 are cell lysates which were either treated (+) or untreated (-) with sorbitol with 1-2 being non-transfected cells and 3-4 were cells transfected with Flag-p38**.**

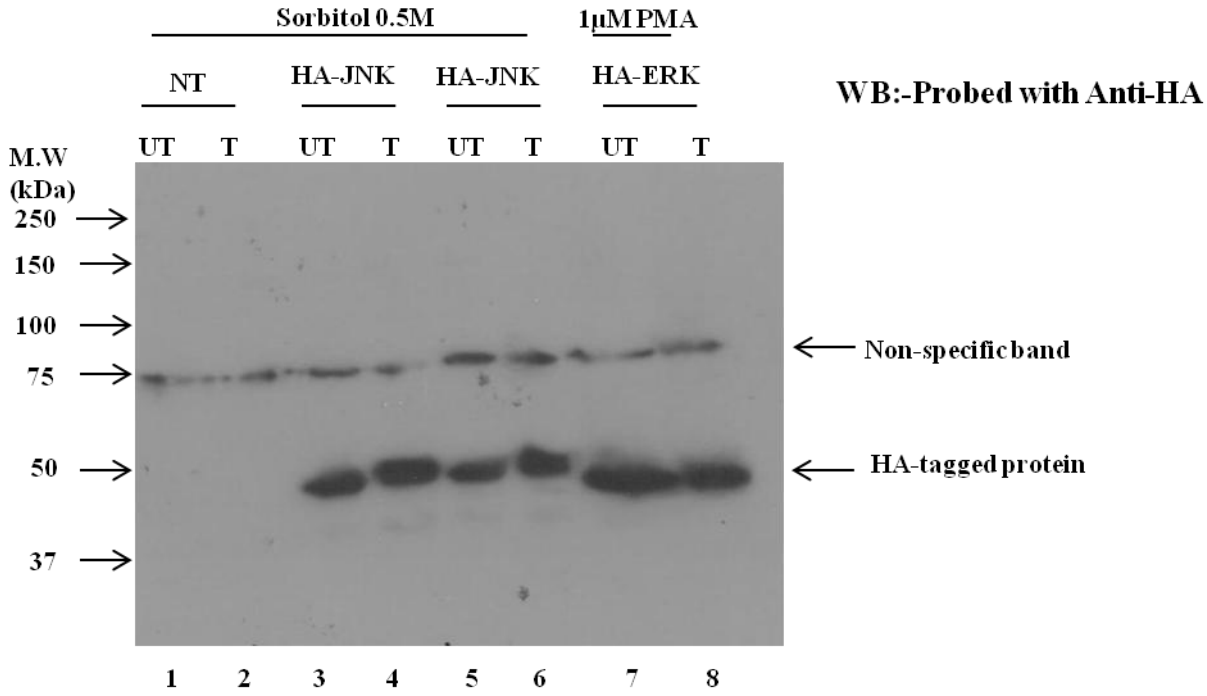

Figure 5.6: Western Blot analysis of HEK293 cell lysates from HEK293 cells transfected with either HA-JNK or HA-ERK.
HEK 293 cells were transfected with either 8 µg of HA-JNK or HA-ERK DNA for 24 hr and then serum starved for 16 hr before treated with either sorbitol (0.5 M) or PMA (1 µM) for activation of JNK and ERK for 30 min. Cell extracts were prepared, centrifu*ge*d and run on a SDS-PA*GE ge*l and western blotted with anti-HA antibodies to ensure that the cells were successfully transfected in order to be used for *in vitro* kinase assay.

5.3.3. In vitro phosphorylation assay to determine whether activated ERK can phosphorylate MS1

To determine whether or not MS1 could be a potential substrate of ERK *in vitro* phosphorylation assays were performed. HEK293 cells transfected with a construct HA-ERK were treated with PMA or left untreated. HA-ERK was immunoprecipitated with anti-HA antibody and *in vitro* phosphorylation assays were performed using three different MS1 protein fragments which were mentioned in section 5.3.1. It should be mentioned that these constructs together would cover the entire length of MS1, however the main emphasis of this study is placed on the N-terminus. Substrate phosphorylation of these fragments was compared with myelin basic protein (MBP), which is a known substrate of ERK and was used as a positive control to confirm ERK activation.

The results in figure 5.7 show phosphorylation of MSD1 in both the treated and untreated samples, however the sample which has been treated to activate ERK increased by 1.8 fold relative to the untreated. The other purified protein N-terminal tandem (1-196 aa) was not phosphorylated even though it has the same residues as MSD1 (2-118 aa). The N-terminal tandem (1-196 aa), protein had comparable levels of phosphorylation when compared with the purified GST protein. In relation to the level of phosphorylation of MBP, which is a known substrate of activated ERK it could be seen that it was almost twice as high in the stimulated sampled than the unstimulated sample.

The GST-MS1 (1-196 aa) was not phosphorylated by ERK, even with all three of the predicted residues present within the construct, however MSD1 was seen to be phosphorylated. Experiments of the immunoprecipitated *in vitro* kinase assays were repeated using MSD1 (2-118 aa), c-terminal tandem (193-375 aa) and the MBP protein. Based on the results in Figure 5.8, it could be seen that in the untreated (-) lane where MSD1 was added there was basal phosphorylation but in the treated (+) sample in comparison to the positive control of MBP phosphorylation half the amount of the positive control (Figure 5.8B). Phosphorylation of MS1 following stimulus was approximately 50% of the lane seen with MSD1.

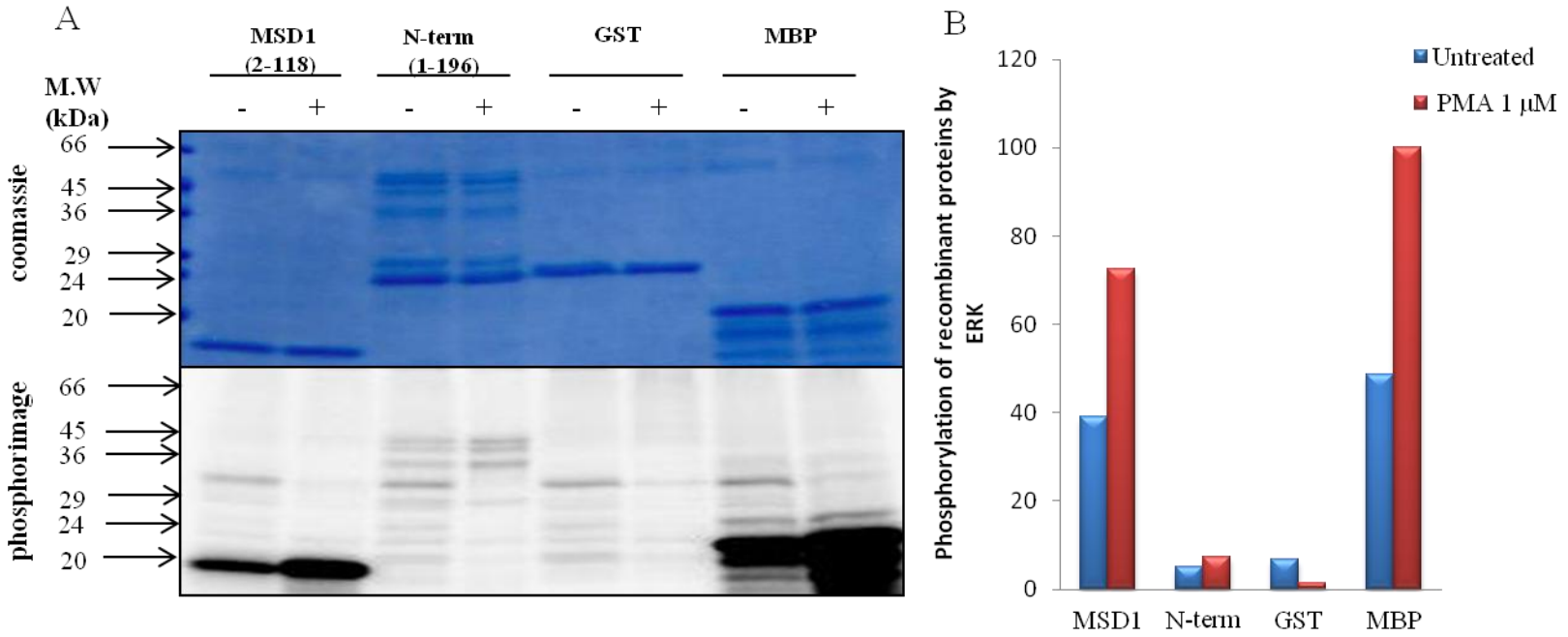

Figure 5.7: *In Vitro* phosphorylation assay showing substrate phosphorylation by activated ERK

A. HEK293 cells which were transiently transfected with HA-ERK (8 µg) for 24 hr and then serum starved for 16 hr were either left untreated or treated with PMA 1µM for 30 min. Lysates were made and immunoprecipitated with anti HA-antibodies. *In vitro* phosphorylation assays were performed using the indicated proteins as substrates. The samples were then analyzed on SDS-PA*GE ge*l, coomassie stained and subjected to autoradiography (32P). Molecular weights (kDa) are seen on the left. **B.** The amount of phosphorylation of each of the proteins was analyzed using a phosphorima*ge*r and the phosphorylation of the proteins was calculated relative to the phosphorylation of positive control MBP.

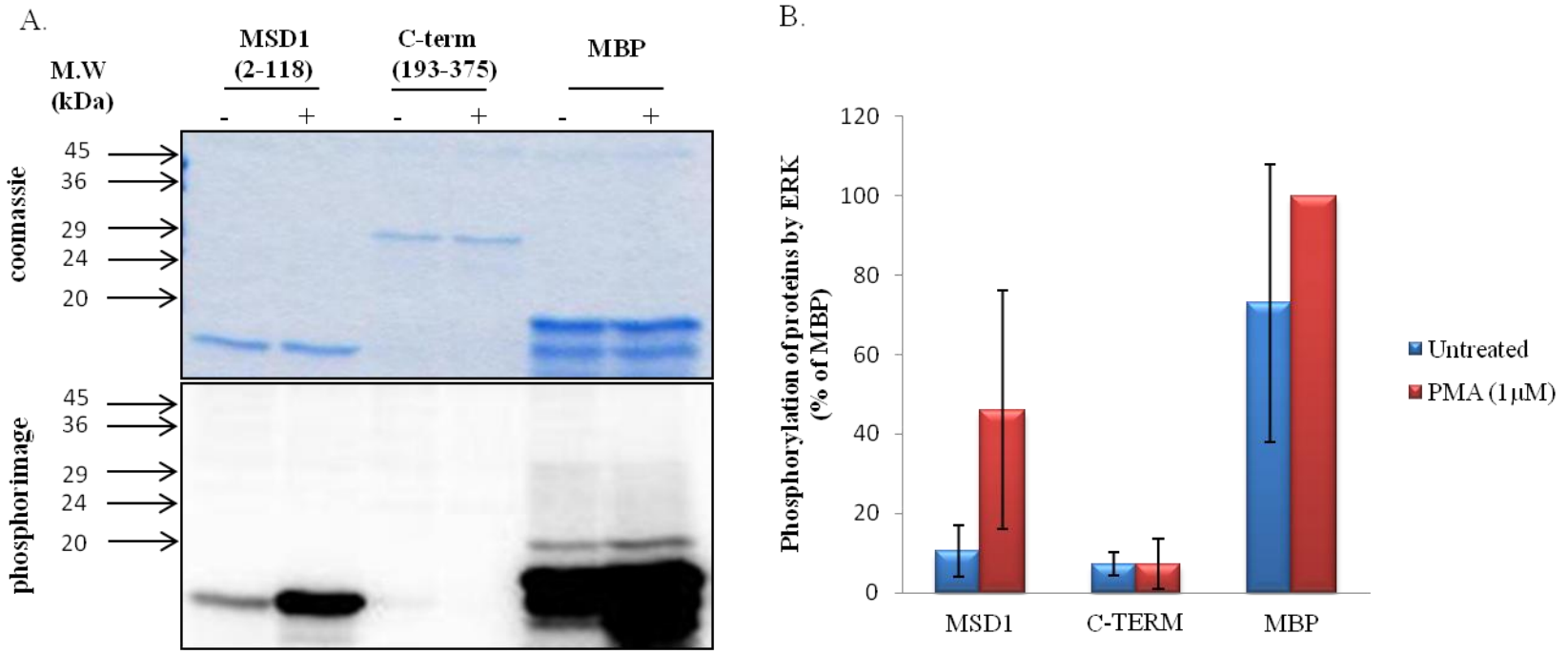

Figure 5.8: *In Vitro* phosphorylation assay showing substrate phosphorylation by activated ERK .
A. HEK293 cells which were transiently transfected with HA-ERK (8µg) for 24 hrs and then serum starved for 16 hrs were either left untreated or treated with PMA 1µM. Lysates were made and immunoprecipitated with anti HA-antibodies.*In vitro* kinase assays were performed using the indicated proteins and substrates above. The samples were then analyzed on SDS-PA*GE ge*l, coomassie stained and subjected to autoradiography. Molecular weights (kDa) indicated. **B.** The amount of phosphorylation of each of the proteins was analyzed using a phosphorima*ge*r and the phosphorylation of the proteins was calculated relative to the phosphorylation of positive control MBP. The data represents the mean of three separate experiments.

5.3.4. In vitro phosphorylation assays of immunoprecipitated p38 to determine phosphorylation of MS1 as a potential substrate

In vitro phosphorylation assays, using immunoprecipitated p38 were done to determine whether activated p38 leads to phosphorylaion of N-terminal MS1 fragments. HEK293 cells which were transiently transfected with pcDNA-Flag-p38 were either left untreated or treated with 0.5 M sorbitol. The cell lysates were prepared and FLAG-p38 was immunoprecipitated with anti-FLAG antibody. *In vitro* phosphorylation assays were performed using MS1 proteins as previously mentioned (Section 5.3.1) and positive control, GST-ATF2 as substrates.

Results from the assay showed that N-terminal tandem (1-196 aa) was not phosphorylated by p38. However, recombinant MSD1 (2-118 aa) protein had a high level of phosphorylation in this experiment, in both the treated and untreated samples when compared with the positive control GST-ATF2 (Figure 5.9). This again raised concern as to why there was evidence of phosphorylation seen for MSD1 (2-118 aa) samples and not the N-terminal tandem (1-196 aa) in the presence of activated p38. When the results of 3 independent experiments were quantified, the amount of phosphorylation by activated p38 on MSD1 is 50% less than the positive control, ATF2 (Figure 5.10). In this phosphorylation assay the C-terminus (193-375 aa) was used as a negative control as seen in Figure 5.10, and did not show any phosphorylation activity.

5.3.5. In vitro phosphorylation assays to determine if phosphorylated immunoprecipitated JNK can lead to substrate phosphorylation of MS1.

The final MAPK to be investigated was the C-Jun N-terminal kinase (JNK). HEK293 cells were transfected with HA-JNK and were either left untreated or treated with sorbitol. Lysates were immunoprecipitated with anti-HA antibody and added to the different substrates for the *in vitro* phosphorylation assay. Strikingly, Figure 5.11A shows that there was phosphorylation of the MSD1 and N-terminal tandem upon activation of JNK. There was more phosphorylation observed in the MSD1 (2-118 aa) protein than N-terminal tandem (1-196 aa) when quantified (Figure 5.11B). Phosphorylation of N-terminal tandem was observed when JNK was phosphorylated, but not when the other MAPKs, ERK and p38 were phosphorylated. Phosphorylation of MSD1 was greater than the positive control substrate, c-jun (Figure 5.11). The negative

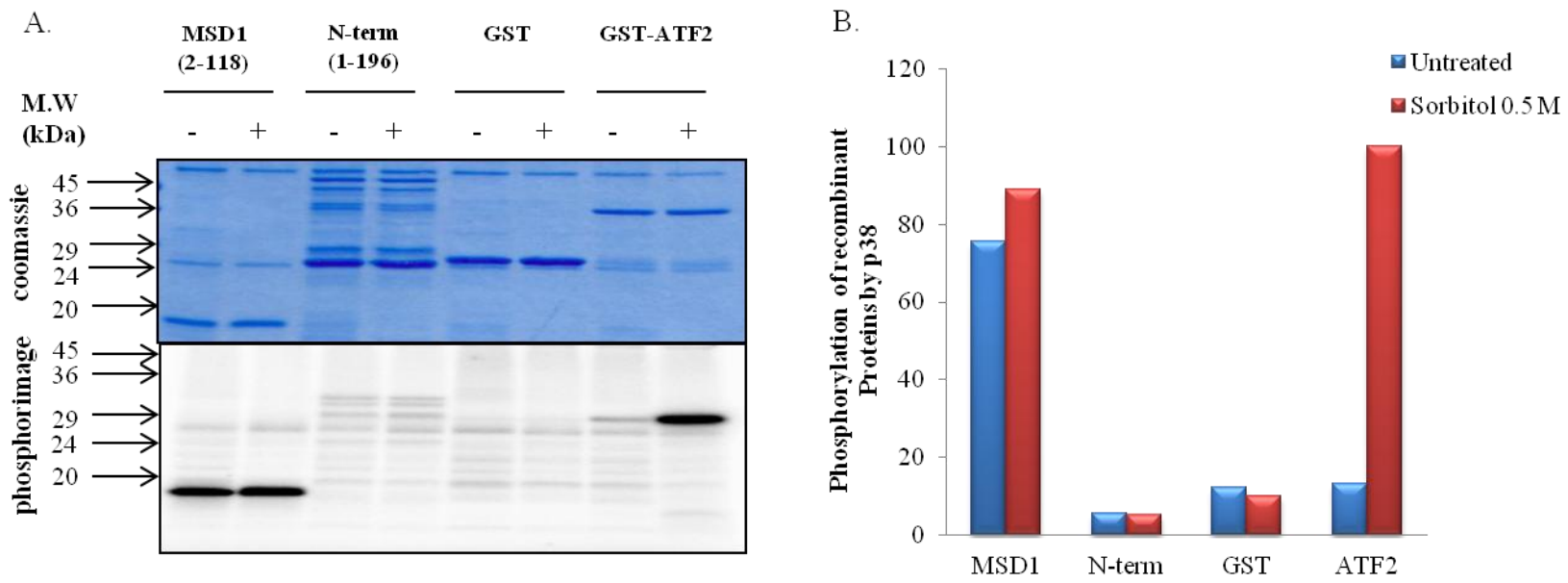

Figure 5.9: *In Vitro* phosphorylation assay showing substrate phosphorylation by p38
A. HEK293 cells which were transiently transfected with Flag-p38 (8 µg) for 24 hr and then serum starved for 16 hr were either left untreated or treated with 0.5 M sorbitol. Lysates were immunoprecipitated with anti Flag-antibodies. Phosphorylation assays were performed using MSD1 (2-118) and MS1 (193-375) as a negative control, GST-ATF2 was the positive control. After, the reaction was stopped, samples were boiled at 100 °C. The samples were then analyzed on an SDS-PA*GE ge*l, coomassie stained and subjected to analysis via the Phosphorima*ger* (^{32}P). Molecular weights (kDa) are seen on the left. **B.** The amount of phosphorylation of each of the proteins was analyzed using a phosphorima*ge*r and the phosphorylation of the proteins was calculated relative to the phosphorylation of positive control GST-ATF2.

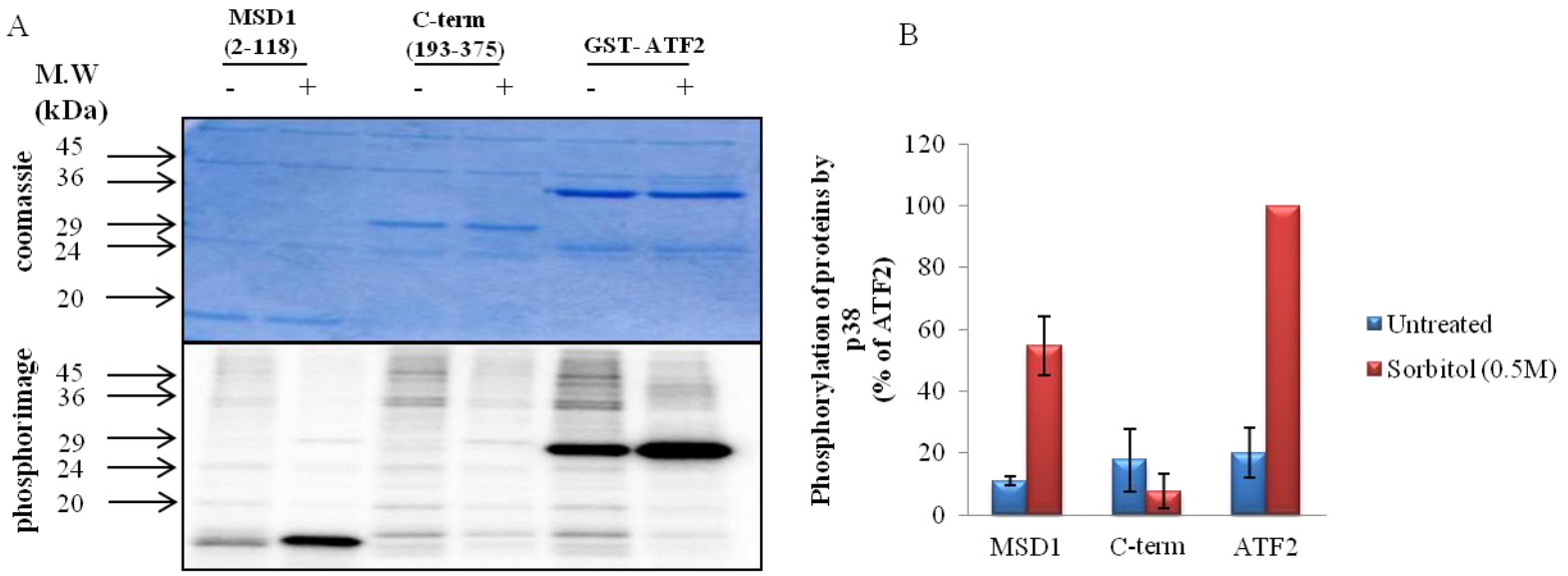

Figure 5.10: ***In Vitro*** **phosphorylation assay showing substrate phosphorylation by p38 .**
A. HEK293 cells were transiently transfected with Flag-p38 (8 µg) for 24 hr and then serum starved for 16 hr were either left untreated or treated with 0.5 M sorbitol. Lysates were made and immunoprecipitated with anti Flag-antibodies. Phosphorylatiom assays were performed using MSD1 as a substrate., C-term tandem was used as a negative control and GST-ATF as a positive control. After the reaction was stopped, samples were boiled at 100 °C. The samples were then analyzed on SDS-PA*GE ge*l which was coomassie stained and subjected to analysis by Phosphorima*ge*r (^{32}P). Molecular weights (kDa) are seen on the left. **B.** The amount of phosphorylation to each of the proteins was analyzed using a phosphorima*ge*r and the phosphorylation of the proteins was calculated relative to the phosphorylation of positive control ATF2. Quntification was done using ima*ge*quant and the data represents the mean (±) SEM of three separate experiments n=3.

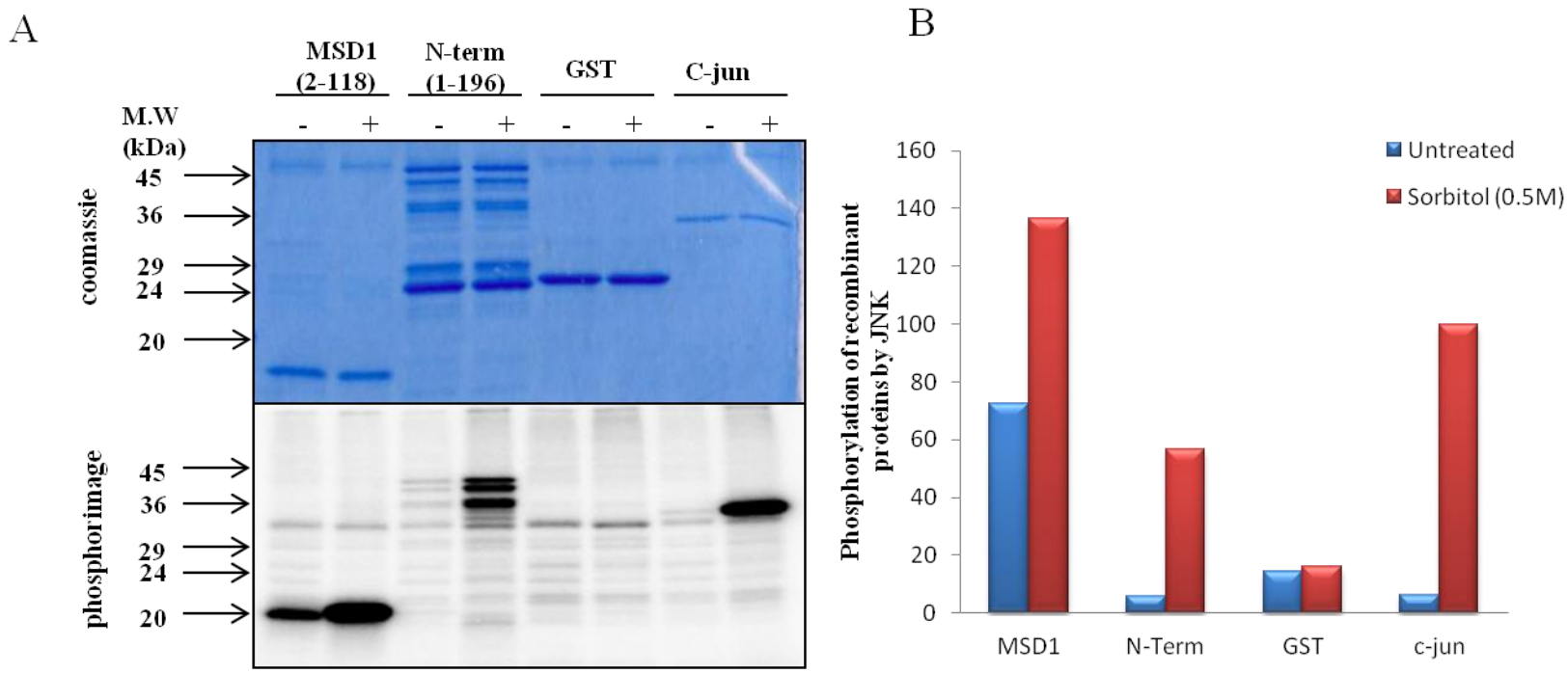

Figure 5.11: *In Vitro* phosphorylation assay showing substrate phosphorylation by JNK.
A. HEK293 cells which were transiently transfected with HA-JNK (8µg) for 24 hrs and then serum starved for 16 hrs were either left untreated or treated with 0.5M sorbitol. Lysates were immunoprecipitated with anti Flag-antibodies. Phosphorylation assays were performed using MSD1, N-terminal tandem as substrate and GST as a negative control and c-jun as a positive control. After, the reaction was stopped, samples were boiled at 100°C. The samples were then analyzed on an SDS-PA*GE ge*l, coomassie stained and subjected to autoradiography (^{32}P). Molecular weights (kDa) are seen on the left. **B.** The amount of phosphorylation to each of the proteins was analyzed using a phosphorima*ge*r and the phosphorylation of the proteins was relative to the phosphorylation of positive control c-jun.

control, GST, was not phosphorylated by activated JNK, which shows that the tag was not the cause of phosphorylation, of the GST tagged N-terminal tandem protein.

Since N-terminal tandem protein (GST-MS1 1-196) did not show additional phosphorylation compared to MSD1 (2-118 aa) the His- tagged MSD1 protein was used for all subsequent phosphorylation assays. *In vitro* phosphorylation assays were repeated three times using MSD1 and the C-terminal fragment (193-375 aa) as a negative control. Based on the results in figure 5.12A and 5.12B the level of phosphorylation of the MSD1 protein increased by over 4 fold compared with the untreated sample.

5.3.6. Mass Spectrometry analysis to identify phosphorylation sites in the N-terminus of MS1 using MSD1 (2-118)

5.3.6.1. Unlabelled in vitro kinase assay using immunoprecipitated MAPKs: HA-JNK, Flag-p38 and HA-ERK

We wanted to investigate the potential phosphorylation sites which were observed at the N-terminus. Having shown that MS1 can be phosphorylated in the region 2-118 aa by JNK and to a lesser extent ERK and p38 we wanted to identify the sites.

Unlabelled *in vitro* phosphorylation was performed using HEK293 cells transfected with the MAPKs Flag-p38, HA-JNK and HA-ERK and then treated with either sorbitol or PMA in order to activate them. The cells were lysed and the lysates were then added to protein G-sepharose beads which either had the antibodies anti-HA or anti-FLAG antibodies bound to them. Samples were then left to bind at 4 °C for 3 hr. The beads with immunoprecipitated kinases were incubated with ATP and appropriate substrates, which were then analyzed by SDS-PAGE and sent for mass spectrometry analysis.

A band shift of MSD1 was clearly observed in the presence of activated JNK which was treated with 0.5 M sorbitol (Figure 5.13). This shift was not seen when the other kinases p38 and ERK were activated (Figure 5.14A and 5.14B). This evidence supports the hypothesis that there could be one or more phosphorylation sites present for this to occur. Samples of each band were removed from the gels and analysed by mass spectrometry (Figure 5.13 and 5.14).

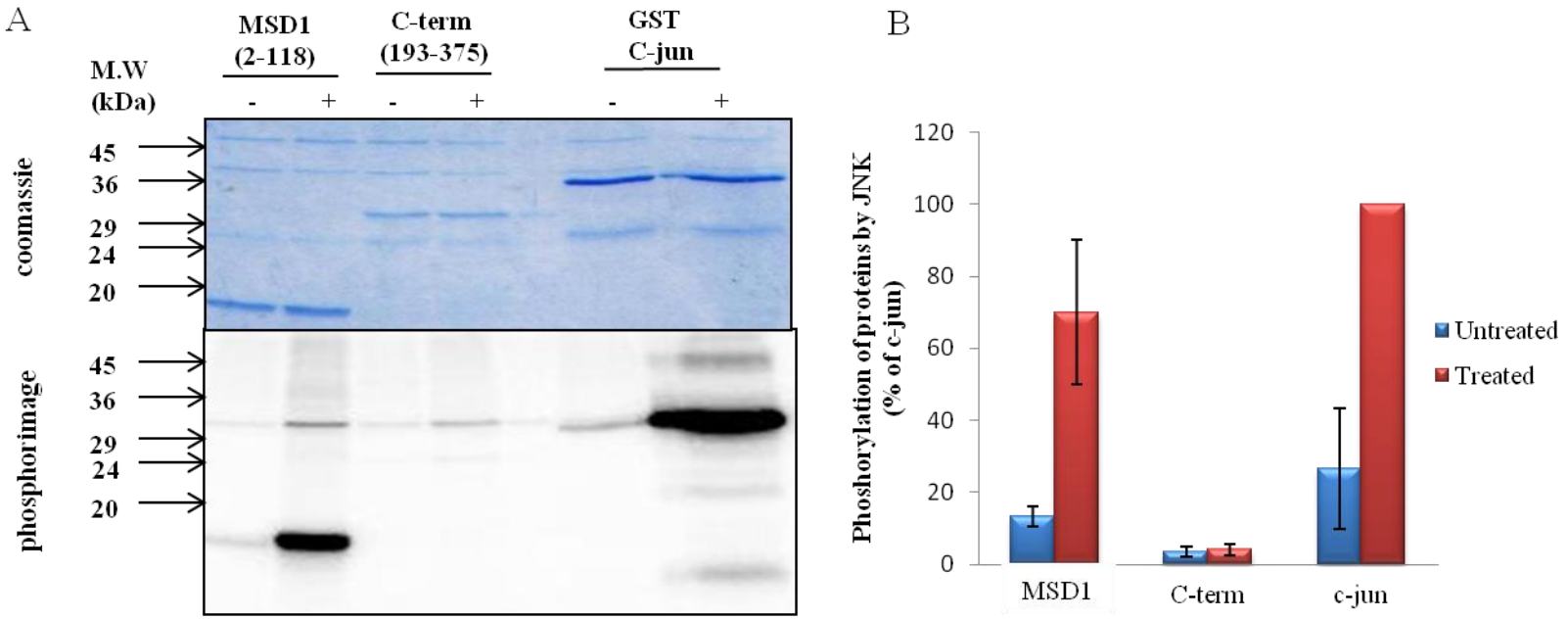

Figure 5.12: *In Vitro* phosphorylation assay showing substrate phosphorylation by activated JNK .
A. Lysates were made from HEK293 cells which were transiently transfected with HA-JNK (8 µg) for 24 hr and then serum starved for 16 hrs were either left untreated or treated with 0.5 M sorbitol. They were immunoprecipitated with anti Flag-antibodies. Phosphorylation assays were performed using MSD1 protein as a substrate, c-terminal tandem as a negative control and c-jun as a positive control. After, the reaction was stopped, samples were boiled at 100°C. The samples were then analyzed on an SDS-PA*GE ge*l, coomassie stained and Phosphorima*ge*r (^{32}P). Molecular weights (kDa) are seen on the left. **B.** The amount of phosphorylation on each of the proteins was analyzed using phosphorima*ge*r and the phosphorylation of the proteins were relative to the phosphorylation of positive control c-jun. Quantification was done using ima*ge*quant and the data represents the mean (±) SEM of three separate experiments n=3.

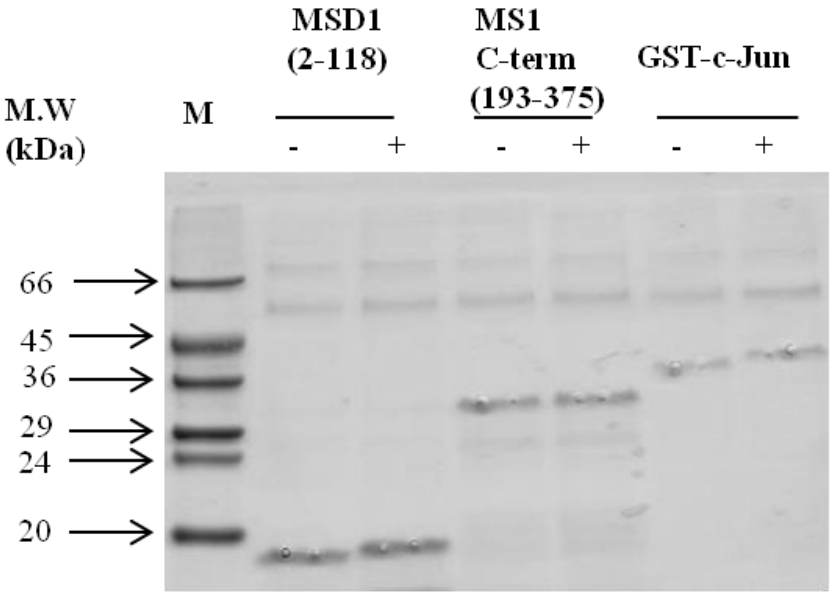

Figure 5.13: Unlabelled In vitro kinase Assay using activated JNK for substrate phosphorylation.

HEK293 cells were plated out on a 10 cm dish and transfected with 8 µg of plasmid DNA of HA-JNK. After 24 hr of transfection, cells were serum starved and subjected to either sorbitol (0.5 M) for 30 min. After cell extracts were made with 1X TLB and left to tumble for 3 hr with protein G sepharose beads bound with anti-HA antibody. Supernatants were removed and beads were washed to remove any unbound proteins and finally in kinase assay buffer. To the beads purified proteins and cold ATP (75 µM) was added to the samples which were treated or untreated. Samples were then left to incubate, then 3X sample buffer was added and the samples were heated for 5 min at 100 $^{\circ}$C and then run on a 15 % SDS-PA*GE ge*l. *Ge*l was stained with coomassie and sent for mass spectrometry.

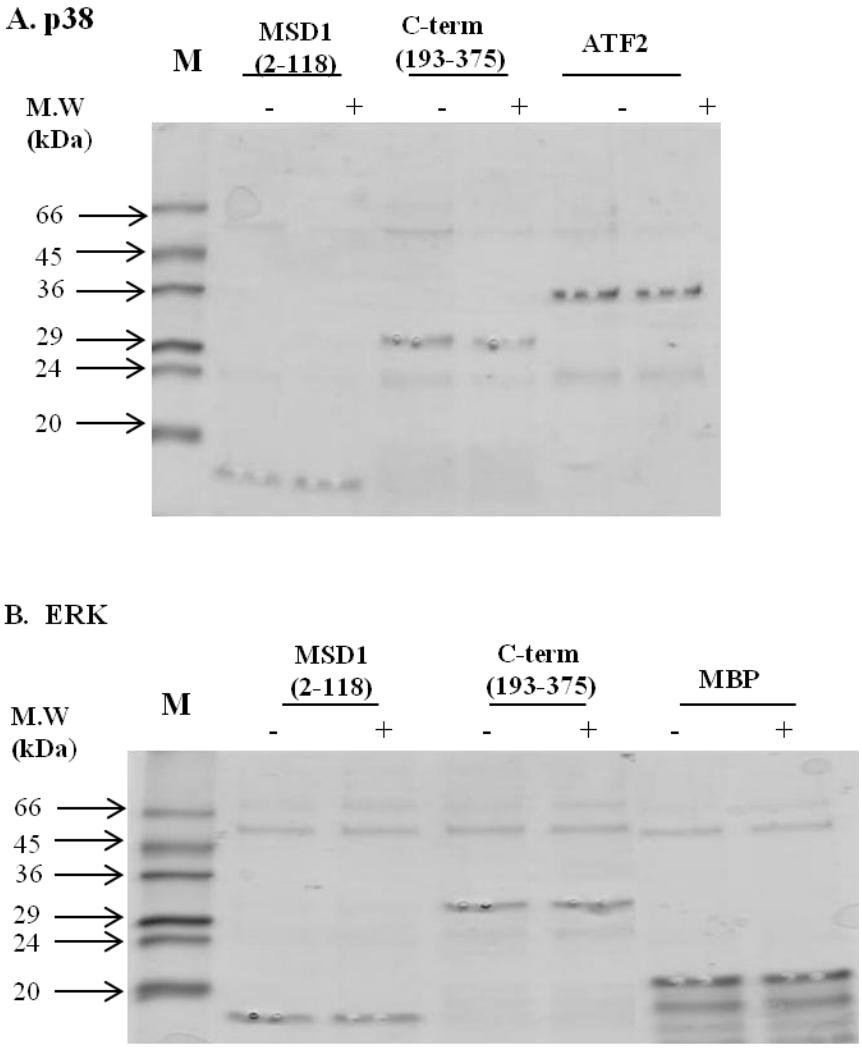

Figure 5.14: Unlabelled In vitro kinase Assay using activated MAPKs for substrate phosphorylation.

HEK293 cells were plated out on a 10cm dish and transfected with 8µg of plasmid DNA of Flag-p38 and HA-ERK. Cells were subjected to either 0.5M sorbitol (A) or 1 µM PMA (B) for 30 min or left untreated, post-transfection. Proteins were immunoprecipitated. Beads were washed 3 times with 1X TLB and once with kinase assay buffer. To the beads purified proteins and cold ATP (75 µM) were added. Samples were then left to incubate at 4° C for 2hrs. 3X sample buffer was added and the samples were heated for 5 min at 100° C and then ran on a SDS-PA*GE ge*l 15%, which were stained with coomassie and sent for Mass spectrometry.

5.3.6.2. Identification of phosphorylation sites in N-terminus of MS1 using MSD1 (2-118)

The coomassie stained gels discussed in **section 5.3.6.1** (Figure 5.13 and 5.14) were taken for phosphopeptide mapping analysis. The bands were excised and digested with trypsin and placed in the LTQ-Orbitrap mass spectrometer. The program, MASCOT was used to analyse the results. Digested peptides were separated by high pressure liquid chromatography (HPLC) where ions are converted to cations by electron removal and then sorted according to mass-to-charge ratio m/z. This is measured in order to produce a spectrum (Wysocki *et al.,* 2005). The results of the phospho-mapping confirmed that there were residues in MS1, which were phosphorylated by the MAPKs (Figure 5.15). The residues which were identified in the MSD1 samples that are phosphorylated were Thr24, Thr62 and Ser77. Phosphorylation of Thr24 was seen in all of the treated and untreated samples by all three of the kinases. However Thr62 phosphorylation was only observed in HA-JNK kinase assays, but was phosphorylated in precipitates from sorbitol treated and untreated cells. Unfortunately, the ion scoring of Ser77 residue was quite low. Although phosphorylation of Ser77 did occur the peptides were too small to bind to the HPLC column which results in insufficient recovery of the phosphorylated peptides.

5.3.7. Site-Directed Mutagenesis of MS1 residues Thr62 and Ser77

The next step was to carry out site directed mutagenesis of the specific sites of interest to determine whether they are necessary for phosphorylation by the activated kinase JNK. It was not necessary to continue with using the other kinases p38 and ERK as Ser77 was not identified as a phophorylation site in these samples.

Thr62 and Ser77 were individually mutated to an alanine in order to generate a non-phosphorylatable version of the constructs. Mutations were also made to convert Thr62 to Glu, and Ser77 to Asp. The Glu and Asp mimic phosphorylation at threonine and serine sites respectively. Two different parental templates were used in order to carry out site directed mutagenesis which was the first domain MSD1 (2-118 aa) for in vitro kinase assays and Flag-MS1 (which is full length MS1) for transfections of mammalian cells in order to carry out *in vivo* cell biology techniques such as immunofluorescence microscopy.

A.

Peptide Sequence	Phosphorylated Residue
K.RA[pT]LVINLAR.G	Thr 24
R.QAQEPAGWLPGATQDLPH[pT]PK.E	Thr 62
R.QHAPKPP[pS]PKPDGDR.E	Ser 77

B.

Sequence Coverage: **74%**
Matched peptides shown in **Bold Red**

1 MAPGETEREA GPAK**SALQKV RRATLVINLA RGWQQWANEN STRQAQEPAG**
51 **WLPGATQDLP HTPKEPGPRQ HAPKPPSPKP DGDREGRGSE EATEVSHIKR**
101 **K**EVTRTVVSK AYERGGDV

Figure 5.15: Phospho-mapping of the amino acid residues: Amino acids highlighted in red were confirmed to be phosphorylated in Table above.
A. Derived MS data summarized as a list of the three phosphorylated peptides found in the sample from *in vitro* phosphorylation assay and the specified phosphorylated residues. **B.** Protein sequence cover*age* of the N-terminal region of MS1 which is high lighted in red.

Following mutagenesis, plasmids were sequenced to ensure the correct alteration was made. Western blot analysis was done to ensure the protein was expressed with the His-tag at the correct size. This was done using either the anti-His antibody (1:1000 dil) to test the bacterial lysates as seen in Figure 5.16, while the Flag-MS1 (full length) mutants which would be used for *in vivo* studies were expressed in HEK293 cells and checked using MS1 antibody (Figure 5.17). This antibody used was a gift from Dr. Mark Pfuhl's laboratory which used the C-terminal end of the protein to make the antibody.

5.3.8. MS1 mutants with mutation at Threonine 62 are not phosphorylated

Having confirmed the correct sequence of the MSD1 mutants and purified each of these proteins. They were then western blotted with appropriate antibodies to determine whether they were the correct size and had their tags. *In vitro* kinase assays were performed with four different mutants to determine whether they still acted as substrates for JNK (Figure 5.18).

HA-JNK was transfected in HEK293 cells as previously described and cells were treated with 0.5 M sorbitol in order to activate JNK. Immunoprecipitation and phosphorylation of the recombinant proteins were carried out using various His-tagged MSD1 (2-118 aa) mutants, wild-type, C-terminal tandem as the negative control and GST-c-Jun as the positive control in this experiment. Following termination of the reactions, the samples were then analyzed on SDS-PAGE gels which were coomassie stained and analysed using an autoradiograph and exposure to film. It was seen that the mutation of MSD1 at Thr62 to alanine or glutamic acid prevented phosphorylation by activated JNK (Figure 5.18). The kinase was active since c-Jun and WT MSD1 were phosphorylated (Figure 5.18). Mutation of Serine77 to alanine or aspartic acid had little effect on phosphorylation of MSD1 (Figure 5.18).

5.3.9. Confirmation of direct interaction between JNK and MS1 through Co-Immunoprecipitation.

Protein:protein interactions between JNK and MS1 were assessed by co-immunoprecipitation, followed by western blotting with the use of HA-JNK and Flag-MS1 proteins. This was to determine whether interaction between JNK and MS1 occurs directly, or indirectly since there is evidence in this chapter that MS1 becomes

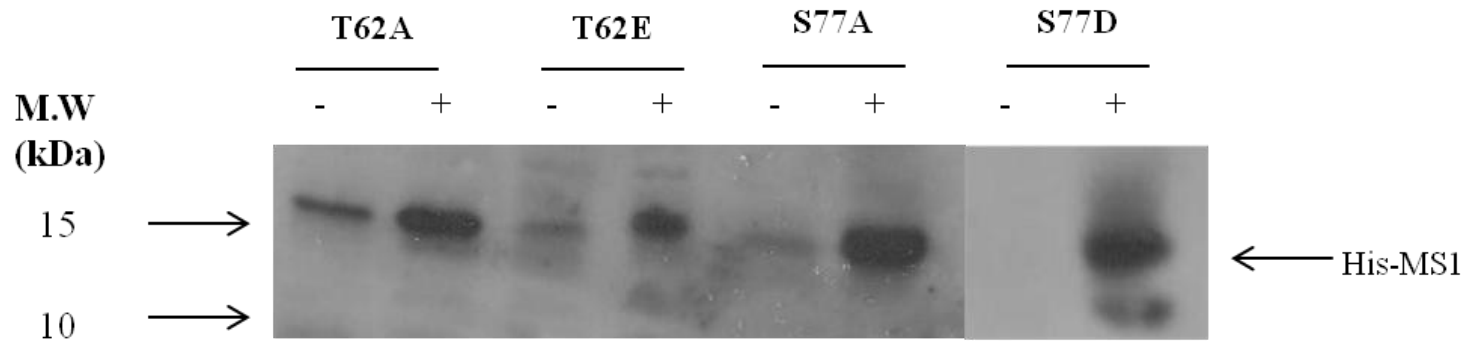

Figure 5.16: Expression of His tag*ge*d MS1 mutants in BL21-DE3 *E. coli* before (-) and following (+) induction with IPTG .
Mutants from site directed muat*ge*nesis were transformed in BL21 DE3 *E. coli.* The fusion protein was induced by IPTG and subsequently purified by a nickel chelating sepharose column chromatography. Lysates from the uninduced and induced samples were run on a SDS-PA*GE ge*l and western blotted for the His-tag using anti-his antibodies (1:2000**)**

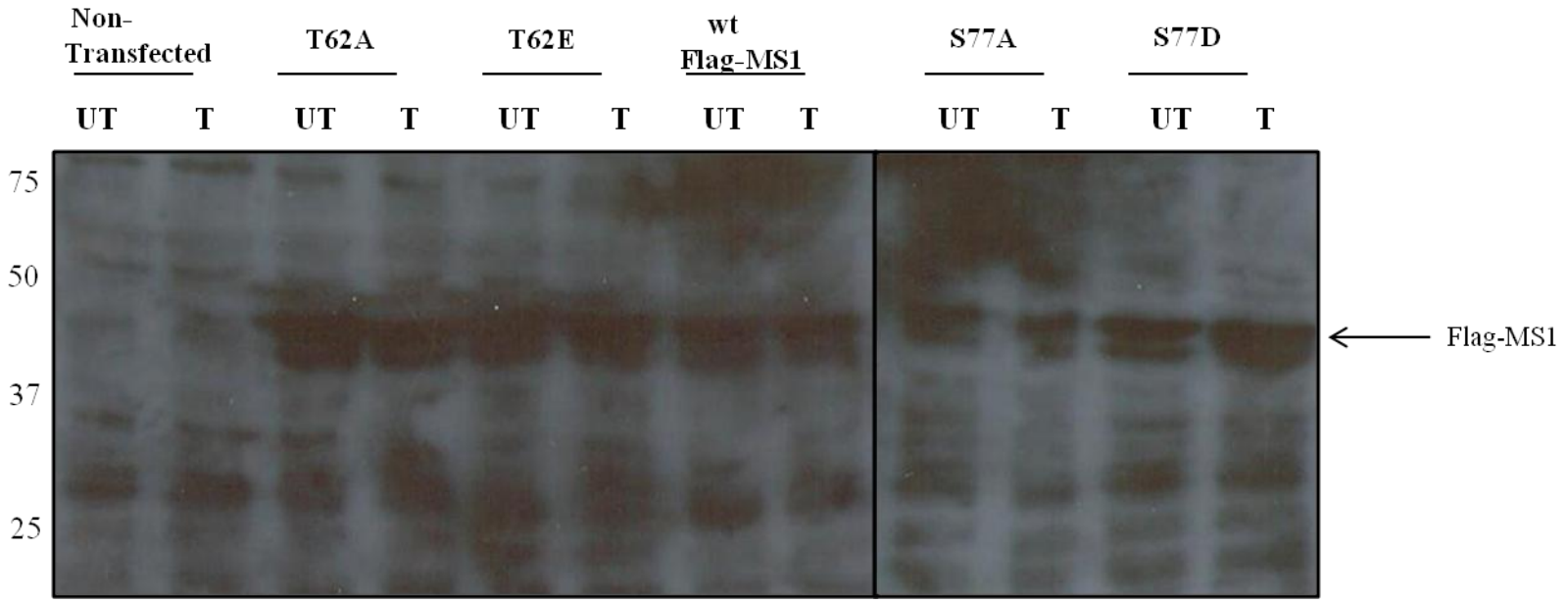

Figure 5.17: Expression of Flag-MS1 mutants in sorbitol treated and untreated samples
H9c2 cells were transfected with 6µg of DNA of the mutants which were made by site directed muta*ge*nesis. After 24 hrs of transfections cells were serum starved for 2 hrs before being treated with sorbitol (0.5M) which others were left untreated (UT). After the cells were washed in 1X PBS and placed directly in 1.5X sample buffer before running on a SDS-PA*GE ge*l and western blotted using the anti-MS1 antibody (1:2000 dil) which was produced by Dr. Mark Pfuhl's lab (made against the C-terminal end of MS1

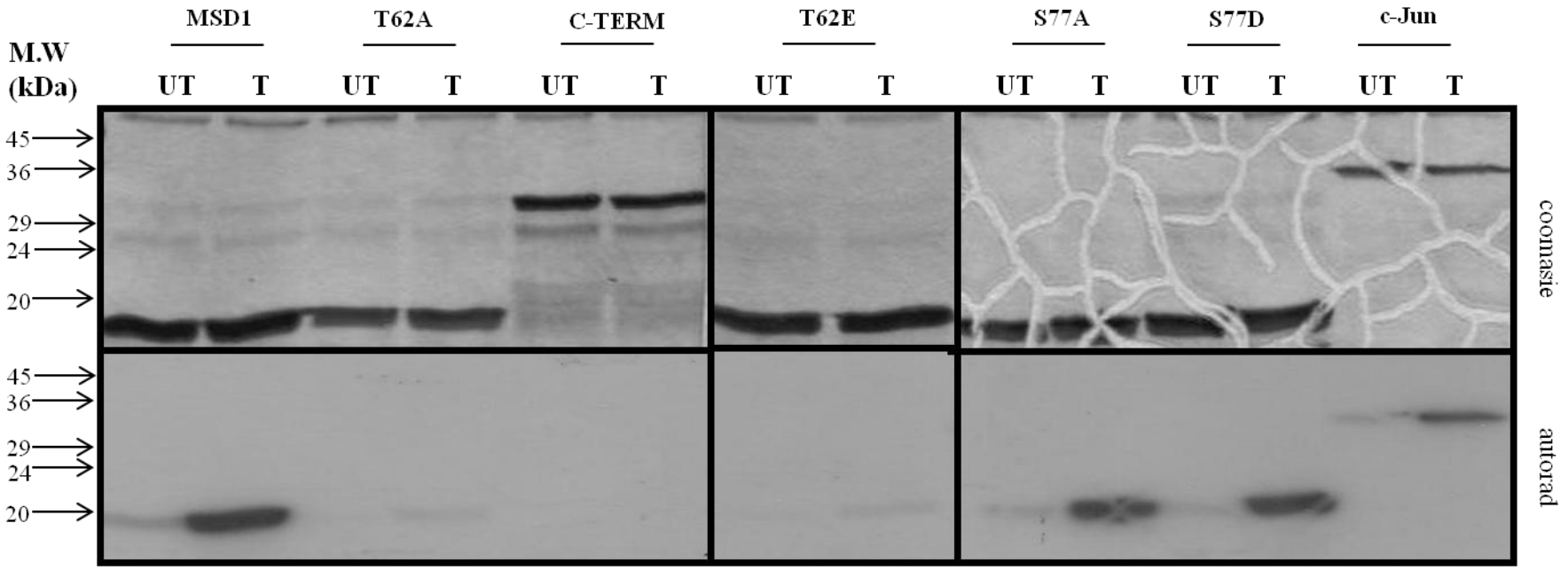

Figure 5.18: *In vitro* phosphorylation Assay Showing Mutants mutated at Threonine 62 were not phosphorylated.
HEK293 cells were plated out on a 10 cm dish and transfected with 8µg of plasmid DNA of HA-JNK . After 24 hr of transfection, cells were serum starved for approximately 16 hr and subjected to sorbitol (0.5 M) for 30 min. After cell extracts were made with 1X TLB and left to tumble for 3 hr with protein G sepharose beads bound with anti-HA antibody. Supernatants were removed and beads were washed to remove any unbound proteins. Beads were washed 3 times with 1X TLB and once with kinase assay buffer. To the beads purified proteins, radiolabelled P^{32} ATP and cold ATP were added to the samples which were treated or untreated. Samples were then left to incubate at 30° C for 30 min. 3X sample buffer was added and the samples were heated for 5 min at 100° C and then analysed on an SDS-PA*GE ge*l 15%.

phosphorylated upon activation of JNK. The detection of Flag-MS1 in JNK precipitates would indicate that MS1 and JNK are present in a stable complex *in vitro*.

HEK293 cells were transfected with HA-JNK and Flag-MS1. Cells were either treated with 0.5 M sorbitol to activate JNK or left untreated. After treatments, the cell lysates were run on a gel to confirm that phospho-JNK was activated (Figure 5.19). Interestingly, Flag-MS1 was able to co-immunoprecipitate with HA-JNK in the absence of activation by sorbitol (Figure 5.20). However, Flag-MS1 was not present in the control immunoprecipitation (IgG) nor in samples from treated cells, which suggests that there was dissociation of JNK after activation (Figure 5.20).

This experiment was repeated four times and each experiment displayed the same result. This could be an indication that JNK protein might phosphorylate MS1 and then dissociate. The interaction between the other kinases p38 and ERK and MS1 by co-immunoprecipitation was not observed (data not shown). This raises questions as to what is the purpose of phosphorylation and how it could affect the subcellular distribution of MS1 or the ability to interact with other proteins. Although phosphorylation occurs in vitro, *in vivo* studies need to be done to determine whether phosphorylation occurs in intact cells.

5.3.10. Immunofluorescence microscopy studies to determine the effect of mutating phosphorylation sites on MS1 co-localization with overexpressed JNK and actin

The N-terminal phosphorylation of MS1 by JNK was observed *in vitro*, however the effects of phosphorylation *in vivo* are unknown. It was of interest to determine the effect of phosphorylation at Thr62 and Ser77 of MS1 on the association with JNK or actin. Therefore immunofluorescence microscopy studies were carried out using Thr62Ala and Thr62Glu mutants and Ser77Ala and Ser77Asp mutants. Since co-immunoprecitation experiments showed interaction between MS1 and JNK, it seemed appropriate to look at the ability of MS1 to co-localise with JNK *in vivo* and to determine whether subcellular distribution of MS1 changed when JNK is activated. Investigations were also carried out to determine whether the mutations at Thr62 and Ser77 would have an effect on the co-localisation of MS1 with actin as it is known that MS1 plays a critical role in SRF activation via actin polymerization (Arai *et al.,* 2002).

H9c2 cells were transiently co-transfected with Wildtype Flag tagged MS1 or phosphorylation site Flag-tagged mutants together with HA-JNK. The cells were either

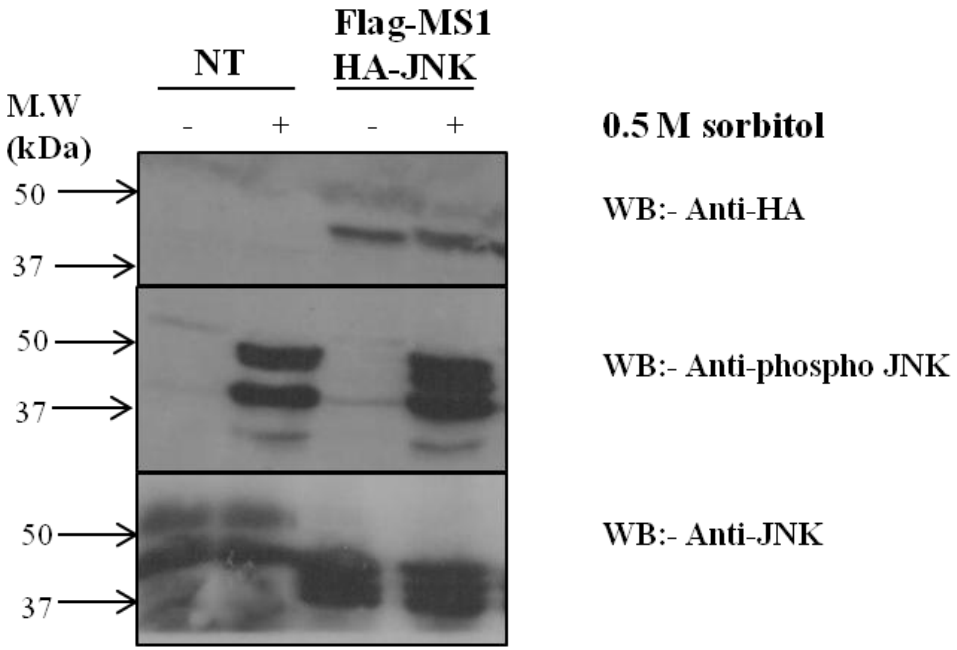

Figure 5.19: Western blot analysis of activated JNK by sorbitol treatment
Cells which were co-transfected with HA-JNK and Flag-MS1were either treated with 0.5 M sorbitol or left untreated for 30 min. Cells were then lysed and western blotted with the antibodies recognising JNK, HA and phospho-JNK.

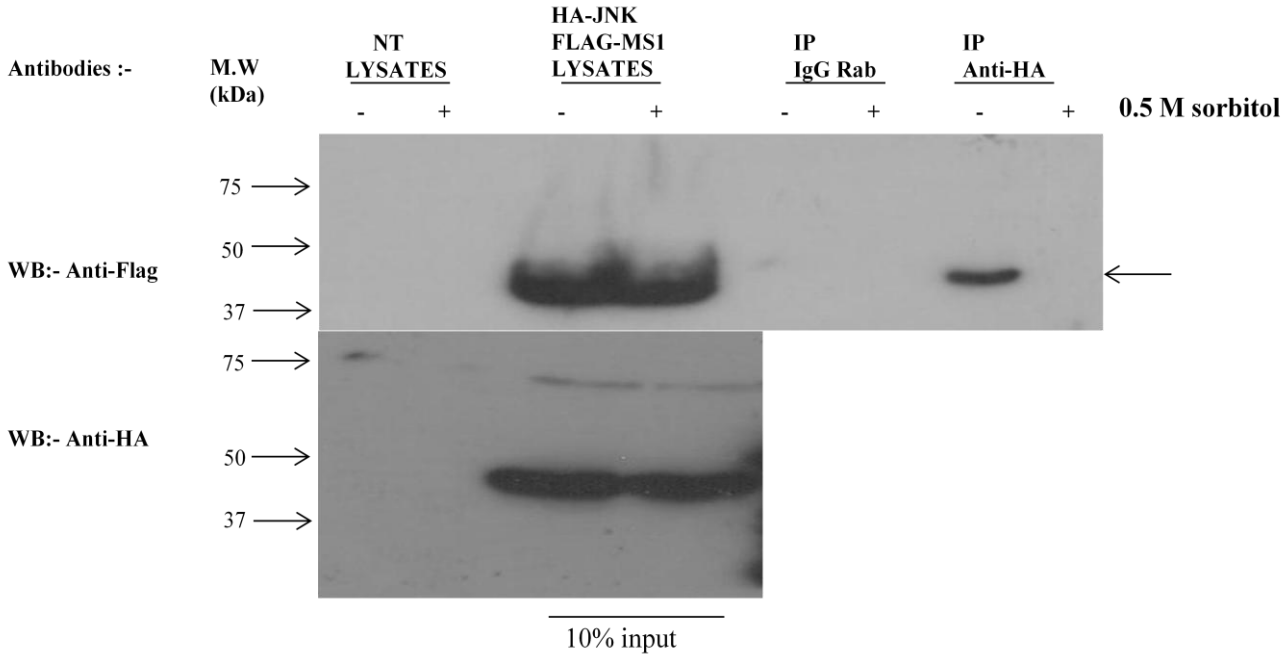

Figure 5.20: Co-immunoprecipitation experiment to determine whether JNK and MS1 are present in the same complex
HEK 293 cells transfected with 8 µg Flag-MS1 and 8 µg HA-JNK DNA were treated (+) with 0.5 M sorbitol or left untreated (-). Cells were lysed with HiLo buffer, then sonicated and clarified cell extract was either immobilised with anti-HA antibody or rabbit IgG (IgG Rab) with tumbling overnight at 4 ºC. Immunoprecipitated proteins along with 1/10 of the cell lysates were resolved on a 12 % SDS-PA*GE ge*l. Western blotting was performed using anti-Flag or anti-HA antibodies at 1:2000 dilution. This experiment was repeated 4 times.

left untreated or treated with 0.5 M sorbitol for 30 min in order to activate JNK. The cells were prepared for immunofluorescence microscopy (**Chapter 2 Section 2.5.18**). In Figure 5.21, cells co-transfected with WT-Flag-MS1 and HA-JNK, showed there was some co-localisation between Flag-MS1 (green fluorescence) and HA-JNK (red fluorescence) around the membrane of the cells as indicated by the arrows (Figure 5.21). HA-JNK was present in the nucleus and the periphery of the cell where there seemed to be some co-localisation with WT-MS1 and presence of membrane ruffling, indicated by the white arrow (Figure 5.21). In cells transfected with WT-MS1 and JNK exposed to sorbitol treatments, HA-JNK was observed only in the nucleus of the cell and there was no co-localisation between WT-MS1 and HA-JNK (Figure 5.21). However, the cells transfected with Thr62Ala mutant and HA-JNK, did not show any co-localisation in the untreated sample, but the treated cell showed there was co-localisation at the edges of the cell membrane indicated by a white arrow in the merge figure 5.22.

Interestingly, in figure 5.22 where cells were transfected with Thr62Ala mutant and HA-JNK, there was no co-localisation observed in the untreated cell (Figure 5.22). HA-JNK which was a red fluorescence was in the nucleus of the cell, while Thr62Ala mutant was distributed evenly in the cytoplasm of the cell, which was identified by green fluorescence (Figure 5.22). In the treated cells, there seemed to be an overlap of HA-JNK and Thr62Ala indicated by the white arrow in the merged figure 5.22 of the treated sample. The untreated Thr62Glu mutant transfected with HA-JNK were both distributed within the cytoplasm of the cell, seen in figure 5.23. The merged image shows there is co-localisation seen throughout the cell and was more pronounced at the periphery of the cell indicated by the white arrow in figure 5.23. In the treated cell with mutant Thr62Glu and HA-JNK, Thr62Glu was distributed around the cytoplasm (indicated by green fluorescence) while HA-JNK was seen concentrated within the nucleus of the cell (red fluorescence) in Figure 5.23. In the merged figure of the treated cell, there was no overlap of green and red fluorescence (figure 5.23). A comparison between the WT-MS1 co-transfected with HA-JNK and Thr62Glu co-transfected with HA-JNK, did not show there was more co-localisation with the mutant than the wildtype MS1 (Figure 5.21 and 5.23). Mutant Ser77Ala co-transfected with HA-JNK in untreated cells, showed there was distribution of MS1 within the cytoplasm which is the green fluorescence and HA-JNK appeared to be seen partly in the nucleus as well as the cytoplasm of the cell in figure

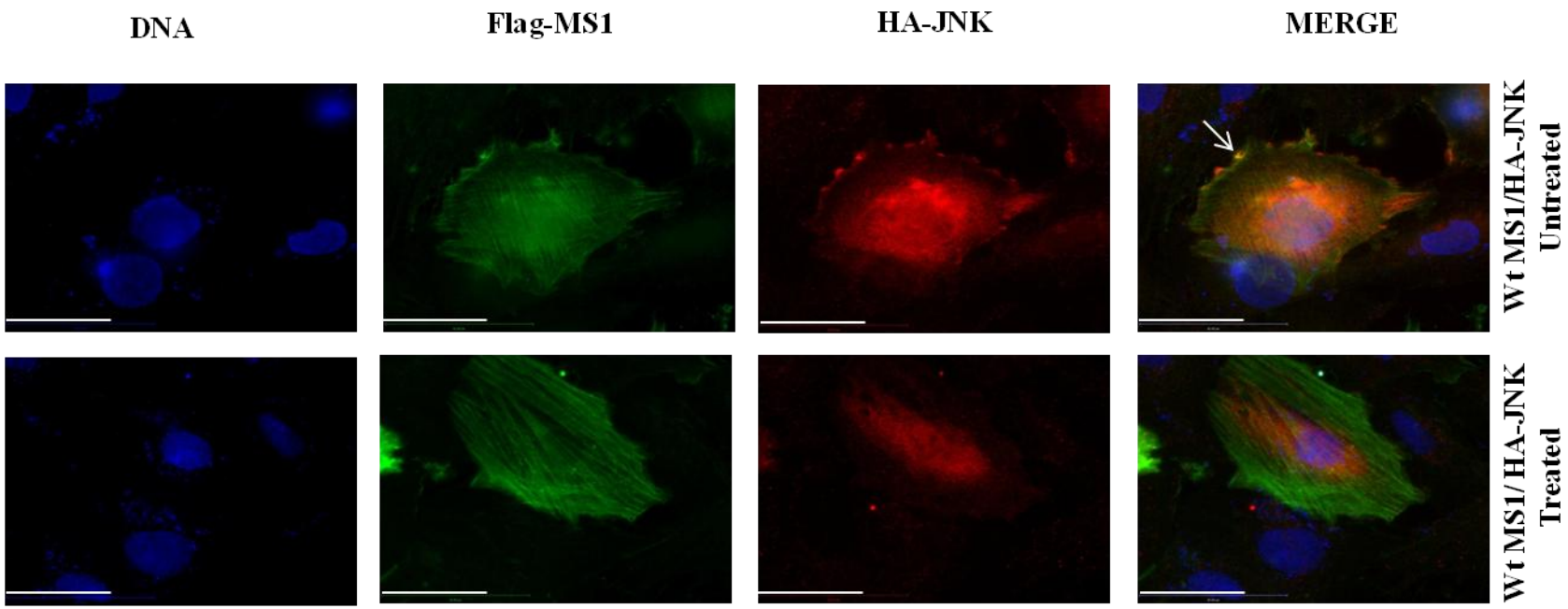

Figure 5.21: Immunofluorescence of wildtype-Flag-MS1 and HA-JNK in H9c2 cells
Cells were transiently co-transfected with Flag-MS1 or mutants and HA-JNK. Cells were either treated with 0.5 M sorbitol or left untreated for 30 min at 37 ºC. The cells were then fixed and permeabilised with methanol. Immunostaining was performed using rabbit anti-HA (red) and mouse anti-Flag (green) antibodies. Hoechst (33258) was used to stain DNA (blue). The cells were visualised using a Nikon inverted microscope. Scale bar represents 60 µm.

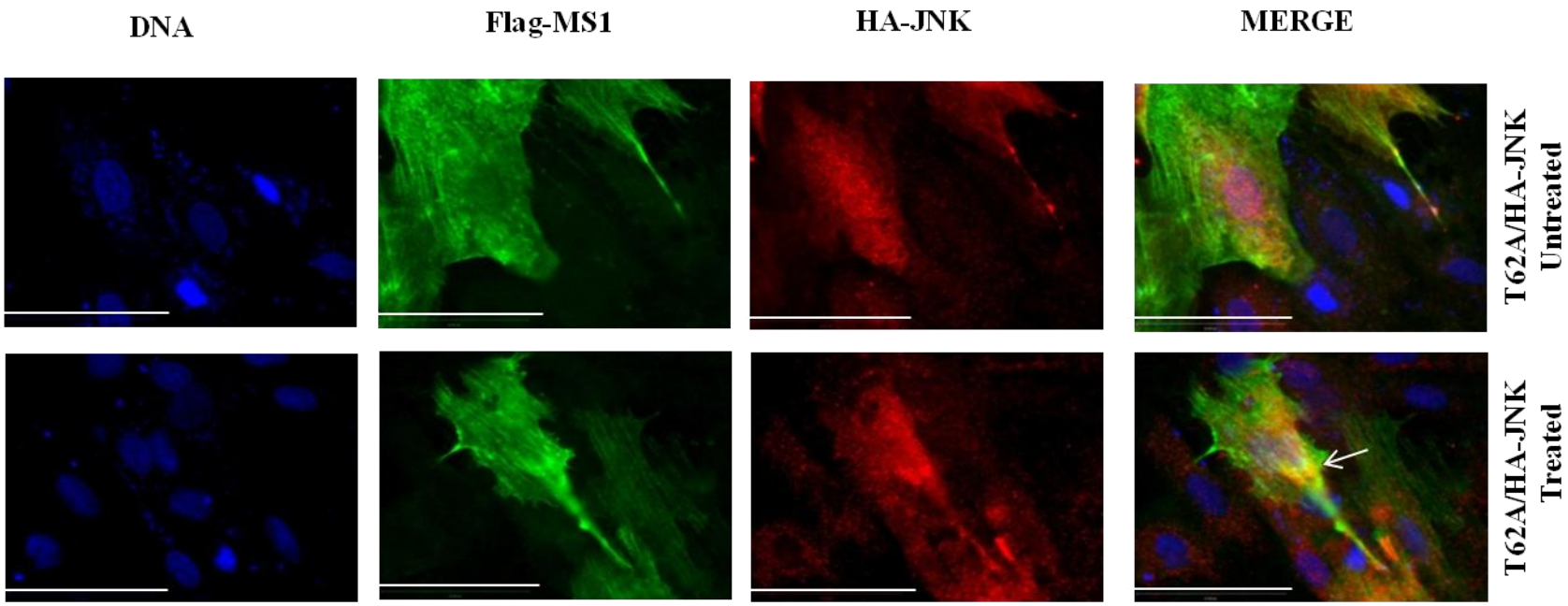

Figure 5.22: Immunofluorescence of mutant T62Ala Flag-MS1 and HA-JNK in H9c2 cells
Cells were transiently co-transfected with Flag-MS1 or mutants and HA-JNK. Cells were either treated with 0.5 M sorbitol or left untreated for 30 min at 37 ºC. The cells were then fixed and permeabilised with methanol. Immunostaining was performed using rabbit anti-HA (red) and mouse anti-Flag (green) antibodies. Hoeschst (33258) was used to stain DNA (blue). The cells were visualised using a Nikon inverted microscope. Scale bar represents 60 µm.

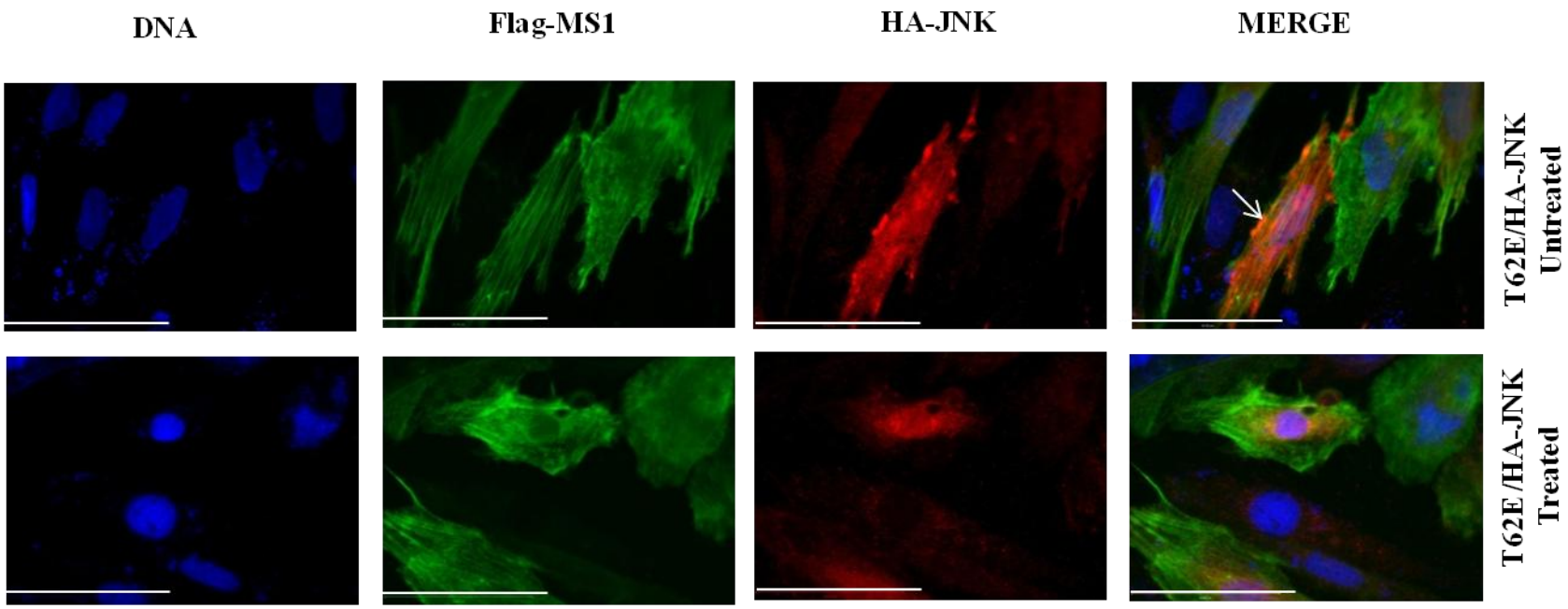

Figure 5.23: Immunofluorescence of mutant T62Glu Flag-MS1 and HA-JNK in H9c2 cells
Cells were transiently co-transfected with Flag-MS1 or mutants and HA-JNK. Cells were either treated with 0.5 M sorbitol or left untreated for 30 min at 37 ºC. The cells were then fixed and permeabilised with methanol. Immunostaining was performed using rabbit anti-HA (red) and mouse anti-Flag (green) antibodies. Hoechst (33258) was used to stain DNA (blue). The cells were visualised using a Nikon inverted microscope. Scale bar represents 60 µm.

5.24. The merged image did not show any co-localisation between the two proteins (Figure 5.24). In the treated cells, Ser77Ala and HA-JNK did not show a change distribution of the cell, when compared to the untreated sample (Figure 5.24).

Disappointingly, Ser77Asp did not transfect as there was not a clear green fluorescence observed nor was there red fluorescence indicating presence of HA-JNK (Figure 5.25). In all figures there was no change in the subcellular distribution of MS1. MS1 remained distributed in the cytoplasm in the MS1 WT and mutants. The HA-JNK secondary antibody showed substantial background, however most of cells showed that HA-JNK was in the nucleus and at some points within the cytoplasm (Figure 5.21, 5.22, 5.23, 5.24). This experiment was only done once and needs to be repeated with better controls and a better antibody. Finally, Thr62Glu and WT showed colocalisation with HA-JNK in untreated cells, while Thr62Ala mutant in treated cells showed co-localisation with HA-JNK to a lesser extent.

Immunofluorescence studies were done using cells transfected with WT-Flag-MS1 or Flag-MS1 phosphorylation site mutants to determine whether there would be a change in co-localisation of MS1 with actin due to mutations of specific amino acids. In order to observe the changes in co-localisation, Texas-Red Phalloidin was used to detect actin and Alexafluor-488 conjugated 2º antibody was used to detect the Flag-epitope. Transfections with Flag-MS1 mutants were compared with WT-Flag-MS1 without treatment. There were no substantial changes seen in the co-localisation of MS1 with actin among the mutants and WT in the untreated cells (Figure 5.26). However, the cells which were transfected with Thr62Glu appeared stressed, with stress fibres (actin filaments) at the periphery of the cell, although they were not subjected to any treatments (Figure 5.26). Overall, there were no other morphological changes seen in the cells in the untreated samples.

Cells subjected to sorbitol treatment appeared stressed overall, with membrane ruffles at the cell perimeter and stress fibres throughout in cells transfected with Thr62Glu, Ser77Ala and Ser77Asp (Figure 5.27). The cells with transfected mutants Thr62Glu, Ser77Ala and Ser77Asp also appeared rounded and actin increased in levels around the periphery compared to the WT-Flag-MS1 (Figure 5.27). F-actin disorganization was observed in sorbitol treated cells, which is indicated by the white arrows and was more predominant in the cells transfected with Thr62Glu, Ser77Ala and Ser77Asp (Figure 5.27). Co-localisation of MS1 with actin was not affected when the mutants were

compared with the WT-FLAG in the treated cells and there was no obvious indication that more co-localisation was taking place among the different mutants (Figure 5.27).

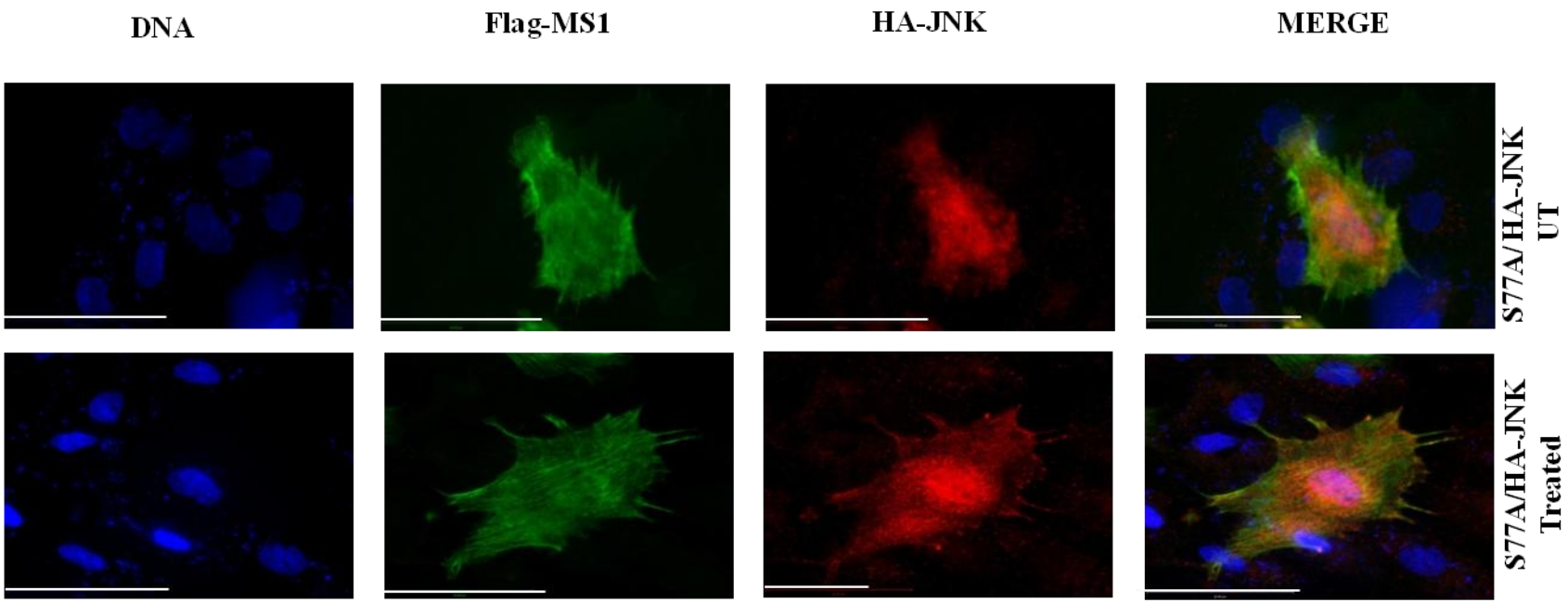

Figure 5.24: Immunofluorescence of mutant S77Ala Flag-MS1 and HA-JNK in H9c2 cells
Cells were transiently co-transfected with Flag-MS1 or mutants and HA-JNK. Cells were either treated with 0.5 M sobritol or left untreated for 30 min at 37 ºC. The cells were then fixed and permeabilized with methanol. Immunostaining was performed using rabbit anti-HA (red) and mouse anti-Flag (green) antibodies. Hoechst (33258) was used to stain DNA (blue). The cells were visualised using a Nikon inverted microscope. Scale bar represents 60 µm.

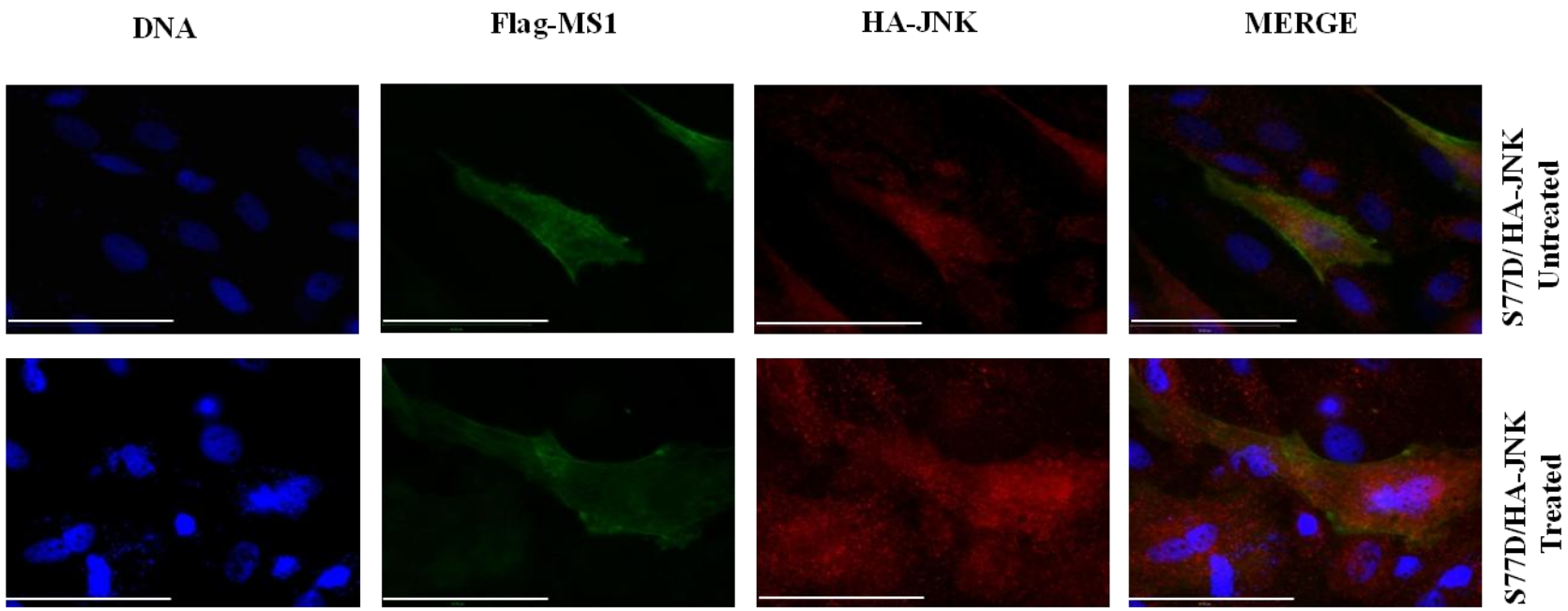

Figure 5.25: Immunofluorescence of mutant S77Asp Flag-MS1 and HA-JNK in H9c2 cells
Cells were transiently co-transfected with Flag-MS1 and HA-JNK. Cells were either treated with 0.5 M sorbitol or left untreated for 30 min at 37 ºC. The cells were then fixed and permeabilized with methanol. Immunostaining was performed using rabbit anti-HA (red) and mouse anti-Flag (green) antibodies. Hoechst (33258) was used to stain DNA (blue). The cells were visualised using a Nikon inverted microscope. Scale bar represents 60µm.

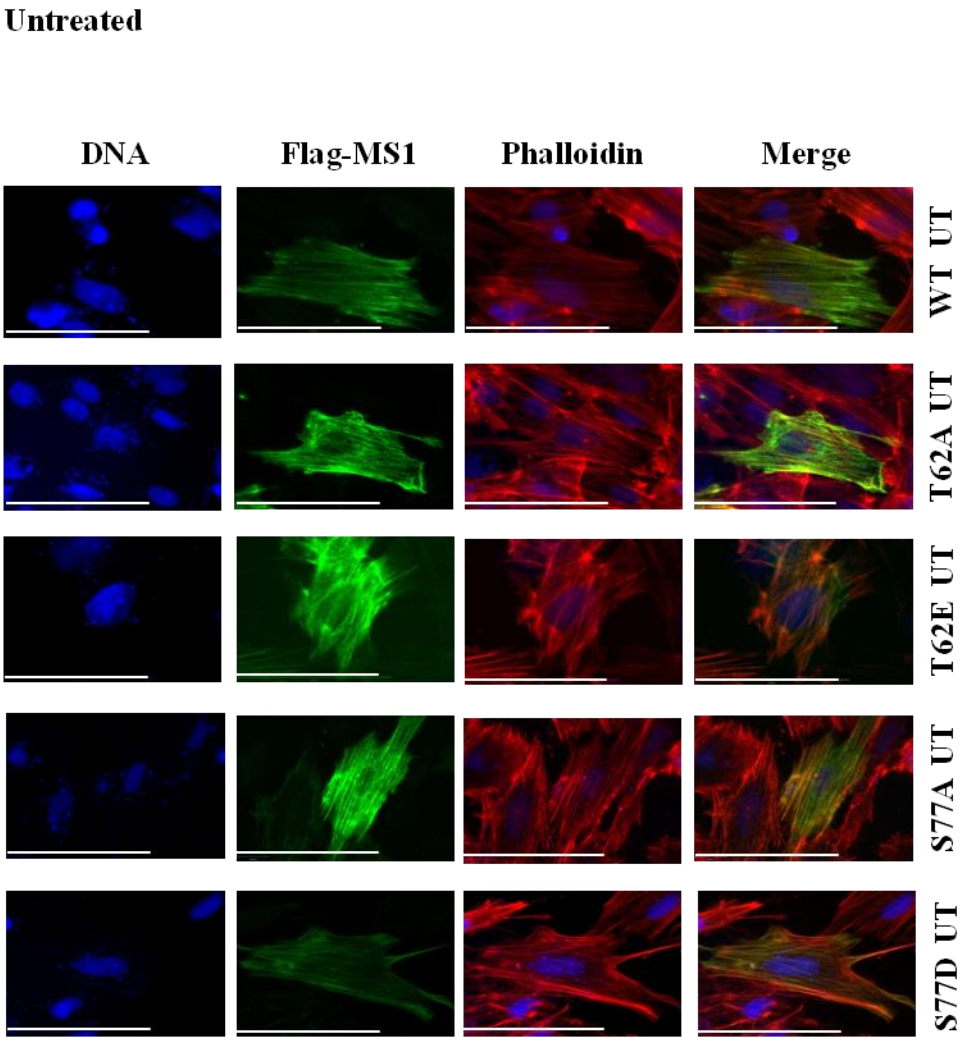

Figure 5.26: Co-localisation of MS1 mutants with Actin in Untreated H9c2 cells.
H9c2 cells were grown on coverslips before being transfected with either Flag-MS1 of Flag-MS1 mutants. After 24 hr of transfection the cells were serum starved for 2 hr before sorbitol treatment or left untreated with the media replaced with DMEM with serum. Cells were fixed with 3.7% (w/v) formaldehyde and permeabilised with 0.1% triton before immunostaining with anti-flag antibody (1:200 dil anti mouse) which was detected by secondary Alexa 488 antibodies (green). Actin staining was done using Phalloidin-Texas Red. Hoechst (33258) was used to stain DNA (blue on mer*ge*). Ima*ge*s were captured using a Nikon TE300 inverted microscope. Scale bar represents 60 µm

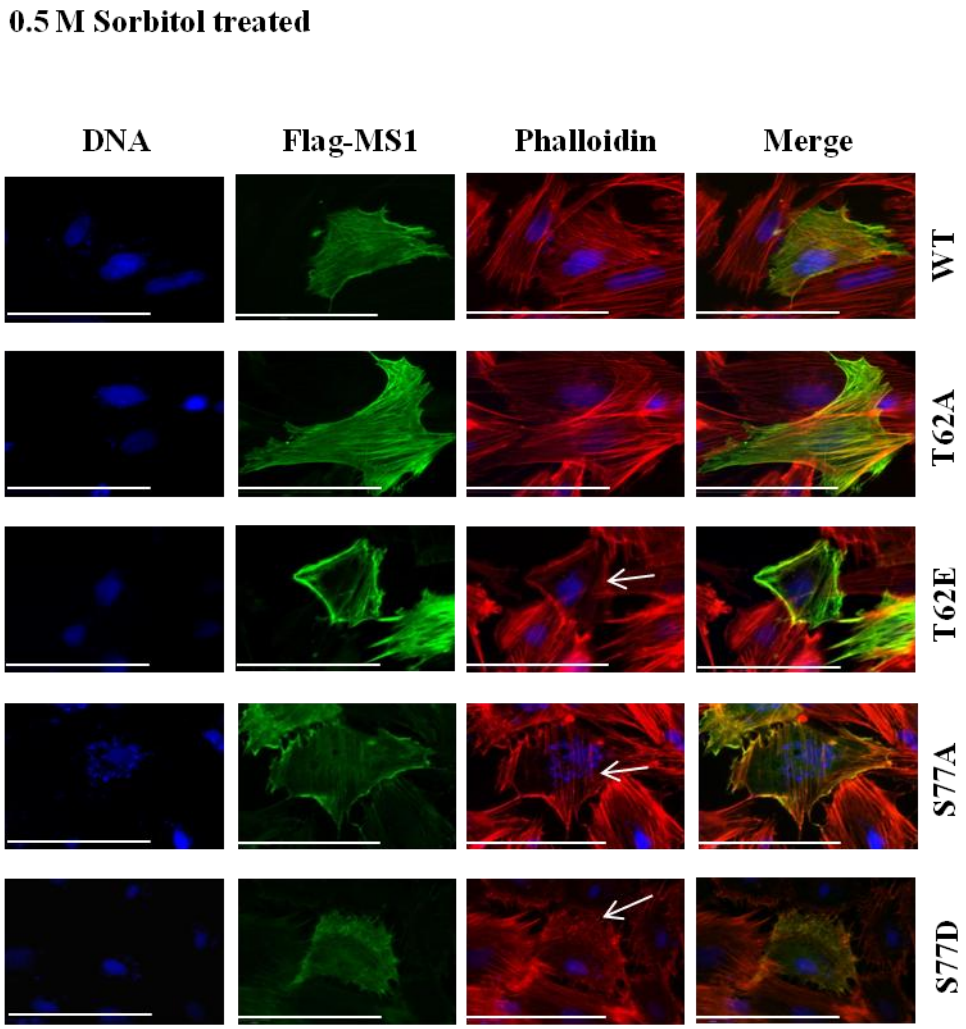

Figure 5.27: Co-localisation of MS1 mutants with Actin in sorbitol treated H9c2 cells.
H9c2 cells were grown on coverslips before being transfected with either Flag-MS1 of Flag-MS1 mutants. After 24 hr of transfection the cells were serum starved for 2 hr before sorbitol treatment or left untreated with the media replaced with DMEM with serum. Cells were fixed with 3.7% (w/v) formaldehyde and permeabilised with 0.1% triton before immunostaining with anti-flag antibody (1:200 dil anti mouse) which was detected by secondary Alexa 488 antibodies (green). Actin staining was done using Phalloidin-Texas Red. Hoeschst (33258) was used to stain DNA (blue on mer*ge*). Ima*ge*s were captured using a Nikon TE300 inverted microscope. Scale bar represents 60 µm

5.4. Discussion

Predicted phosphorylation sites at Threonine 62, Serine 77 and Serine 150 at the N-terminus of MS1 may be potential candidates for MAPK substrate phosphorylation, based on the presence of SAPK substrate motif Ser-Thr-Pro. Since no research to date has looked at the phosphorylation of MS1, it was decided to investigate whether MS1 could be a substrate for MAPK mediated phosphorylation. No function has been identified for the N-terminus of MS1, however recent research within the C-terminus resulted in the identification of various actin binding domains (Arai *et al*., 2002). MAPK mediated interactions are of particular interest since JNK was previously thought to play a role in the regulation of MS1 mRNA expression during simulated ischaemia reperfusion with the use of JNK inhibitor SP600125 (Hay *et al*., 2006). ERK mediated interactions are also of interest since they play a major role in cardiovascular pathology, through the calcium/calmodulin signalling pathway, which leads to the phosphorylation of sarcomeric proteins located at the z-disk and I-band region of the sarcomere, where MS1 is also localised (Hidalgo *et al.*, 2009 and Kruger *et al*., 2011).

5.4.1. *In vitro* phosphorylation of MSD1 (2-118 aa) by activated JNK, ERK and p38

In vitro phosphorylation confirmed MSD1 (2-118 aa) was phosphorylated by activated-JNK, ERK and p38. Phosphorylation at the N-terminus of MS1 is thought to be specific since no substrate phosphorylation within the C-terminal tandem fragment which acted as a negative control was observed. Unfortunately, the GST tagged N-terminal tandem (1-196 aa) did not appear to display any additional phosphorylation than activated JNK phosphorylated MSD1 (2-118 aa) and was not observed to be phosphorylated by phospho-p38 nor phospho-ERK in the phosphorylation assays.

This was a concern since there were additional potential phosphorylation sites, however a possible reason could be due to the large GST tag which could have caused steric hindrance. Steric hindrance by GST could have prevented phosphorylation by blocking the sites which were necessary for substrate phosphorylation by phospho-ERK, since the tag is also located at the N-terminus of the construct.

5.4.2. Phosphorylation sites: Thr24 Thr62 and Ser77 Identified by Mass Spectrometry

Mass spectrometry using LTQ-Orbitrap confirmed two of the three predicted sites which were Thr62 and Ser77 and an additional phosphorylation site, Thr24. Ser77 was identified with less confidence due to insufficient recovery of phosphorylated peptides, as a result of in-gel tryptic digestion. The area of the sequence of MSD1 where Ser77 is present has many lysine and arginine residues. Lysine and arginine are the amino acids that are cleaved by trypsin for digestion during mass spectrometry analysis, this would also result in small peptides being produced and insufficient coverage of the protein (Dephoure and Gygi; 2012).

The additional site which was identified was Thr24 which was phosphorylated by all three of the kinases used, in the presence and absence of stimulation. Thr24 is seen highly conserved in different species and using GPS prediction program was predicted to be phosphorylated by many different kinases (**Appendix 1.0**). Non-specific phosphorylation at Thr24 could be a reason why MSD1 was phosphorylated by all three kinases. However, Thr24 does not correspond to the MAPK substrate phosphorylation motif and was not further investigated. The amino acid residues which were identified to be phosphorylated may explain the band shift which was seen for MSD1 after activation of JNK. There is more substrate phosphorylation in the *in vitro* assay when JNK is activated rather than unstimulated.

Mass spectrometry analysis using LC-MS/MS is limited, because it does not detect differences in the amount of phosphorylation for each residue. The phosphopeptides which were present in untreated and treated samples could not determine whether more phosphorylation occurred when JNK was actived than in the untreated. Quantifying the amount of phosphorylation seen should be carried out in the future since Thr62 was identified in the untreated sample which suggests a basal phosphorylation. Also, since Thr62 was identified in substrate phosphorylation by ERK it should be investigated further in future.

5.4.3. D-docking Domains or Kinase interacting motif present in the N-terminal region of MS1

Supporting evidence that could suggest all these phosphopeptides are genuine is the presence of a kinase interacting motif (KIM) or D-docking domain (D domain) sequence which is recognised by MAP kinases has this motif; X_2-(Arg/Lys)(Arg/Lys)-

X_{3-6} (MacKenzie *et al.,*2000 Bardwell *et al*.,2003; Sharrocks *et al*., 2003). These docking sites or motifs allows for the direct interaction between a protein and a kinase (Caldwell *et al.,* 2006). At the N-terminius MS1 has a peptide sequence which is characteristic of this kinase interacting motif or docking site which is; Leu-Gln-Lys-Val-Arg-Arg-Ala-Thr-Leu-Val-Ile-Asn-Leu as seen in figure 5.28. Coincidentally, this sequence contains the Threonine which is not characteristic of MAPK phosphorylation but may possibly regulate association and dissociation might explain perhaps why this became phosphorylated. This D-domain sequence also allows for ERK substrate phosphorylation and JNK substrate phosphorylation, with a characteristic hydrophobic patch where "ϕ" is representative of either Leucine, Isoleucine or Valine, following the residues after the recognition sequence (Arg/Lys)(Arg/Lys)-X_{3-6}-ϕ-X-ϕ that substrates conform to which is present at the N-terminus in figure 5.28 (Tanoue *et al.,* 2000; Liu *et al*.,2006).

These docking domains can be specific for MAPKs such as JNK and ERK; which can use the same recognition sequence but not by p38, as seen for example with Elk1 (Yang *et al.,*1998, Galanis *et al.,*2001; Reviewed in Caldwell *et al.,* 2006). That might also explain why phosphorylation was not as high when MSD1 was phosphorylated by p38 as opposed to JNK and ERK. What also supports these results is the peptide sequence mentioned, is also highly conserved in different species and is located within the MSD1 domain where the phosphorylation sites are located (Figure 5.28).

Further observation into the N-terminus of MS1, where the predicted phosphorylation site Ser150 was located also has D-domains present which are also known as DEJL domains (Ubersax and Ferrell, 2007; Jacobs *et al.,* 2009). The DEJL domain has a motif of Leu-X-Leu which preceeds the phosphoaccepter, Ser150 (Figure 5.28). This site was present within the N-terminal tandem construct but was not sent for phosphopeptide analysis. A construct should be made with a smaller tag which has both MSD1 and MSD2 domains present. The smaller tag would eliminate steric hindrance and further investigation of these MAPK docking sites could be carried out.

Mutants should also be tested with ERK to determine whether they interrupt phosphorylation and Thr24 may need to be investigated further with site directed mutagenesis. Another experiment that should be carried out is mutation of the sites within the recognition sequence in order to determine whether this leads to the

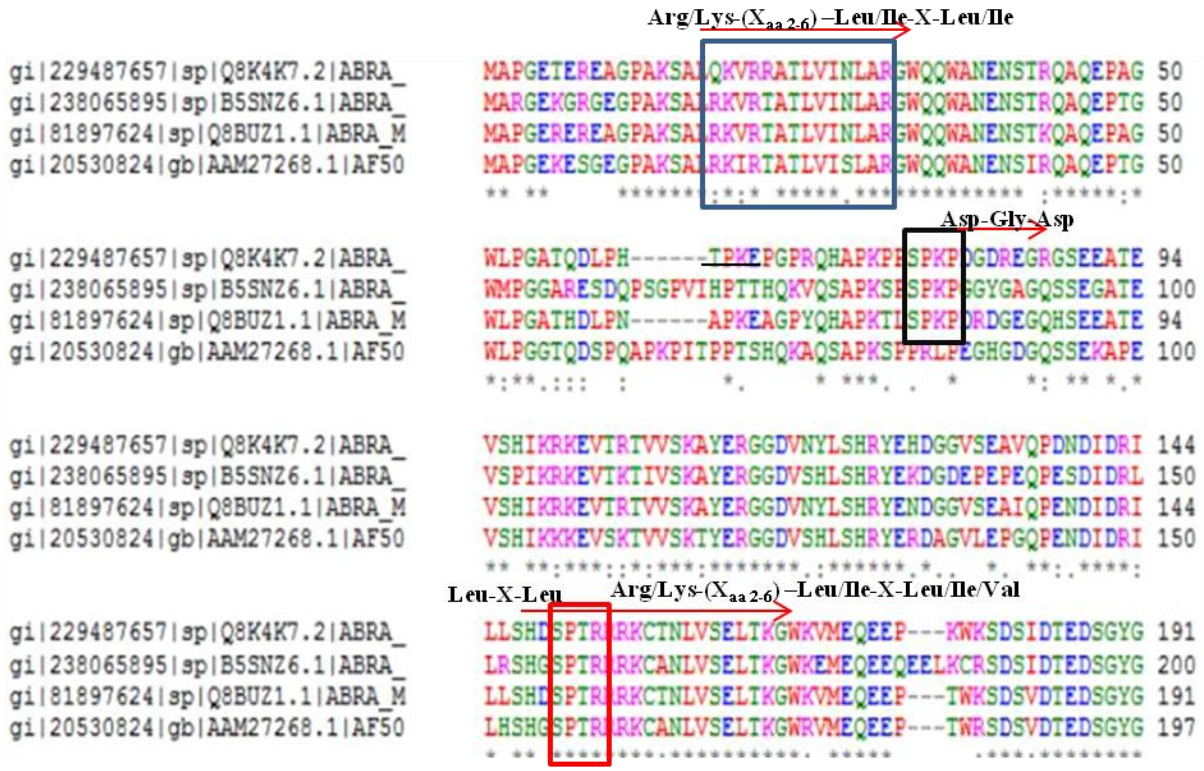

Figure 5.28: An Alignment using Clustalw showing the N-terminus of MS1 where one of the phosphopeptides confirmed is conserved in 4 different species and D-domains.

The alignment which was done using MS1 from pig, rat, mouse and human shows that Thr24 is conserved (blue box), Thr62 (underlined in black) is not conserved throughout the species however, Ser77 is conserved in rat, mouse and pig which is grouped by the black box. In human, there is an upstream SP present. Ser150 is seen conserved in all species present which is grouped by the red box. The red arrows show the D-domains and Kinase interacting motifs near phosphorylated amino acids within the N-terminus for JNK and ERK recognition.

abolishment of phosphorylation of the identified phosphorylation sites. Site directed mutagenesis confirmed that the major site of phosphorylation by JNK is Thr62.

5.4.4. Co-localisation of overexpressed MS1 with JNK

Phosphorylation can influence the nuclear localisation of proteins and we know that increasing levels of MS1 leads to the regulation of transcription factors which promote hypertrophy, myogenesis and expression of other muscle specific genes (Mahadeva *et al.,* 2002, Kuwahara e*t al*., 2007 and Koekemoer *et al.,* 2009). Whether phosphorylation leads to the translocation of MS1 to the nucleus could shed light into the definitive role of MS1. Phosphorylation of JNK had no effect on the subcellular distribution of MS1 and the protein remained localised in the cytoplasm of the cells. However, immunofluorescence results looking at MS1 and JNK co-localisation, did show some overlap but this needs to be repeated since the antibody used for the HA-JNK was not very clear and also needs to be quantified.

Although it has been suggested that MS1 has the ability to be a transcriptional activator (Pfuhl, unpublished) and domain prediction programs have shown MS1 to have three DNA binding domains, with one located at the N-terminus at amino acid 33 and 35, there was no increase in nuclear MS1 with the presence of HA-JNK in these experiments.

Immunofluorescence experiments using phosphorylation site mutants were used to determine whether or not there would be a change between co-localisation of MS1 and actin. In figure 5.21, cells transfected with WT-Flag-MS1 and HA-JNK displayed membrane ruffles at the periphery and co-localisation was observed between WT-MS1 and HA-JNK in the area of membrane ruffling (figure 5.21). The same was seen with phosphorylation site mutant Thr62Glu and HA-JNK in the untreated sample and Thr62Ala and HA-JNK in the treated sample also showed co-localisation but no ruffling of the membranes (figure 5.22 and 5.23).

Membrane ruffling is the formation of motile cell surface protrusions containing a meshwork of newly polymerized actin and bundles of actin fibres run perpendicular to the plasma membrane (Ridley, 1994; Hall, 1998). The key regulator of membrane ruffling is Ras related GTP-binding protein, Rac1 and also newly discovered Rac2 (Reviewed in Hall, 1998; Manhankali *et al.,* 2011). The lamellipodia, filopodia and membrane ruffles are essential for cell motility and at the periphery of the cell is a recruitment of molecular scaffolds to their tip where actin polymerization is localised

(Small *et al.,* 2002; Manhankali *et al.,* 2011). MS1 directly interacts with RhoA, of the Rho-GTPase family, to enhance actin polymerization of G-actin monomers to make F-actin (Arai *et al.,* 2002). The presence of JNK makes this even more interesting as there is evidence that JNK interacts with Rho, Rac1 and Cdc42 in the Rho-GTPase family (Minden *et al.,* 1995; Coso *et al.,* 1995).

The family of Rho proteins are well studied and involved in regulation of actin cytoskeletal organization that in turns influences cell shape, adhesion and motility (Reviewed in Narumiya *et al.,* 1997; Zohn *et al.,* 1998; Burridge and Wennerberg, 2004; Ridley and Hall, 1992; Sorokina and Chernoff, 2005). MS1 plays a key role in actin dynamics and regulation and perhaps JNK may form the link between RhoA and MS1 working together in actin dynamics due to extracellular stress signals. Studies have also revealed that Rho1 regulates apoptosis via activation of JNK at the plasma membrane (Neisch *et al.,* 2010). MS1 is also believed to reduce chemically induced apoptosis and this could link the role of the two proteins in the plasma membrane (Koekemoer *et al.,* 2009). Although co-localisation and membrane ruffling was seen for Wt-MS1 and phosphorylation site mutants Thr62Glu and Thr62Ala (with cells sorbitol treated) in the presence of overexpressed HA-JNK, it could not be determined whether there was more co-localisation compared to the wild-type. Unfortunately this experiment did not show any change in MS1 subcellular distribution and was not observed in the nucleus of the cell. There were other problems encountered as Ser77Asp did not co-transfect with HA-JNK. This experiment needs to be repeated to confirm what was observed is reproducible.

Co-localisation of MS1 and phosphorylation site mutants with actin was also investigated to determine whether MS1:actin interaction is attenuated with mutations of the amino acids. In treatments with sorbitol, Thr62Glu, Ser77Asp and Ser77Ala all appeared stressed, with disorganization of actin observed and distribution of actin concentrated around the periphery, with presence of membrane ruffling and stress fibres. This was not observed in the samples which were left untreated. However, although the cells appeared very stressed it did not alter interaction between MS1 and actin. Based on these studies there is no doubt that MS1 is not involved in actin dynamics but may play a role in cell motility (Olson and Nordheim, 2010). These results may contribute to confirming the relationship between MS1 linked to F-actin interaction that leads to regulation of transcription factors such as SRF to allow

regulation of cell motile function, which was speculated and not fully confirmed (Olson and Nordheim, 2010).

In these experiments, we showed that MS1 is in a complex with JNK by co-immunoprecipitation experiments and the *in vitro* kinase assays. There was some evidence that shows interaction between MS1 and JNK *in vivo*. Co-localisation of the WT-MS1, Thr62Glu and Thr62Ala with HA-JNK was observed. The interaction between MS1 and JNK might be linked to cell migration and cell motility. Therefore more work needs to be done to determine whether MS1 is becoming inactivated, activated or relocated when phosphorylation takes place. Based on the results in chapter 4 where MS1 was seen to potentially interact with new proteins at the N-terminus, it would be interesting to test whether these interactions are influenced by phosphorylation of Thr 62 and Ser 77 residues.

Three phosphoprylation sites within the N-terminus of MS1 were identified, these were; Thr24, Thr62 and Ser77 by *in vitro* phosphorylation by JNK and ERK and p38 to a lesser extent. Supporting evidence also identifies a kinase interacting motif at the N-terminus which is specific to ERK and JNK phosphorylation called a D-domain or KIM motif which is upstream of the phosphoacceptor Thr62 and Ser77. This sequence is highly conserved in different species and could confirm that the phosphorylation seen by the MAPKs are genuine. Site directed mutagenesis confirmed Thr62 as the main site for MS1 phosphorylation. *In vitro* Co-immunoprecipitation experiments confirmed MS1 directly interacts with JNK but not with ERK nor p38. Preliminary attempts to determine the function of Thr62 and Ser77 shows a possible link between MS1 and JNK interaction with cell motility. However these experiments needs to be repeated since it was only done once and there were problems with Ser77Asp transfection. Co-localisation of MS1 with actin was not affected by mutations in MS1. However, the role of phosphorylation of MS1 by MAPKs remains to be elucidated.

.

Chapter 6. Discussion

MS1 plays a role in cardiac stress responses such as left ventricular hypertrophy, which was seen as a result of aortic banding in mice, which leads to increased pressure overload (Mahadeva *et al., 2002).* Studies which substantiate these findings also demonstrated that when MS1 is overexpressed, it leads to increased expression of genes involved in cardiac remodelling and hypertrophy (Koekemer *et al.,*2007 and Kuwahara *et al.,* 2007). MS1 is also implicated in the regulation of skeletal muscle (Reviewed in Lamon *et al.,* 2014). Previous studies in the laboratory by Dr. Joanna Hay showed that MS1 mRNA expression levels increased as a consequence of simulated ischaemia/reperfusion in H9c2 cells. The increase was prevented by JNK inhibitors and actinomycin-D, providing strong evidence that MS1 expression levels could be potentially regulated by the JNK pathway at the transcriptional level (Hay, 2006).

This research aimed to build on previous studies and confirm that MS1 protein levels also increase following simulated ischaemia/reperfusion. Since MS1 mRNA levels increase during simulated ischaemia/reperfusion we wanted to determine whether the MS1 promoter is responsive to stress known to activate the JNK pathway. MS1 is rather poorly characterized, and in particular there has been no function assigned to the N-terminal region. It was therefore aimed to characterize the MS1 protein further by identifying proteins that interact with the N-terminal region. This was to be achieved by affinity purification of binding partners from mouse heart extract. Sequence analysis of the N-terminal region also revealed potential phosphorylation sites for MAP kinases and stress activated kinases. Therefore studies were designed whether MS1 acts as a substrate for these kinases.

6.1. MS1 is expressed at the protein level during simulated Ischaemia/reperfusion injury

In order to investigate endogenous levels of in H9c2 cells, MS1 antisera were generated as MS1 protein levels increased following simulated ischaemia/reperfusion injury after 2hr and 4hr of reperfusion. Supporting what was seen at the mRNA level during reperfusion injury, JNK is known to become activated (Bogyevitch *et al.,* 1996, Clerk *et al.,* He *et al.,*1999 and Knight *et al.,* 1996) which supports the theory that JNK could potentially be playing a role in the expression of MS1. Although other MAPKs such as

p38 and ERK also become activated during ischaemia/reperfusion injury, their specific inhibitors did not have any effect on the expression of MS1 mRNA levels (Hay, 2006).

6.2. Promoter studies

6.2.1. MS1 promoter is responsive to activators of cellular stress

Studies in H9c2 cells, using a luciferase reporter under the control of the MS1 promoter, showed the promoter was responsive to UV, and sorbitol had an even greater effect on the promoter. Serum withdrawal also displayed a significant effect on the MS1 promoter, with a 6 fold increase seen in 48 hrs being left without serum. These different types of stress are known to be major activators of the JNK and p38 pathway (Wang *et al.*,1998).

6.2.2. MS1 promoter is responsive to hypertrophic agonists

MS1 has been implicated in left ventricular hypertrophy by Mahadeva *et al.*, 2002 where this leads to the re-establishment of the foetal gene program. Hypertrophic stimulation is asscosiated with activation of a number of intracellular signalling pathways which include the MAPKs (Force *et al.*, 1999), calcineurin and PKC. Promoter studies carried out by Kuwahara *et al.*, 2002 showed that MS1 expression was mediated by MEF2 and SRF as a result of hypertrophic stress. More recently promoter studies carried out by Ounzain *et al.*, 2012 has shown that GATA4 is involved in regulation of MS1 expression. MS1 is known to be involved in the SRF signaling pathway leading to the activation of sarcomeric genes such as alpha-actinin and alpha-MHC. MEF2 is also known to be a downstream target of the SAPKs (Wang.,2007). This evidence prompted us to look at the effect of, hypertrophic agonists, known to cause the activation of JNK to determine whether this will have an effect on the promoter activity of MS1. The two hypertrophic agonists which were selected to carry out these experiments were PE and ET-1. Both of these hypertrophic agonists activate the PKC pathway which is activated by IP3 and diacyglycerol (Hilal-Dandan *et al.*, 1992). 100 µM of PE caused a 2.5 fold increase in the promoter activity of MS1 after 1 hour treatment, whereas Endothelin-1 (100nm) did not cause an increase in promoter activity (Fig. 3.8). Previous studies showed that the promoter of MS1 is responsive to the hypertrophic agonists (Kuwahara *et al.*, 2007).

6.3. Mass spectrometry identifies putative myofibrillar proteins from binding assays

Research on the C-terminal domain of MS1 has been of great interest. Studies of the c-terminus demonstrated that deletion of residues 234-375 resulted in the loss of binding of actin (Arai *et al.,* 2002). Research done by Dr. Cladia Fogl showed that MS1 consists of four different domains, two are actin binding domains ABD1 and ABD2 which have independent actin binding activity and are located in the C-terminal half of the protein (Fogl *et al.,* 2011). MS1 is known to stimulate the SRF-pathway by interacting with Rho-A (Kuwahara *et al.,* 2005). There have been other proteins recently discovered which are known to interact with the C-terminus which are ABLIM-2 and ABLIM-3 (Barrientos *et al.,* 2006). It was of interest to look at the N-terminal domain of MS1 which is poorly characterized to determine whether there are any proteins within the heart which would bind to this domain. In order to investigate this, affinity purification was performed using purified MS1 protein fragments coupled to sepharose beads, to determine whether any proteins from Mouse heart extract would be bound. The N-terminal domain of MS1 was investigated using purified N-terminal tandem as a bait protein, this purified construct consisted of MSD1 and MSD2 together (1-196 residues). Binding assays using both the C and N-terminus of MS1, pulled out proteins from mouse heart extract. These bound proteins identified by mass spectrometry were Myosin heavy chain (MHC), actin, α- topomyosin, troponin I, troponin T and myosin LC2.

There has never been any indication that there are potential actin binding sites within the N-terminal domain of MS1. α-MHC and LC myosin were only seen to be binding at the N-terminal domain. These proteins are all known to interact with each other as they are all myofibrillar proteins which are found within the sarcomere. Myofibrillar proteins have been implicated in hypertrophic cardiomyopathies (Ruparelia *et al.,* 2012; Peddy *et al.,* 2006, Rao *et al.,* 2007). These proteins are also seen located within the I-band and z-disk region where MS1 is also located. These putative interacting proteins could interact with MS1 directly or via actin which binds to MS1 at the C-terminal region.

C-terminal tandem (193-375) was also investigated to determine whether any other proteins might potentially be pulled down from heart extract that had not been previously identified. The results of mass spectrometry identified that actin, troponin T and α-tropomyosin were present.

Although putative interacting proteins have been identified by mass spectrometry it is not certain how they interact with the MS1 protein itself. Binding studies using N-terminal tandem coupled to sepharose incubated with individual purified proteins did not confirm the interaction (data not shown). The proteins did not successfully bind and it was thought perhaps they need to be in complex with each other to bind with MS1. Therefore we did a series of actin co-sedimentation assays to determine whether the presence of actin is required for other proteins to bind. Actin was seen to interact with the C-terminal tandem domain (193-375) while this was not seen for the N-terminal tandem domain (1-196).

Based on what was observed in this study, myofibrillar proteins were identified to bind to both the N-terminal and C-terminal tandem MS1 proteins. However Myosin was seen binding at the N-terminal domain and not the C-terminal domain which could be a reason why actin is being pulled down at the N-terminal domain. Although this is preliminary data it is novel and more needs to be done in order to determine whether these interactions are directed or facilitated through one of the proteins present and not all of them.

Future work to confirm the association identified, could involve co-immunoprecipitation experiments. Evidence from experiments carried out in chapter 5, identified MS1 as being a substrate of JNK/SAPK. This could mean that phosphorylation is required for binding to occur, therefore it would be interesting to design binding assays using phosphorylated N-terminal tandem or the mutant proteins with Ser to Asp, or Thr to Glu that mimic the phosphorylated protein.

6.4. Thr 62 and Ser 77 of MS1 are phosphorylated by JNK *in vitro*.

MS1 is still poorly understood in terms of what is responsible for its activation and what pathways it is associated with. MS1 is known to activate the SRF which is involved in myocyte differentiation and regulation of developing hearts (Arai *et al.,* 2002, Wong *et al.,* 2011; Pipes *et al.,* 2006; Niu *et al.,* 2005 and Takano *et al.,*1998). There have not been any previous studies which have investigated MS1 in terms of its phosphorylation. The sequence of MS1 showed potential SAPK phosphorylation sites within the N-terminal domain due to the presence of the conserved phosphorylation sequence that had the classic motif of MAPK substrates SP/SPT (Cargnello and Roux, 2011; The predicted phosphorylation sites were Thr62, Ser77 and Ser-150. In vitro kinase assays

were carried out using the MAPK's JNK, p38 and ERK were used to determine whether MS1 is a potential substrate when any of the kinases are activated.

Mass spectrometry results identified that there were 3 amino acid residues which were being phosphorylated by MAPKs *in vitro*. Thr24, Thr62 and Ser77 were the sites which were phosphorylated, however site directed mutagenesis was only carried out on two of the putative sites which were Thr62 and Ser-77. These sites were identified to be phosphorylated by JNK, ERK and p38 to a lesser extent. Site directed mutagenesis prevented phosphorylation of Thr62 but not Ser77. Co-IP experiments were done to investigate whether FLAG-MS1 and JNK can directly interact with each other. The results confirmed direct interaction between MS1 and JNK *in vitro*.

We wanted to explore further the function of these phosphorylation sites. Immunofluorescence studies were done to determine whether phosphorylation of these sites led to change in subcelluar distribution of MS1 and also to determine whether MS1 phosphorylation has an effect on actin and MS1 interaction. Results from these experiments did not show any change in colocalisation of MS1 with actin but cells appeared stressed and there was disorganization of the cytoskeleton. Colocalisation experiments using WT or phosphorylation site mutants transfected with HA-JNK were subjected to sorbitol treatment. There was observed *in vivo* co-localisation between MS1 and JNK at the periphery of the cell with WT MS1 and Thr62E.

6.5. Overall summary

In this study we were able to determine that expression of MS1at the protein level increased after 2hr and 4hr of simulated reperfusion. This supports what was seen previously by Dr. Joanna Hay, where levels of MS1 mRNA increased during simulated ischaemia/reperfusion injury. MS1 promoter studies provided strong evidence that the MS1 promoter is responsive to the cellular stresses that have been shown to activate JNK and p38. The MS1 promoter was also responsive to phenylephrine which is a strong hypertrophic agonist and leads to the activation of JNK via the PKC pathway.

Mass spectrometry confirmed binding of, Myosin HC and LC, α-tropomyosin, and troponin to the N-terminal region. Similarly the C-terminal domain of MS1 was able to bind α-actin, α-tropomyosin- and troponin but not β-Myosin of LC-Myosin which was quite interesting. This is the first time that the N-terminal domain has been shown to bind actin and is worthy of further investigation. Lastly we showed via *in vitro* kinase assays, that MS1 is a substrate for JNK phosphorylation, at Thr62 and Ser77. Co-

immunoprecipitation studies indicated that JNK and MS1 interact directly with each other and there is little co-localisation between MS1 and JNK *in vivo.* However, where there was evidence of interaction between them, the cells appeared stressed with membrane ruffles at the periphery and observed disorganization of actin. Membrane ruffling is controlled by the Rho-GTPase family that interact with JNK (Hall, 2008, Borm *et al.,* 2005, Demali *et al.,* 2003; Johansen *et al*., 2007)

These studies have provided evidence that MS1 is associated with the JNK pathway. MS1 could potentially be regulated by JNK activation and this needs to be explored more in depth. A possible role for JNK in MS1 expression and function is illustrated in figure 6.1. Activation of the MAPK/JNK as a result of stress, targets the MS1 promoter which could be targeting the GATA4 sites within the promoter (Ouzain *et al.*, 2012). MS1 protein is phosphorylated by JNK at two positions; Ser77 and Thr62. Phosphorylation of these sites may lead to increased levels of MS1 within the cytosol where it may promote interactions with other proteins. The increase of MS1 levels leads to polymerization of G-actin to F-actin. When G-actin levels become depleted, this results in the release of MRTF, which is translocated from the cytoplasm to the nucleus. MRTF activates SRF which leads to the expression of hypertrophic genes such as myosin, alpha actinin, and others. Hypertrophic proteins which are expressed could be in a feedback mechanism interacting with MS1 to aid in myogenic differentiation, and may interact with other proteins to aid in myofibrillar disarray. Phosphorylation of MS1 by JNK could also have an impact on its localization and could potentially promote translocation to the nucleus where it could act as a transcription factor.

The data provided has shown for the first time that the MS1 protein is a substrate for phosphorylation by JNK and it will be important to determine the functional significance of this phosphorylation. JNK is also involved in induction of MS1 expression as no other studies have reported protein interacting with the N-terminus of MS1. Although the studies are preliminary, they are novel and have given more insight into the potential function of MS1.

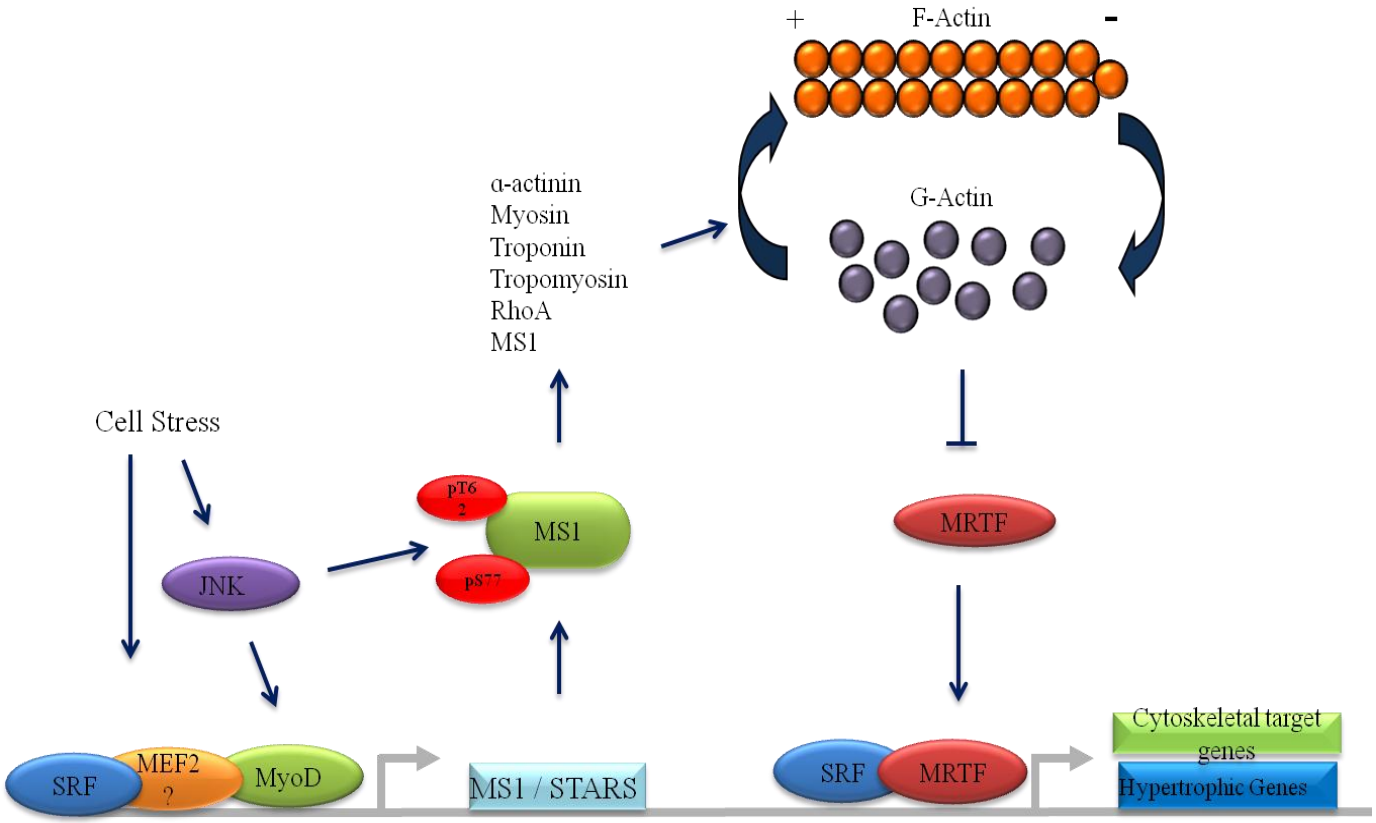

Figure 6.1: An overview of how MS1 links stress signals & actin dynamics to hypertrophic gene expression and cytoskeletal target genes.
Extracellular stress signals are transmitted into the cell, where proteins upstream of JNK become activated. JNK activation leads to direct phosphorylation of MS1 or targeting specific sites within the promoter to drive MS1 expression. Phosphorylation at Thr62 and S77 may facilitate interaction with myofibrillar proteins,that in turn assist in actin dynamics. F-actin increases in concentration in the cytoplasm while G-actin becomes depleted. G-actin depletion allows for the translocation of MRTF-A into the nucleus, where it binds SRF. SRF activation regulates hypertrophic and cytoskeletal genes, that become expressed and lead to interactions with MS1.

References

Abas, L; Bogoyevitch, M.A and Guppy, M. (2000) Mitochondrial ATP production is necessary for activation of the extracellular-signal-regulated kinases during ischaemia/reperfusion in rat myocyte-derived H9c2 cells. *Biochem. J*. 349:119-126.

Acehan, D; Jiang, X; Morgan, D; heuser, J; Wang, X and Akey, C. (2002) Three-Dimensional Structure of the Apoptosome: Ipmlications for Assembly, Procaspase-9 Binding, and Activation. *Mol. Cell*. 9:423-432.

Aceto A., Mezzetti A., Di-llio C., Calafiore A.M., De Cesare D., Bosco G., Accai N., Cappalletti L., Federici G. And Cuccurullo F. (1990) Effect of ischaemia-reperfusion on glutathione peroxidise, glutathione reductase and glutathione transferase activities in human heart protected by hypothermic cardioplegia. *Free Rad. Res. Commun.* 8:85-91.

Agarkova, I and Perriard, J. (2005) The M-band: an elastic web that crosslinks thick filaments in the center of the sarcomere. *Trends Cell Biol*. 15(9):477-485.

Ahmed S.H. and Lindsey M.L. (2009) Titin phosphorylation myocardial passive stiffness regulated by the intracellular giant. *Circ. Res.* 105(7):611-613.

Aikawa, R; Komuro, I; Yamazaki, T; Zou, Y; Kudoh, S; Zhu, W; Kadowaki, T and Yazaki, Y. (1999) Rho family small G proteins play critical roles in mechanical stress-induced hypertrophic responses in cardiac myocytes. *Circ Res*. 84(4):458-66.

Akazawa, H and Komuro, I. (2003) Roles of cardiac transcription factors in cardiac hypertrophy. *Circ Res*. 92(10):1079-88.

Alberts, A.S and Treisman, R. (1998) Activation of RhoA and the SAPK/JNK signalling pathways by the RhoA-specific exchange factor mNET1. *EMBO J*. 17(14):4075-4085.

Allard S.M. and Kopish K. (2008) Luciferase reporter assays: powerful, adaptable tools for cell biology research. *Cell Notes.*21:23-26.

Altman C.D., Fulton D.R. and Weisman L.E. (2014) Congenital heart disease (CHD) in the newborn: Presentation and screening for critical CHD. May 2013. [Online] Available from: http://www.uptodate.com/contents/congenital-heart-disease-chd-in-the-newborn-presentation-and-screening-for-critical-chd. [Accessed 1st June 2014]

Ambrosio, G and Tritto, I. (1999) Reperfusion injury: Experimental evidence and clinical implications. *Am Heart J*. 138(2 Pt2):69-75.

Ambrosio G., Weisman H.F., Mannisi J.A and Becker L.C. (1989) Progressive impairment of regional myocardial perfusion after initial restoration of postischaemic blood flow. *Circulation.*80(6):1846-1891.

Aneba, S; Chen, Y; Mateasik, A; Comte, B; Chorvat, D and Chorvatova, A. (1997) Probing of Cardiomyocyte Metabolism by Spectrally Resolved Lifetime Detection of NAD(P)H Fluorescence. *Computers in Cardiology*. 34:349-352.

Aoki, H; Izumo, S and Sadoshima, J. (1998) Angiotensin II activates RhoA in cardiac myocytes: a critical role of RhoA in angiotensin II- induced pre-myofibril formation. *Circ. Res*. 82:666-676.

Aoyagi, T and Matsui, T. (2011) Phosphoinositide-3 kinase signaling in cardiac hypertrophy and heart failure. *Curr Pharm Des*. 17(18):1818-1824.

Arai, A; Spencer, J.A and Olson, E.N. (2002) STARS, a Striated Muscle Activator of Rho Signaling and Serum Response Factor-dependent Transcription. *J. Biol. Chem,* 277: 24453-24459.

Aravind L., and Koonin E.V. (2000) SAP- a putative DNA binding motif involved in chromosomal organization. *Trends Biochem Sci.* 25(3):112-114.

Armstrong S. C. (2004) Protein kinase activation and myocardial ischaemia/reperfusion injury. *Eur. Soc. Of Cardol.*

Aronheim A., Broder Y.C., Cohen A., Fritsch A., Belisle B. and Abo A. (1998) Chp, a homologue of the GTPase Cdc42Hs activates the JNK pathway and is implicated in reorganizing the actin cytoskeleton. *Curr. Biol.* 8:1125-1128.

Ashley E. A., Niebauer J. (2004) Cardiology Explained. (*London) Remedica.*

Avkiran M. and Marber M.S. (2002) Na^+/ H^+ exchange inhibitors for cardioprotective therapy: progress, problems and prospects. *J Am Cell Cardiol.* 39(5):747-753.

Avruch J. (2007) MAP kinase pathways: the first twenty years. *Biochem Biophys Acta.* 1773: 1150- 1160.

Baines C.P and Molkentin J.D. (2005) STRESS signalling pathways that modulate cardiac myocyte apoptosis. *J Mol. Cell Cardiol.* 38(1): 47-62.

Balakumar P. and Jagadeesh G. (2010) Multifarious molecular signalling cascades of cardiac hypertrophy: can the muddy waters be cleared? *Pharmacol Res.* 62(5):365-383.

Bang M.L., Caremani M., Brunello E., Littlefield R., Leiber R.L. Chen J., Lombardi V. and Linari M. (2009) Nebulin plays a direct role in promoting strong actin-myosin interactions. *FASEB J.* 23:4117-4125.

Baker, J.L and Voth, G.A. (2013) Effects of ATP and Actin-Filament Binding on the Dynamics of the Myosin II S1 Domain. *Biophys J*. 105(7):1624-1634.

Barany, M and Barany K. (1980) Phosphorylation of the myofibrillar proteins. *Ann Rev Physiol*. 42:275-292.

Barany M and Barany K. (2003) The imoact of the paper if Edsall and Mehl (1949) on actin and actomyosin research. *Biophys Chem.* 100(1-3):177-182.

Bardwell L. (2006) Mechanisms of MAPK signalling specificity. *Biochem. Soc. Trans.* 34(Pt5):837- 841.

Bardwell, A.J; Abdollahi, M and Bardwell, L. (2003) Docking sites on mitogen-activated protein kinase (MAPK) kinases, MAPK phosphatases and the Elk-1 transcription factor compete for MAPK binding and are crucial for enzymic activity. *Biochem J*. 370(Pt3):1077-1085.

Bardwell A.J., Frankson E. and Bardwell L. (2009) Selectivity of docking sites in MAPK kinases. *J. Biol. Chem.* 284(19): 13165-13173.

Barouch, L.A; Gao, D; Chen, L; Miller, K.L; Xu, W; Phan, A.C; Kittleson, M.M; Minhas, K.M; Berkowitz, D.E; Wei, C and Hare, J.M. (2005) Cardiac Myocyte Apoptosis Is Associated With Increased DNA Damage and Decreased Survival in Murine Models of Obesity. *Circ Res*. 98(1):119-124.

Barr R.K. and Bogoyevitch M.A. (2001) The c-Jun N-terminal protein kinase family of mitogen-activated protein kinase (JNK MAPs). *Int J Biochem Cell Biol.* 33:1047-1063.

Barrientos, T; Frank, D; Kuwahara, K; Bezprozvannaya, S; Teg Pipes, G.C; Bassel-Duby, R; Richardson, J.A; Katus, H.A; Olson, E.N and Frey, N. (2007) Two Novel Members of the ABLIM Protein Family, ABLIM-2 and -3, Associate with STARS and Directly Bind F-actin. *J. Biol. Chem*. 282(11): 8393-8403.

Barry, S.P; Davidson, S.M and Townsend, P.A. (2008) Molecular regulation of cardiac hypertrophy. *Int J Biochem Cell Biol.* 40(10):2023-2039.

Bassi R., Heads R., Marber S. and Clark J.E. (2008) Targeting p38-MAPK in the ischaemic heart: kill or cure? *Curr Opinion in Pharmacol*. 8(2):141-146.

Bedard, E; Shore, D.F and Gatzoulis, M.A. (2008) Adult congenital heart disease: a 2008 overview. *Br Med Bull*. 85:151-180.

Behrmann, E; Müller, M; Penczek, P.A; Mannherz, H. G; Manstein, D.J and Raunser, S. (2012) Structure of the Rigor Actin-Tropomyosin-Myosin Complex. *Cell*. 150: 327-338.

Belaguli, N.S; Sepulveda, J.L; Nigam, V; Charron, F; Nemer, M and Schwartz, R.J. (2000) Cardiac tissue enriched factors serum response factor and GATA-4 are mutual coregulators.*Mol Cell Biol*. 20(20):7550-7558.

Berkes, C.A and Tapscott, S.J. (2005) MyoD and the transcriptional control of myogenesis. *Semin Cell Dev Biol*. 16(4-5):585-595.

Berry C.E. and Hare J.M. (2004) Xanthine oxidoreductase and cardiovascular disease: molecular mechanisms and pathophysiological implications. *J of Physiol*. 555(Pt3):589-606.

Bialik, S; Geenen, D.L; Sasson, I.E; Cheng, R; Horner, J.W; Evans, S.M; Lord, E.M; Koch, C.J and Kitsis, R.N (1997) Myocyte Apoptosis During Acute Myocardial Infarction in the Mouse Localizes to Hypoxic Regions but Occurs Independently of p53. *J. Clin. Invest.* 100: 1363-1372.

Bird T.M., Hobbs C.A., Cleves M.A., Tilford J.M. and Robbins J.M. (2006) National rates of birth defects among hospitalized newborns. *Clinc and Mol Teratology.* 76(11):762-769.

Bisno A.L., Campo R.E and Schultz D.R. (1995) M proteins of group G streptococci: mechanisms of resistance to phagocytosis. *J Infect Dis.* 17(3):601-606.

Black, B.L and Cripps, R.M. (2010) Myocyte Enhancer Factor 2 Transcription Factors in Heart Development and Disease. In: Rosenthal, N and Harvey, R.P. ed. *Heart Development and Re*generation. Oxford: Academic Press, pp. 673-699.

Blackwell, T.K and Weintraub, H. (1990) Differences and similarities in DNA-binding preferences of MyoD and E2Aprotein complexes revealed by binding site select ion. *Science*. 250(4984):1104-1110.

Bogoyevitch, M.A; Boehm, I; Oakley, A; Ketterman, A.J and Barr, R.K. (2004) Targeting the JNK MAPK cascade for inhibition: basic science and therapeutic potential. *Biochim Biophys Acta*. 1697(1-2):89-101.

Bogoyevitch, M.A; Gillespie-Brown, J; Ketterman, A.J; Fuller, S.J; Ben-Levy, R; Ashworth, A; Marshall, C.J and Sugden P.H. (1996) Stimulation of the Stress-Activated Mitogen Activated Protein Kinase Subfamilies in Perfused Heart; p-38/RK Mitogen-Activated Protein Kinases and c-Jun N-Terminal Kinases are activated by Ischaemia/Reperfusion *Circ. Res,* 79, 161-172.

Bogoyevitch, M.A; Ketterman, A.J and Sugden P.H. (1995) Cellular Stresses Differentially Activate c-Jun N-Terminal Protein Kinases and Extracellular Signal-regulated Protein Kinases in Cultured Ventricular Myocytes. *J. Biol. Chem*, 270: 29710-29717

Bogoyevitch, M.A; Ketterman, A.J and Sugden P.H. (1995) Cellular stresses activate c-Jun N-terminal protein kinases (JNKs) in ventricular myocytes cultured from neonatal rat hearts. *J Biol Chem*. 270: 29710-29717.

Bogoyevitch M.A. and Kobe B. (2006) Uses for JNK: the many and varied substrates of the c-Jun N-terminal kinases. *Microbiol Mol Biol Rev.* 70: 1061-1095.

Bolli R., Jeroudi M.O., Patel B.S., Aruoma O.I., Halliwell B., Lai E.K. and McCay P.B. (1989) Marked reduction of free radical generation and contractile dysfunction by antioxidant therapy begun at the time of reperfusion. Evidence that myocardial "stunning" us a manifestation of reperfusion injury. *Circ. Res.*65 (3): 607-622.

Bolli R., Li Q.H., Tang X.L., Guo Y., Xuan Y.T., Rokosh G. and Dawn B. (2007) The late phase of preconditioning and its natural clinical application – gene therapy. *Heart Fail Rev.* 292(1):19-27.

Boneva R.S., Botto L.D., Moore C.A., Yang Q., Correa A. and Erickson J.D. (2001) Mortality associated with congenital heart defects in the United states: Trends and racial disparities 1979-1997. *Circulation.* 103:2376-2381.

Bottcher R.T. and Niehrs C. (2005) Fibroblast growth factor signalling during early vertebrate development. *Endocr. Rev.* 26:63-77.

Bradford, M. M. (1976) A rapid and sensitive method for the quantitation of microgram quantities of protein utilizing the principle of protein-dye binding. *Anal. Biochem*. 72:248-254.

Bratton, D. L; Fadok, V. A; Richter, D. A; Kailey, J. M; Guthrie, L. A and Henson, P. M. (1997) Appearance of Phosphatidylserine on Apoptotic Cells Requires Calcium-mediated Nonspecific Flip-Flop and Is Enhanced by Loss of the Aminophospholipid Translocase. *J. Biol. Chem*. 272(42): 26159-26165.

Braun, T and Gautel, M. (2011) Transcriptional mechanisms regulating skeletal muscle differention, growth and homeostasis. *Nat Rev Mol Cell Biol*. 12(6):349-361.

Braunwald E. and Kloner R.A. (1985) Myocardial reperfusion: a double edged sword? *J clin Invest.* 1719: 761713- 761719.

Brickner, M.E; Hillis, L.D and Lange, R.A. (2000) Congenital heart disease in adults. First of two parts. *N Engl J Med*. 342(4):256-263.

Broderick T.L., Parrott C.R., Wang D., Jankowski M. and Butkowska J. (2012) Expression of cardiac GATA4 and downstream genes after exercise training in the db/db mouse. *Pathology.* 19(3): 193-203.

Bromme, H.J and Holtz,J. (1996) Apoptosis in the Heart, When and Why? *Mol. Cell. Biochem.*163-164: 271-275.

Buchwalter G., Gross C., Wasylyk B (2004) Ets ternary complex transcription factors. Ge*ne* 324:1-14.

Buja, L.M. (2005) Myocardial ischemia and reperfusion injury. *Cardiovasc Pathol*. 14(4):170-175.

Buja, L.M and Weerasinghe, P. (2010) Unresolved issues in myocardial reperfusion injury. *Cardiovasc Pathol*. 19(1):29-35.

Burke, A.P. 2013. Pathology of Rheumatic Heart Disease. WedMD. Available at: http://emedicine.medscape.com/article/1962779-overview [Accessed: 28th July, 2014].

Burridge K., Wennerberg K. (2004) Rho and Rac take center stage. *Cell* 116:167-179.

Bustelo X.R., Sauzeau V. and Berenjeno I.M. (2007) GTP-binding proteins of the Rho/Rac family:regulation, effectors and functions in vivo. *Bioessays*. 29:356-370.

Caldwell K. K., Sosa M. and Buckley C. T. (2006) Identification of mitogen-activated kinase docking sites in enzymes that metabolize phosphatidylinositols and inositol phosphates. *Cell Commun Signal*. 4:2.

Canagarajah B., Khokhlatchev A., Cobb M. and Goldsmith E. (1997) Activation mechanism of the MAP kinase ERK2 by dual phosphorylation. *Cell*. 90:859-869.

Canton, M., Menazza S., Sheeran F.L., Polverino de Laureto P., Di Lisa F., Pepe S. (2011) Oxidation of Myofibrillar proteins in human heart failure. *J. Of the Am. Col. Of Cardiology* 57(1): 300-309.

Carden, D.L and Granger, D.N. (2000) Pathophysiology of ischemia-reperfusion injury. *J Pathol*. 190(3):255-266.

Cargnello, M and Roux, P.P. (2011) Activation and Function of the MAPKs and Their Substrates, the MAPK-Activated Protein Kinases. *Microbiol Mol Biol Rev*. 75(1):50-83.

Carlier M.F. and Pantaloni D. (1997) Control of actin dynamics in cell motility. *J Mol Biol*. 269(4):459-467. Review.

Carnac G., Primig M., Kitzmann M., Chafey P., Tuil D., Lamb N., Fernandez A. (1998) RhoA GTPase and serum response factor control selectively the expression of MyoD without affecting Myf5 in mouse myoblasts. *Mol. Biol. Cell* 9:1891-1902.

Carreño, J.E; Apablaza, F; Ocaranza, M.P and Jalil, J.E. (2006) Cardiac hypertrophy: molecular and cellular events. *Rev Esp Cardiol*. 59(5):473-486.

Cartoni, R; Leger, B; Hock, B.M; Prazl, M; Crettenand, A; Pich, S; Ziltener, J; Luthi, F; Deriaz, O; Zorzano, A; Gobelet, C; Kralli, A and Russell, A.P. (2005) Mitofusins ½ and ERRα expression are increased in human skeletal muscle after physical exercise. *J Physiol*. 567(Pt 1):349-358.

Chandra M., Mamidi R., Ford S., Hidalgo C., Witt C., Ottenheijm C., Labeit S. and Granzier H. (2009) Nebulin alters cross-bridge cycling kinetics and increases think filament activation: a novel mechanism for increasing tension and reducing tension cost. *J. Biol. Chem.* 284: 30889-30896.

Chaudry, I.H; Clemens, M.G and Baue, A.E. (1981) Alterations in cell function with ischemia and shock and their correction. *Arch Surg*. 116:1309-1317.

Chen, H; Bernstein, B.W and Bamburg, J.R. (2000) Regulating actin-filament dynamics in vivo. *Trens Biochem. Sci*. 25:19-23.

Chen L., Kuo W., Yang J., Wang S., Yeh Y., Tsai F., Ho Y., Chang M., Huang C. and Lee S. (2007) Eccentric cardiac hypertrophy was induced by long-term intermittent hypoxia in rats. *Exp. Physiol.* 92: 409-416.

Chilton, R.J. (2004) Pathophysiology of coronary heart disease: a brief review. *J Am Osteopath Assoc*. 104(9Suppl7):S5-8.

Cho, Y; Hazen, B.C; Russell, A.P and Kralli, A. (2013) Peroxisome Proliferator-activated Receptor Coactivator 1(PGC-1)- and Estrogen-related Receptor (ERR)-induced Regulator in Muscle 1 (PERM1) Is a Tissue-specific Regulator of Oxidative Capacity in Skeletal Muscle Cells. *J Biol Chem*. 288(35):25207-25018.

Chong, N. W; Koekemoer, A. L; Ounzain, S; Samani, N. J; Shin, J. T and Shaw, S. Y. (2012) STARS is essential to maintain cardiac development and function *in vivo* via a SRF pathway. *PLoS ONE*. 7(7):e40966.

Choukroun G., Hijar R., Fry S., del Monte F., Haq S., Guerrero J., Picard M., Rosenzweig A. and Force T. (1999) Regulation of cardiac hypertrophy in vivo by the stress-activated protein kinases/c-Jun NH2-terminal kinases. *J Clinc. Invest.* 104:391-398.

Cisterna, B; Necchi, D; Prosperi, E and Biggiogera, M. (2006) Small ribosomal subunits associate with nuclear myosin and actin in transit to the nuclear pores. *FASEB J.* 20: 1901-1903.

Clark K. A; McElhinny A. S; Beckerle M. C and Gregorio C. C. (2002) Striated muscle cytoarchitecture: An intricate web of form and function. *Annu. Rev. Cell Dev. Biol.* 18: 637-706.

Clements R.T., Feng J., Cordeiro B., Bianchi C. and Selke F.W. (2011) p38 MAPK-dependent small HSP27 and alphaB-crystallin phosphorylation in regulation of myocardial function following cardioplegic arrest. *Am. J Physiol.* 35(3):474-483.

Clerk, A; Fuller, S.J; Michael, A and Sugden, P.H. (1998) Stimulation of " Stress-regulated" Mitogen-Activated Protein Kinasses (Stress-activated Protein Kinases/c-Jun N-terminal Kinases and p38-Mitogen-activated Protein Kinases) in Perfused Rat Hearts by Oxidative and Other Stresses. *J. Biol. Chem*, 273(13), 7228-7234.

Clerk A. and Sugden P.H. (1997) Activation of p-21 activated protein kinase alpha (alpha PAK) by hyperosmotic shock in neonatal ventricular myocytes. *FBBS Lett.* 403(1):23-25.

Clerk A. and Sugden P.H. (1997) Cell stress-induced phosphorylation of ATF2 and c-Jun transcription factors in rat ventricular myocytes. *Biochem J.* 325(Pt3): 801-810.

Clerk A. and Sugden P.H. (1997) Cell stresses regulate the phosphorylation state of c-Jun and ATF-2 in ventricular myocytes. *Biochem Soc. Trans.* 25(2):221S.

Clerk A. and Sugden P.H. (2004) Regulation of phospholipases C and D in rat ventricular myocytes: stimulation by endothelin-1,bradykinin and phenylephrine. *J Mol Cell Cardiol.* 29(6):1593- 15604.

Clerk A. and Sugden P.H. (2004) Signalling through the extracellular signal-regulated kinase ½ cascadein cardiac myocytes. *Biochem Cell Biol.* 82(6): 603-609. Review

Collard, C.D and Gelman, S. (2001) Pathophysiology, Clinical Manifestations, and Prevention of Ischemia-Reperfusion Injury. *Anesthesiology*. 94(6):1133-1138.

Cooper J.A. (2002) Actin dynamics: tropomyosin provides stability. *Curr. Biol.* 12:R523-R525.

Cooper J. A., Schafer D. A. (2000) Control of actin assembly and disassembly at filament ends. *Curr. Opin. Cell Biol.* 12:97-103.

Coso O. A., Chiariello M., Yu J.C., Teramoto H., Crespo P., Xu N., Milki T. And Gutkind S. (1995) The small GTP-Binding Proteins Rac1 and Cdc42 regulate the activity of the JNK/SAPK Signalling Pathway. *Cell* 81:1137-1146.

Creyghton M.P., Cheng A.W., Welstead G.G., Kooistra T., Carey B.W., Steine E.J., Hanna J., Lodato M.A. Frampton G.M., Sharp P.A., Boyer L.A., Young R.A. and Jaenisch R. (2010) Histone H3K27ac separates active from poised enhancers and predicts developmental state. *Proc. Natl Acad Sci U.S.A.* 107(50): 21931-21936.

Crossland H., Constantin-Teodosiu D., Gardiner S.M., Constantin D. and Greenhaff P.L. (2008) A potential rold for Akt/FOXO signalling in both protein loss and the impairment of muscle carbohydrate oxidation during sepsis in rodent skeletal muscle. *J. Physiol.* 586(Pt22):5589-5600.

Cuenda A. and Rousseau S. (2007) p38 MAP-kinase pathway regulation, function and role in human disease. *Biochem. Biophys. Acta.* 1773(8): 1358-1375.

Cunningham, M.W. (2000) Pathogenesis of Group A Streptococcal Infections. *Clin Microbiol Rev*. 13(3):470-511.

Davies M.J. (2000) The physiology of acute coronary syndromes. *Heart.* 366: 83361-83366.

Davies, S.W., Ranjadayalan, K., Wickens D.G., Dormandy T.L. and Timmis A.D. (1990) Lipid peroxidation associated with successful thrombolysis. *Lancet.* 335: 741-743.

Davis P.J., Davis F.B and Lin H.Y. (2010) Roles and controls of mTOR in the heart. Focus on "mTOR attenuates the inflammatory response in cardiomyocytes and prevent dysfunction in pathological hypertrophy. *Am. J of Physiol.* 299(6): 1250-1252

Davis R.J. (2000) Signal transduction by the JNK group of MAP kinases. *Cell.* 103:239-252.

DeBosch B., Treskov I., Lupu T.S. Weinheimer C., Kovacs A., Courtsois M. and Muslin A.J. (2006) Akt1 is required for physiological cardiac growth. *Circulation.* 113(17):2097-2104.

De Groot, H and Rauen, U. (2007) Ischemia-reperfusion injury: processes in pathogenetic networks: a review. *Transplant Proc*. 39(2):481-4.

Dephoure N. and Gygi S.P. (2012) Hyperplexing: a method for high-order quantitative proteomics provides a map of the dynamic response to rapamycin in yeast. *Sci. Signal.* 5(217):rs2.

Dhalla N.S., Elmoselhi A.B., Hata T. and Makino N. (2000) Status of myocardial antioxidants in ischaemia-reperfusion injury. *Cardiovasc. Res.* 47 (3): 446-8211,56.

Dhanasekaran D., Kashef K., Lee C., Xu H. and Reddy E. (2007) Scaffold protein of MAPK-kinase modules. *Oncogene*. 26: 3185-3202.

Di Napoli, P; Taccardi, A.A; De Caterina, R and Barsotti, A. (1997) Pathophysiology of ischemia-reperfusion injury: experimental data. *Ital Heart J.* 3 suppl 4:24S-28S.

Dickens, M; Rogers, J.S; Cavanagh, J; Raitano, A; Xia, Z; Halpern, J.R; Greenber, M.E; Sawyers, C.L and Davis, R.J. (1997) A cytoplasmic inhibitor of the JNK signal transduction pathway. *Science*. 277:693-696.

Dirksen, M.T; Laarman, G.J; Simoons, M.L and Duncker, D.J.G.M. (2007) Reperfusion injury in humans: A review of clinical trials on reperfusion injury inhibitory strategies. *Cardiovasc Res*. 74(3):343-355.

Dirwan A. and Dorn G.W II. (2007) Decompensation of cardiac hypertrophy: cellular mechanisms and novel therapeutic targets. *Physiology*. 22: 56-64.

Djinovic-Carugo K., Young P., Gautel M. and Saraste M. (1999) Structure of the alpha-actinin rod: molecular basis for cross-linking of actin filaments. *Cell.* 98(4):537-546.

Dorn G.W. (2009) Apoptotic and non-apoptotic programmed cardiomyocytes death in ventricular remodelling. *Cardiovasc. Res.* 81, 465-473.

Dorn, GW 2nd; Robbins, J; Sugden, P.H. (2003) Phenotyping hypertrophy: eschew obfuscation. *Circ Res.* 92: 1171-1175.

Dos Remedios C.G., Chabra D., Kekic M., Dedova I.V., Tsubakihara M., Berry D.A. and Nosworthy N.J. (2003) Actin binding proteins: Regulation of cytoskeletal microfilaments. *Physiol Rev.* 83:433-473.

Dos Remedios C.G., Chabra D. and Nosworthy N.J. (2005) The N-terminal fragment of gelsolin inhibits the interaction of DNAse1 with isolated actin, but not with the cofilin actin complex. *Proteomics.* 5(12):3131-3136.

Doucet M., Russell A.P., Leger B., Debigare R., Joanisse D.R., Caron M.A., LeBlanc P. and Maltais F. (2007) Muscle atrophy and hypertrophy signalling in patients with chronic obstructive pulmonary disease. *Am J Respir Crit Care*, 176(3):261-269.

Dreisher T.A., Garcia I. And Harlan J.M. (1993) Cytokine-induced adhesion molecule exoression on human umbilical vein endothelial cells is not regulated by cyclic adenosine monophosphate accumulation. *Life Sci.* 53(4):365-370.

Duilio C., Ambrosio G., Kuppusamy P., DiPaula A., Becker L.C. and Zweier J.L. (2001) Neutrophils are primary source of O2 radicals during reperfusion after prolonged myocardial ischaemia. *Am J Physiol Heart Circ Physiol.* 280(6):H2649-H2657.

Ehler E. and Gautel M. (2008) The sarcomere and sarcomerogenesis. *Adv Exp Med Biol.*642:1-14.

Elliott, P; Andersson, B; Arbustini, E; Bilinska, Z; Cecchi, F; Charron, P; Dubourg, O; Kühl, U; Maisch, B; McKenna, W.J; Monserrat, L; Pankuweit, S; Rapezzi, C; Seferovic, P; Tavazzi, L and Keren, A. (2008) Classification of the cardiomyopathies: a position statement from the European Society Of Cardiology Working Group on Myocardial and Pericardial Diseases. *Eur heart J*. 29(2):270-276.

Elmore, S. (1997) Invited Review: Apoptosis: A Review of Programmed Cell Death. *J. Toxicol. Pathol*. 35:495-516.

Eltzschig, H.K and Collard, C.D. (2004) Vascular ischemia and reperfusion injury. *Br Med Bull*. 70:71-86.

Engel F., Schbesta M., Duong M., Lu G., Ren S., Madwed J., Jiang H., Wang Y. and Keating M. (2005) p38 MAP kinase inhibition enables proliferation of adult mammalian cardiomyocytes. G*enes Dev.* 19: 1175-1187.

Engel F.B., Hsieh P.C., Lee R.T. and Keating M.T. (2006) FGF/p38 MAP kinase inhibitor therapy induces cardiomyocytes mitosis, reduces scarring, and rescues function after myocardial infarction. *Proc Natl Acad Sci U.S.A.* 103: 15546- 15551.

Enslen H., Raingeaud J. and Davis R.J. (1998) Selective activation of p38 mitogen-activated protein (MAP) kinase isoforms by the MAP kinase Kinases MKK3 and MKK6. *J Biol Chem.* 273(3):1741-1748.

Evelyn, C.R; Wade, S.M; Wang, Q; Wu, M; Iñiguez-Lluhí, J.A; Merajver, S.D and Neubig, R.R. (2007) CCG-1423: a small-molecule inhibitor of RhoA transcriptional signaling. *Mol Cancer Ther*. 6(8):2249-2260.

Fagard R.H. (1997) Impact of different sports and training on cardiac structure and function. *Cardiol Clin.*15(3):397-412.

Falk E., Shah P.K. and Fuster V. (1995) Coronary plaque disruption. *Circulation* 92:657-671.

Fauci A. S., Braunwald E., Isselbacher K. J. (1998) Harrison's principles of internal medicine, 14th Ed. Chap. 234:p.1279.

Ferdinandy P., Schulz R., Baxter G. F. (2007) Interaction of cardiovascular risk factors with myocardial ischaemia/reperfusion injurt, preconditioning and postconditioning. *Pharmacol. Rev.* 59: 5418-458

Fernandes, T; Soci, U.P.R; Melo, S.F.S; Alves, C.R and Oliveira, E.M. (2012). Signaling Pathways that Mediate Skeletal Muscle Hypertrophy: Effects of Exercise Training.

Ferrari R., Curello S., Boffa G.M., Condorelli E., Pasini E., Guanieri G. and Albertini A. (1989) Oxygen free radical-mediated heart injury in animal models and during bypass surgery in humans. Effects of alphatocopherol. *Ann NY Acad Sci.* 570: 237-253.

Filatov, V.L; Katrukha, A.G; Bulargina, T.V and Gusev, N.B. (1999) Troponin: Structure, Properties, and Mechanism of Functioning. Biochemistry (Moscow). 64(9):969-985.

Fluck, M. (2006) Functional, structural and molecular plasticity of mammalian skeletal muscle in response to exercise stimulus. *J. Of Expt. Biol.* 209: 2239-2248.

Fogl, C; Puckey, L; Hinssen, U; Zaleska, M; El-Mezgueldi, M; Croasdale, R; Bowman, A; Matsukawa, A; Samani, N. J; Savva, R and Pfuhl, M. (2011) A structural and functional dissection of the cardiac stress response factor MS1. *Proteins*. 80:398-409

Force T., Haiiar R., Del Monte F., Rosenzweig A. and Choukroun G (1999) Signalling pathways mediating the response to hypertrophic stress in the heart. G*ene Expr*. 7:337-348.

Frank, D and Frey, N. (2011) Cardiac Z-disc Signaling Network. *J Biol Chem*. 286:9897-9904. InTech. Available at: http://www.intechopen.com/books/skeletal-muscle-from-myogenesis-to-clinical-relations/signaling-pathways-that-mediate-skeletal-muscle-hypertrophy-effects-of-exercise-training [May 14th, 2014]

Frey, N; Katus, H.A and Olson, E.N. (2004) Hypertropy of the heart: A new therapeutic target? *Circ Res.* 109: 1580-1589

Friedrich, R; Hirche, H; Kebbel,V; Zylka,V; Bissig,R. (1981) Changes in intracellular Na , K , Ca and H of the ischaemic myocardium in pigs. *Basic Res. Cardiol.* 76:453-456.

Fritz G. And Kaina B. (2006) Late activation of stress kinases (SAPK/JNK) by genotoxins requires the DNA repair proteins DNA-PKcs and CSB. *Mol. Biol. Cell.* 17: 851-861.

Fuller S.J., Finn S.G., Downward J. and Sugden P.H. (1998) Stimulation of gene expression in neonatal rat ventricular myocytes by Ras is mediated by Ral guanine nucleotide dissociation stimulator (RalGDS) and phosphatidylinositol 3-kinase in addition to Raf. *Biochem J.* 335:241-246.

Furst D.O., Osborn M. and Weber K. (1989) Myogenesis in the mouse embryo: differential onset of expression of myogenic proteins and the involvement of titin in myofibril assembly. *J. Cell Biol*. 109:517- 527.

Fusello A.M., Mandik-Nyak L., Shih F., Lewis R.E., Allen P.M and Shaw A.S. (2006) The MAPK Scaffold Kinase Suppressor of Ras is involved in ERK activation by stress and proinflammatory cytokines and induction of arthritis. *The J. Of Immunology* 177:6152-6158.

Galanis A., Yang S.H. and Sharrocks A.D. (2001) Selective targeting of MAPKs to the ETS domain transcription factor SAP-1. *J Biol Chem.* 276:965-973.

Galis Z. S., Sukhova G. K., Lark M. W., Libby P. (1994) Increased expression of matrix metalloproteinases and matrix degrading activity in vulnerable regions of human atherosclerotic plaques. *J. Clin. Invest.* 94:2493-2503.

Gallo, K.A and Johnson, G. L. (2002) Mixed-Lineage Kinase Control of JNK and p38 MAPK Pathways. *Nat Rev Mol Cell Biol*. 3(9):663-672.

Ganote C. E. (1983) Contraction Band Necrosis and Irreversible myocardial Injury, *J. Mol. Cell Cardiol.* Vol 15:67-73.

Garcia-Dorado D., Theroux P., Munoz R., Alonso J., Elizaga J., Fernandez-Aviles F., Botas J., Solares J., Soriano J. and Duran J.M. (1992) Favourable effects of hyperosmotic reperfusion on myocardial edema and infarct size. 262(Pt2): H17-22.

Gatzoulis M.A. (2006) Adult congenital heart disease: education, education, education. *Nat Clin. Prac. Cardio. Med.* 3: 1743-4297.

Gautel M. (2008) The sarcomere and the nucleus: functional links to hypertrophy, atrophy and sarcopenia. *Adv. Exp. Med. Biol.* 642:176-191.

Gautel M. (2011) The sarcomeric cytoskeleton: who picks up the strain? *Curr. Opin. Cell Biol.* 23(1):39-46.

Ge B., Gram H., Di Padova F., Huang B., New L., Ulevitch R.J. and Luo J.H. (2002) MAPKK-independent activation of p38alpha mediated by TAB1-dependent autophosphorylation of p38alpha. *Science.* 295:1291-1294.

Geisler, H.W.S; Shi, H and Gerrard, D.E. (2013) MAPK Pathway in Skeletal Muscle Diseases. *J Vet Sci Anim Husb*. 1(1):1-4.

Gertis N., Kostenko S. and Moens U. (2007) In vivo functions of mitogen-activated protein kinases: conclusions from knock-in and knockout mice. *Transgenic Res.* 16:281-314.

Gewies, A. (2003) An Introduction to Apoptosis. *Apo Review*. 1-26.

Giordano F. J. (2005) Oxygen, oxidative stress, hypoxia and heart failure. *J. Clin. Invest.* 115(3): 500-508.

Goldhaber S.Z. and Bounameaux H. (2012) Pulmonary embolism and deep vein thrombosis. *Lancet*. 379(9828):1835-1846.

Goldhaber S.Z. and Morrison R.B. (2002) Pulmonary Embolism and Deep Vein Thrombosis. *Circulation*. 106:1436-1438.

Goldhaber S.Z. and Ridker P.M. (2002) Thrombosis and Thromboembolism.

Goll D. E., Neti G., Mares S. W. and Thompson V. F. (2008) Myofibrillar protein turnover: The proteasome and the calpains. *J. Anim. Sci*. Vol 86(14): E19-E35.

Grace, P.A. (1994) Ischaemia-reperfusion injury. *Br. J. Surg*. 81:637-647.

Grech E.D., Jack C.I.A., Bleasdale C., Jackson M.J., Hind C.R.K. and Perry R.A. (1993) Differential free radical activity (FRA) after successful and unsuccessful thrombolytic reperfusion in acute myocardial infarction. *Lancet.* 341: 990-991.

Green, D. R and Amarante-Mendes, G. P. (1998) The Point of no Return: Mitochondria, caspases and the commitment to cell death. *Results Probl Cell Differ*. 24:45-61.

Greenblatt, M.B; Shim, J; Zou, W; Sitara, D; Schweitzer, M; Hu, D; Lotinun, S; Sano, Y; Baron, R; Park, J.M; Arthur, S; Xie, M; Schneider, M.D; Zhai, B; Gygi, S; Davis, R and Glimcher, L.H. (2010) The p38 MAPK pathway is essential for skeletogenesis and bone homeostasis in mice. *J Clin Invest*. 120(7):2457-2473.

Gregorio C.C and Fowler V. M. (1995) Mechanism of thin filament assembly in embryonic chick cardiac myocytes: tropomodulin requires tropomyosin for assembly. *J. Cell Biol.* 129: 683-695.

Gregorio C.C., Weber A., Bondad M., Pennise C.R. and Fowler V.M. (1995) Requirement of pointed-end capping by tropomodulin to maintain actin filament length in embryonic chick cardiac myocytes. *Nature.* 377: 83-86.

Grewal S., Molina D.M. and Bardwell L. (2006) Mitogen-activated protein kinase (MAPK)-docking sites in MAPK kinases function as tethers that are crucial for MAPK regulation in vivo. *Cell Signal.* 18: 123-134.

Grossman W., Jones D. and McLaurin L.P. (1975) Wall stress and patterns of hypertrophy in the human left ventricle. *J clin invest.* 56(1):55-64.

Grummt I. (2006) Actin and myosin as transcription factors. *Curr Opin* G*enet Dev.* 16(2):191-196. Epub 2006 Feb 21.Review.

Guba, F and Straub, F.B. (1942) Extraction of myosin.

Guettler S., Vartiainen M.K., Miralles F., Larijani B. and Treisman R. (2008) REPL motifs link the serum response factor cofactor MAL but not myocardin to Rho signalling via actin binding. *Mol Cell Biol.* 28(2):732-742.

Guilherme L., Cury P., Demarchi L.M., Coelho V., Abel L., Lopez A.P., Oshiro S.E., Aliotti S., Cunha-Neto E., Pomerantzeff P.M., Tanaka A.C. and Kalil J. (2004)

Rheumatic heart disease: proinflammatory cytokines play a role in the progression and maintenance of valvular lesions. *Am. J Pathol.* 165(5):1583-1591.

Guilherme L. and Kalil J. (2004) Rheumatic fever: from sore throat to autoimmune heart lesions. *Int Arch Allergy Immunol.* 134(1):56-64. Epub 2004 Apr 16. Review.

Gutkowska, J; Broderick, T.L; Bogdan, D; Wang, D; Lavoic, J and Jankowski, M. (2009) Downregulation of oxytocin and natriuretic peptides in diabetes: possible implications in cardiomyopathy. *J Physiol*. 587(Pt 19):4725-4736.

Gwechenberger, M; Mendoza, L. H; Youker, K. A; Frangogiannis, N. G; Smoth, W. C; Michael, L. H and Entman, M.L. (1999) Cardiac Myocytes Produce Interleukin-6 in Culture and in Viable Border Zone of Reperfused Infarctions. *Circulation*. 99(4):546-51.

Halestrap, A.P; Clarke, S.J and Javadov, S.A. (2004) Mitochondrial permeability transition pore opening during myocardial reperfusion – a target for cardioprotection. *Cardiovasc Res*. 61(3):372-385.

Hall A. (1998) Rho GTPases and the actin cytoskeleton. *Science.* 279(5350):509-514. Review.

Hall R. A. and Lefkowitz R. J. (2002) Regulation of G protein-coupled receptor signalling by scaffold proteins. *Circ. Res.* 91: 672-680.

Hammill, A. K; Uhr, J. W and Scheuermann, R. H. (1999) Annexin-V staining due to loss of membrane asymmetry can be reversible and precede commitment to apoptotic death. *Exp Cell Res*. 251(1):16-21.

Han J., Lee J., Bibbs L. and Ulevitch R. (1994) A MAP kinase targeted by endotoxin and hyperosmolarity in mammalian cells. *Science.* 265: 808-811.

Han J. and Molkentin J.D. (2000) Regulation of MEF2 by p38 MAPK and its implication in cardiomyocte biology. *Trends Cardiovasc Med.* 10(1):19-22.

Hansen, P.R. (1995) Myocardial reperfusion injury: experimental evidence and clinical relevance. *Eur Heart J*. 16(6):734-740.

Hansson, G.K. (2005) Inflammation, Atherosclerosis, and Coronary Artery Disease. *N Engl J Med*. M52:1685-1695.

Haq S.E., Clerk A. and Sugden P.H. (1998) Activation of mitogen-activated proein kinases (p38-MAPKs, SAPKs/JNKs and ERKs) by adenosine in the perfused rat heart. *FBBS Lett.* 424(3): 305-308.

Harvey, P.A and Leinwand, L.A. (2011) Cellular mechanisms of cardiomyopathy. *J. Cell Biol*. 194(3): 355-365.

Hausenloy, D.J and Yellon, D.M. (2013) Myocardial ischemia-reperfusion injury: a neglected therapeutic target. *J Clin Invest*. 123(1):92-100.

Hay, J. (2006) Regulation of Gene Expression during Myocardial Ischaemia and reperfusion. PhD (Thesis) Dissertation, Leicester, England

Hefti, M.A; Harder, B.A; Eppenberger, H.M and Schaub, M.C. (1997) Signaling Pathway in Cardiac Myocyte Hypertrophy. *J Mol Cell Cardiol*. 29:2873-2892.

Helbig L., Damrot J., Hulsenbeck J., Koberle B., Brozovic A., Osmak M., Fiket Z., Kaina B., Fritz G. (2011) Late activation of stress-activated protein kinases/ c-Jun N-terminal kinases triggered by cisplatin-induced DNA damage in repair-defective cells. *J. Biol. Chem.* 286: 12991-13001.

Heineke, J and Molkentin, J.D. (2006) Regulation of cardiac hypertrophy by intracellular signalling pathways. *Nat Rev Mol Cell Biol*. 7(8):589-600.

Heineke J., Ruetten H., Willenbockel C., Gross S. C., Naguib M., Schaefer A., Kempf T., Hilfker-Kleiner D., Caroni P., Kraft T., Kaiser R. A., Molkentin J. D., Drexler H., Wollert K. C. (2005) Attenuation os cardiac remodelling after myocardial infarction by

muscle LIM proyein-calcineurin signalling at the sarcomeric z-disc. *Proc. Natl. Acad. Sci. USA* 102:1655-1660.

Helisch, A and Schaper, W. (2003) Arteriogenesis: the development and growth of collateral arteries. *Microcirculation*. 10(1):83-97.

Herskowitz, A; Choi, S; Anasari, A and Wesselingh, S. (1995) Cytokine mRNA expression in postischaemic/reperfused myocardium. *Am. J. Pathol*. 146:419-428.

Hescheler, J; Meyer, R; Plant, S; Krautwurst, D; Rosenthal, W and Schultz, G (1991) Morphological, biochemical, and electrophysiological characterization of a clonal cell (H9c2) line from rat heart. *Circ Res*. 69(6): 1476-1486.

Hidalgo, C; Hudson, B; Bogomolovas, J; Zhu, Y; Anderson, B; Greaser, M; Labeit, S and Granzier, H. (2009) PKC Phosphorylation of Titin's PEVK Element: A Novel and Conserved Pathway for Modulating Myocardial Stiffness. *Circ Res*. 105:631-638.

Hilal-Dandan R., Urasawa K. and Brunton L.L. (1992) Endothelin inhibits adenylate cyclise and stimulates phosphoinositide hydrolysis in adult cardiac myocytes. *J. Biol Chem.* 267(15):10620-10624.

Hilfiker-Kleiner D., Hilfiker A., Castellazzi M., Wollert K.C., Trautwein C., Schunkert H. and Drexler H. (2006) JunD attenuates phenylephrine-mediated cardiomyocytes hypertrophy by negatively regulating AP-1 transcriptional activity. *Cardiovasc. Res.* 71:108-117.

Hilfiker-Kleiner D., Hilfiker A., Kaminski K., Schaefer A., Park J.K., Michel K., Quint A., Yaniv M., Weitzman J.B. and Drexler H. (2005) Lack of JunD promotes pressure overload-induced apoptosis, hypertrophic growth and angiogenesis in the heart. *Circulation.* 112: 1470-1477.

Hilgers, R.H and Webb, R. C. (2005) Molecular aspects of arterial smooth muscle contraction: focus on Rho. *Exp Biol Med (Maywood)*. 230(11):829-835.

Hill C.S., Wynne J. and Treisman R. (1995) The Rho family GTPases RhoA, Rac1 and CDC42Hs regulate transcriptional activation by SRF. *Cell.* 81(7):1159-1170.

Hock, B.M and Kralli, A. (2009) Transcriptional Control of Mitochondrial Biogenesis and Function. *Annu Rev Physiol*. 71:177-203.

Homey, C. J. (1998) Signaling hypertrophy: how many switches, how many wires. *Circulation*. 97:1890-1892.

Horowits R. (2006) Nebulin regulation of actin filament lengths: new angles. *Trends Cell Biol.* 16: 121-124.

Hoshijima, M. (2006) Mechanical stress-strain sensors embedded in cardiac cytoskeleton: Z disk, titin, and associated structures. *Am J Physiol Heart Circ Physiol*. 290:H1313-H1325.

Huang, C; Jacobson, K and Schaller, M.D. (2004) MAP kinases and cell migration. *J Cell Sci*. 117(20):4619-4628.

Inserte, J; Garcia-Dorao, D; Ruiz-Meana, M; Solares, J and Solar,J. (1997) The Role of Na+/H+ Exchange Occurring During Hypoxia in the Genesis of Reoxygenation-induced Myocardial Oedema *J Mol Cell Cardiol* 29, 1167–1175.

Inserte, J; Garcia-Dorao, D; Ruiz-Meana, M; Padilla, F; Barrabes, J.A; Pina, P; Agullo, L; Piper, H.M and Soler-Soler, J. (2002) Effect of inhibition of Na^{+}/Ca^{2+} exchanger at the time of myocardial reperfusion on hypercontracture and cell death. *Cardio Res*. 55:739-748.

Iyer, D; Chang, D; Marx, J; Wei, L; Olsen, E.N; Parmacek, M.S; Balasubramanyam, A and Schwartz, R.J. (2006) Serum response factor MADS box serine-162 phosphorylation switches proliferation and myogenic gene programs. *Proc Natl Acad Sci U S A*. 103(12):4516-4521.

Jacobs L., Nawrot T.S., de Geus B., Meeusen R., Degraeuwe B., Bernard A., Sughis M., Nemery B. and Panis L.I. (2010) Subclinical responses in healthy cyclists briefly exposed to traffic related air pollution. *Environ Health.* 9:64.

Janknecht R., Ernst W.H., Pingoud V. and Nordheim A. (1993) Activation of ternary complex factor ELK-1 by MAP kinases. *EMBO J.* 12(13):5097-5104.

Jankecht R. and Nordheim (1993) Gene regulation by Ets proteins. *Biochem Biophys Acta.* 1155(3):346-356. Review

Jennings, R. B. (2013) Historical Perspective on the Pathology of Myocardial Ischemia/Reperfusion Injury. *Circ Res*. 113:428-438.

Jennings, R; Reimer, R.K and Steenbergen, C.J. (1986) Myocardial Ischaemia revisited. The osmolar load,membrane damage and reperfusion *J. Mol. Cel Cardiol.*,18:769-780

Jennings, R.B; Hawkins, HK; Lowe, J.E. (1978) Relation between high energy phosphate and lethal injury in myocardial ischaemia in the dog. *Am J Pathol,*92:187

Jennings, R; Schaper, J; Hill, M; Steenbergen, C.J and Reimer, K. (1985) Effect of reperfusion late in the phase of reversible ischaemic injury. Changes in cell volume, electrolytes, metabolites and ultrastructure. *Circ. Res.*56:262-278.

Jennings, R.B. and Reimer, K.A. (1991) The Cell Biology of acute Myocardial Ischaemia. *Annual Review of Medicine,* 42: 225-246.

Johnson G.L and Lapadat R. (2002) Mitogen activated protein kinase pathway mediated by ERK, JNK and p38 protein kinases. *Science.* 298:1911-1912.

Johnson S.A. and Hunter T. (2005) Kinomics: methods for deciphering the kinome. *Nat Methods.*2(1): 17-25.

Jiang, Y; Gram, H; Zhao, M; New, L; Feng, L; DiPadova,F;Ulevitch, R.J and Han, J. (1996) Characterization of the structure and function of the fourth member of p38 group mitogen-activated protein kinases,p38δ. *J Biol. Chem.* 272: 30122-30128.

Jin, W; Goldfine, A.B; Boes, T; Henry, R.R; Ciaraldi, T.P; Kim, E; Emecan, M; Fitzpatrick, C; Sen, A; Shah, A; Mun, E, Vokes, M; Schroeder, J; Tatro, E; Jimenez-Chillaron, J and Patti, M. (2011) Increased SRF transcriptional activity in human and mouse skeletal muscle is a signature of insulin resistance. *J Clin Invest*. 121(3):918-929.

Jolly S.R., Kane W.J., Ballie M.B., Abrams G.D. and Lucchesi B.R. (1984) Canine myocardial reperfusion injury, its reduction by the combined administration of superoxide dismutase and catalase. *Circ. Res.* 54(3):277-285.

Jolly S.R., Kane W.J., Hook B.G., Abrams G.D., Kunkel S.L. and Lucchesi B.R. (1986) Reductiom of myocardial infarct size by neutrophil depletion: effect of duration of occlusion. *J Am Heart.* 112 (4):682-690.

Jordan J.E., Thourani V.H., Auchampach J.A., Robinson J.A., Wang N.P. and Vinten-Johansen J. (1999) A3 adenosine receptor activation attenuates neutrophile function and neutrophil-mediated reperfusion injury. *Am. J of Physiol.* 277(5): H1895-H1905.

Jordan J.E., Zhao Z.Q. and Vinten-Johnson J. (1999) The role of neutrophils in myocardial ischaemia-reperfusion injury. *Cardiovascular Research.* 43(4):860-878.

Kadrmas, J. L and Beckerle, M. C. (2004) The LIM domain: from the cytoskeleton to the nucleus. *Nat Rev Mol Cell Biol*. 5(11):920-31.

Kai H., Muraishi A., Sugiu Y., Nishi H., Seki Y., Kuwahara F., Kimura A., Kato H. and Imaizumi T. (1998) Expression of proto-oncogenes and gene mutation of sarcomeric proteins in patients with hypertrophic cardiomyopathy. *Circ Res.* 83:594-601.

Kaminski K.A., Bonda T.A., Korecki J. and Musial W.J. (2002) Oxidative stress and neutrophil activation two keystones of ischaemia/reperfusion injury. *Int J Cardiol.* 86(1):41-59.

Kamisago, M; Sharma, S.D; DePalma, S.R; Solomon, S; Sharma, P; McDonough, B; Smoot, L; Mullen, M.P; Woolf, P.K; Wigle, E.D; Seidman, J.G and Seidman, C.E. (2000) Mutations in sarcomere protein genes as a cause of dilated cardiomyopathy. *N Engl J Med*. 343(23):1688-1696.

Kang, P. M; Haunstetter, A; Aoki, H; Usheva, A and Izumo, S. (2000) Morphological and molecular characterization of adult cardiomyocyte apoptosis during hypoxia and reoxygenation. *Circ. Res.* 87:118-125.

Kaplan, E.L. (2005) Pathogenesis of acute rheumatic fever and rheumatic heart disease: evasive after half a century of clinical, epidemiological, and laboratory investigation. *Heart*. 91:3-4.

Katsch, K; de Jong, S.J; Albrecht, J.C; Steger, J; Genth, H; Posern, G and Biesinger, B. (2012) Actin-dependent activation of serum response factor in T cells by the viral oncoprotein tip. *Cell Commun Signal*. 10(1):5.

Kaunas, R; Usami, S and Chien, S. (2006) Regulation of stretch-induced JNK activation by stress fiber orientation. *Cellular Signalling*. 18:1924-1931.

Kaur S., Kumar D., Grover A., Khanduja K.L., Kaplan E.L., Gray E.D. and Ganguly N.K. (1998) Ethnic differences in expression of susceptibility marker(s) in rheumatic fever/rheumatic heart disease patients. *Intl. J Cardiol.* Vol 64 (1): 9-14.

Kayali A.G., Austin D.A. and Webster N.J. (2000) Stimulation of MAPK cascades by insulin and osmotic shock: lack of an involvement of p38 mitogen-activated protein kinase in glucose transport in 3T3-L1 adipocytes. *Diabetes.* 49(11):1783-1793.

Kee H.J. and Kook H. (2011) Roles and targets of class I and IIa histone deacetylases in cardiac hypertrophy. *J Biomed Biotechnol.* 928326, doi:10.1155/2011/928326. Epub 2010 Nov 29 Review.

Keesler G.A., Bray J., Junt J., Johnson D.A., Gleason T., Yao Z., Wang S.W., Parker C., Yamane H., Cole C. and Lichenstein H.S. (1998) Purification and activation of recombinant p38 isoforms alpha,beta,gamma and delta. *Protein Expr Purif.* 14(2):221-228.

Kelly, D. P and Scarpulla, R.C. (2004) Transcriptional regulatory circuits controlling mitochondrial biogenesis and function. G*enes Dev*. 18:357-368.

Kensler R.W., Shaffer J.F. and Harris S.P. (2011) Binding of the N-terminal fragment CO-C2 of cardiac MyBP-C to cardiac F-actin. *J Struct Biol.* 174(1): 44-51.

Keren, A; Tamir, Y and Bengal, E. (2006) The p38 MAPK signaling pathway: A major regulator of skeletal muscle development. *Mol Cell Endocrinol*. 252(1-2):224-230.

Kerkela, R and Force, T. (2006) p38 mitogen-activated protein kinase: a future target for failure therapy? *J. Am. Coll. Cardiol.* 48: 556-558.

Kerkela, R and Force, T. (2006) Recent Insights into Cardiac Hypertrophy and Left Ventricular Remodeling. *Curr Heart Fail Rep*. 3: 14-18.

Kerr, J.F; Wyllie, G and Currie, A.R. (1972) Apoptosis: a basic biological phenonmenon with wide-ranging implication in tissue kinetics. *Br. J. Cancer*. 26:239-257.

Keshari R.S., Verma A., Barthwal M.K. and Dikshit M. (2013) Reactive oxygen species-induced activation of ERK and p38 MAPK mediates PMA-induced NETs release from human neutrophils. *J Cell Biochem.* 114(3):532-540.

Keyse, S.M. (2000) Protein phosphatases and the regulation of mitogen-activated protein kinase signalling. *Curr Opin Cell BiolI.* 12(2):186-192.

Kho, A.L; Perera, S; Alexandrovich, A and Gautel, M. (2012) The sarcomeric cytoskeleton as a target for pharmacological intervention. *Curr Opin Pharmacol*. 12(3):347-354.

Klatsky A.L., Armstrong M.A., Poggi J. (2000) Risk of pulmonary embolism and/or deep venous thrombosis in Asian-Americans. *Am. J. Cardiol.* 85: 1334-1337.

Kloner, R.A. (1993) Does Reperfusion Injury Exist in Humans? *J Am Coll Cardiol*. 21(2):537-545.

Kniffin W.D., Baron J.A., Barrett J., Birkmeyer J.D., Anderson F.A. Jr. (1994) The Epidemiology of Diagnosed Pulmonary Embolism and Deep Venous Thrombosis in the Elderly. *Arch. Intern Med.* 154(8):861-866.

Knight, R.J and Buxton, D.B. (1996) Stimulation of c-Jun kinase and mitogen-activated protein kinase by ischemia and reperfusion in the perfused rat heart. *Biochem Biophys Res Commun*. 218(1):83-88.

Knoll R., Buyandelger B., Lab M. (2011) The sarcomeric Z-disc and z-discopathies. *J. Biomed. Biotechnol.* 2011:569628.

Knoll R., Hoshijima M., Hoffman H. M., Person V., Lorenzen-Schmidt I., Bang M. L., Hayashi T., Shiga N., Yasukawa H., Schaper W., McKenna W., Yokoyama M., Schrock N. J., Omens J. H., McCulloch A. D., Kimura A., Gregorio C. C., Poller W., Schaper J., Schultheiss H. P., Chien K. R. (2002) The cardiac mechanical stretch sensor machinery involves a Z disc complex that is defective in a subset of human dilated cardiomyopathy. *Cell* 111(7): 943-955.

Knoll R., Kostin S., Klede S., Savvatis K., Klinge L., Stehle I., Gunkel S., Kotter S., Babicz K., Sohns M., Miocic S., Didie M., Knoll G., Zimmermann W. H., Thelen P., Bickeboller H., Maier L. S., Schaper W., Schaper J., Kraft T., Tschope C., Linke W. A., Chien K. R. (2010) A common MLP (muscle LIM protein) variant is associated with cardiomyopathy. *Circ. Res.* 106:695-704.

Knutti, D and Kralli, A. (2001) PGC-1, a versatile coactivator. *Trends Endocrinol Metab*. 12(8):360-365.

Knutti, D; Kressler, D and Kralli, A. (2001) Regulation of the transcriptional coactivator PGC-1 via MAPK-sensitive interaction with a repressor. *Proc Natl Acad Sci U S A*. 98(17):9713-9718.

Kobayashi, S; Mao, K; Zheng, H; Wang, X; Patterson, C; O'Connell, T.D and Liang, Q. (2007) Diminished GATA4 Protein Levels Contribute to Hyperglycemia-induced Cardiomyocyte Injury. *J Biol Chem*. 282(30):21945-21952.

Koekemoer, A.L; Chong, N.W; Goodall, A.H and Samani, N.J (2009) Myocyte stress 1 plays an important role in cellular hypertrophy and protection against apoptosis. *FEBS Lett*. 583: 2964-2967.

Komuro, I and Yazaki, Y. (1994) Intracellular Signaling Pathways in Cardiac Myocytes Induced by Mechanical Stress. *Trends Cardiovasc Med.* 4(3):117-121.

Kong Y., Flick M. J., Kudla A. J. and Konieczny S.F. (1997) Muscle LIM protein promotes myogenesis by enhancing the activity of MyoD. *Mol. Cell. Biol.* 17:4750-4760.

Kramer, H.F and Goodyear, L.J. (2007) Exercise, MAPK, and NF-κB signaling in skeletal muscle. *J Appl Physiol*. 103:388-395.

Krijnen, P.A., Nijimeijer, R., Meijer, C.J., Visser, C.A., Hack, C.E. and Niessen H.W. (2002) Apoptosis in myocardial ischaemia and infarction. *Int. J Pathol.* 55(11): 801-811.

Krüger M. and Linke W.A (2009) Titin-based mechanical signalling in normal and failing myocardium. *J Mol Cell Cardiol.* 46(4):490-498, Review.

Krüger, M and Linke, W.A. (2011) The Giant Protein Titin: A Regulatory Node That Integrates Myocyte Signaling Pathways. *J Biol Chem*. 286(12): 9905-9912.

Kucher N. (2011) Deep-Vein Thromosis of the Upper Extremities. *N Engl. J. Med.* 364: 861- 869.

Kuwahara, K; Barrientos, T; Pipes, G.C.T; Li, S and Olson, E.N. (2005) Muscle-Specific Signaling Mechanism That Links Actin Dynamics to Serum Response Factor. *Mol. Cell. Biol.*, 25(8): 3173-3181.

Kuwahara K., Teg Pipes, G.C., McAnally J., Richardson J.A., Hill J.A., Bassel-Duby, R and Olson, E.N (2007) Modulation of adverse cardiac remodeling by STARS, a mediator of MEF2 signaling and SRF activity. *J Clin Invest*. 117(5): 1324-1334.

Kyriakis J.M and Avruch J. (1996) Sounding the Alarm:Protein Kinase Cascades Activated by Stress and Inflammation. *J. Bio. And Chem. Rev.* 271, 24313-24316.

Kyriakis J.M and Avruch J. (2001) Mammalian Mitogen-Activated Protein Kinase Signal Transduction Pathways Activated by Stress and Inflammation. *Physiol Rev*. 81(2):807-869.

Kyriakis J.M., Brautigan D., Ingebritsen T. And Avruch J. (1991) pp54 microtubule-associated protein-2 kinase requires both tyrosin and serine/Threonine phosphorylation for activity. *J Biol Chem.* 266:10043-10046.

Kyrle P. and Eichinger P. (2005) Deep Vein Thrombosis. *Lancet.* 365(9465): 1163-1174.

Labeit S., Gautel M., Lakey A. and Trinick J. (1992) Towards a molecular understanding of titin. *EMBO J.* 11(5):1711-1716.

Labeit S., Kohl C.H., Witt C.C., Labeit D., Jung J. and Granzier H. (2010) Modulation of muscle atrophy, fatigue and MLC phosphorylation by MURF1 as indicated by hindlimb suspension studies on MuRF1-KO mice. *J Biomed Biotechnol.* 2010:693741.

Labeit S. and Kolmerer B. (1995) Titins: giant proteins in charge of muscle ultrastructure and elasticity. *Science.* 270(5234): 293-296.

Labeit S. and Kolmerer B. (1995) The complete primary structure of human nebulin and its correlation to muscle structure. *J Mol Biol.* 248(2):308-315.

Labeit S., Ottenheijm A.C. and Granzier H. (2011) Nebulin, a major player in muscle health and disease *FASEB J.* 25(3):822-829.

Laderoute K.R. and Webster K.A. (1997) Hypoxia/reoxygenation stimulates jun kinase activity through redox signalling in cardiac myocytes. *Circ Res.* 80: 336-344.

Lamon, S; Wallace, M.A; Leger, B and Aaron, P.R. (2009) Regulation of STARS and its downstream targets suggest a novel pathway involved in human skeletal muscle hypertrophy and atrophy. *J Physiol*. 587(8):1795-1803.

Lamon, S; Wallace, M.A; Stefanetti, R. J; Rahbek, S. K; Vendelbo, M. H; Russel, A. P and Vissing, K. (2013) Regulation of the STARS signalling pathway in response to endurance and resistance exercise and training. *Pflu*g*ers Arch.*

Lamon S., Wallace M.A and Russell A. (2014) The STARS signalling pathway: a key regulator of skeletal function. *Pflu*g*ers Arch.*

Lange, S; Ehler, E and Gautel, M. (2006) From A to Z and back? Multicompartment proteins in the sarcomere. *Trends Cell Biol*. 16(1):11-18.

Lanna, A; Henson, S.M; Escors, D and Akbar, A.N. (2014) The kinase p38 activated by the metabolic regulator AMPK and scaffold TAB1 drives the senescence of human T cells. *Nat Immunol*. 15(10):965-972.

Lazou, A; Sugden, P. H and Clerk, A. (1998) Activation of mitogen-activated protein kinases (p38-MAPKs, SAPKs/JNKs and ERKs) by the G-protein-coupled receptor agonist phenylephrine in the perfused rat heart. 1;332 (Pt 2):459-65.

Lee R.E. and Megeney L.A. (2005) The yeast kinome displays scale free topology with functional hub clusters. *BMC Bioinformatics.* 6:271.

Lee, S; Vasishtha, M and Prywes, R. (2010) Activation and repression of Cellular Immediate Early Genes by Serum Response Factor Cofactors. *J Biol Chem*. 285:22036-22049.

Leger B., Cartoni R., Praz M., Lamon S., Deriaz O., Crettenand A., Gobelet C., Rohmer P., Konzelmann M., Luthi F. and Russell A.P. (2006) Akt signalling through GSK-3beta, mTOR and FOXO1 is involved in human skeletal muscle hypertrophy and atrophy. *J Physiol.* 576(Pt3):923-933.

Leger B., Derave W., De Bock K., Hespel P. and Russell A.P. (2008) Human sarcopenia reveals an increase in SOC-3 and myostatin and a reduced efficiency of Akt phosphorylation. *Rejuvenation Res.* 11(1):163-175.

Leone, T.C and Kelly, D.P. (2011) Transcriptional control of cardiac fuel metabolism and mitochondrial function. *Cold Spring Harb Symp Quant Biol*. 76:175-182.

Levy D., Garrison R.J., Savage D.D., Kannel W.B. and Castelli W.P. (1990) Prognostic implications of echocardiographically determined left ventriucular mass in the Framingham Heart Study. *J of Med.* 322:1561-1566.

Levy D., Labib S.B., Anderson K.M., Christiansen J.C., Kannel W.B. and Castelli W.P. (1990) Determinants of sensitivity and specificity of electrocardiographic criteria of left ventricular hypertrophy. *Circulation.* 81(3):815-820.

LeWinter M. A. and Granzier H. Cardiac (2010) Titin: A multifunctional giant. *Cardio. Med.* 12:2137-2145

L'honore, A; Rana, V; Arsic, N; Franckhauser, C; Lamb, N.J and Fernandez, A. (2007) Identification of a new hybrid serum response factor and myocyte enhancer factor 2-binding element in MyoD enhancer required for MyoD expression during myogenesis. *Mol Biol Cell*. 18(6):1992-2001.

Li G.. Ali I.S and Currie R.W. Insulin induced myocardial protection in isolated ischaemic rat hearts requires p38 MAPK phosphorylation of Hsp27. *Am J of Physiol.* 294(1):H74-H87.

Liang, Q; De Windt, L.J; Witt, S.A; Kimball, T.R; Markham, B.E and Molkentin, J.D. (2001) The Transcription Factors GATA4 and GATA6 Regulate Cardiomyocyte Hypertrophy *in Vitro* and *in Vivo*. *J Biol Chem*. 276:30245-30253.

Liang Q. And Molkentin J.D. (2003) Redefining the role of p38 and JNK signalling in cardiac hypertrophy: dichotomy between cultured myocytes and animal models. *J Mol Cell Cardiol.* 35(12): 1385-1394. Review.

Lifton, R.P. (2007) Lasker Award to heart valve pioneer. *Cell*. 130(6):971-974.

Linke, W.A and Kruger, M. (2010) The Giant Protein Titin as an Interogator of Myocyte Signaling Pathways. *Physiology*. 25:186-198.

Liu, S; Sun, J.P; Zhou, B and Zhang, Z.Y. (2006) Structural basis of docking interactions between ERK2 and MAP kinase phosphatase 3. *Proc Natl Acad Sci U S A*. 103(14):5326-5331.

Lodish H., Berk A. and Zipursky S.L. (2000) Actin and myosin in nonmuscle cells . *W.H. Freeman* (Ed). Molecular cell biology.

Lopez-Carmarillo C., Ocampo E.A; Casamichana, M.L; Pérez-Plasencia, C; Álvarez-Sánchez, E and Marchat, L.A. (2012) Protein kinases and transcription factors activation in response to UV-radiation of skin: implications for carcinogenesis. *Int J Mol Sci*. 13(1):142-172.

Louis H. A., Pino J. D., Schmeichel K. L., Pomies P., Beckerle M. C., (1997) Comparison of three members of cysteine-rich protein family reveals functional conservation and divergent patterns of gene expression. *J. Biol. Chem.* 272(43):27484-27891.

Lu J., Landerholm T.E., Wei J.S., Dong X.R., Wu S.P., Liu X., Nagata K., Inagaki M. and Majesky M.W. (2001) Coronary smooth muscle differentiation from proepicardial cells requires rhoA-mediated actin reorganization and p160 rho-kinase activity. *Dev. Biol.* 240:404-418.

Luther P.K . and Craig R. (2011) Modulation of striated muscle contraction by binding of myosin binding protein C to actin. *Bioarchitecture.* 1(6): 277-283.

MacKenzie S.J., Baillie G.S., McPhee I., Bolger G.B. and Houslay M.D. (2000) ERK2 mitogen-activated protein kinase binding phosphorylation and regulation of the PDE4D cAMP-specific phosphodiesterases. *J Biol Chem.* 275:16609-16617.

MacNeil. L.G., Melov S., Hubbard A.E., Baker S.K. and Tampolsky M.A. (2010) Eccentric exercise activates novel transcriptional regulation of hypertrophic signalling pathways not affected by hormone changes. *PLoS ONE.* 5:e10695 10.1371/journal.pone.0010695.

Mahadeva, H; Brooks, G; Lodiwck, D; Chong, N.W and Samani, N.J. (2002) ms1, a novel stress-responsive, muscle-specific gene that is up-regulated in the early stages of pressure overload-induced left ventricular hypertrophy. *FEBS Letters*, 521: 100-104.

Maillet, M; van Berlo, J. H and Molkentin, J. D. (2013) Molecular basis of physiological heart growth: fundamental concepts and new players. *Nat Rev Mol Cell Biol*. 14(1):38-48.

Malliopoulou, V., Xinaris C., Mourouzis I., Cokkinos A.D., Katsilambros N., Pantos C., Kardami E, Cokkinos DV.High glucose protects embryonic cardiac cells against simulated ischemia. *Mol Cell Biochem*. 284(1-2):87-93.

Manhankali M., Peng H. J., Cox D., and Gomez-Cambronero J. (2011) The mechanism of cell membrance ruffling relies on a phospholipase D2(PLD2), Grb2 and Rac2 association. *Cell Signal.* 23(8): 1291-1298.

Manning G., Whyte D.B., Martinez R., Hunter T. and Sudarsanam S. (2002) The protein kinase complement of the human genome. *Science.* 298:1912-1934.

Marion A.J., Senthil V., Chen S.N and Lombardi R. (2006) Antifibrotic effects of antioxidant N-acetylcysteine in a mouse model of human hypertrophic cardiomyopathy mutation. *J Am. Coll. Cardiol.* 47:827-834.

Maron, B.J and Maron, M.S. (2013) Hypertrophic cardiomyopathy. *Lancet*. 381:242-255.

Martindale J.J., Wall J.A., Martinez-longoria D.M., Aryal P., Rockman H.A., Guo Y., Bolli R. and Glembotski C.C. (2005) Overexpression of mitogen-activated protein kinase kinase 6 in the heart improves functional recovery from ischaemia in vitro and protects against myocardial infarction in vivo. *J Biol Chem.* 280(1):669-676.

Martineau, L.C and Gardiner, P.F. (2001) Insight into skeletal muscle mechanotransduction: MAPK activation is quantitatively related to tension. *J Appl Physiol*. 91:693-702.

Maruyama K., Kimura S., Yamamoto K., Wakabayashi T. and Suzuki T. (1985) Connectin causes aggregation of myosin rods but not myosin heads. *Biomed Res.* 6:423-427.

Maxwell, L and Gavin J.B. (1991) The role of post-ischaemic reperfusion in the development of microvascular incompetence and ultrastructural damage in the myocardium. *Basic. Res. Cardiol.* 86: 544-553.

Maxwell, S.R.J; and Lip, G.Y.N. (1997) Reperfusion injury: a review of the pathophysiology, clinical manifestations and therapeutic options. *J. Cardiol.* 58: 95-117

Maxwell, S.R.J; and Lip, G.Y.N. (1997) Free Radicals and antioxidants in cardiovascular disease. *Br. J Clin Pharmacol.* 44(4): 307-317.

McCain, M.L and Parker, K.K. (2011) Mechanotransduction: the role of mechanical stress, myocyte shape, and cytoskeletal architecture on cardiac function. *Pflugers Arch*. 462(1):89-104.

McCord J.M. (1985) Oxygen-derived free radicals in post-ischaemic tissue injury. *N Engl J* Med. 312, 159-163.

McElhinny A.S., Kolmerer B., Fowler V.M., Labeit S. and Gregorio C.C. (2001) The N-terminal end of nebulin interacts with tropomodulin at the pointed ends of the titin filaments. *J. Biol. Chem.* 276: 583-592.

McMullen J.R., Amirahmadi F., Woodcock E.A., Schinke-Braun M., Bouwman R.D., Hewitt K.A., Mollica J.P., Zhang L., Zhang Y., Shioi T., Buerger A., Izumo S., Jay P.Y. and Jennings G.L. (2007) Protective effects of exercise and phosphoinositide 3-kinase (p110 alpha) signalling in dilated and hypertriphic cardiomyopathy. *Proc. Natl Acad. Sci USA.* 104(2):612-617.

McMullen J.R. and Izumo S. (2006) Role of the insulin-like growth factor 1 (IGF1)/ phosphoinositide-3-kinase (PI3K) pathway mediating physiological cardiac hypertrophy. *Novartis Found Symp.* 274: 90-111.

McMullen, J.R and Jennings, G.L. (2007) Differences between pathological and physiological cardiac hypertrophy: Novel therapeutic strategies to treat heart failure. *Clin Exp Pharmacol Physiol*. 34(4):255-262.

McMullen J.R., Sherwood M.C., Tarnavski O., Zhang L., Dorfman A.L., Shioi T. And Izumo S. (2004) Inhibition of mTOR signalling with rapamycin regresses established cardiac hypertrophy induced by pressure overload. *Circulation.* 109(24): 3050- 3055.

McMullen J.R., Shioi T., Zhang L., Tarnavski O., Sherwood M.C., Kang P.M and Izumo S. (2003) Phosphoinositide-3-kinase (p110 alpha) plays a critical role for the induction of physiological, but not pathological cardiac hypertrophy. *Proc. Natl Acad Sci. U.S.A.* 100(21):12355-12360.

Meldrum D.R., Dinarello C.A., Cleveland J.C., Cain B.S., Shames B.D., Meng X. and Harken A.H. (1998) Hydrogen peroxide induces tumpr necrosis factor alpha-mediated cardiac injury by a p38 mitogen-activated protein kinase dependent mechanism. *Surgeon.* 124(2):291-297.

Menown I.B and Adgey A.A. (2001) Cardioprotective therapy and sodium-hydrogen exchange inhibition: current concepts and future goals. *J Am Coll Cardiol.* 38(6):1651-1653.

Mewton, N; Ivanes, F; Cour, M and Ovize, M. (2010) Postconditioning: from experimental proof to clinical concept. *Dis Model Mech*. 3(1-2):39-44.

Meyer, L.C and Wright, N.T. (2013) Structure of giant muscle proteins. *Front Physiol*. 4:368.

Miano, J.M. (2010) Role of serum response factor in the pathogenesis of disease. *Lab Invest*. 90(9):1274-1284.

Miano J.M. (2003) Serum response factor:toggling between disparate programs of gene expression. *J Mol Cell Cardiol.* 35(6):577-593. Review.

Miano, J.M; Long, X and Fujiwara, K. (2007) Serum response factor: master regulator of the actin cytoskeleton and contractile apparatus. *Am J Physiol Cell Physiol*. 292:C70-C81.

Miano J.M., Ramanan N., Georger M.A., de Mesy Bently K.L., Emerson R.L., Balza R.O., Xiao Q., Weiler H., Ginty D.D. and Misra R.P. (2004) Restricted inactivation of serum response factor to the cardiovascular system. *Proc. Natl. Acad Sci U.S.A.* 101(49):17132-17137.

Michelsen J.W., Sewell A.K., Louis H.A., Olsen J.L., Davis D.R., Winge D.R. and Beckerle M.C. (1994) Mutational analysis of the metal sites in an LIM domain. *J Biol Chem.* 269(15):11108-11113.

Mikhailov, A.T and Torrado, M. (2012) In Search of Novel Targets for Heart Disease: Myocardin and Myocardin-Rekated Transcriptional Cofactors. *Biochem Res Int*. 2012:973723.

Milano G., Morel S., Bonny C., Samaja M., Von Segesser L.K., Nicod P. and Vassalli G. (2007) A peptide inhibitor of c-Jun NH2-terminal kinase reduces myocardial ischaemia-reperfusion injury and infarct size in vivo. *Am J Physiol Heart Circ Physiol.* 292(4):H1828-1835.

Minamino T., Yujuri T., terada N., Taffet G., Michael L., Johnson G. and Schneider M. (2002) MEKK1 is essential for cardiac hypertrophy and dysfunction induced by Gq. *Proc. Natl. Acad. Sci U.S.A.* 99: 3866-3871.

Minden A., Lin A., Claret F.X., Abo A. and Karin M. (1995) Selective activation of the JNK signalling cascades and c-jun transcriptional activity by the small GTPases Rac and Cdc42Hs. *Cell.* 81(7):1147-1157.

Miralles, F; Posern, G; Zaromytidou, A.L and Treisman, R. (2003) Actin Dynamics Control SRF Activity by Regulation of Its Coactivator MAL. *Cell*. 113:329-342.

Miyamoto T., Takeishi Y., Takahashi H., Shishido T., Arimoto T., Tomoike H. and Kubota .I. (2004) Activation of distinct signal transduction pathways in hypertrophied hearts by pressure and colume overload. *Basic Res. Cardiol.* 99:328-337.

Mohinder, N.S and Belgrave,R. (2004) Regulation of Ca^{2+} homeostasis by glucose metabolism in rat brain. *J. Mol. And Cell Bio.*176, 317-326.

Mocanu M.M., Baxter G.F., Yue Y., Critz S.D. and Yellon D.M. (2000) The p38 MAPK inhibitor SB203580, abrogates ischaemic preconditioning in rat heart but timing of administration is critical. *Basic Res. Cardiol.* 95: 472-478.

Molkentin, J. D. (2000) The zinc finger-containing transcription factors GATA-4, -5 and -6. Ubiquitously expressed regulators of tissue-specific gene expression. *J, Biol, Chem*. 275: 38949-38952.

Molkentin J. D. (2004) Calcineurin-NFAT signalling regulates the cardiac hypertrophic response in coordination with the MAPKs. *Cardiovasc. Res.* 63:467-475.

Molkentin, J. D. and Dorn, G. W. (2001) cytoplasmic signalling pathways that regulate cardiac hypertrophy. *Annu. Rev Physiol.* 63: 391-426.

Molkentin, J.D., Lu, J.R; Antos, C.L; Markham, B; Richardson, J; Robbins, J; Grant, S.R and Olson, E.N. (1998) A Calcineurin-Dependent Transcriptional Pathway for Cardiac Hypertrophy. *Cell*. 93:215-228.

Monzen, K; Shiojima, I; Hiroi, Y; Kudoh, S; Oka, T; Takimoto, E; Hayashi, D; Hosoda, T; Habara-Ohkubo, A; Nakaoka, T; Fujita, T; Yazaki, Y and Komuro, I. (1999) Bone morphogenetic proteins induce cardiomyocyte differentiationthrough the mitogen-activated protein kinase kinase kinase TAK1 andcardiac transcription factors Csx/Nkx-2.5 and GATA-4. *Mol Cell Biol*. 19(10):7096-7105.

Moore, M.L; Wang, G; Belaguli, N.S; Schwartz, R.J and McMillin, J.B. (2001) GATA-4 and Serum Response Factor Regulate Transcription of the Muscle-specific Carnitine Palmitoyltransferase I β in Rat Heart. *J Biol Chem*. 276:1026-1033.

Mootha, V.K; Handschin, C; Arlow, D; Xie, X; St Pierre, J; Sihag, S; Yang, W; Altshuler, D; Puigserver, P; Patterson, N; Willy, P.J; Schulman, I.G; Heyman, R.A; Lander, E.S and Spiegelman, B.M. (2004) Erralpha and Gabpa/b specify PGC-1alpha-dependent oxidative phosphorylation gene expression that is altered in diabetic muscle. *Proc Natl Acad Sci U S A*. 101(17):6570-6575.

Morimoto, S. (2008) Sarcomeric proteins and inherited cardiomyopathies. *Cardio Res*. 77:659-666.

Morrison D.K. and Davis R. (2003)Regulation of MAP kinase signalling module by scaffold proteins in mammals. *Annu Rev Cell Dev Biol.* 19:91-118.

Mudry R.E., Perry C.N., Richards M., Fowler V.M. and Gregorio C.C. (2003) The interaction of tropomodulin with tropomyosin stabilizes thin filaments in cardiac myocytes. *J. Cell Biol.* 162: 1057-1068.

Murai K and Treisman R. (2002) Interaction of the serum response factor (SRF) with the ELK-1 B box inhibits RhoA-actin signalling to SRF and potentiates transcriptional activation by Elk-1. *Mol. Cell. Biol.* 22:7083-7092.

Muslin, A.J. (2008) MAPK Signaling in Cardiovascular Health and Disease: Molecular Mechanisms and Therapeutic Targets. *Clin Sci (Lond)*. 115(7):203-218.

Myhre, J.L and Pilgrim, D.B. (2012) At the Start of the Sarcomere: A Previously Unrecognized Role for Myosin Chaperones and Associated Porteins during Early Myofibrillogenesis. *Biochem Res Int*. 2012:712315.

Nabel E. G. (2003) Cardiovascular Disease. *N. Engl. J. Med.* 349 (1): 60-72.

Naghavi M., Madjid M., Khan M.R., Mohammadi R.M., Willerson J.T. and Casscells S.W (2001) New developments in the detection of vulnerable plaque. *Curr. Atheroscler. Rep.* 3(2):125-135.

Nakamura K. and Johnson G. (2003) PB1 domains of MEKK2 and MEKK3 interact with the MEK5 PB1 domain for activation of the ERK5 pathway. *J Biol. Chem.* 278:36989-36992.

Narumiya S., Ishizaki T. and Watanabe N. (1997) Rho effectors and reorganization of actin cytoskeleton. *FEBS Lett.* 410:68-72.

Naya, F.J; Black, B.L; Wu, H; Bassel-Duby, R; Richardson, J.A; Hill, J.A and Olsen, E.N. (2002) Mitochondrial deficiency and cardiac sudden death in mice lacking the MEF2A transcription factor. *Nat.Med*. 8:1963-1973.

Neisch A.L., Speck O., Stronach B. and Fehon R.G. (2010) Rho1 regulates apoptosis via activation of the JNK signalling pathway at the plasma membrane. *J Cell Biol.* 189(2): 311-323.

Nemoto S., Sheng Z. And Lin A. (1998) Opposing effects of jun kinase and p38 mitogen-activated protein kinases on cardiomyocytes hypertrophy. *Mol Cell Biol.* 18: 3518-3526.

Nishimoto S. and Nishida E. (2006) MAPK signalling ERK5 versus ERK1/2. *EMBO*. 7: 782-786.

Niu, Z., Li, A., Zhang, S. X and Schwartz, R.J. (2007) Serum response factor micromanaging cardiogenesis. *Curr. Opin, Cell Biol*. 19: 618-627.

Niu Z., Yu W., Zhang S.X., Barron M., Melaguli N.S., Schneider M.D., Parmacek M., Nordheim A. and Schwartz R.J. (2005) Conditional mutagenesis of the murine serum response factor gene blocks cardiogenesis and the transcription of downstream gene targets. *J Biol Chem.* 280:32531-32538.

Nurrish, S.J and Treisman, R. (1995) DNA Binding Specificity Determinants in MADS-Box Transcription Factors. *Mol Cell Biol*. 15(8):4076-4085.

Oka, T; Maillet, M; Watt, A.J; Schwartz, R.J; Aronow, B.J; Duncan, S.A and Molkentin, J.D. (2006) Cardiac-Specific Deletion of *Gata4* Reveals Its Requirement for Hypertrophy Compensation, and Myocyte Viability. *Circ Res*. 98:837-845.

Olsen, E.N. (2006) Gene regulatory networks in the evolution and development of the heart. *Science*. 313: 1922-1927.

Olson E. N. and Nordheim A. (2010) Linking actin dynamics and gene transcription to drive cellular motile functions. *Nat. Rev. Mol. Cell Biol.* 11:353-365.

Ono K. and Han J. (2000) The p38 signal transduction pathway activation and function. *Cell Signal.* 12:1-13.

Ota, A; Zhang, J; Ping, P; Han, J and Wang, Y. (2010) Specific Regulation of Noncanonical p38α Activation by Hsp90-Cdc37 Chaperone Complex in Cardiomyocyte. *Circ Res*. 106:1404-1412.

Ottenheijm C.A. and Granzier H. (2010) New Insights into the structural roles of nebulin in skeletal muscle. *J Biomed Biotechnol.* 968139. Doi:10.1155/2010/968139.

Ottenheijm C.A. and Granzier H. (2010) Role of titin in skeletal muscle function and disease. *Adv. Exp Med Biol.* 682:105-122.

Ottenheijm C.A., Hooijman P., DeChene E.T., Stienen G.J., Beggs A.H. and Granzier H. (2010) Althered myofilament function depresses force generation in patients with nebulin-based nemaline myopathy (NEM). *J Struct. Biol.* 170(2):334-343.

Ounzain, S; Dacwag, C.S; Samani, N; Imbalzano, and Chong, N. (2008) Comparative *in silico* analysis identifies bona fide MyoD binding sites within the Myocyte Stress 1 gene promoter. *BMC Mol. Bio.* 1471:2199/9/50

Ounzain, S; Kobayashi, S; Peterson, R.E; He, A; Motterle, A; Samani, N.J; Menick, D. R; Pu, W. T; Liang, Q and Chong, N. W (2012) Cardiac expression of *ms1/STARS*, a novel gene involved in cardiac development and disease, is regulated by GATA4. *Mol, Cell, Biol*. 32: 1830-1843.

Owens, D.M and Keyse, S.M. (2007) Differential regulation of MAP kinase signalling by dual-specificity protein phosphatises. *Oncoge*n*e*. 26:3203-3213.

Panes J. And Granger D.N. (1998) Leukocyte-endothelial cell interactions: molecular mechanisms and implications in gastrointestinal disease. *Gastroenterology.*114: 1066-1090.

Panes J., Perry M. and Granger D.N. (1999) Leukocyte-endothelial cell adhesion: avenues for therapeutic intervention. *Br. J Pharmacol.* 126(3): 537-550.

Pappas C.T., Bhattacharya N., Cooper J.A. and Gregorio C.C. (2008) Nebulin interacts with CapZ and regulates thin filament architecture within the Z-disc. *Mol. Biol. Cell.* 19: 1837-1847.

Pappas C.T., Kreig P.A. and Gregorio C.C. (2010) Nebulin regulates actin filaments lengths by a stabilization mechanism. 189 (5):859.

Paradies, G; Petrosillo, G; Pistolese, M; Di Venosa, N; Serena, D and Ruggiero, F.M. (1999) Lipid peroxidation and alterations to oxidative metabolism in mitochondria isolated from rat heart subjected to ischemia and reperfusion. *Free Radic Biol Med*. 27(1-2):42-50.

Parlakpinar, H; Orum, M.H and Sagir, M. (2013) Pathophysiology of Myocardial Ischemia Reperfusion Injury: A Review. *Med Sci Rev*. 2(4):935-954.

Parmacek, M.S. (2007) Myocardin-Related Transcription Factors: Critical Coactivators Regulating Cardiovascular Development and Adaptation. *Circ Res*. 100:633-644.

Passier R., Zeng H., Frey N., Naya F.J., Nicol R.L., Mckinsey T.A., Overbeek P., Richardson J.A., Grant S.R. and Olson E.N. (2000) CaM kinase signalling induces cardiac hypertrophy and activates the MEF2 transcription factor in vivo. *J clin invest.* 105(10):1395-1406.

Patel R.K., Lambie J., Bonner L., Arya R. (2004) Venous thromboembolism in the black population. *Arch. Intern. Med.* 164: 1348-1349.

Peddy S.B., Vricella L.A., Crosson J.E., Oswald G.L., Cohn R.D., Cameron D.E., Valle D. and Loeys B.L. (2006) Infantile restrictive cardiomyopathy resulting from a mutation in the cardiac troponin T gene. *Pediatrics*. 117(5):1830-1833.

Peng, Y.B; Guan, H.P; Fan, B; Zhao, S.H; Xu, X.W; Li, K; Zhu, M. J; Yerle, M and Liu, B. (2008) Molecular characterization and expression pattern of the porcine STARS, a striated muscle-specific expressed gene. *Biochem* Ge*net*. 46: 644-651.

Petrich, B.G; Gong, X; Lerner, D.L; Wang, X; Brown, J.H; Saffitz, J.E and Wang, Y. (2002) c-Jun N-Terminal Kinase Activation Mediates Downregulation of Connexin43 in Cardiomyocytes. *Circ Res*. 91:640-647.

Petrich B.G. and Molkentin J.D. (2003) Temporal activation of c-Jun N-terminal kinase in adult transgenic heart via cre loxP-mediated DNA recombination. *FASEB J.* 02-0438fje.

Petrich B.G and Wang Y. (2004) Stress-activated MAP kinases un cardiac remodelling and heart failure new insights from transgenic studies. *Cardiovasc. Med.*14: 50-55.

Pierpont M.E., McGee G., Sable C.A., Srivastava D. and Webb C. (2007) Genetic basis for congenital heart defects: current knowledge. *Circulation.* 115: 3015-3038.

Ping P. and Murphy E. (2000) Role of p38 mitogen-activated kinases in preconditioning: a detrimental factor or a protective kinase? *Circulation Research.* 86(9):921-922.

Piper, H.M; Garcia-Dorado, D and Ovize, M. (1998) A Fresh Look at reperfusion Injury. Review. *Cardio. Res* 38: 291-300.

Pipes, G. C; Creemers, E. E and Olson, E.N. (2006) The myocardin family of transcriptional coactivators: versatile regulators of cell growth, migration, and myogenesis. Ge*nes Dev*. 20(12):1545-56.

Pipp F., Boehm S., Cai W.J., Adili F., Ziegler B., Karanovic G., Ritter R., Scheler C., Schaper W. and Schmitz-Rixen T. *Arterioscler Thromb Vasc. Biol.* 24(9):1664-`1668.

Pluim B.M., Zwinderman A.H., van der Laarse A. and van der Wall E.E. (2000) The athlete's heart. A meta-analysis of cardiac structure and function. 101(3):336-344.

Podrid, P.J; Ganz, L.I; Knight, B.P and Downey, B.C. 2014. Pathogenesis of ventricular tachycardia and ventricular fibrillation during acute myocardial infarction. UpToDate. Available at: http://www.uptodate.com/contents/pathogenesis-of-ventricular-

tachycardia-and-ventricular-fibrillation-during-acute-myocardial-infarction [July 15th ,2014].

Pollanen, E; Fey, V; Tormakangas, T; Ronkainen, P.H.A; Taaffe, D. R; Takala, T; Koskinen, S; Cheng, S; Puolakka, J; Kujala, U.M; Suominen, H; Sipila, S and Kovanen, V. (2010) Power training and postmenopausal hormone therapy affect transcriptional control of specific co-regulated gene clusters in skeletal muscle. *A*ge. 32:347-363.

Posern, G and Treisman, R. (2006) Actin' together: serum response factor, its cofactors and the link to signal transduction. *Trends Cell Biol*. 16(11):588-596.

Pulakanti, K; Pinello, L; Stelloh, C; Blinka, S; Allred, J; Milanovich, S; Kiblawi, S; Peterson, J; Wang, A; Yuan, G and Rao, S. (2013) Enhancer transcribed RNAs arise from hypomethylated, Tet-occupied genomic regions. *Epigenetics*. 8(12):1303-1320.

Qi M. and Elion E.A. (2005) MAP kinase pathways. *J Cell Sci*. 118:3569-3572.

Raingeaud J., Gupta S., Rogers J., Dickens M., Han J., Ulevitch R. and Davis R. (1995) Pro-inflammatory cytokines and environmental stress cause p38 mitogen-activated protein kinase transactivation by dual phosphorylation on tyrosine and theronine. *J Biol Chem.* 270: 7420-7426.

Raman M., Chen W. and Cobb M.H. (2007) Differential regulation and properties of MAPKs. Oncogene. 26: 3100-3112.

Ramos J.W. (2008) The regulation of extracellular signal-regulated kinase (ERK) in mammalian cells. *Int J Biochem Cell Biol.* 40: 2707-2719.

Raza, H and John, A. (2012) Streptozotocin-Induced Cytotoxicity, Oxidative Stress and Mitochondrial Dysfunction in Human Hepatoma HepG2 Cell. *Int J Mol Sci*. 13:5751-5767.

Reich S., Puckney L. H., Cheetham C. L., Harris R., Ali A. A., Bhattacharyya U., Maclagan K., Powell K. A., Prodromou C., Pearl L. H., Driscoll P. C. and Savva R.

(2006) Combinatorial Domain Hunting: An effective approach for the identification of soluble protein domains adaptable to high-throughput applications. Protein Sci. vol 15:2356-2365

Reimer, K.A and Ideker,R.E. (1987) Myocardial Ischaemia and Infarction: Anatomic and Biochemical Substrates for Ischaemic cell death and Ventricular Arrythmias. *Human Pathology*, vol. 18: 462-475.

Remenyi A., Good M., Bhayyacharyya R. and Lim W. (2005) The role of docking interaction in mediating signalling input, output and discrimination in the yeast MAPK network. *Mol. Cell.* 20:951-962.

Ridley A. J., Hall A. (1992) The small GTP-binding protein rho regulates the assembly of focal adhesions and actin stress fibers in response to growth factors. *Cell.* 70:389-399

Riccardi, C and Nicoletti, I. (2006) Analysis of apoptosis by propidium iodide staining and flow cytometry. *Nat. Protoc* 1(3):1458-1461.

Risco, A and Cuenda, A. (2011) New Insights into the p38γ and p38δ MAPK Pathways. *J Signal Transduct*. 2012:520289.

Roberts A., Allanson J., Jadico S.K., Kavamura M.I., Noonan J., Optiz J.M., Young T. and Neri G. (2006) The cardiofaciocutaneous syndrome. *J Med* G*enet.* 43:833-842.

Roberts, W.C and Ko, J.M. (2008) Some observations on mitral and aortic valve disease. *Proc (Bayl Univ Med Cent).* 21(3):282-299.

Roger, V.L; Go, A.S; Lloyd-Jones, D.M; Benjamin, E.J; Berry, J.D; Borden, W.B; Bravata, D.M; Dai, S; Ford, E.S; Fox, C.S; Fullerton, H.J; Gillespie, C; Hailpern, S.M; Heit, J.A; Howard, V.J; Kissela, B.M; Kittner, S.J; Lackland, D.T; Lichtman, J.H; Lisabeth, L.D; Makuc, D.M; Marcus, G.M; Marelli, A; Matchar, D.B; Moy, C.S; Mozaffarian, D; Mussolino, M.E; Nichol, G; Paynter, N.P; Soliman, E.Z; Sorlie, P.D; Sotoodehnia, N; Turan, T.N; Virani, S.S; Wong, N.D; Woo, D and Turner, M.B.

(2012) Heart disease and stroke statistics—2012 update: a report from the American Heart Association. *Circulation*. 125(1):e1002.

Rohilla, A; Kumar, P; Rohilla, S and Kushnoor, A. (2012) Cardiac Hypertrophy: A Review on Pathogenesis and Treatment. *Pharmacol Res*. 63(1):8-12.

Roof, D.J; Hayes, A; Adamian, M; Chishti, A.H and Li, T. (1997) Molecular Characterization of abLIM, a Novel Actin-binding and Double Zinc Finger Protein. *J Cell Biol*. 138(3):575-588.

Rose B. A., Force T., Wang Y. (2010) Mitogen-activated protein kinase signalling in the heart: angels versus demons in a heart-breaking tale. *Physiol. Rev.* 90: 1507-1546

Rouse J., Cohen P., Trigon S., Morange M., Alonso-Llamazares A., Zamanilo D., Hunt T. and Nebreda A.R. (1994) A novel kinase cascade triggered by stress and heat shock that stimulates MAPKAP-kinase 2 and phosphorylation of the small heat shock proteins. *Cell.* 78:1027-1037.

Roux P. and Blenis J. (2004) ERK and p38 MAPK-activated protein kinases: a family of protein kinases with diverse biological functions. *Microbiol. Mol Biol Rev.* 68: 320-344.

Rubinfeld H. and Serger R. (2005) The ERK cascade: a prototype of MAPK signalling. *Mol. Biotechnol.* 31:151-174.

Ruiz-Meana, M; Garcia-Dorado ,D; Gonzhlez, M.A; Barrabks,Jo and A and soler-Soler,J. (1995) Effect of osmotic stress on sarcolemmal integrity of isolated cardiomyocytes following transient metabolic inhibition. *Cardio. Res*, 30,64-69.

Ruiz-Meana M., Garcia-Dorado D., Hofstaetter B., Piper H.M. and Soler-soler J. (1999) Propagation of cardiomyocytes hypercontracture by passage of Na+ through gap junctions. *Circ Res.* 85(3):280-287.

Ruparelia A.A., Zhao M., Currie P.D. and Bryson-Richardson R.J. (2012) Characterization and investigation of zebrafish models of Filamin related myofibrillar myopathy. *Hum. Mol.* Ge*net.* 21(18): 4073-4083.

Russell, A.P. (2010) Molecular regulation of skeletal muscle mass. *Clin Exp Pharmacol Physiol*. 37(3):378-384.

Sadoshima J. and Izumo S. (1997) The cellular and molecular response of cardiac myocytes to mechanical stress. *Annu. Rev. Physiol.* 59: 551-571. Review.

Sadoshima J. and Izumo S. (1997) Tyrosine kinases mediation of c-fos expression by cell swelling in cardiac myocytes. *Heart Vessels.* 12:194-197.

Sadoshima J., Montagne O., Wang Q., Yang G., Warden J., Liu J., Takagi G., Karoor V., Hong C., Johnson G.L., Vatner D.E. and Vatner S.F. (2002) The MEKK1-JNK pathway plays a protective role in pressure overload bit does not mediate cardiac hypertrophy. *J Clin Invest.* 110(2):271-279.

Sahai, E; Alberts, A.S and Treisman, R. (1998) RhoA effector mutants reveal distinct effector pathways for cytoskeletal reorganization, SRF activation and transformation. *EMBO J*. 17:5)1350-1361.

Sahna E., Parlakpinar H. Turkoz Y. and Acet A. (2005) Protective effects of melatonin on myocardial ischaemia-reperfusion induced infarction size and oxidative changes. *Physiol. Res.* 54(5):491-495.

Sakabe N.J., Savic D. and Nobrega M.A. (2012) Transcriptional enhancers in development and disease. Ge*nome Biol.* 13(1): 238.

Sakuma, K; Akiho, M; Nakashima, H; Akima, H and Yasuhara, M. (2008) Age-related reductions in expression of serum response factor and myocardin-related transcription factor A in mouse skeletal muscles. *Biochim Biophys Acta*. 1782(7-8):453-461.

Sakuma K., Nishikawa J., Nakao R., Nakano H., Sano M. and Yashara M. (2003) Serum response factor plays an important role in the mechanically overloaded plantaris muscle of rats. *Histochem Cell Biol.* 119-149-160.

Sakuma, K; Watanabe, K; Hotta, N; Koike, T; Ishida, K; Katayama, K and Akima, H. (2009) The adaptive responses in several mediators linked with hypertrophy and atrophy of skeletal muscle after lower limb unloading in humans. *Acta Physiol (Oxf)*. 197(2):151-159.

Sala, V; Gallo, S; Leo, C; Gatti, S; Gelb, B.D and Crepaldi, T. (2012) Signaling to Cardiac Hypertrophy: Insights from Human and Mouse RASopathies. *Mol Med*. 18:938-947.

Salvador, J.M; Mittelstadt, P.R; Guszczynski, T; Copeland, T.D; Yamaguchi, H; Appella, E; Fornace, A.J. Jr and Ashwell, J.D. (2005) Alternative p38 activation pathway mediated by T cell receptor-proximaltyrosine kinases. *Nat Immunol*. 6(4):390-395.

Sanger J.W., Wang J., Fan Y., White J. and Sanger J.M. (2010) Assembly and dynamics of myofibrils. *J Biomed Biotechnol.*Epub 2010 Jun 10. Review.

Saraswat, M; Musante, L; Ravida, A; Shortt, B; Byrne, B and Holthofer, H. (2013) Preparative Purification of Recombinant Proteins: Current Status and Future Trends. *Biomed Res Int*. 2013:12709.

Sarkozy A., Obregon M.G., Conti E., Esposito G., Mingarelli R., Pizzuti A. and Dallapiccola B. (2004) A novel PTPN11 gene mutation bridges Noonan syndrome, multiple lenines/ LEOPARD syndrome and Noonan like multiple giant cell lesion syndrome. *Eur J Hum* G*enet.* 12:1069:1072.

Saurin A., Martin J., Heads R., Mockridge J., Foley C., Wright M., Wang Y. and Marber M.S. (2000) The role of differential activation of p38-mitogen-activated protein kinase in preconditioned ventricular myocytes. *FASEB J.* 14: 2237-2246.

Schaper, W and Scholz, D. (2003) Factors Regulating Arteriogenesis. *Arterioscler Thromb Vasc Biol*. 23:1143-1151.

Scheer, U; Hinssen, H; Franke, W.W and Jockusch, B.M. (1984) Microinjection of actin-binding proteins and actin antibodies demonstrates involvement of nuclear actin in transcription of lampbrush chromosomes. *Cell*. 39: 111-122.

Schiaffino, S and Mammucari, C. (2011) Regulation of skeletal muscle growth by the IGF1-Akt/PKB pathway: insights from genetic models. *Skeletal Muscle*. 1:4.

Schiaffino, S and Reggiana, C. (1996) Molecular Diversity of Myofibrillar Proteins: Gene Regulation and Functional Significance. *Physiol Rev*. 76(2):371-423.

Schlesinger, J; Schueler, M; Grunert, M; Fischer, J.J; Zhang, Q; Kreuger, T; Lange, M; Tonjes, M; Dunkel, I and Sperling, S.R. (2011) The Cardiac Transcription Network Modulated by Gata4, Mef2a, Nkx2.5, Srf, Histone Modifications, and MicroRNAs. *PLoS* G*enet*. 7(2):1-16.

Schmeichel K.L and Beckerle M.C. (1994) The LIM domain is a modular protein-binding interface. *Cell.* 79(2):211-219.

Schreiber, S.N; Emter, R; Hock, B; Knutti, D; Cardenas, J; Podvinec, M; Oakeley, E.J and Kralli, A. (2004) The estrogen-related receptor (ERR) functions in PPAR coactivator 1 (PGC-1)-induced mitochondrial biogenesis. *PNAS*. 101(17):6472-6477.

Schulz R., Belosjorow S., Gres P., Jansen J., Michel M.C. Heusch G. (2002) p38 MAP kinase is a mediator of ischemic preconditioning in pigs. *Cardiovasc Res.* 55(3):626-632.

Schulz R., Gres P., Skyschally A., Duschin A., Belosjorow S., Konietzka I. and Heusch G. (2003) Ischemis preconditioning preserves connexion 43 phosphorylation during sustained ischamia in pig hearts in vivo. *FASEB J.* 17(10):1355-1357.

Seger, R and Krebs, E. G. (1995) The MAPK signalling cascade. *FASEB J*. 9(9):726-

35.

Sediman J.G. and Seidman C. (2001) The genetic basis for cardiomyopathy: from mutation identification to mechanistic paradigms. *Cell.* 104(4):557-567.

Settleman, J. (2003) A nuclear MAL-function links Rho to SRF. *Mol Cell*. 11(5):1121-1123.

Shaffer J.F., Kensler R.W. and Harris S.P. (2009) The myosin-binding protein C motif binds to F-actin in a phosphorylationp-sensitive manner. *J Biol. Chem.* 284(18):12318-12327.

Sharrocks A.D., Yang S.H. and Galanis A. (2000) Docking domains and substrate-specificity determination for MAP kinases. *Rends Biochem Sci.* 25(9): 448-453.

Shaw J.E., Sicree R.A. and Zimmet P.Z. (2009) Global estimates of the prevalence of diabtetes. *Diabetes Res and Clinc Prac.* 87:4-14.

Shaw, P.E; Frasch, S and Nordheim, A. (1989) Repression of c-fose transcription is mediated through $p67^{SRF}$ bound to the SRE. *EMBO J*. 8(9):2567-2574.

Shaw, P.E; Schroter, H and Nordheim, A. (1989) The ability of a ternary complex to form over the serum response element correlates with serum inducibility of the human c-fos promoter. *Cell*. 56:563-572.

Shioi T., McMullen J.R., Tarnavski O., Converso K., Sherwood M.C., Manning W.J. and Izumo S. (2003) Rapamycin attenuates load-induced cardiac hypertrophy in mice. *Circulation.* 107(12): 1664-1670.

Shore, P and Sharrocks, A.D. (1995) The MADS-box family of transcription factors. *Eur. J. Biochem*. 229:1-13.

Sicard P., Clark J.E., Jacquet S., Mohammadi S., Arthur J.S. O'Keefe S.J. and Marber M.S. (2010) The activation of p38 alpha and not p38 beta, mitogen-activated protein kinase is required for ischemic preconditioning. *J Mol Cell Cardiol.* 48(6):1324-1328.

Sipila S., Taaffe D. R., Cheng S., Puolakka J., Toivanen J. and Suominen H. (2001) Effects of hormone replacement therapy and high-impact physical exercise on skeletal muscle in post-menopausal women: a randomized placebo-controlled study. *Clin. Sci. (Lond.)* 101:147-157.

Slezak, J; Tribulova, N; Pristacova, J; Uhrik, B; Thomas, T; Khaper, N; Kaul, N and Singal, P.K. (1995) Hydrogen peroxide changes in ischemic and reperfused heart: cytochemistry and biochemical and X-ray microanalysis. *Am J Pathol*. 147: 772-781.

Song X., Kusakuri Y., Xiao C.Y., Kinselle S.D., Rosenberg M.A., Scherrer-Crosbie M., Hara K., Rosenzweig A. and Matsui T. (2010) mTOR attenuated the inflammatory response in cardiomyocytes and prevents cardiac dysfunction in pathological hypertrophy. *Am. J Physiol Cell Physiol.* 299(6): 1256-1266.

Sorokina E.M. and Chernoff J. (2005) Rho-GTPases: new members, new pathways. *J Cell Biochem.* 94(2):225-231.

Soteriou A., Gamage M. and Trinick J. (1993) A survey of interactions made by the giant protein titin. *J Cell Sci.* 104:119-123.

Sotiropoulos A., Ginetis D., Copeland J. and Treisman R. (1999) Signal-regulated activation of serum response factor is mediated by changes in actin dynamics. *Cell*. 98(2):159-169.

Sparrow J.C. and Shöck F. (2009) The initial steps of myofibril assembly: integrins pave the way. *Nat Rev Mol Cell Biol.* 10(4):293-298.

Spiering, D and Hodgson, L. (2011) Dynamics of the Rho-family small GTPases in actin regulation and motility. *Cell Adh Migr*. 5(2):170-180.

Srivastava, J. and Barber, D. (2008) Actin Co-sedimentation assay; for the analysis of Protein Binding to F-actin. *Joirdanl of Visualized Experiments :JoVE*, (13), 690. doi:10. 3791/690.

Srivastava D. and Olson E. N. (2000) A genetic blueprint for cardiac development. *Nature* 407 :796-801.

Steenbergen C. (2002) The role of p38 mitogen-activated protein kinase in myocardial ischaemia/reperfusion injury: relationship to ischaemic preconditioning. *Basic Res. Cardiol.* 97:276- 285.

Steenbergen, C; Jennings, R.B. (1984) Relationship between lysophospholipis accumulation and plasma membrane injury during total in vitro ischaemia in dog heart. *J. Mol. Cell. Cardiol.* 16: 605-621.

Steinberg S. F. (2013) Oxidative Stress and sarcomeric proteins. *Circ. Res.* 112(2): 393-405.

Stockli, J; Fazakerley, D.J and James, D.E. (2011) GLUT4 exocytosis. *J Cell Sci*. 124(Pt 24):4147-4159.

Stollerman G.H. (1995) Rheumatic carditis. *Lancet*. 346(8972):390-392.

Stollerman G.H. (1991) Rheumatogenic streptococci and autoimmunity. *Clin. Immunol Immunopathol.*61(2Pt1):131-142.

Sugden P.H and Clerk A. (2006) Oxidative stress and growth-regulating intracellular signalling pathways in cardiac myocytes. *Antioxid Redox Signal.* 8(11-12):2111-2124. Review

Sugden P.H and Clerk, A. (1997) Regulation of the ERK subgroup of MAP kinase cascades through G protein-coupled receptors. *Cell Signal.* 9: 337-351.

Sugden, P.H and Clerk, A. (1998) “Stress-Responsive” Mitogen-Activated Protein Kinases (c-Jun N-Terminal Kinases and p38 Mitogen-Activated Protein Kinases) in the Myocardium. *Cir. Res.* 83: 345-352.

Sun Q., Chen G., Streb J.W., Long X., Yang Y., Stoeckert C.J. Jr. and Miano J.M. (2006) defining the mammalian CArGenome. G*enome Res.* 16(2): 197-207.

Sutton, M. G. St. J and Sharpe, N. (2000) Left ventricular remodelling after myocardial infarction. Pathophysiology and therapy. *Circulation*. 101:2981-2988.

Svendsen J.H. and Bjerrum P.J. (1992) Effects pf exogenous oxygen derived free radicals on myocardial capillary permeability, vascular tone, and incidence of ventricular arrhythmias in the canine heart. *Cardiovasc Res.* 26(12): 1181-1188.

Swan L., Lupton M., Anthony J., Yentis S.M., Steer P.J. and Gatzoulis M.A. (2006) Controversies in pregnancy and congenital heart disease. *Con. Heart Dis.* 1: 27-34.

Szent-Gyorgyi A. G. (2004) The early history of the biochemistry of Muscle contraction. *J.* G*en. Physiol.* 123 (6):631-641.

Szkudelski, T. (2001) The Mechanism of Alloxan and Streptozotocin Action in B Cells of Rat Pancreas. *Physiol Res*. 50:536-546.

Takano, H; Komuro, I; Oka,T; Shiojima, I; Hiroi, Y; Mizuno, T and Yazaki, Y. (1998) The Rho family G proteins play a critical role in muscle differentiation.*Mol. Cell. Biol*. 18: 1580-1589.

Tanno M., Bassi R., Gorog D.A., Saurin A.T., Jiang J., Heads R.J., Martin J.L., Davis R.J. and Flavell R.A. (2003) Diverse mechanisms of myocardial p38 mito-activated protein kinase activation: evidence for MKK-independent activation by a TAB-1 associated mechanism contributing to injury during myocardial ischaemia. *Circ Res.* 93:254-261.

Tanoue T., Adachi M., Moriguchi T. and Nishidi E. (2000) A conserved docking motif in MAP kinases common to substrates, activators and regulators. *Nat Cell Biol.* 2(2):110-116.

Tapscott, S.J. (2005) The circuitry of a master switch: Myod and the regulation of skeletal muscle gene transcription. *Development*. 132(12):2685-2695.

Tartaglia M., Mehler E.L., Goldberg R., Zampino G., Brunner H.G., Kremer H., van der Burgt I., Crosby A.H., Ion A., Jeffrey S., Kalidas K., Patton M.A., Kucherlapati R.S. and Gelb B.D. (2001) Mutations in PTPN11, encoding the protein tyrosine phosphatase SHP-2, cause Noonan syndrome. *Nat* Ge*net.* 29: 465-468.

Tennant P.W., Pearce M.S., Bythell M. and Rankin J. (2010) 20-year survival of children born with congenital anomalies: a population-based study. *Lancet.* 375: 649-656.

Thornburn A., Thornburn J., Chen S.Y., Powers S., Shubeita H.E., Feramisco J.R. and Chien K.R. (1993) HRas dependent pathways can activate morphological and genetic markers of cardiac hypertrophy. *J Biol Chem.* 268:2244-2249.

Thornton T. and Rincon M. (2008) Non-classical p38 map kinase functions: cell cycle checkpoints and survival. *Int J Biol. Sci.* 5:44-52.

Treisman, R. (1986) Identification of a Protein-Binding Site That Mediates Transcriptional Response of the c-fos Gene to Serum Factors. *Cell*. 46:567-574.

Treisman R. (1995) DNA binding proteins inside the MADS box. *Nature.* 376 (6540):468 -469

Treisman, R. (1995) Journey to the surface of the cell: Fos regulation and the SRE. *EMBO J*. 14(20):4905-4913.

Treisman R. (1994) Ternary complex factors: growth factor regulated transcriptional activators. G*en and Dev.* 4(1):96-101.

Trinick, J. (1992) Understanding the functions of titin and nebulin. *FEBS*. 307(1):44-48.

Trinick, J. (1996) Titin as a scaffolding and spring. Cytoskeleton. *Curr Biol.* 6(3):258-260.

Trinick, J. (1996) Interaction of titin/connectin with the thick filament. *Adv. Biophys.* 33: 81- 90.

Troidl, K; Rüding, I; Cai, W.J; Mücke, Y; Grossekettler, L; Piotrowska, I; Apfelbeck, H; Schierling, W; Volger, O.L; Horrevoets, A.J; Grote, K; Schmitz-Rixen, T; Schaper, W and Troidl, C. (2009) Actin-binding rho activating protein (Abra) is essential for fluid shear stress-induced arteriogenesis. *Arterioscler Thromb Vasc Biol*. 29(12):2093-2101.

Troidl, K and Schaper, W. (2012) Arteriogenesis versus angiogenesis in peripheral artery disease. *Diabetes Metab Res Rev*. 28(Suppl 1):27-29.

Tskhovrebova, L and Trinick, J. (2010) Roles of Titin in the Structure and Elasticity of the Sarcomere. *J Biomed Biotechnol*. 2010:612482.

Ubersax J. A. and Ferrell J. E. (2007) Mechanisma of specificity in protein phosphorylation. *Nat. Rev. Mol. Cell Biol.* 8(7): 530-541

Van Bilsen, M and Chien, K.R. (1993) Growth and hypertrophy of the heart: towards an understanding of cardiac specific and inducible gene expression. *Cardio. Res.* 27:1140-1149.

Vanden Hoek, T.L; Li, C; Shao, Z; Schumacker, P.T and Becker, L.B (1997) Significant levels of oxidants are generated by isolated cardiomyocytes during ischemia prior to reperfusion. *J Mol Cell Cardiol*. 29: 2571-2583.

Van der wal A.C; Becker A.E; Van der Loos C.M and Das P.K. (1994) Site of intimal rupture or erosion thrombosed coronary atherosclerotic plaques is characterized by an

inflammatory process irrespective of the dominant plaque morphology. American Heart Association *Circukation* 89:36-44.

Van Oostrom, M.C; Van Oostrom, O; Quax, P.H; Verhaar, M.C and Hoefer, I.E. (2008) Insights into mechanisms behind arteriogenesis: what does the future hold? *J Leukoc Biol*. 84(6):1379-1391.

VanTeeffelen J.W. (2008) How to prevent leaky vessels during repersufion? Just keep that glycocalyx sealant in place! *Crit. Care.* 12(4): 167-8.

Vassalli G., Milano G., and Moccetti T. (2012) Role of Mitogen-activated protein kinases in myocardial ischaemia-reperfusion injury during heart transplantation. *J. Of Trans.* Article ID 928954, 16 pg doi:10.1155/2012/928954.

Verma R., Aravind L., Oania R., McDonald W.H., Yates J.R. (2002) Role of Rpn11 metalloprotease in deubiquination and degradation by the 26S proteasome. *Science* 298:611-615.

Virmani R; Kolodgie, F.D; Burke, A.P; Finn, A.V; Gold, H.K; Tulenko, T.N; Wrenn, S.P and Narula, J. (2005) Atherosclerotic Plaque Progression and Vulnerability to Rupture: Angiogenesis as a Source of Intraplaque Hemorrhage. *Arterioscler Thromb Vasc Biol*. 25:2054-2061.

Vissing K., Rahbek S. K., Lamon S., Farup J., Stefanetti R. J., Wallace M. A., Vendelbo M. H., Russell A. (2013) Effect of resistance exercise contraction mode and protein supplementation on members of the STARS signalling pathway. *J. Physiol.* 591(Pt 15):3749-3763.

Von Harsdorf, R; Li, P.F and Dietz, R. (1999) Signaling pathways in reactive oxygen species-induced cardiomyocyte apoptosis. Circulation. 99(22):2934-2941.

Wada, A; Fukuda, M; Mishima, M and Nishida, E. (1998) Nuclear export of actin: a novel mechanism regulating the subcellular localization of a major cytoskeletal protein. *EMBO J*. 17:1635-1641.

Wallace M. A; Hock, M.B; Hazen, B.C; Kralli, A; Snow, R.J and Russel, A.P. (2011) Striated muscle activator of Rho signalling (STARS) is a PGC-1α/oestrogen-related receptor- α target gene and is upregulated in human skeletal muscle after endurance exercise. *J Physiol*. 589(8):2027-2039.

Wallace M.A and Russell, A. P. (2013) Striated muscle activator of Rho signaling (STARS) is required for myotube survival but does not influence basal protein synthesis or degradation. *Am J Physiol Cell Physiol*. 2013 May 29. [Epub ahead of print]

Wallace, M.A., Lamon S. And Russell A.P. (2012) The regulation and function of the striated muscle activator of rho signalling (STARS) protein. *Front Physiol.* 3:469.

Wang D., Chang P.S., Wang Z., Sutherland L., Wang Z., Richardson J.A., Small E., Kreig P.A. and Olson E.N. (2001) Activation of cardiac gene expression by myocardin a transcriptional cofactor of serum response factor. *Cell.* 105:851-862.

Wang, D.Z; Li, S; Hockemeyer, D; Sutherland, L; Wang, Z; Schratt, G; Richardson, J.A; Nordheim, A and Olson, E.n. (2002) Potentiation of serum response factor activity by a family of myocardin-related transcription factors. *Proc Natl Acad Sci U S A*. 99(23):14855-14860.

Wang D.Z. and Olson E.N. (2004) Control of smooth muscle development by the myocardin family of transcriptional coactivators. *Curr Opin* G*enet Dev.* 14:558-566.

Wang J., Van De Water T., Bonny C., de Ribaupierre F., Puel J and Zine A. (2003) A peptide inhibitor of c-Jun N-terminal kinase protects against both aminoglycoside and acoustic trauma-induced hair cell death and hearing loss. *J Neurosci.* 23:8596-8607.

Wang, K. (1996) Titin/Connectin and Nebulin: Giant Protein Rulers of Muscle Structure and Function. *Adv Biphys*. 33:123-134.

Wang, L; Tanaka, S and Ramirez, F. (2005) GATA-4 binds to an upstream element of the human alpha2(I) collagen gene (COL1A2) and inhibits transcription in fibroblasts. *Matrix Biol.*24: 333-340.

Wang, Y. (2007) Mitogen-activated protein kinases in heart development and diseases. *Circulation*. 116(12):1413-23.

Wang Y., Su B., Ssh V., Brown J.H., Han J. and Chien K.R. (1998) Cardiac hypertrophy induced by mitogen-activated protein kinase kinase 7, a specific activator for c-Jun NH2-terminal kinase in ventricular muscle cells. *J Biol Chem.* 273: 5423-5426.

Wang Z., Wand D.Z., Hockemeyer D., McAnally J., Nordheim A. and Olson E.N. (2004) Myocardin and ternary complex factors for SRF to control smooth muscle gene expression. *Nature.* 428:185-189.

Watkins, S.J and Borthwick, G.M. (2011) The H9C2 cell line and primary neonatal cardiomyocyte cells show similar hypertrophic responses in vitro. *In Vitro Cell Dev Biol Anim.* 47:125-131.

Wear, M.A; Schafer, D.A and Cooper, J.A. (2000) Actin dynamics: assembly and disassembly of actin networks. *Curr. Biol*. 10: 891-895.

Weinberg, R. (2007) The Biology of Cancer, Garland Science.

Willis, M.S; Schisler, J.C; Portbury, A.L and Patterson, C. (2009) Build it up–Tear it down: protein quality control in the cardiac sarcomere. *Cardiovasc Res*. 81:439-448.

Winder S.J. and Ayscough K.R. (2005) Actin-binding proteins. *J Cell Sci.* 118(Pt4):651-654.

Winegrad, S. (1999) Cardiac Myosin Binding Protein C. *Circ Res*. 84(10):1117-1126.

Witt C.C., Burkart C., Labeir D., McNabb M., Wu Y., Granzier H. and Labeit S. (2006) Nebulin regulates thin filament length, contractility and Z-disk structure in vivo. *EMBO J.* 25: 3843-3855.

Wright J., Huang Q.Q. and Wang K. (1993) Nebulin is a full-length template of actin filaments in the skeletal muscle sarcomere: an immunoelectron microscope study of its orientation and span with site- specific monoclonal antibodies. *J. Muscle Res. Cell Motil.* 14:476-483.

Wright, J.W; Mizuutani, S and Harding, J.W. (2008) Pathways involved in the transition from hypertension to hypertrophy to heart failure. Treatment strategies. *Heart. Fail. Rev*. 13:367-375.

Wu, H and Olson, E.N. (2002) Activation of the MEF2 transcription factor in skeletal muscles from myotonic mice. *J Clin Invest*. 109:1327-1333.

Wu, W; Huang, X; Cheng, J; Li, Z; de Folter, S, Huang, Z; Jiang, X; Pang, H and Tao, S. (2011) Conservation and evolution in and among SRF- and MEF2- type MADS domains and their binding sites. *Mol Biol Evol*. 28(1):501-511.

Wysocki V.H., Resing K.A., Zhang Q. And Cheng G. (2005) Mass spectrometry of peptides and proteins. *Methods.* 35:211-222.

Xing, W; Zhang, T. C; Cao, D; Wang, Z; Antos, C. L; Li, S; Wang, Y; Olson, E. N and Wang, D.Z. (2006) Myocardin induces cardiomyocyte hypertrophy. *Circ Res*. 98(8):1089-1097.

Yang S.H., Whitmarsh A.J., Davis R.J. and Sharrocks A.D. (1998) Differential targeting of MAP kinases to the ETS-domain transcription factor ELK-1. *EMBO J.* 17:1740-1749.

Yamada Y., Nezu J.I., Shimane M. and Hirata Y. (1997) Molecular cloning of a novel vascular endothelial growth factor, VEGF-D. *Genomics.*42:483-488.

Yamakazi, T; Komuro, I; Shiojma, I and Yakazi, Y. (1999) The Molecular Mechanism of Cardiac Hypertrophy Failure. *Annals of the New York Academy of Science*. 874:38-48

Yamakazi, T; Komuro, I and Yakazi, Y. (1995) Molecular mechanism of cardiac cellular hypertrophy by mechanical stress. *J. Mol. Cell. Cardiol*. 27:133-140.

Yin, T; Sandhu, G; Wolfgang, C.D; Burrier, A; Webb, R.L; Rigel, D.F; Hai, T and Whelan, J. (1997) Tissue-specific Pattern of Stress Kinase Activation in Ischaemic/Reperfused Heart and Kidney. *J. Biol. Chem;* 272, 19943-19950.

Young, P; Ehler, E and Gautel, M. (2001) Obscuring, a giant sarcomeric Rho guanine nucleotide exchange factor protein involved in sarcomere assembly. *J Cell Biol*. 154(1):123-136.

Zarubin T and Han J. (2005) Activation and signalling of the p38 MAP kinase pathway. *Cell Res.* 15: 11-18.

Zechner D., Thuerauf D.J., Hanford D.S., McDonough P.M. and Glembotski C.C. (1997) A role for the p38 mitogen-activated protein kinase pathway in myocardial cell growth, sarcomeric organization and cardiac-specific gene expression. *J Cell Biol.* 139: 115-127.

Zhang, D; Gaussin, V; Taffet, G.E; Belaguli, N.S; Yamada, M; Schwartz, R.J; Michael, L.H; Overbeek, P.A and Schneider, M.D. (2000) TAK1 is activated in the myocardium after pressure overload and is sufficient to provoke heart failure in transgenic mice. *Nat Med*. 6(5):556-563.

Zhang, X; Azhar, G; Chai, J; Sheridan, P; Nagano, K; Brown, T; Yang, J; Khrapko, K; Borras, A.M; Lawitts, J; Misra, R.P and Wei, J.Y. (2001) Cardiomyopathy in transgenic mice with cardiac-specific overexpression of serum response factor.*Am J Physiol Heart Circ Physiol.* 280(4): 1782-1792.

Zhang, X**;** Chai, J; Azhar, G; Sheridan, P; Borras, A.M; Furr, M.C; Khrapko, K; Lawitts, J; Misra, R.P and Wei, J.Y. (2001) Early postnatal cardiac changes and premature death in transgenic mice overexpressing a mutant form of serum response factor. *J Biol Chem.* 276(43): 40033-40040.

Zhao, T.C. (2013) Glucagon-like peptide-1 (GLP-1) and protective effects in cardiovascular disease: a new therapeutic approach for myocardial protection. *Cardiovasc Diabetol*. 12:90.

Zheng, B; Han, M; Bernier, M and Wen, J.K. (2009) Nuclear actin and actin-binding proteins in the regulation of transcription and gene expression. *FEBS J*. 276:2669-2685.

Zhivotovsky, B and Orrenius, S. (2003) Defects in the apoptotic machinery of cancer cells: role in drug resistance. *Semin. Cancer. Biol*. 13:125-134.

Zhou, P; He, A and Pu, W.T. (2012) Regulation of GATA4 transcriptional activity in cardiovascular development and disease. *Curr Top Dev Biol*. 100:143-169.

Zhou, T; Sun, L; Humphreys, J and Goldsmith, E.J. (2006) Docking Interactions Induce Exposure of Activation Loop in the MAP Kinase ERK2. *Structure*. 14(6)1011-1019.

Zweier J.L., Flaherty J.T and Weisfeldt M.L (1987) Direct measurement of free radical generation following reperfusion of ischaemic myocardium. *Proc. Natl. Acad. Sci. USA.* 84: 1404-1407.

Appendices

APPENDIX 1:- GPS 2.1 OUTPUT Data of predicted phosphorylation sites within MS1 and their cognate protein kinases

ID	Position	Code	Kinase	Peptide	Score	Cutoff
sp|Q8K4K7|ABRA_RAT Actin-binding Rho-activating protein OS=Rattus norvegicus GN=Abra PE=1 SV=2	77	S	CMGC/MAPK	QHAPKPPSPKPDGDR	5.04	3.757
sp|Q8K4K7|ABRA_RAT Actin-binding Rho-activating protein OS=Rattus norvegicus GN=Abra PE=1 SV=2	104	T	STE/STE7	HIKRKEVTRTVVSKA	1.7	1.65
sp|Q8K4K7|ABRA_RAT Actin-binding Rho-activating protein OS=Rattus norvegicus GN=Abra PE=1 SV=2	24	T	STE/STE20	LQKVRRATLVINLAR	2.985	2.088
sp|Q8K4K7|ABRA_RAT Actin-binding Rho-activating protein OS=Rattus norvegicus GN=Abra PE=1 SV=2	106	T	STE/STE20	KRKEVTRTVVSKAYE	2.103	2.088
sp|Q8K4K7|ABRA_RAT Actin-binding Rho-activating protein OS=Rattus norvegicus GN=Abra PE=1 SV=2	24	T	TKL/IRAK	LQKVRRATLVINLAR	6.5	4.5
sp|Q8K4K7|ABRA_RAT Actin-binding Rho-activating protein OS=Rattus norvegicus GN=Abra PE=1 SV=2	89	S	TKL/IRAK	GDREGRGSEEATEVS	6	4.5
sp|Q8K4K7|ABRA_RAT Actin-binding Rho-activating protein OS=Rattus norvegicus GN=Abra PE=1 SV=2	56	T	Atypical/PIKK	AGWLPGATQDLPHTP	6.074	5.585
sp|Q8K4K7|ABRA_RAT Actin-binding Rho-activating protein OS=Rattus norvegicus GN=Abra PE=1 SV=2	24	T	Other/AUR	LQKVRRATLVINLAR	4.365	3.784
sp|Q8K4K7|ABRA_RAT Actin-binding Rho-activating protein OS=Rattus norvegicus GN=Abra PE=1 SV=2	62	T	Other/PEK	ATQDLPHTPKEPGPR	2.875	2.5
sp|Q8K4K7|ABRA_RAT Actin-binding Rho-activating protein OS=Rattus norvegicus GN=Abra PE=1 SV=2	106	T	Other/PEK	KRKEVTRTVVSKAYE	3	2.5
sp|Q8K4K7|ABRA_RAT Actin-binding Rho-activating protein OS=Rattus norvegicus GN=Abra PE=1 SV=2	6	T	Other/Wnk	**MAPGETEREAGPA	4.833	4.167
sp|Q8K4K7|ABRA_RAT Actin-binding Rho-activating protein OS=Rattus norvegicus GN=Abra PE=1 SV=2	15	S	Other/Wnk	REAGPAKSALQKVRR	4.333	4.167
sp|Q8K4K7|ABRA_RAT Actin-binding Rho-activating protein OS=Rattus norvegicus GN=Abra PE=1 SV=2	56	T	Other/Wnk	AGWLPGATQDLPHTP	5	4.167
sp|Q8K4K7|ABRA_RAT Actin-binding Rho-activating protein OS=Rattus norvegicus GN=Abra PE=1 SV=2	106	T	Other/Wnk	KRKEVTRTVVSKAYE	4.667	4.167
sp|Q8K4K7|ABRA_RAT Actin-binding Rho-activating protein OS=Rattus norvegicus GN=Abra PE=1 SV=2	120	Y	TK/Abl	ERGGDVNY*******	4.22	1.72
sp|Q8K4K7|ABRA_RAT Actin-binding Rho-activating protein OS=Rattus norvegicus GN=Abra PE=1 SV=2	112	Y	TK/Alk	RTVVSKAYERGGDVN	3.667	2.667
sp|Q8K4K7|ABRA_RAT Actin-binding Rho-activating protein OS=Rattus norvegicus GN=Abra PE=1 SV=2	120	Y	TK/EGFR	ERGGDVNY*******	2.97	2
sp|Q8K4K7|ABRA_RAT Actin-binding Rho-activating protein OS=Rattus norvegicus GN=Abra PE=1 SV=2	120	Y	TK/Eph	ERGGDVNY*******	3.909	3.773
sp|Q8K4K7|ABRA_RAT Actin-binding Rho-activating protein OS=Rattus norvegicus GN=Abra PE=1 SV=2	120	Y	TK/Fak	ERGGDVNY*******	5.308	4.923

sp|Q8K4K7|ABRA_RAT Actin-binding Rho-activating protein OS=Rattus norvegicus GN=Abra PE=1 SV=2	112	Y	TK/InsR	RTVVSKAYERGGDVN	1.636	1.606
sp|Q8K4K7|ABRA_RAT Actin-binding Rho-activating protein OS=Rattus norvegicus GN=Abra PE=1 SV=2	120	Y	TK/InsR	ERGGDVNY*******	3.379	1.606
sp|Q8K4K7|ABRA_RAT Actin-binding Rho-activating protein OS=Rattus norvegicus GN=Abra PE=1 SV=2	120	Y	TK/JakA	ERGGDVNY*******	5.024	3.195
sp|Q8K4K7|ABRA_RAT Actin-binding Rho-activating protein OS=Rattus norvegicus GN=Abra PE=1 SV=2	120	Y	TK/Met	ERGGDVNY*******	2.8	2.067
sp|Q8K4K7|ABRA_RAT Actin-binding Rho-activating protein OS=Rattus norvegicus GN=Abra PE=1 SV=2	112	Y	TK/Src	RTVVSKAYERGGDVN	1.042	0.743
sp|Q8K4K7|ABRA_RAT Actin-binding Rho-activating protein OS=Rattus norvegicus GN=Abra PE=1 SV=2	120	Y	TK/Src	ERGGDVNY*******	1.552	0.743
sp|Q8K4K7|ABRA_RAT Actin-binding Rho-activating protein OS=Rattus norvegicus GN=Abra PE=1 SV=2	120	Y	TK/Syk	ERGGDVNY*******	2.862	1.662
sp|Q8K4K7|ABRA_RAT Actin-binding Rho-activating protein OS=Rattus norvegicus GN=Abra PE=1 SV=2	120	Y	TK/PDGFR	ERGGDVNY*******	4.614	2.273
sp|Q8K4K7|ABRA_RAT Actin-binding Rho-activating protein OS=Rattus norvegicus GN=Abra PE=1 SV=2	24	T	AGC/DMPK/ ROCK	LQKVRRATLVINLAR	2.474	2.158
sp|Q8K4K7|ABRA_RAT Actin-binding Rho-activating protein OS=Rattus norvegicus GN=Abra PE=1 SV=2	93	T	AGC/DMPK/ ROCK	GRGSEEATEVSHIKR	2.289	2.158
sp|Q8K4K7|ABRA_RAT Actin-binding Rho-activating protein OS=Rattus norvegicus GN=Abra PE=1 SV=2	41	S	AGC/PKC/Alpha	QQWANENSTRQAQEP	4.743	4.59
sp|Q8K4K7|ABRA_RAT Actin-binding Rho-activating protein OS=Rattus norvegicus GN=Abra PE=1 SV=2	41	S	AGC/PKC/Delta	QQWANENSTRQAQEP	4.452	3.806
sp|Q8K4K7|ABRA_RAT Actin-binding Rho-activating protein OS=Rattus norvegicus GN=Abra PE=1 SV=2	106	T	AGC/PKC/Iota	KRKEVTRTVVSKAYE	3.769	3.692
sp|Q8K4K7|ABRA_RAT Actin-binding Rho-activating protein OS=Rattus norvegicus GN=Abra PE=1 SV=2	24	T	AGC/PKG/PKG2	LQKVRRATLVINLAR	4.8	3.5
sp|Q8K4K7|ABRA_RAT Actin-binding Rho-activating protein OS=Rattus norvegicus GN=Abra PE=1 SV=2	24	T	CAMK/CAMK2/CAMK2a	LQKVRRATLVINLAR	3.333	2.917
sp|Q8K4K7|ABRA_RAT Actin-binding Rho-activating protein OS=Rattus norvegicus GN=Abra PE=1 SV=2	24	T	CAMK/DAPK /DAPK3	LQKVRRATLVINLAR	9	4.222
sp|Q8K4K7|ABRA_RAT Actin-binding Rho-activating protein OS=Rattus norvegicus GN=Abra PE=1 SV=2	89	S	CAMK/DAPK /DAPK3	GDREGRGSEEATEVS	4.389	4.222
sp|Q8K4K7|ABRA_RAT Actin-binding Rho-activating protein OS=Rattus norvegicus GN=Abra PE=1 SV=2	104	T	CAMK/DAPK /DAPK3	HIKRKEVTRTVVSKA	6.111	4.222
sp|Q8K4K7|ABRA_RAT Actin-binding Rho-activating protein OS=Rattus norvegicus GN=Abra PE=1 SV=2	89	S	CK1/CK1/CK1a	GDREGRGSEEATEVS	1.647	1.588
sp|Q8K4K7|ABRA_RAT Actin-binding Rho-activating protein OS=Rattus norvegicus GN=Abra PE=1 SV=2	56	T	CK1/CK1/CK1e	AGWLPGATQDLPHTP	1.429	1
sp|Q8K4K7|ABRA_RAT Actin-binding Rho-activating protein OS=Rattus norvegicus GN=Abra PE=1 SV=2	62	T	CMGC/CDK/ CDC2	ATQDLPHTPKEPGPR	3.947	2.512
sp|Q8K4K7|ABRA_RAT Actin-binding	77	S	CMGC/CDK/	QHAPKPPSPKPDGDR	3	2.512

Rho-activating protein OS=Rattus norvegicus GN=Abra PE=1 SV=2			CDC2			
sp|Q8K4K7|ABRA_RAT Actin-binding Rho-activating protein OS=Rattus norvegicus GN=Abra PE=1 SV=2	62	T	CMGC/CDK/CDK4	ATQDLPHTPKEPGPR	7.385	5.077
sp|Q8K4K7|ABRA_RAT Actin-binding Rho-activating protein OS=Rattus norvegicus GN=Abra PE=1 SV=2	77	S	CMGC/CDK/CDK4	QHAPKPPSPKPDGDR	9.846	5.077
sp|Q8K4K7|ABRA_RAT Actin-binding Rho-activating protein OS=Rattus norvegicus GN=Abra PE=1 SV=2	62	T	CMGC/CDK/CDK5	ATQDLPHTPKEPGPR	10.579	9.158
sp|Q8K4K7|ABRA_RAT Actin-binding Rho-activating protein OS=Rattus norvegicus GN=Abra PE=1 SV=2	77	S	CMGC/CDK/CDK5	QHAPKPPSPKPDGDR	13.263	9.158
sp|Q8K4K7|ABRA_RAT Actin-binding Rho-activating protein OS=Rattus norvegicus GN=Abra PE=1 SV=2	104	T	CMGC/CDK/CDK7	HIKRKEVTRTVVSKA	4.5	2.278
sp|Q8K4K7|ABRA_RAT Actin-binding Rho-activating protein OS=Rattus norvegicus GN=Abra PE=1 SV=2	77	S	CMGC/DYRK/Dyrk1	QHAPKPPSPKPDGDR	4.714	3
sp|Q8K4K7|ABRA_RAT Actin-binding Rho-activating protein OS=Rattus norvegicus GN=Abra PE=1 SV=2	62	T	CMGC/GSK/GSK3A	ATQDLPHTPKEPGPR	4.167	4
sp|Q8K4K7|ABRA_RAT Actin-binding Rho-activating protein OS=Rattus norvegicus GN=Abra PE=1 SV=2	77	S	CMGC/GSK/GSK3A	QHAPKPPSPKPDGDR	4	4
sp|Q8K4K7|ABRA_RAT Actin-binding Rho-activating protein OS=Rattus norvegicus GN=Abra PE=1 SV=2	77	S	CMGC/GSK/GSK3B	QHAPKPPSPKPDGDR	5.041	4.102
sp|Q8K4K7|ABRA_RAT Actin-binding Rho-activating protein OS=Rattus norvegicus GN=Abra PE=1 SV=2	62	T	CMGC/MAPK/ERK	ATQDLPHTPKEPGPR	7.377	5.91
sp|Q8K4K7|ABRA_RAT Actin-binding Rho-activating protein OS=Rattus norvegicus GN=Abra PE=1 SV=2	77	S	CMGC/MAPK/ERK	QHAPKPPSPKPDGDR	8.671	5.91
sp|Q8K4K7|ABRA_RAT Actin-binding Rho-activating protein OS=Rattus norvegicus GN=Abra PE=1 SV=2	62	T	CMGC/MAPK/JNK	ATQDLPHTPKEPGPR	4.812	4.688
sp|Q8K4K7|ABRA_RAT Actin-binding Rho-activating protein OS=Rattus norvegicus GN=Abra PE=1 SV=2	62	T	CMGC/MAPK/p38	ATQDLPHTPKEPGPR	5.224	4.776
sp|Q8K4K7|ABRA_RAT Actin-binding Rho-activating protein OS=Rattus norvegicus GN=Abra PE=1 SV=2	77	S	CMGC/MAPK/p38	QHAPKPPSPKPDGDR	6.328	4.776
sp|Q8K4K7|ABRA_RAT Actin-binding Rho-activating protein OS=Rattus norvegicus GN=Abra PE=1 SV=2	6	T	STE/STE7/MAP2K1	**MAPGETEREAGPA	7	7
sp|Q8K4K7|ABRA_RAT Actin-binding Rho-activating protein OS=Rattus norvegicus GN=Abra PE=1 SV=2	93	T	STE/STE7/MAP2K1	GRGSEEATEVSHIKR	9	7
sp|Q8K4K7|ABRA_RAT Actin-binding Rho-activating protein OS=Rattus norvegicus GN=Abra PE=1 SV=2	104	T	STE/STE7/MAP2K2	HIKRKEVTRTVVSKA	9	7
sp|Q8K4K7|ABRA_RAT Actin-binding Rho-activating protein OS=Rattus norvegicus GN=Abra PE=1 SV=2	104	T	STE/STE7/MAP2K3	HIKRKEVTRTVVSKA	6.75	3.25
sp|Q8K4K7|ABRA_RAT Actin-binding Rho-activating protein OS=Rattus norvegicus GN=Abra PE=1 SV=2	106	T	STE/STE7/MAP2K7	KRKEVTRTVVSKAYE	4.6	3.2
sp|Q8K4K7|ABRA_RAT Actin-binding Rho-activating protein OS=Rattus norvegicus GN=Abra PE=1 SV=2	24	T	STE/STE20/PAKA	LQKVRRATLVINLAR	4.431	3.052
sp|Q8K4K7|ABRA_RAT Actin-binding Rho-activating protein OS=Rattus	24	T	TKL/MLK/ILK	LQKVRRATLVINLAR	3.667	3.556

norvegicus GN=Abra PE=1 SV=2						
sp|Q8K4K7|ABRA_RAT Actin-binding Rho-activating protein OS=Rattus norvegicus GN=Abra PE=1 SV=2	109	S	TKL/MLK/ILK	EVTRTVVSKAYERGG	3.889	3.556
sp|Q8K4K7|ABRA_RAT Actin-binding Rho-activating protein OS=Rattus norvegicus GN=Abra PE=1 SV=2	56	T	Atypical/PIKK/DNAPK	AGWLPGATQDLPHTP	3.333	2.952
sp|Q8K4K7|ABRA_RAT Actin-binding Rho-activating protein OS=Rattus norvegicus GN=Abra PE=1 SV=2	62	T	Atypical/PIKK/FRAP	ATQDLPHTPKEPGPR	7.4	5.8
sp|Q8K4K7|ABRA_RAT Actin-binding Rho-activating protein OS=Rattus norvegicus GN=Abra PE=1 SV=2	77	S	Atypical/PIKK/FRAP	QHAPKPPSPKPDGDR	6.667	5.8
sp|Q8K4K7|ABRA_RAT Actin-binding Rho-activating protein OS=Rattus norvegicus GN=Abra PE=1 SV=2	24	T	Other/AUR/AUR-B	LQKVRRATLVINLAR	5.931	5.69
sp|Q8K4K7|ABRA_RAT Actin-binding Rho-activating protein OS=Rattus norvegicus GN=Abra PE=1 SV=2	24	T	Other/AUR/IPL1-yeast	LQKVRRATLVINLAR	8.053	6.211
sp|Q8K4K7|ABRA_RAT Actin-binding Rho-activating protein OS=Rattus norvegicus GN=Abra PE=1 SV=2	104	T	Other/NEK/NEK2	HIKRKEVTRTVVSKA	8	6.667
sp|Q8K4K7|ABRA_RAT Actin-binding Rho-activating protein OS=Rattus norvegicus GN=Abra PE=1 SV=2	109	S	Other/NEK/NEK2	EVTRTVVSKAYERGG	7.333	6.667
sp|Q8K4K7|ABRA_RAT Actin-binding Rho-activating protein OS=Rattus norvegicus GN=Abra PE=1 SV=2	24	T	Other/NEK/NEK9	LQKVRRATLVINLAR	8.667	8.333
sp|Q8K4K7|ABRA_RAT Actin-binding Rho-activating protein OS=Rattus norvegicus GN=Abra PE=1 SV=2	77	S	Other/Other-Unique/KIS	QHAPKPPSPKPDGDR	5.6	5.2
sp|Q8K4K7|ABRA_RAT Actin-binding Rho-activating protein OS=Rattus norvegicus GN=Abra PE=1 SV=2	89	S	Other/Other-Unique/KIS	GDREGRGSEEATEVS	6.8	5.2
sp|Q8K4K7|ABRA_RAT Actin-binding Rho-activating protein OS=Rattus norvegicus GN=Abra PE=1 SV=2	62	T	Other/PEK/PKR	ATQDLPHTPKEPGPR	2.875	2.562
sp|Q8K4K7|ABRA_RAT Actin-binding Rho-activating protein OS=Rattus norvegicus GN=Abra PE=1 SV=2	106	T	Other/PEK/PKR	KRKEVTRTVVSKAYE	3	2.562
sp|Q8K4K7|ABRA_RAT Actin-binding Rho-activating protein OS=Rattus norvegicus GN=Abra PE=1 SV=2	6	T	Other/PLK/PLK1	**MAPGETEREAGPA	1.362	1.298
sp|Q8K4K7|ABRA_RAT Actin-binding Rho-activating protein OS=Rattus norvegicus GN=Abra PE=1 SV=2	120	Y	TK/Abl/Abl	ERGGDVNY*******	3.354	1.333
sp|Q8K4K7|ABRA_RAT Actin-binding Rho-activating protein OS=Rattus norvegicus GN=Abra PE=1 SV=2	112	Y	TK/Axl/Mer	RTVVSKAYERGGDVN	6.667	4.34
sp|Q8K4K7|ABRA_RAT Actin-binding Rho-activating protein OS=Rattus norvegicus GN=Abra PE=1 SV=2	120	Y	TK/EGFR/EGFR	ERGGDVNY*******	3.918	2.197
sp|Q8K4K7|ABRA_RAT Actin-binding Rho-activating protein OS=Rattus norvegicus GN=Abra PE=1 SV=2	120	Y	TK/EGFR/ErbB2	ERGGDVNY*******	2.8	2.2
sp|Q8K4K7|ABRA_RAT Actin-binding Rho-activating protein OS=Rattus norvegicus GN=Abra PE=1 SV=2	112	Y	TK/InsR/IGF1R	RTVVSKAYERGGDVN	2	1.839
sp|Q8K4K7|ABRA_RAT Actin-binding Rho-activating protein OS=Rattus norvegicus GN=Abra PE=1 SV=2	120	Y	TK/InsR/InsR	ERGGDVNY*******	3.911	2.489
sp|Q8K4K7|ABRA_RAT Actin-binding Rho-activating protein OS=Rattus norvegicus GN=Abra PE=1 SV=2	120	Y	TK/JakA/Tyk2	ERGGDVNY*******	4.375	4.25

sp|Q8K4K7|ABRA_RAT Actin-binding Rho-activating protein OS=Rattus norvegicus GN=Abra PE=1 SV=2	112	Y	TK/Src/HCK	RTVVSKAYERGGDVN	5	3.917
sp|Q8K4K7|ABRA_RAT Actin-binding Rho-activating protein OS=Rattus norvegicus GN=Abra PE=1 SV=2	120	Y	TK/Src/Lck	ERGGDVNY*******	5.352	2.889
sp|Q8K4K7|ABRA_RAT Actin-binding Rho-activating protein OS=Rattus norvegicus GN=Abra PE=1 SV=2	112	Y	TK/Src/Src	RTVVSKAYERGGDVN	1.369	0.832
sp|Q8K4K7|ABRA_RAT Actin-binding Rho-activating protein OS=Rattus norvegicus GN=Abra PE=1 SV=2	120	Y	TK/Src/Src	ERGGDVNY*******	1.497	0.832
sp|Q8K4K7|ABRA_RAT Actin-binding Rho-activating protein OS=Rattus norvegicus GN=Abra PE=1 SV=2	120	Y	TK/Syk/ZAP70	ERGGDVNY*******	2.75	2.15
sp|Q8K4K7|ABRA_RAT Actin-binding Rho-activating protein OS=Rattus norvegicus GN=Abra PE=1 SV=2	120	Y	TK/Tec/ITK	ERGGDVNY*******	8.286	3.571
sp|Q8K4K7|ABRA_RAT Actin-binding Rho-activating protein OS=Rattus norvegicus GN=Abra PE=1 SV=2	120	Y	TK/PDGFR/CSF1R	ERGGDVNY*******	11.625	3.25
sp|Q8K4K7|ABRA_RAT Actin-binding Rho-activating protein OS=Rattus norvegicus GN=Abra PE=1 SV=2	24	T	AGC/DMPK/ROCK/ROCK1	LQKVRRATLVINLAR	4.6	3.4
sp|Q8K4K7|ABRA_RAT Actin-binding Rho-activating protein OS=Rattus norvegicus GN=Abra PE=1 SV=2	77	S	AGC/GRK/BARK/GRK-3	QHAPKPPSPKPDGDR	7	5.75
sp|Q8K4K7|ABRA_RAT Actin-binding Rho-activating protein OS=Rattus norvegicus GN=Abra PE=1 SV=2	106	T	AGC/GRK/GRK/GRK-1	KRKEVTRTVVSKAYE	4.625	3.75
sp|Q8K4K7|ABRA_RAT Actin-binding Rho-activating protein OS=Rattus norvegicus GN=Abra PE=1 SV=2	24	T	AGC/PKC/Alpha/PKCa	LQKVRRATLVINLAR	4.291	3.97
sp|Q8K4K7|ABRA_RAT Actin-binding Rho-activating protein OS=Rattus norvegicus GN=Abra PE=1 SV=2	77	S	AGC/PKC/Alpha/PKCg	QHAPKPPSPKPDGDR	3.2	2.6
sp|Q8K4K7|ABRA_RAT Actin-binding Rho-activating protein OS=Rattus norvegicus GN=Abra PE=1 SV=2	41	S	AGC/PKC/Delta/PKCd	QQWANENSTRQAQEP	3.826	3.478
sp|Q8K4K7|ABRA_RAT Actin-binding Rho-activating protein OS=Rattus norvegicus GN=Abra PE=1 SV=2	6	T	AGC/PKC/Delta/PKCt	**MAPGETEREAGPA	5.25	4.125
sp|Q8K4K7|ABRA_RAT Actin-binding Rho-activating protein OS=Rattus norvegicus GN=Abra PE=1 SV=2	41	S	AGC/PKC/Delta/PKCt	QQWANENSTRQAQEP	4.5	4.125
sp|Q8K4K7|ABRA_RAT Actin-binding Rho-activating protein OS=Rattus norvegicus GN=Abra PE=1 SV=2	106	T	AGC/PKC/Eta/PKCh	KRKEVTRTVVSKAYE	5.25	4.75
sp|Q8K4K7|ABRA_RAT Actin-binding Rho-activating protein OS=Rattus norvegicus GN=Abra PE=1 SV=2	15	S	AGC/PKC/Iota/PKCz	REAGPAKSALQKVRR	3.615	3.615
sp|Q8K4K7|ABRA_RAT Actin-binding Rho-activating protein OS=Rattus norvegicus GN=Abra PE=1 SV=2	106	T	AGC/PKC/Iota/PKCz	KRKEVTRTVVSKAYE	3.615	3.615
sp|Q8K4K7|ABRA_RAT Actin-binding Rho-activating protein OS=Rattus norvegicus GN=Abra PE=1 SV=2	24	T	AGC/RSK/RSK/RSK1	LQKVRRATLVINLAR	4.2	4.2
sp|Q8K4K7|ABRA_RAT Actin-binding Rho-activating protein OS=Rattus norvegicus GN=Abra PE=1 SV=2	89	S	AGC/RSK/RSK/RSK1	GDREGRGSEEATEVS	4.7	4.2
sp|Q8K4K7|ABRA_RAT Actin-binding Rho-activating protein OS=Rattus norvegicus GN=Abra PE=1 SV=2	62	T	CMGC/CDK/CDC2/CDC2	ATQDLPHTPKEPGPR	6.784	4.072
sp|Q8K4K7|ABRA_RAT Actin-binding	62	T	CMGC/CDK/	ATQDLPHTPKEPGPR	7.622	3.095

Rho-activating protein OS=Rattus norvegicus GN=Abra PE=1 SV=2			CDC2/CDK2			
sp|Q8K4K7|ABRA_RAT Actin-binding Rho-activating protein OS=Rattus norvegicus GN=Abra PE=1 SV=2	77	S	CMGC/CDK/CDC2/CDK2	QHAPKPPSPKPDGDR	5.473	3.095
sp|Q8K4K7|ABRA_RAT Actin-binding Rho-activating protein OS=Rattus norvegicus GN=Abra PE=1 SV=2	62	T	CMGC/CDK/CDK4/CDK4	ATQDLPHTPKEPGPR	7.385	5
sp|Q8K4K7|ABRA_RAT Actin-binding Rho-activating protein OS=Rattus norvegicus GN=Abra PE=1 SV=2	77	S	CMGC/CDK/CDK4/CDK4	QHAPKPPSPKPDGDR	9.846	5
sp|Q8K4K7|ABRA_RAT Actin-binding Rho-activating protein OS=Rattus norvegicus GN=Abra PE=1 SV=2	15	S	CMGC/CDK/CDK4/CDK6	REAGPAKSALQKVRR	6.25	5.25
sp|Q8K4K7|ABRA_RAT Actin-binding Rho-activating protein OS=Rattus norvegicus GN=Abra PE=1 SV=2	62	T	CMGC/MAPK/ERK/MAPK1	ATQDLPHTPKEPGPR	8.583	6.557
sp|Q8K4K7|ABRA_RAT Actin-binding Rho-activating protein OS=Rattus norvegicus GN=Abra PE=1 SV=2	77	S	CMGC/MAPK/ERK/MAPK1	QHAPKPPSPKPDGDR	10.548	6.557
sp|Q8K4K7|ABRA_RAT Actin-binding Rho-activating protein OS=Rattus norvegicus GN=Abra PE=1 SV=2	62	T	CMGC/MAPK/ERK/MAPK3	ATQDLPHTPKEPGPR	10.322	7.747
sp|Q8K4K7|ABRA_RAT Actin-binding Rho-activating protein OS=Rattus norvegicus GN=Abra PE=1 SV=2	77	S	CMGC/MAPK/ERK/MAPK3	QHAPKPPSPKPDGDR	10.172	7.747
sp|Q8K4K7|ABRA_RAT Actin-binding Rho-activating protein OS=Rattus norvegicus GN=Abra PE=1 SV=2	62	T	CMGC/MAPK/ERK/MAPK7	ATQDLPHTPKEPGPR	3.286	3.214
sp|Q8K4K7|ABRA_RAT Actin-binding Rho-activating protein OS=Rattus norvegicus GN=Abra PE=1 SV=2	77	S	CMGC/MAPK/ERK/MAPK7	QHAPKPPSPKPDGDR	4.071	3.214
sp|Q8K4K7|ABRA_RAT Actin-binding Rho-activating protein OS=Rattus norvegicus GN=Abra PE=1 SV=2	77	S	CMGC/MAPK/JNK/MAPK8	QHAPKPPSPKPDGDR	16.778	15.889
sp|Q8K4K7|ABRA_RAT Actin-binding Rho-activating protein OS=Rattus norvegicus GN=Abra PE=1 SV=2	62	T	CMGC/MAPK/JNK/MAPK9	ATQDLPHTPKEPGPR	4.947	4.947
sp|Q8K4K7|ABRA_RAT Actin-binding Rho-activating protein OS=Rattus norvegicus GN=Abra PE=1 SV=2	77	S	CMGC/MAPK/JNK/MAPK10	QHAPKPPSPKPDGDR	10.571	8.857
sp|Q8K4K7|ABRA_RAT Actin-binding Rho-activating protein OS=Rattus norvegicus GN=Abra PE=1 SV=2	62	T	CMGC/MAPK/p38/MAPK14	ATQDLPHTPKEPGPR	6.4	5.72
sp|Q8K4K7|ABRA_RAT Actin-binding Rho-activating protein OS=Rattus norvegicus GN=Abra PE=1 SV=2	77	S	CMGC/MAPK/p38/MAPK14	QHAPKPPSPKPDGDR	7.58	5.72
sp|Q8K4K7|ABRA_RAT Actin-binding Rho-activating protein OS=Rattus norvegicus GN=Abra PE=1 SV=2	24	T	STE/STE20/PAKA/PAK1	LQKVRRATLVINLAR	6.679	5.5
sp|Q8K4K7|ABRA_RAT Actin-binding Rho-activating protein OS=Rattus norvegicus GN=Abra PE=1 SV=2	24	T	STE/STE20/PAKA/PAK2	LQKVRRATLVINLAR	4.882	3.118
sp|Q8K4K7|ABRA_RAT Actin-binding Rho-activating protein OS=Rattus norvegicus GN=Abra PE=1 SV=2	106	T	STE/STE20/PAKA/PAK2	KRKEVTRTVVSKAYE	4.471	3.118
sp|Q8K4K7|ABRA_RAT Actin-binding Rho-activating protein OS=Rattus norvegicus GN=Abra PE=1 SV=2	93	T	STE/STE20/PAKA/PAK3	GRGSEEATEVSHIKR	2.2	2
sp|Q8K4K7|ABRA_RAT Actin-binding Rho-activating protein OS=Rattus norvegicus GN=Abra PE=1 SV=2	15	S	TKL/MLK/MLK/MAP3K11	REAGPAKSALQKVRR	6.333	4.667